Epigenetic control of the post-bariatric phenotype: The role of microRNAs

A thesis submitted for a Doctor of Philosophy

Abdullah Alkandari

2015

Department of Surgery and Cancer

Imperial College London

Statement of Originality

The work presented in this thesis is my own unless otherwise stated. All other work is appropriately referenced.

Copyright

Abstract

The rising obesity pandemic and the concomitant rise in its co-morbidities are leading causes of global morbidity and mortality. Bariatric surgery is a form of gastrointestinal surgery that leads to sustained weight loss, diabetes resolution, reduction in cancer risk and other improvements in health. MicroRNAs are a family of small, endogenous, non-coding RNAs that regulate gene expression at the post-transcriptional level. MicroRNAs control expression of over half the human transcriptome and are involved in processes fundamental to both normal physiology and disease, including obesity and diabetes. This study hypothesizes that microRNAs are biomarkers for health improvements following bariatric surgery. Using quantitative PCR, a microRNA baseline was established in the serum and urine of an obese human population and increases in three anti-fibrotic microRNAs were found in urine following bariatric surgery. Circulating microRNA profiles were characterised in Roux-en-Y gastric bypass patients preoperatively and at 5 timepoints postoperatively. Roux-en-Y gastric bypass significantly altered circulating microRNA profiles in a time dependent manner. Relative to preoperative levels, of the 159 circulating microRNAs assayed 2 were significantly deregulated 1 month postoperatively, 5 were deregulated at 3 months, 10 at 6 months, 28 at 9 months and 31 at 12 months. Target prediction and pathway analysis revealed that these differentiated microRNAs regulate biological pathways that are involved in obesity and that microRNAs may contribute to the development of the beneficial post-bariatric phenotype. Both circulating and urinary post-bariatric microRNA levels correlated with measured clinical biomarkers such as BMI and blood glucose. These results indicate that bariatric operations fundamentally alter microRNA expression both in urine and in circulation and suggest that microRNAs represent not only potentially novel biomarkers for improvements in health following surgery, but are possible biological effectors that contribute to the mechanisms behind bariatric surgery. MicroRNA expression profiles could potentially be used to monitor operative outcomes and understanding the role of these differentially expressed microRNAs could shed light behind the mechanism by which bariatric surgery improves health.

Acknowledgments

Firstly, I would like to thank my two supervisors. Thank you to Professor Nigel Gooderham for giving me the opportunity to embark on this PhD and for his advice and direction. Thank you as well to Dr Hutan Ashrafian, for providing big ideas, enthusiasm and encouragement. I would also like to thank my sponsors the Ministry of Higher Education of the State of Kuwait for funded this degree and the two before it. I am also grateful to the Cultural Office for taking care of me over the last ten years.

Thank you to Professor Stephen Atkin and his colleagues at the University of Hull and Hull and East Yorkshire Hospitals NHS Trust for kindly supplying a lot of my samples and the corresponding clinical data. Thanks too to Dr Simon Rowland and Dr Mariam Ali for collecting samples and clinical data. Thank you to Dr Jia Li for sharing and managing samples. I would also like to thank all of those who helped me within the department, including Dr Paul Benton and Dr Marcelo Segura-Lepe for patiently teaching me R.

Thank you to all members of the Gooderham lab, past and present. Thank you to Dr Rhiannon David for managing the lab so well. Thank you to Michael Osborne, Saroor Patel, Mariana Flores Torres, Dr Leanne Harling, Oliver Graham, Durr Malik and Tianlai Yang for all their help and advice. Special thanks to Dr Qianxin Wu for her tutelage, training and (limited) patience.

Thank you to all the good friends I made in Imperial, during my MRes and this PhD both within and outside of the department. There are too many to name but they all have my gratitude for their continued friendship, great conversations and company. They made my PhD very enjoyable.

Lastly, I would like to thank my family, in particular my father. Without their support, in every sense, this PhD and all that came before it would not have been possible.

Table of Contents

List of Figures

List of Tables

Abbreviations

AGB	Adjustable Gastric Band
ANOVA	Analysis of Variance
BMI	Body Mass Index
C. elegans	Caenorhabditis elegans
CART	Cocaine and Amphetamine Regulated Transcript
CCK	Cholecystokinin
CCKR	Cholecystokinin Receptor
cDNA	Complementary DNA
cel.	Caenorhabditis elegans
CKD	Chronic Kidney Disease
Ct	Threshold Cycle
CV	Coefficient of Variances
CVD	Cardiovascular Disease
DMSO	Dimethyl Sulphoxide
DN	Diabetic Nephropathy
dNTP	Deoxynucleotides
eGFR	Estimated Glomerular Filtration Rate
EMT	Epithelial and Mesenchymal Transition
FAM	6-carboxyfluorescein
FBS	Foetal Bovine Serum
FDA	Food and Drug Administration
FSH	Follicle stimulating hormone
GDP	Gross Domestic Product
GLP-1	Glucagon-like Peptide 1

GLUT	Glucose Transporter
GnRHR	Gonadotropin Releasing Hormone Receptor
GSH	Follicle Stimulating Hormone
HbA1c	Glycated Haemoglobin
HDL	High-density Lipoprotein
HK-2	Human Kidney-2
LDL	Low-density Lipoprotein
LH	Luteinizing Hormone
LNA	Locked nucleic acid
MCH	Melanin-Concentrating Hormone
MDS	Myelodysplastic syndrome
MiR	MicroRNA
miRNA	MicroRNA
mRNA	Messenger RNA
NF-κB	Nuclear factor-κB
NHS	National Health Service
NICE	National Institute of Health and Care Excellence
PAF	Population Attributable Fractions
PANTHER	Protein Annotation Through Evolutionary Relationship
PBS	Phosphate-buffered Saline
PCA	Principal Component Analysis
PCR	Polymerase Chain Reaction
PDGF	Platelet Derived Growth Factor
Pre-miRNA	Precursor microRNA
Pri-miRNA	Primary microRNA

PTC	Proximal Tubular Cell
PYY	Peptide YY
qPCR	Quantitative Polymerase Chain Reaction
RISC	RNA-inducing Silencing Complex
RT	Reverse Transcription
RYGB	Roux-en-Y Gastric Bypass
SEM	Standard Error of Mean
SG	Sleeve Gastrectomy
SOS	Swedish Obese Subjects
T2DM	Type 2 Diabetes Mellitus
TGF-β	Transforming Growth Factor Beta
TNF-α	Tumour Necrosis Factor Alpha
UTR	Untranslated Region
WHO	World Health Organisation
ZEB	Zinc E-box Coding Homeobox

1 Introduction

1.1 Obesity

Obesity is a global pandemic with prevalence having more than doubled since 1980 [1]. The number of overweight and obese individuals rose from 857 million in 1980 to 2.1 billion in 2013 [2]. In the United Kingdom prevalence of obesity was 24.4% in adult males and 25.1% in adult females in 2013, a sharp increase from 1993 when 13.2% of men and 16.4% of women were obese [3]. Unlike other global health risks such as tobacco, alcoholism and malnutrition, obesity is not decreasing and is now established as one of the leading public health challenges of the 21st century. If the current trajectory holds approximately half of the world will be overweight or obese by 2030 [4].

Obesity is excessive weight in the form of fat and is measured through the body mass index (BMI), which is calculated by dividing weight in kilograms by height in metres squared. The World Health Organisation (WHO) defines healthy weight as a BMI between 18.5 and 25, overweight as a BMI between 25 and 30 and obesity as a BMI over 30 (Table 1.1). Obesity is caused by an energy imbalance where calorific intake exceeds expenditure. Globally there's been an increase in intake of high fat food and a decrease in physical activity due to environmental and societal changes caused by the rapid urbanisation and industrialisation of the 20th century.

Table 1.1: The WHO classification of obesity

Classification	BMI
Underweight	<18.50
Normal weight	18.50-24.99
Overweight	25-29.99
Obese (Obese Class I)	30-34.99
Severely Obese (Obese Class II)	35-39.99
Morbidly Obese (Obese Class III)	>40

Obesity is a risk factor for a number of other disorders including type 2 diabetes mellitus, cardiovascular disease and cancer [5]. Together, obesity and its co-morbidities form a cluster of related physiological disorders collectively known as the metabolic syndrome, and are leading causes of global morbidity and mortality, imposing substantial burdens on health services. Relative to individuals with a healthy BMI, severely and morbidly obese individuals have a higher all cause mortality [6, 7]. Over 3 million deaths were caused by excessive weight in 2010, leading to almost 4% of years of life lost [2]. In 2012/13 there were 10,957 hospital admissions in England with a primary diagnosis of obesity, a 9 fold increase from 2002/03 (1,275). There were 292,404 admissions with a primary or secondary diagnosis in 2012/13 [3]. There were 34,100 deaths attributed to obesity in 2004, equating to 6.8% of all deaths in England [8]. Obesity mortality statistics are thought to be underestimated as obesity is not always cited as a cause of death even when it's an important underlying cause [9].

The direct cost of obesity and related disorders to the National Health Service (NHS) in England was £4.2 billion in 2007, up from £470 million in 1998 [10]. Between 2 and 7% of health care funding is used to treat obesity in developed countries. That figure rises to 20% when factoring in the cost of obesity-associated disorders [4]. The indirect global socioeconomic cost of obesity is estimated to be $2 trillion, or 2.8% of global gross domestic product (GDP). That is roughly equivalent to the cost of smoking or armed conflict. In the UK, the economic impact of obesity is almost £50 billion, or 3% of national GDP [4]. The direct healthcare costs were calculated by applying population attributable fractions (PAF) to GP consultation rates, hospital admissions and outpatient attendances [10]. PAF is defined by the WHO as the proportional reduction in population disease or mortality that would occur if exposure to a risk factor was reduced to an alternative ideal exposure scenario (i.e. no obesity) [11]. Disability due to obesity leads to lost work days, physical limitations and decreased productivity [12]. The indirect costs of obesity and related disorders on years of working life lost and estimated lost earnings were calculated from age and sex-specific obesity mortality and morbidity rates [10].

1.1.1 Obesity co-morbidities

1.1.1.1 Type 2 diabetes

The emerging obesity epidemic has lead to a concomitant rise in prevalence of type 2 diabetes mellitus (T2DM), obesity's principal co-morbidity. T2DM is a chronic, progressive metabolic disease that manifests as hyperglycaemia and is caused by diminished insulin secretion and pancreatic β-cell function and increased insulin resistance and glucagon synthesis. Obesity contributes to the development of T2DM as adipose tissues in obese individuals release increased amounts of fatty acids, glycerols, hormones and pro-inflammatory cytokines that lead to insulin resistance [13]. Diabetes increases the risk of cardiovascular disease and stroke and is one of the leading causes of kidney failure [14]. Type 2 diabetes accounts for 90% of all diabetic cases and approximately 80-90% of all type 2 diabetics are overweight or obese [15]. The risk of developing diabetes is elevated with excess weight, increasing 5 fold with a BMI between 25 and 30 and 93 fold with a BMI over 35 [16]. Global prevalence of T2DM is 8.3%. There are 382 million diabetics worldwide and prevalence is expected to rise to 592 million by 2035 [17]. About half of those living with type 2 diabetes are undiagnosed. In the UK over 3 million people are diabetic, with prevalence at 6%. The NHS spends approximately £10 billion on diabetes annually [18].

1.1.1.2 Cancer

There were 14 million cases and 8.2 million deaths in 2012 due to cancer, another disease in which obesity is an established independent risk factor [19]. An epidemiological study initiated by the American Cancer Society in 1959 reported higher cancer mortality in individuals 40% above the average weight [20]. More recently obesity has been shown to increase cancer death rates by 52% in men and 62% in women [21]. In the UK a large study of 1 million women over a 5 year period revealed a significant association between obesity and cancer risk, especially in postmenopausal women [22]. Obesity increases the risk of developing colorectal, endometrial, breast, renal, oesophagus, pancreatic, gallbladder, liver and haematological cancers, including lymphoma,

leukaemia and myeloma [23-25]. The direct and indirect mechanisms linking obesity and cancer risk are multi-factorial and include obesity-related hormones and growth factors, impaired insulin signalling, regulation of energy balance, calorie restriction, signalling pathways and inflammation [26].

1.1.1.3 Cardiovascular disease

Obesity also has adverse effects on cardiac health. Over 17 million people died from cardiovascular disease (CVD) in 2008 and this is projected to rise to over 23 million by 2030 [27]. Obesity is an independent risk factor of CVD. A large prospective study found that obese individual were twice as likely to have heart failure than healthy weight individuals, and that the risk of heart failure increases between 5 and 7% for every increasing unit of BMI [28]. Excessive BMI is significantly associated with the development of angina, myocardial infarction, ischemic heart disease and heart failure [29, 30]. In addition, obesity also indirectly promotes cardiovascular disease by promoting intermediate risk factors including hypertension, dyslipidemia, insulin resistance, inflammation and endothelial dysfunction [31].

1.1.2 Treatment of obesity

A holistic public policy initiative is being implemented to prevent obesity and halt its pandemic rise. These include taxation of high fat foods, advertisement restriction, regulation of portion sizes and attempts to increase social awareness [32]. When obesity is established, the first line of therapy is often intensive lifestyle intervention which encompasses dietary restrictions, physical activity and cognitive behavioural therapy. Dietary programmes are designed to simply limit calorie intake or limit specific macronutrients such as carbohydrates, fat and glycaemic load. There is no significant difference in the efficacy of specific diets and choice of diet is down to preference, ease of adherence and the need to control specific co-morbid conditions [33]. Studies have shown lifestyle interventions can be successful at inducing modest weight loss and reducing risk of developing co-morbidities [34, 35]. However, long-term many patients return to baseline weight levels [36]. Physical activity alone is insufficient at inducing weight loss in obese individuals but is vital for long-term weight management and improving cardiovascular health [37, 38]. Regular exercise maintains weight loss achieved through behavioural therapy at significantly greater levels [39].

Obesity can also be treated pharmaceutically by altering appetite or the absorption of nutrients. Orlistat is a pancreatic and gastric lipase inhibitor that decreases the hydrolysis of ingested triglycerides and is currently the only anti-obesity agent approved in Europe. Lorcaserin and phentermine plus topiramate are approved by the American Food and Drug Administration (FDA) and suppress appetite by targeting the central nervous system [34]. All three when used together with lifestyle intervention are effective at inducing modest reductions in weight over 12 months [34, 40]. However, adverse side effects are common and up to 60% of patients don't respond to the medication [40]. Tachyphylaxis can also occur and weight is often regained when the drug is withdrawn. There is also no concrete evidence that obesity drugs have any impact on co-morbid conditions [34]. The history of obesity drug therapy is beset with failure. Despite early promise fenfluramine, sibutramine and rimonabant have been discounted due to safety fears [41].

1.2 Bariatric surgery

The most effective treatment for morbid obesity is the surgical approach. Termed bariatric surgery, weight-loss operations typically incorporate gastric restriction with a possible bypass of part of the small intestine. Bariatric operations achieve greater and sustained weight loss when compared to non-surgical treatments [42]. In addition, they result in improvements in a host of co-morbid conditions including type 2 diabetes and cardiovascular disease [43]. Once seen as a drastic last-resort, bariatric surgery is increasingly recognised as an important strategy in treating morbid obesity. The last decade has seen a steep rise in the number of bariatric surgeries. There were over 450,000 bariatric procedures performed worldwide in 2013 [44], a figure that has more than tripled since 2003 [45]. The vast majority (95.7%) of operations are performed laparoscopically [44] and overall mortality due to surgery is well under 1% [46]. The rate of bariatric complications, the most common of which include staple line leaks, stenosis and reflux, is also low [47]. In the UK over 6,000 bariatric operations are performed annually with the majority being a Roux-en-Y gastric bypass [48].

The National Institute for Health and Care Excellence (NICE) recommends bariatric surgery as a treatment option in the UK for the morbidly obese with a BMI of 40 kg/m^2 or greater or between 35 kg/m^2 and 40 kg/m^2 if accompanied by a significant co-morbid disease and if behavioural and/or pharmacological therapies have proved unsuccessful [49]. This is identical to the criteria set by the National Institute of Health in the US [50]. However, given the profound benefits of bariatric surgery, particularly with regards to the resolution of co-morbid conditions, there have been recent calls to expand the guidelines for surgery [51]. NICE have recently updated their bariatric criteria and now recommend that bariatric surgery be considered as a treatment option for obese individuals with a BMI between 30 and 35 kg/m^2 and a recent onset of type 2 diabetes [52]. In 2013 0.01% of the world's population underwent a bariatric procedure, a figure that is dwarfed by the estimated 10% of the world that is obese [44].

1.2.1 Types of bariatric procedures

The three most common bariatric procedures performed globally are the Roux-en-Y gastric bypass (45%), the sleeve gastrectomy (37%) and the adjustable gastric band (10%). Other minimally performed procedures include the biliopancreatic diversion (with or without duodenal switch) and the vertical banded gastroplasty [44]. A recent meta-analysis of 19 randomised controlled bariatric trials found that although all bariatric procedures resulted in greater weight loss compared to non-surgical treatment, the biliopancreatic diversion induced the most amount of weight loss, followed by the sleeve gastrectomy, the Roux-en-Y gastric bypass and lastly banding procedures [53]. Improvements in co-morbidities is also greatest following biliopancreatic diversion, followed by Roux-en-Y gastric bypass and banding procedures [42].

1.2.1.1 Roux-en-Y gastric bypass

First developed in the 1960s [54] and modified in the 1970s [55], the Roux-en-Y gastric bypass (RYGB) has become the most common bariatric procedure worldwide. A small gastric pouch (15-30mL) is created and separated from the larger stomach remnant. The jejunum is then incised from the duodenum and anastomised to the small stomach pouch forming a distinctive 'Y' shape that gives this procedure its name [56]. The duodenum is anastomised to the distal end of the jejunum. This allows nutrients to bypass the majority of the stomach as well as the duodenum. Gastric, pancreatic and biliary secretions mix with nutrients when they enter the small intestine (Figure 1.1A). RYGB is the most commonly performed bariatric procedure worldwide. Almost 200,000 RYGB are performed a year [44], over 9,000 in the UK alone [48].

1.2.1.2 Sleeve gastrectomy

The sleeve gastrectomy (SG) requires simpler surgical technique compared to RYGB. The procedure was originally described in 1993 as an alternative stomach resection to improve biliopancreatic diversion results [57]. A longitudinal gastric sleeve is created running from the oesophagus to the small intestine that is separated for the larger excised stomach (Figure 1.1B). This procedure reduces the stomach size by approximately 75%. A relatively new procedure, the SG has gained in popularity over the last decade. In 2013, 172,320 SG were preformed [44], an 852% increase from 2008 [58]. No SG were performed in 2003 [45]. These procedures are the second most common bariatric operations in the world and the most common in North America and Asia [44].

1.2.1.3 Adjustable gastric band

Once the preferred weight loss operation, the adjustable gastric band (AGB) has lost favour of late. In 2008 42.3% of bariatric procedures worldwide were the AGB. In 2013 the percentage of AGB procedures had fallen to 10% [44]. Almost two-thirds of bariatric procedures in the North America were AGB in 2003 [45]. The AGB consists of an inflatable silicone band placed laparoscopically around the upper stomach that can be readily and repeatedly adjusted to restrict gastric size by injecting or withdrawing saline through a subcutaneous port (Figure 1.1C).

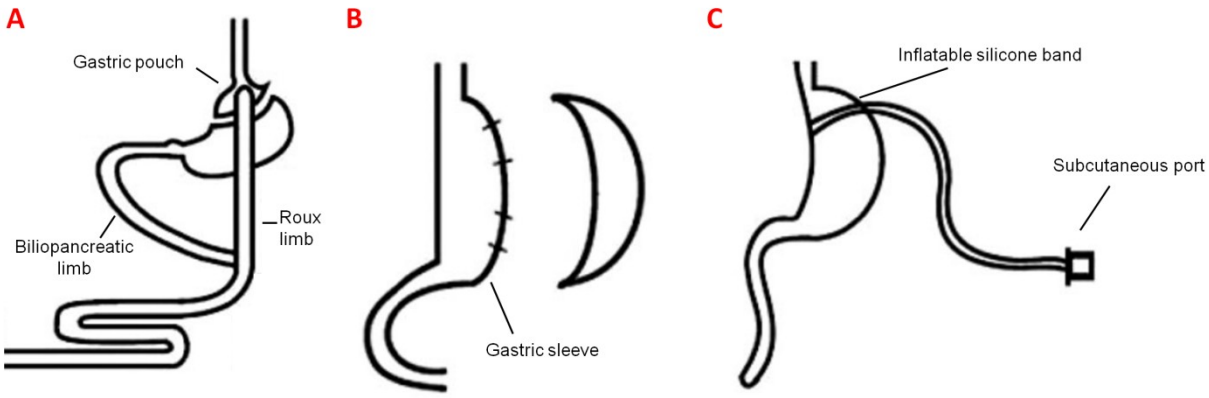

Figure 1.1: Bariatric procedures.

(A) Roux-en-Y gastric bypass, (B) sleeve gastrectomy and (C) adjustable gastric band. Adapted from [59].

1.2.2 Bariatric outcomes

1.2.2.1 Weight loss

Bariatric surgery results in greater weight loss than non-surgical treatment. The Swedish Obese Subjects (SOS) study was a prospective trial of 4,047 obese individuals treated either surgically (banding or gastric bypass) or non-surgically. They reported a mean maximum weight loss of 1% in non-surgical patients compared to 38% in gastric bypass, 26% in vertical banded gastroplasty and 21% in gastric banding patients [60]. Ten, fifteen and twenty years following intervention non-surgical patients had remained at baseline weight whereas surgical patients had maintained a statistically significant amount of their postoperative weight loss [60-62]. Other studies on adjusted gastric banding, gastric bypass, sleeve gastrectomy and biliopancreatic diversion patients have also reported greater weight loss when compared to obese patients treated medically [63-66]. Three meta-analyses of bariatric studies conducted in 2005 [67], 2009 [42] and 2013 [68] all concluded that surgical treatment for obesity is the most effective strategy at inducing and maintaining substantial weight loss.

1.2.2.2 Resolution of diabetes

The anti-diabetic effects of bariatric surgery were first observed by Pories and colleagues in 1995 who reported normal plasma glucose, glycated haemoglobin (HbA1c) and insulin in diabetics following RYGB [69]. The SOS study reported 72% of diabetics were in remission 2 years following bariatric surgery and that surgery reduces the incidence of non-diabetics developing type 2 diabetes by approximately 75%, figures much higher than in the control, non-surgical group [60]. Buchwald *et al.* reported a 57% remission in diabetics after AGB and an 80% remission after RYGB [42]. RYGB, SG and AGB have all been shown to be more effective at achieving glycaemic control than conventional drug therapy in randomised trials [63-66, 70]. These studies differ in the percentage of diabetics achieving remission, likely due to the variable definition of remission used. For example, the Buse

criteria defines remission as a HbA1c level under 6% and a fasting glucose level of under 100mg/dl [71], while the American Diabetes Association defines remission as a HbA1c level under 5.6% [72].

However, recurrence of diabetes has been reported at a rate of 19-35% 5 years [73, 74] and 50% 10 years following surgery [60]. Remission and recurrence rates appear to correlate with preoperative duration of diabetes and the level of glycaemic control [73, 74]. Preoperative BMI did not predict diabetes remission [75] and improvements in diabetes are often independent of weight loss [76]. In fact, preliminary data has suggested bariatric surgery is effective at treating type 2 diabetes in individuals with a BMI 35 or under [77, 78]. Additionally, bariatric surgery also improves renal function and prevents or delays end-organ diabetic complications such as nephropathy and retinopathy [79].

1.2.2.3 Other outcomes

Bariatric surgery has other health benefits beyond weight loss and diabetes remission. Epidemiological data has shown that RYGB, SG and to lesser degree AGB resolves hypertension [80-82]. Remission of dyslipidemia, characterised by high levels of low-density lipoprotein (LDL) and triglycerides and low levels of high-density lipoproteins (HDL), has been reported in almost 70% of RYGB patients [83]. An increase in HDL and decrease in triglycerides levels have also been shown following bariatric surgery in randomised trials [66, 84]. As diabetes, hypertension and dyslipidemia are all risk factors of cardiovascular disease, it is not surprising that their remission following bariatric surgery leads to improved cardiac health. The SOS study reported fewer cardiovascular events and deaths in the surgical compared to the non-surgical group [62]. Other studies have also found reduced cardiovascular risks and mortality [85-87]. Another study reported that the metabolic syndrome was presented preoperatively by 87% of bariatric patients. Less than 4 years following RYGB the metabolic syndrome was only present in 29% of patients. In comparison prevalence of the metabolic syndrome in non-surgical patients only decreased from 85% to 75% over the same period [88]. Bariatric surgery also resolves obstructive sleep apnea in patients with the condition

preoperatively [89]. Cancer events, cancer risk and mortality all decrease following surgery, particularly in women [61, 90, 91]. Overall, all-cause mortality is also reduced between 24-89% in surgical patients compared to non-surgical controls [61, 86, 87]. Bariatric surgery also improves quality of life [92] and is cost-effective long-term based on both direct and indirect savings [93].

1.2.3 Mechanisms

Bariatric surgery is often referred to as metabolic surgery in acknowledgments of its multiple beneficial results with regards to overall health. The mechanistic elements behind this process are multi-factorial and likely intertwined [94, 95]. They can be broadly summarised as the BRAVE effects - bile flow alteration, reduction of gastric size, anatomical gut rearrangement and altered flow of nutrients, vagal manipulation and enteric gut hormone modulation with the associated modulation of the gut microbiome [96].

1.2.3.1 Gastric restriction

It was initially thought that the beneficial results of bariatric surgery were in large part due to a reduction in gastric size and malabsorption in procedures that include intestinal bypass. However, the evidence supporting the notion that the volume of the gastric pouch or sleeve influences weight loss is inconsistent [95]. Gastric emptying appears to have a bigger role following surgery with the rapid delivery of nutrients into the gut initiating a neurohormonal cascade reducing hunger and ameliorating glycaemic mismanagement. Counter-intuitively gastric emptying is faster in SG than RYGB [97], but in RYGB nutrients bypass the duodenum and enter the distal small intestine faster than usual. In AGB, patients reach satiation faster when the band is optimally adjusted compared to when the band in partially or completely deflated, suggesting AGB does not restrict meal size but reduces hunger [98, 99]. The contribution of malabsorption has also been dismissed [94]. As such it appears the perception of bariatric surgery as malabsorptive and/or restrictive procedures is outdated and it's metabolic changes that drive the mechanisms underlying the surgeries.

1.2.3.2 Food appetite and preference

The failure of dietary interventions in sustaining long-term weight loss has been attributed to an evolutionary compensatory programming that attempts to maintain energy homeostasis [100]. Patients attempting to restrict calorie intake often report increase in appetite [101]. In contrast bariatric patients report less hunger and reach satiation quicker [98, 102]. RYGB patients also develop distaste for food high in fat or sugar [103, 104], as do rats in an animal RYGB and SG models [105, 106]. In fact, some RYGB patients report nauseousness and abdominal pain after eating food high in sugar or fat, a phenomenon referred to as dumping syndrome [107]. Neuroimaging has also demonstrated decreased activation of brain reward areas in response to eating or seeing calorific food [108, 109]. The underlying mechanisms behind these changes in appetite and food preference are still not fully understood but there have been some suggestions that changes in gut hormones could play a role.

1.2.3.3 Gut hormones

There is increasing evidence that bariatric surgery modifies hormonal gut-brain signalling. Preserving the vagus nerve, which links the brain stem to the abdomen, leads to greater and more sustained loss in animal RYGB models [110] and inflating the AGB in rodents stimulates vagal afferents [111]. Peptide YY (PYY) and glucagon-like peptide-1 (GLP-1) are gut hormones secreted by the L cells of the small bowel after a meal and act on the vagus nerve. PPY signals satiety, decreases food intake, increases energy expenditure and slows gastric emptying [112]. GLP-1 plays a similar role to PYY but also inhibits glucagon release and promotes pancreatic insulin secretion. This is known as the incretin effect. The postprandial levels of both in RYGB and SG patients are increased within days and in the case of RYGB remain high for at least 10 years postoperatively. PPY and GLP-1 are not increased following AGB or dietary therapy and inhibiting PPY increases food intake following RYGB but not AGB. It has been suggested that the bypass of the small intestine in RYGB and the rapid gastric emptying in SG could be the reason for the increase in gut hormone levels. Blocking a GLP-1 receptor during a meal test decreases glucose tolerance. A third gut hormone, Ghrelin, is also

thought to contribute to the effects of bariatric surgery. Ghrelin is secreted during fasting by the stomach and acts to increase food intake. Levels are decreased following SG and RYGB, although its increase has also been reported following RYGB [113-115].

1.2.3.4 Hindgut and foregut theories

Gut hormones have a central role in the hindgut mechanism behind diabetes resolution, which theorises that the direct entry of nutrients into the distal gut following bariatric surgery increases secretion of PPY and GLP-1. The foregut mechanism theorises that the bypass of the proximal small intestine prevents the release of, as of yet, undiscovered 'anti-incretin' agents resulting in an anti-diabetic effect [116]. A study involving the bypass of the duodenum in Goto-Kakizaki rats demonstrated improved glycaemic control when compared to sham operated rats, independent of weight loss [117]. A similar study in mice resulted in increased intestinal gluconeogenesis, increased glucose levels in the portal vein and enhanced glucose sensing. This led to improved glucose tolerance when compared to AGB mice [118]. However, mice deficient in glucose-transporter-2 (GLUT2) did not improve glucose tolerance following duodenal bypass. Neither did mice with impaired portal-vein signalling, suggesting intestinal gluconeogenesis improves glucose tolerance in a GLUT2-dependent hepatoportal sensory pathway [118]. Recently, it has also been shown that the exposure of the Roux limb to undigested nutrients leads to a reprogramming of intestinal glucose metabolism, increasing aerobic glycolysis and glucose uptake through glucose-transporter-1 (GLUT1), rendering the intestine a major user of glucose, improving glycaemic control in the process [119]. Duodenal-jejunal exclusion also leads to glycaemic improvements in humans [120]. This has led to the development of the EndoBarrier, an impermeable duodenojejunal plastic sleeve. Preliminary data is promising, indicating the EndoBarrier improves glycaemic control by decreasing HbA1c and increasing insulin sensitivity [121].

1.2.3.5 Bile

Bile acids are synthesised in the liver from cholesterol or oxysterols and can regulate food intake, energy expenditure and glucose metabolism by acting on the bile acid receptors Farnesoid X receptor and TGR5 in the liver and intestine [122, 123]. Fasting and postprandial bile acid levels are increased in circulation following RYGB [124, 125], with an accompanied decrease in conjugated bile acids [126]. These negatively correlate with postprandial glucose concentrations [124]. Patients who demonstrated remission of diabetes following RYGB had larger increases in bile acids than patients who failed to achieve remission or non-diabetics [127]. Recently plasma bile levels have also been shown to be increased in a mouse VSG model with associated changes in gut microbiota. Knocking-out FXR attenuates weight loss and improvements in glucose tolerance [128], suggesting bile acids have an important role in promoting the beneficial results of bariatric surgery.

1.2.3.6 Gut microbiota

The role of gut bacterial composition in obesity is being increasingly recognised. Gut microbial composition differ between lean and obese individuals and the colonisation of certain bacteria that have an increased ability to harvest energy alters host metabolism and promotes obesity [129]. RYGB shifts gut microbiota in humans and rodents [130-132], and the transfer of bacteria from the gut of RYGB mice to the gut of un-operated, germ-free mice led to weight loss in the later [133]. This suggests that altered gut microbiota contributes to the beneficial bariatric phenotype and is not merely a consequence of surgery.

1.2.3.7 Energy expediture

Bariatric surgery also modifies the way the body expends energy. Whereas energy expended during rest is either reduced or stable after bariatric surgery [95], postprandial energy expenditure is increased following RYGB [134, 135].

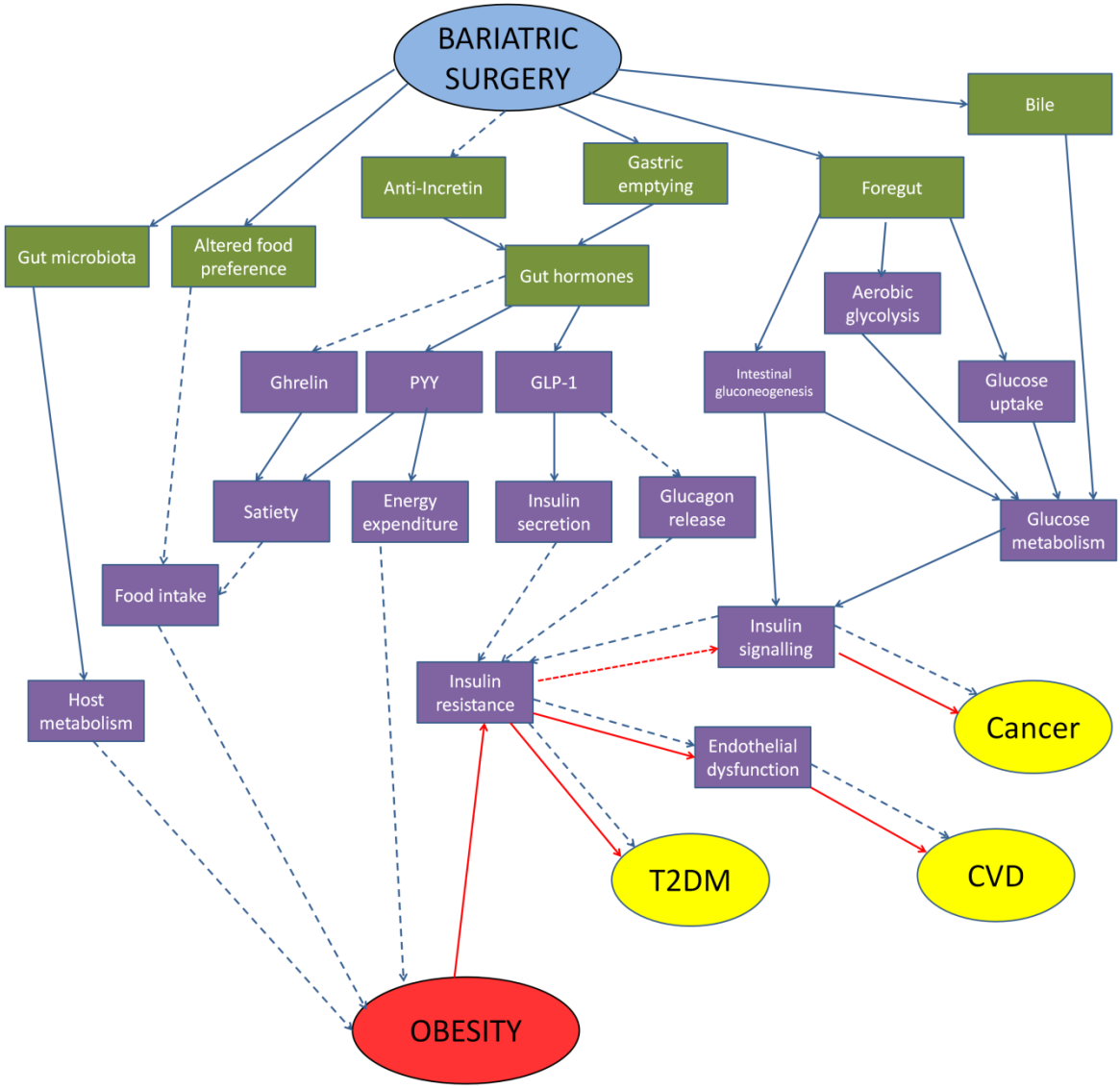

Figure 1.2: Mechanisms of obesity co-morbidities and the beneficial effects following bariatric surgery.

Red lines represent mechanisms of obesity. Blue lines represent mechanisms following bariatric surgery. Solid lines indicate improvement, dashed lines indicate impairment.

1.3 MicroRNAs

MicroRNAs (miRNA) are a family of endogenous, non-coding RNAs that regulate gene expression at the post-transcriptional level. These evolutionally conserved super-regulators bind to target messenger RNA (mRNA) silencing their translation to protein. Since their discovery in the nematode *Caenorhabditis elegans* (*C. elegans*) in 1993 [136], thousands of miRNAs have been identified across organisms. The mirBASE database lists almost 2,600 mature miRNA sequences in humans [137].

Biogenesis of the archetypical microRNA is a multi-step process which is initiated by the transcription of primary miRNA (pri-miRNA) from introns or intergenic transcripts by RNA polymerase II/III [138]. Pri-miRNA is then cleaved into an 80-100 nucleotide hairpin structure called precursor miRNA (pre-miRNA) by a nuclear microprocessor composed of the RNA endonuclease Drosha and the RNA-binding protein DGCR8. Pre-miRNAs are exported from the nucleus into the cytoplasm by exportin 5 and undergo further processing by a second endonuclease, Dicer, into mature, double stranded miRNAs 18-22 nucleotides in length [139]. The knock-out of Dicer [140] and DGCR8 [141] in mice results in defective embryonic development, indicating microRNAs are essential for mammalian development.

One strand of the mature miRNA is then loaded into an RNA-induced silencing complex (RISC), a multi-protein complex at the heart of which lies a member of the Argonaute protein subfamily. RISC directs the seed region (nucleotides 2-7) of miRNA into binding to 3' UTR (untranslated region) of its target mRNA, although there is evidence to suggest that microRNAs can also bind to other regions of a target mRNA. Perfect, complementary hybridisation leads to cleavage of the mRNA by RISC. Imperfect binding leads to an inhibition of translation and mRNA degradation [142, 143]. This allows each miRNA to target multiple mRNAs and each mRNA to be targeted by multiple microRNAs. Distinct microRNAs can also share targets, regulating certain genes in unison. MicroRNAs therefore form a complex layer of post-transcriptional regulation, controlling the expression of over half the human transcriptome [144].

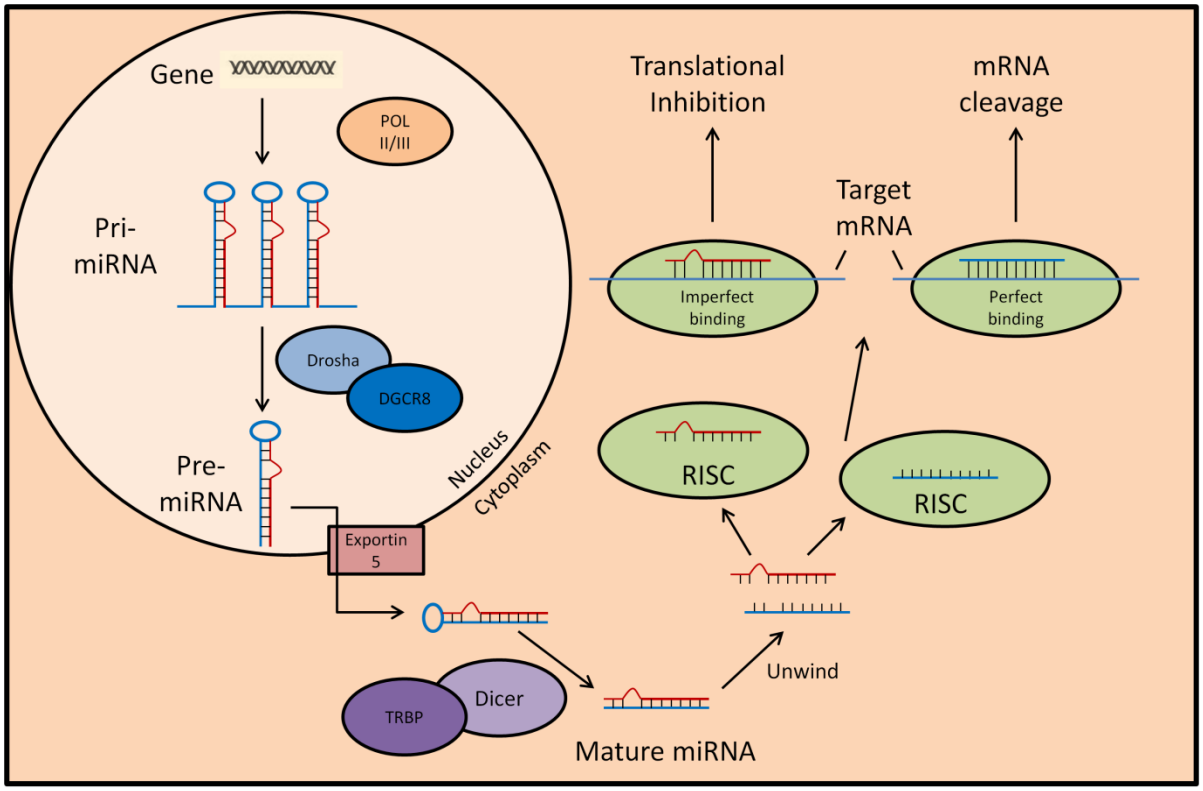

Figure 1.3: MicroRNA biogenesis and function.

However, the concept of microRNAs as purely negatively regulators of translation has recently been challenged. MicroRNAs can switch between repressing and activating translation under certain conditions such as cell cycle arrest [145]. During amino acid starvation the microRNA miR 10a can also interact with 5' UTR of mRNAs encoding for ribosomal protein increasing their translation and global protein synthesis in the process [146]. Another study has also shown that miR 328 can indirectly increase translation by binding to an mRNA translational regulator independent of its seed sequence [147]. As such it would appear that microRNAs do not simply silence but fine-tune gene expression.

1.3.1 MicroRNAs, obesity and the metabolic syndrome

Given their comprehensive role in gene regulation it is not surprising that microRNAs are involved in processes fundamental to both normal physiology and disease. MicroRNAs regulate cell proliferation, cell signalling and apoptosis [148] and have been widely implicated in a range of disorders including cancer [149], cardiovascular disease [150] and neurological disorders [151]. This has led to interest in microRNAs as potential novel therapeutics [152].

The evidence linking miRNAs to obesity is vast and is summarised in Table 1.2. The dysregulation of microRNAs has been linked to virtually every process involved in the progression and complications of obesity, diabetes and the metabolic syndrome. The roles of microRNAs in adipogenesis, insulin secretion and resistance and lipid metabolism is particularly extensive [153].

1.3.1.1 Adipogenesis

Adipocytes are a primary source of free fatty acid storage and release during consumption and fasting and are responsible for the synthesis of leptin. A number of studies have shown that microRNA expression profiles differ between obese and lean white adipose tissue in mice and humans, both in diabetics and non-diabetics, the preeminent of which is miR 221. Multiple microRNAs also have reported involvement both in the promotion and inhibition of adipogensis [154]. MiR 146b is upregulated during differentiation of the mouse adipocyte cell line 3T3-L1 [155]. Another microRNA that regulates adipose differentiation is miR 143, which reportedly inhibits adipogenesis in the earlier clonal stage and promotes adipogenesis in the later terminal stages [156]. Both miR 26a and miR 196a promote brown adipocyte differentiation while miR 21 is differentially expressed in white adipose tissue [157-159]. Inhibitors of adipogenesis include miR 27, which targets brown adipose tissue transcription factors [160]. Another inhibitor of brown adipose tissue adipogenesis is miR 155 [161]. MiR 540 also inhibits adipogenesis by binding the 3'UTR of PPARγ [162].

1.3.1.2 Insulin secretion and resistance

Poy *et al.* were the first to link microRNAs with diabetes when they demonstrated the key regulatory role of miR 375 in insulin secretion [163]. MiR 375 is now known to be essential for maintaining pancreatic α and β-cell function and glycaemic control as its knockout results in hyperglycaemia and glucose intolerance [164]. Since then more microRNAs have demonstrated regulatory roles in pancreatic β-cell development, insulin secretion and resistance. MicroRNAs 126 and 193b are downregulated in subcutaneous adipose tissue of obese individuals. Both inhibit CCL2, a cytokine release during obesity induced inflammation, and as such guard against the development of insulin resistance [165]. On the other hand, miR 221 is upregulated in subcutaneous adipose tissue and promotes insulin resistance, reportedly by targeting ADIPOR1, a receptor for adiponectin [166]. MiR 130a-3p improves glucose homeostasis by targeting the growth factor receptor bound protein GRB10 [167]. High levels of miR 802 are linked with glucose intolerance and insulin resistance [168], whereas the overexpression of miR 26a improves insulin sensitivity [169]. MiR 93, a regulator of the glucose transporter GLUT4, is upregulated in patients with polycystic ovary syndrome, which is associated with insulin resistance [170]. MicroRNAs have also been shown to have regulatory roles in other diabetic complications including diabetic nephropathy and diabetic cardiomyopathy [171].

1.3.1.3 Lipid metabolism

The most abundant microRNA in the liver is miR 22, which regulates cholesterol and fatty acid metabolism. Blocking miR 122 in mice on both normal and high-fat diets inhibits fatty-acid and cholesterol synthesis in the liver and decreases plasma triglycerides levels [172]. MiR 27b also regulates lipid metabolism through its target PPARγ. Plasma levels of miR 27b correlates strongly with hyperlipidemia [173]. MiR 33 is another key regulator of lipid and cholesterol homeostasis. MiR 33 targets various members of the cholesterol synthesis and transport pathway, increasing intracellular cholesterol concentrations. MiR 33 also raises intracellular lipid concentrations by regulating fatty acid oxidation and insulin signalling [174, 175]. In fact, blocking miR 33 reduces hyperlipidemia in mouse models [176]. Inhibiting miR 33 also improves lipid metabolism in primates

[177], solidifying miR 33's candidacy as an attractive therapeutic target against lipid metabolism dysfunction.

Table 1.2: MicroRNAs associated with the metabolic syndrome.

	MicroRNA		References
Process	**Up**	**Down**	
Adipogenesis	146b	27	[154-162]
	143	155	
	26a	540	
	196a		
	21		
β-cell development and Insulin Secretion	375	221	[163-171]
	126	802	
	193b	93	
	26a		
	130a		
Diabetic Nephropathy	192	192	[178-187]
	200	200	
	377	29	
	21	215	
Diabetic Cardiomyopathy	21	29	[188-191]
	206	30	
	1		
Lipid Metabolism		122	[172-177]
		27b	
		33	

1.3.2 MicroRNAs as biomarkers

MicroRNA expression profiles offer a wealth of biological information, as the changes in the regulation of several core physiological processes can be seen in the expression of a few microRNAs that regulate them. MicroRNAs are relatively abundant and stable in tissue and biofluids are able to withstand numerous freeze-thaw cycles allowing for long-term storage [192]. They can also be measured with speed, ease and sensitivity through a number of platforms including quantitative Polymerase Chain Reaction (PCR), next generation deep sequencing and microarray hybridisation [193, 194]. As a result microRNAs have become the focus of rigorous research over the past decade and their expression profiles have been used to map species development and tissue differentiation [195, 196] and can predict type, origin and prognosis of cancer [197-201].

Their expression in extracellular biofluids is of particular interest given the potential of novel non- or minimally invasive biomarkers. Extracellular microRNAs are packaged in membrane-covered exosomes or are present in complexes with high-density lipoproteins or argonaute protein protecting them from ribonuclease degradation, and circulating miRNAs can be taken up in active form by recipient cells, suggesting a potential hormonal tissue-to-tissue communicative role [202-204]. Circulating miRNAs have been proposed as potential novel biomarkers of cancer [192], cardiovascular disease [205] and tissue injury [206]. Distinct obese and diabetic circulating microRNA profiles have also recently been characterised. The metabolic syndrome is characterised by the deregulation of 7 circulating miRNAs [207] and a number of miRNAs have been put forward as candidate biomarkers of obesity including miR 15a, miR 142-3p and miR 221 in men [208] and miR 28-3p and miR 130b in children [209]. Similarly, microRNAs, including miR 192 and miR 125b, have been proposed as circulating biomarkers of T2DM [210]. Urinary microRNAs have also been reported markers of disease including type 1 diabetes-induced nephropathy [211], bladder cancer [212] and drug-induced nephrotoxicity [213].

1.4 Hypothesis

MicroRNAs are biomarkers of the beneficial effects of bariatric surgery.

The premise of this thesis is that bariatric surgery modulates the expression of microRNAs in extracellular biofluids and this can in turn explain some of the beneficial effects of these operations. A bariatric circulating microRNA signature has recently been characterised in a rat bariatric model and the downregulation of miR 122, a key player in lipid and glucose metabolism, was found [214]. MiR 122 has also been reported to be downregulated in human circulation following RYGB [208]. However, this is the extent of the published work with regards to role of microRNAs in bariatric surgery. To investigate this hypothesis studies were conducted assessing:

1. Urinary and circulating microRNAs associated with obesity
2. Urinary microRNA biomarkers after bariatric surgery2
3. Circulating microRNA biomarkers after bariatric surgery

All urinary and circulating microRNAs assessed at the obesity baseline were assessed in the subsequent bariatric studies.

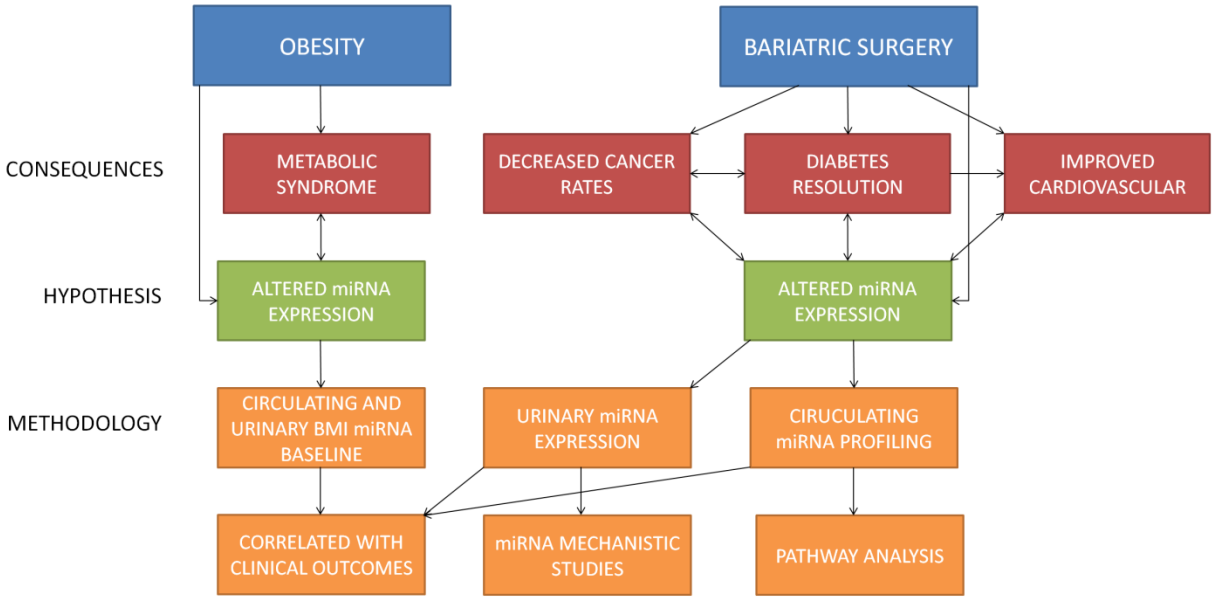

Figure 1.4: A flow chart outlining the structure of this thesis.

2 Circulating and urinary microRNAs in obesity

2.1 Justification

Circulating and urinary microRNAs are reported biomarkers for obesity and diabetes [208, 210]. The objectives of this chapter were to establish a microRNA obesity baseline in serum and urine, anchoring the phenotypic setting for subsequent bariatric chapters, to correlate microRNA levels with standard clinical blood biochemistry markers, and to potentially identify novel microRNA biomarkers of obesity.

2.2 Aims

1. To establish an obesity microRNA baseline in serum and urine
2. To correlate microRNA expression with clinical parameters
3. To identify circulating and/or urinary obesity microRNA biomarkers

2.3 Study design

Samples were collected from 47 volunteers in collaboration with Prof. Stephen Atkin at the University of Hull under ethics approval 09/H1304/46 with the informed consent of each participant. Individuals in this dataset had BMIs ranging from 19 to 47 and were stratified into 5 BMI groups, 9 to 11 each in the under 25, 25-30, 30-35 and 35-40 BMI groups and 7 in the over 40 BMI group. Table 2.1 provides a study summary. Participants donated serum and urine samples and were subject to a blood biochemistry profile, the complete results of which are summarised in Table 2.1. RNA was obtained from all samples and the expression levels of 8 microRNAs were determined in serum and 3 microRNAs in urine using quantitative PCR. These microRNAs were chosen for three reasons; (a) due to their reported association with the metabolic syndrome, (b) due to their known presence in circulation/urine and (c) because they have been previously identified to be deregulated in obesity and its co-morbidities (Table 2.2). Figure 2.1 is a flowchart outlining Chapter 2's study design.

Table 2.1: Study summary and blood biochemistry [ǂ].						
	BMI					
	Total	Under 25	25-30	30-35	35-40	Over 40
n	47	10	11	9	10	7
BMI (kg/m^2)	31.9 (7.59)	22.0 (1.68)	27.2 (1.34)	32.4 (1.34)	37 (1.23)	44.4 (2.15)
Weight (kg)	90.1 (23.3)	63.3 (11.4)	76.7 (6.82)	99 (11.1)	104.4 (11.4)	125.1 (10.5)
Age	48.2 (16)	39.2 (16.4)	42.4 (16.3)	51.2 (12.7)	56 (16)	55.4 (11.9)
% female	57.4	80	50	50	60	42.9
Fasting glucose (mmol/L)	5.69 (1.92)	4.63 (0.31)	5.97 (2.85)	5.9 (1.61)	5.04 (0.4)	7.12 (2.46)
Insulin (µIU/mL)	14.5 (13.4)	3.65 (1.1)	7.11 (4.87)	22.4 (17.3)	21.3 (10.6)	20.5 (14.1)
CRP (mg/L)	2.85 (2.76)	1.92 (2.1)	1.37 (1.8)	2.68 (2.77)	4.28 (3.05)	4.62 (3.44)
Hb (g/L)	13.8 (1.37)	13.4 (1.17)	13.9 (1.63)	14 (1.29)	13.4 (1.44)	14.5 (1.52)
WCC (x10^9/L)	5.86 (1.43)	5.63 (1.62)	5.54 (0.99)	6.11 (2.04)	6.22 (1.04)	5.94 (1.45)
Platelet Count (x10^9/L)	234.5 (59.3)	239 (47.9)	219 (52.3)	237 (90)	263 (32.9)	218 (61)
Sodium (mmol/L)	139 (1.67)	138 (1.63)	140 (1.51)	139 (1.77)	140 (1.1)	139 (2.07)
Potassium (mmol/L)	4.27 (0.33)	4.2 (0.29)	4.26 (0.3)	4.23 (0.39)	4.4 (0.43)	4.34 (0.3)
Chloride (mmol/L)	104.5 (2.57)	104 (2.43)	106 (1.51)	104 (2.37)	106 (3.46)	104 (2.95)
BiCarb (mmol/L)	27.3 (2.42)	27.6 (2.57)	27.6 (1.81)	27.7 (1.25)	27.2 (1.92)	26 (4.53)
Urea (mmol/L)	4.89 (1.42)	4.84 (1.91)	4.47 (1.16)	4.56 (1.15)	4.98 (1.81)	5.94 (0.66)
Creatinine (umol/L)	75.3 (17.8)	74.4 (17)	74.1 (10.4)	75.3 (18.6)	80 (27.9)	73.4 (21.3)
eGFR (mL/min)	81.8 (10.4)	79.4 (11.2)	85.7 (4.08)	82.4 (9.18)	80 (18.7)	81.2 (10.8)
Calcium (mmol/L)	2.31 (0.08)	2.34 (0.09)	2.28 (0.06)	2.33 (0.07)	2.34 (0.08)	2.29 (0.13)
Phospate (mmol/L)	1.19 (0.19)	1.32 (0.14)	1.22 (0.13)	1.21 (0.23)	1 (0.18)	1.15 (0.13)
Bilirubin (umol/L)	15.3 (5.41)	17.1 (6.82)	15.4 (3.87)	16.3 (7.61)	12.8 (3.03)	13.4 (3.37)
Alk Phos (iu/L)	57.5 (19.3)	44.1 (7.48)	51.9 (14)	56.6 (21.3)	79.6 (24.3)	63.6 (11.2)
Albumin (g/L)	40.4 (2.85)	42.1 (3.44)	38.7 (1.89)	42 (2.08)	40.2 (1.48)	38.4 (3.05)
Total protein (g/L)	67.7 (4.85)	67.4 (4.54)	64.4 (5.68)	68.6 (3.69)	71.4 (2.51)	67.8 (5.72)
Cholestrol (mmol/L)	4.6 (1.07)	4.58 (0.88)	4.64 (1.18)	4.83 (1.24)	4.23 (1.57)	4.37 (0.3)
Triglycerides (mmol/L)	1.72 (1.14)	0.74 (0.21)	1.38 (0.29)	1.76 (1.39)	2.05 (0.76)	2.97 (1.35)
HDL (mmol/L)	1.24 (0.49)	1.80 (0.75)	1.17 (0.23)	1.14 (0.42)	1.12 (0.31)	0.94 (0.13)
LDL (mmol/L)	2.57 (0.86)	2.6 (0.33)	2.84 (1.06)	2.89 (0.79)	2.18 (1.16)	2.08 (0.72)
L-Tyr (µM)	73.7 (18.4)	67.4 (19.9)	67.9 (16.2)	78.7 (16.7)	77.3 (27.2)	76.7 (15.1)
L-Phe (µM)	78.2 (12.6)	77.3 (14.1)	76.3 (19.9)	79 (8.73)	79.2 (8.56)	79.4 (13.7)
L-Phe : L-Tyr Ratio	1.1 (0.22)	1.2 (0.27)	1.12 (0.13)	1.04 (0.23)	1.11 (0.33)	1.04 (0.05)
GLP-1 (pM)	29 (13.6)	21.7 (7.65)	21.6 (10.1)	30.1 (12)	34.1 (16.1)	38.1 (17.9)
GIP (pg/mL)	78.7 (33.1)	58.9 (26.6)	81.5 (28.5)	90.6 (42.2)	69.5 (29)	89.7 (29.7)

[ǂ]Values represent mean unless otherwise stated. Standard deviation in parentheses.

Table 2.2: Targeted microRNAs and their involvement in obesity and associated co-morbidities.			
MicroRNA	**Expression measured in**	**Involved in**	**References**
15a	Serum	Insulin biosynthesis	[208]
22-5p	Serum	Haematopoietic malignancies	[209, 210]
122	Serum	Cholesterol and fatty-acid metabolism	[184]
125b	Serum	Adipocyte differentiation	[211, 212]
142-3p	Serum	Diabetic cardiomyopathy	[213]
145-5p	Serum	Lipolysis	[214]
192	Serum and Urine	Diabetic nephropathy	[170, 173, 174]
200a	Urine	Diabetic nephropathy	[172, 215]
200b	Urine	Diabetic nephropathy	[172, 215]
221	Serum	Diabetes-associated CVD	[216]

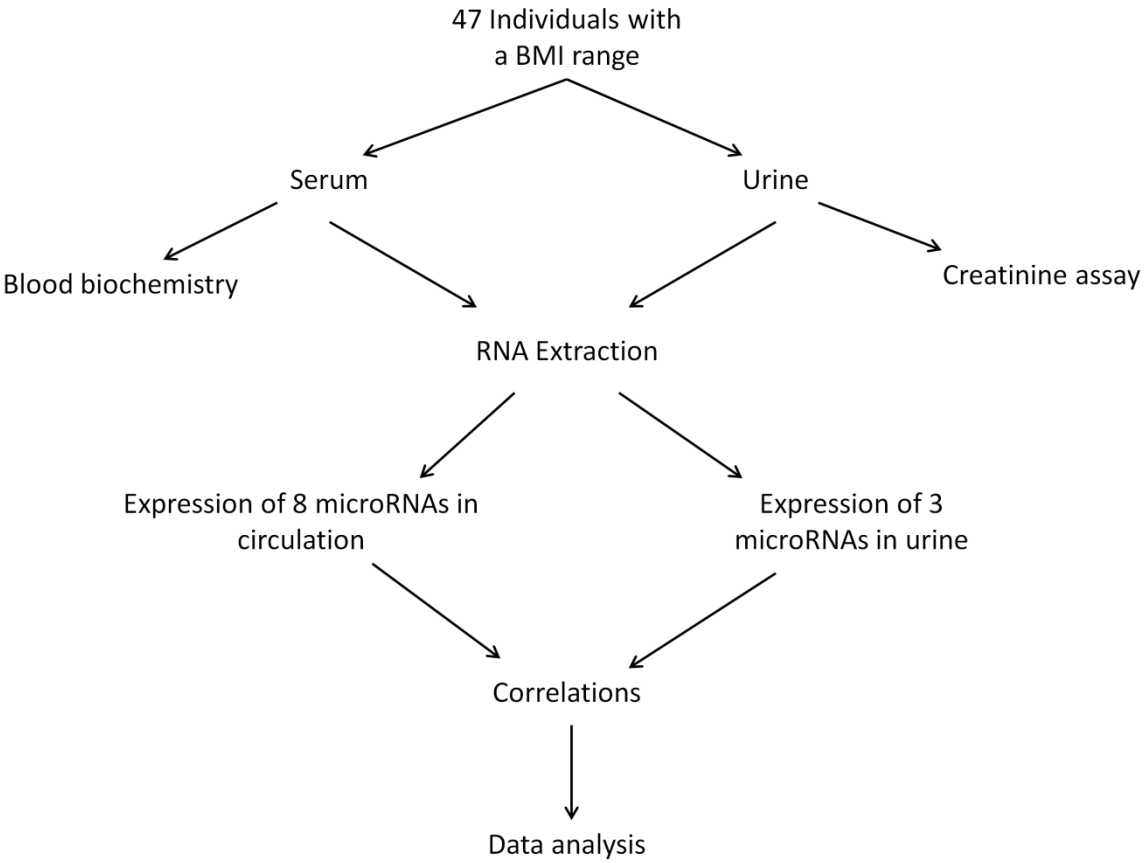

Figure 2.1: A flow chart illustrating the workflow of Chapter 2.

2.4 Materials and methods

2.4.1 Samples

Serum was obtained using standard venipuncture and centrifugation technique at the University of Hull. Urine samples were received neat in urine donation tubes and were filtered through a 0.2µm filter prior to analysis. All samples were aliquoted into 0.2ml and 0.5ml centrifuge tubes and stored in -80^{o}C until use. Clinical parameters, including BMI and blood biochemistry, were obtained in collaboration with the University of Hull.

2.4.2 Serum RNA extraction

RNA was extracted from serum using the *mir*Vana PARIS kit (Ambion, Paisley, UK). In this procedure an organic extraction is followed by immobilisation of RNA on glass-fibre filters to allow purification. The manufacturer's protocol was followed with slight modifications. Briefly, samples were thawed on ice and 100µl cell disruption buffer was added to 100µl of serum. Pre-warmed 200µl of denaturing solution was added and the mixture was incubated on ice for 10 minutes. Following denaturation 30 attomoles of synthetic *C. elegans* (cel.) microRNA 39 (Ambion) was spiked into the mixtures for normalisation purposes. *C. elegans* miR-39 was selected due to its lack of sequence homology with endogenous human microRNAs. The optimal concentration of cel. miR-39 spike-in was determined through method development on archived serum. Equal volume (400µl) of Acid-Phenol:Chloroform was then added and the mixture was vortexed and centrifuged at 10,000g for 5 minutes, separating RNA (upper aqueous phase) from DNA (lower phase) and protein (interphase). The aqueous upper phase was transferred to a fresh centrifuge tube and 1.25X 100% ethanol was added. Lysate/ethanol mixture was then loaded onto a silica filter cartridge placed within a centrifuge tube and centrifuged briefly at 1,000g for 30 seconds to immobilise total RNA. The flow-through was discarded and the filter was washed once with 700µl Wash Solution 1 and then twice with 500 µl Wash Solution 2/3 to purify RNA. RNA was then eluted in 100µl nuclease-free water preheated to 95^{o}C. RNA extracts were stored at -20^{o}C until use.

2.4.3 Urinary RNA extraction

RNA was extracted from urine samples using the *mir*Vana PARIS kit (Ambion). Extraction was as described in 2.4.2 for serum with a couple of modifications. RNA was extracted from 250µl of urine. To normalise 30 femtomoles of synthetic *C. elegans* miR-39 (Ambion) was spiked into urine samples following denaturing. The optimal concentration of cel. miR-39 spike-in was determined through method development on archived urine. As with serum RNA was eluted in 100µl nuclease free water and stored at -20^{o}C until use.

2.4.4 Polymerase Chain Reaction (PCR)

MicroRNA quantification in serum and urine was determined through reverse transcription PCR (RT-PCR) using TaqMan Small RNA assays (Applied Biosystems, Paisley, UK). This was a two-step process [215]:

1. RT Step – Small miRNA-specific, stem-loop RT primers hybridise to the 3' end of miRNA and are then reverse transcribed to produce complementary DNA (cDNA) through the enzymatic action of reverse transcriptase.
2. PCR Step – cDNA is amplified with the use of fluorescent microRNA probes, which anneal complementarily to specific targets. Each probe has a 6-carboxyfluorescein (FAM) fluorescent reporter dye and a non-fluorescent quencher. The quencher suppressors the reporter fluorescence when not bound. Once the probe hybridises to the target it is cleaved by DNA polymerase, separating the reporter dye from the quencher, resulting in increased fluorescence by the reporter. This only occurs following complimentary hybridisation, eliminating non-specific amplification. Fluorescence is captured real-time and corresponds to the amount of cDNA product amplified.

2.4.4.1 cDNA synthesis through reverse transcription

cDNA was synthesised from extracted RNA by reverse transcription (RT) through the reverse transcriptase enzyme contained in the TaqMan MicroRNA Reverse Transcription kit (Applied Biosystems). The manufacture's protocol was followed. A master mix was initially made consisting of deoxynucleotides (dNTPs), reverse transcriptase, 10X reverse transcriptase buffer, RNase Inhibitor and nuclease-free water as described in Table 2.3.

Table 2.3: RT Master Mix components

Component	Volume, per reaction (µl)
100mM dNTPs (with dTTP)	0.15
Reverse Transciptase 50 U/µl	1
10X Reverse Transcriptase Buffer	1.5
RNase Inhibitor, 20U/µl	0.19
Nuclease-free water	4.19
Total volume	7

Once created the master mix was manually mixed and 7µl was dispensed into a 0.2ml PCR polypropylene reaction tube per reaction. To this 5µl of RNA and 3 µl of the relevant 5X TaqMan microRNA RT primer was added to produce a 15µl RT reaction. Reaction tubes were loaded onto a MJ Research PTC-200 Thermo Cycler (GMI, Ramsey, MN, USA) and reactions were incubated at 16^{o}C for 30 minutes, then 42^{o}C for another 30 minutes, 85^{o}C for 5 minutes and finally 4^{o}C until the samples tubes were retrieved. cDNA products were stored at -20^{o}C until use.

2.4.4.2 Quantitative Polymerase Chain Reaction (qPCR)

cDNA product was amplified through qPCR using TaqMan Fast Universal Master Mix. A master mix was made consisting of 10µl of Universal PCR Master Mix, 1µl relevant 20X TaqMan microRNA PCR probe and 6µl nuclease-free water per reaction. Master mix was manually mixed and 17µl was dispensed into a 0.2ml PCR polypropylene reaction tube per reaction, to which 3µl of cDNA per reaction was added. The 20µl reaction mixture was then loaded into an assigned well of a 96-well PCR plate, which was sealed when fully loaded with optical film. The PCR plate was then centrifuged briefly before being run on Applied Biosystems 7500 Fast System PCR machine. The PCR reaction consisted of 95^{o}C for 10 minutes to activate the enzyme followed by 40 cycles of 95^{o}C for 15 seconds to denature and 60^{o}C for 60 seconds to anneal/extend. PCR reactions were run with three technical replicates and one no-template control reaction, with nuclease-free water replacing cDNA, to ensure the absence of contaminants.

2.4.4.3 Data analysis

A graphical representation of typical PCR amplification curves can be found in Figure 2.2. cDNA product is doubled with each reaction cycle for a total of 40 cycles and until the exhaustion of reaction reagents. A threshold of 0.2 ΔRn (Rn is the fluorescence of the reporter dye divided by the fluorescence of a passive reference dye) was arbitrarily set and this remained consistent for every PCR reaction. C_t (threshold cycle) was obtained for every reaction, measured as the point the threshold is met by the amplification curve.

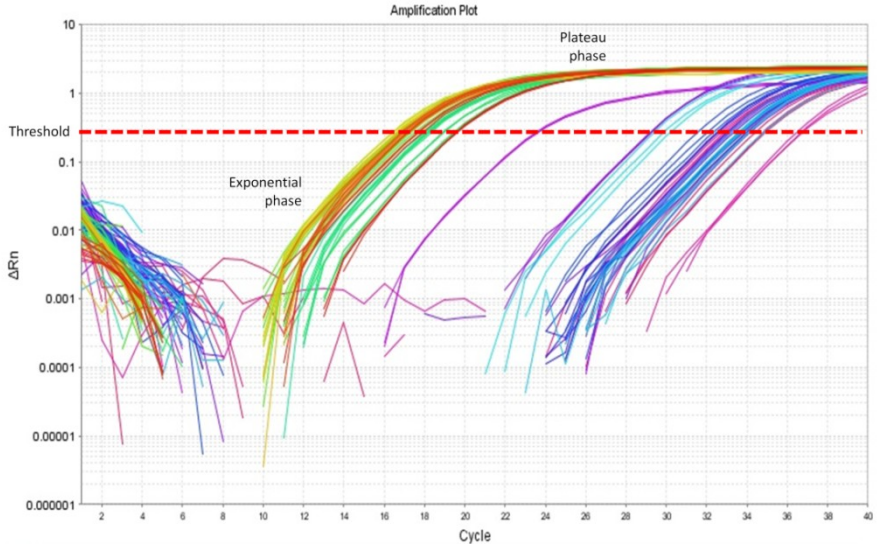

Figure 2.2: Typical PCR amplification curves.

Levels are detected during the exponential phase when a threshold is met.

PCR data was analysed through the $2^{-\Delta Ct}$ method, first described by Livak and Schmittgen [216]. In this method ΔC_t was calculated for each sample by subtracting the C_t of the reference microRNA (cel. miR-39) from the C_t of the target microRNA. ΔC_t was then linearised by log-transformation ($2^{-\Delta Ct}$). The mean was calculated within a biological group and fold change was calculated relative to a control group.

2.4.4.4 Normalisation

The purpose of normalisation is to minimise technical variation in data not related to biological changes. Accuracy of results and the validity of the interpretation that follows are largely dependent on accurate data normalisation. This is particularly important when assessing biofluids as yields following RNA extraction can be too low to accurately quantify using standard spectrophotometry techniques. The absence in the circulation of consistently stable reference microRNAs and small RNAs to normalise microRNA expression means there is no general consensus as to how to best normalise circulating microRNA data. Serum and urinary microRNA expression measured through TaqMan PCR was normalised to cel. miR-39 spike-in levels. Urinary microRNA expression was further normalised to creatinine to correct for diuretic effect.

2.4.5 Creatinine normalisation

Creatinine is a product of creatine and creatine phosphate metabolism in the muscle, which is sourced from the diet and through *de novo* synthesis from arginine, glycine and methionine in the kidney and liver [217, 218]. Creatinine production is non-enzymatic and irreversible. Under normal conditions creatinine diffuses into circulation and is excreted by the kidneys into urine at a relatively constant rate. In human, approximately 2% of creatine is converted to creatinine daily [217]. Therefore, urinary biomarkers including markers of kidney damage are frequently normalised to urinary creatinine, and serum creatinine is used to determine estimated glomerular filtration rate [219].

Urinary creatinine levels were determined using a creatinine assay kit (R&D Systems, Abingdon, UK). When treated with picric acid in an alkaline solution creatinine produces quantitatively an orange colour through the Jaffe reaction [220]. Briefly, creatinine standards (0-20mg/dl) were prepared by serial dilution and 50µl was dispensed into assigned wells of a 96 well plate. Urine samples were diluted 1 in 20 in nuclease-free water and dispensed into assigned wells and 100µl of alkaline picrate solution was added to each well. The plate was incubated at room temperature for 30 minutes. Absorbance was then read at 490nm. Urinary creatinine levels were determined using a standard curve.

2.4.6 Statistical analysis

PCR data is expressed as fold change relative to a control group. Data is represented as mean ± standard error of mean (SEM). Statistical significance was determined using one-way analysis of variance (ANOVA) with a linear trend and Student's t-test where appropriate. The relationship between microRNA expression and clinical parameters was determined by Pearson's correlation. Significance was considered as $p<0.05$. Statistical analysis was performed using GraphPad Prism (La Jolla, CA, USA).

2.5 Results

2.5.1 Method optimisation

Synthetic C. elegans microRNA 39 was spiked into all samples during RNA extraction to act as an internal standard, necessitated by the lack of a stable, endogenous microRNA in biofluids. Optimal cel. mIR 39 spike-in concentration was determined by method development on archived serum and urine samples. In serum, 30 femtomole of cel. miR-39 was initially spiked in, which corresponded to a raw C_t value of 16-18, whereas endogenous, circulating miR 122 and miR 223 C_t levels came in between 23 and 32 (Figure 2.3A). Spike in concentration was then decreased to 30 attomole, which corresponded to a more comparable miR 122 and miR 223 raw C_t value of 23-25 (Figure 2.3B). It was therefore determined that 30 attomole was the optimal cel. miR-39 spike in level in serum.

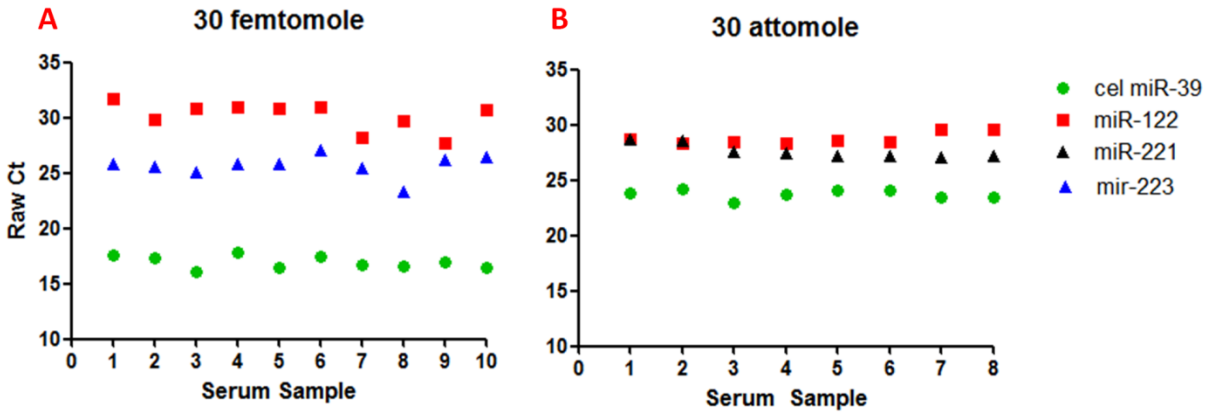

Figure 2.3: Optimal serum cel. miR-39 spike-in.

Raw Ct values as determined by qPCR of miR-122, miR-221, miR-223 and spiked in cel. miR-39 in archived serum samples**.** (A) cel miR-39 spike in level of 30 femtomoles. (B) cel. miR-39 spike in level of 30 attomoles.

Thirty attomole of cel. miR-39 resulted in inconsistent and variable expression levels of both target microRNAs and cel. miR-39 in urine (Figure 4A). A fivefold increase to 150 attomole resulted in similar inconsistency (Figure 4B). A further increase to 30 femtomole produced consistent and reproducible expression (Figure 4C). At higher concentrations cel. miR-39 appears to act as an RNA carrier, required due to the scarcity of endogenous microRNA in urine. Indeed, subsequent to this study Exiqon's commercially available microRNA extraction kit specific to biofluids was released and recommends the use of a bacterial plasmid as an RNA carrier [221]. In urinary RNA extraction optimised here cel. miR-39 appears to act both as an internal standard and an RNA carrier. It was therefore determined that 30 femtomole was the optimal cel. miR-39 spike in level in urine.

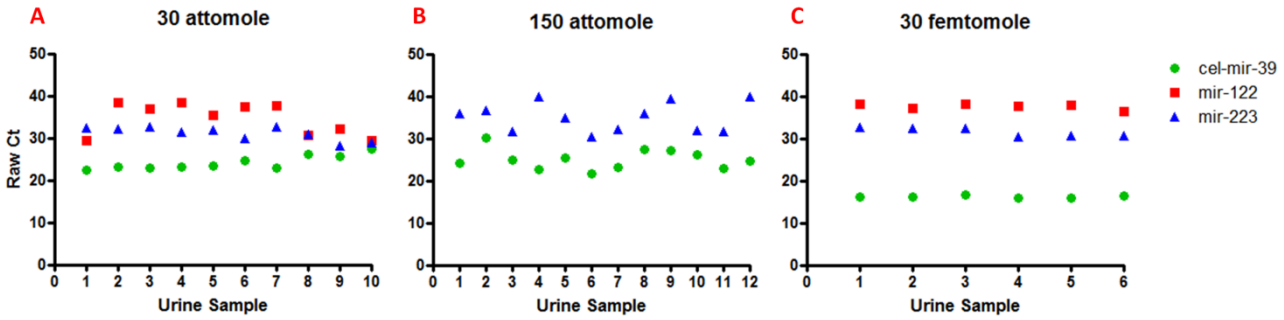

Figure 2.4: Optimal urinary cel. miR-39 spike-in.

Raw Ct values as determined by qPCR of miR 122, miR 223 and spiked in cel. miR 39 in archived urine samples. (A) cel miR 39 spike in level of 30 attomoles. (B) cel. miR 39 spike in level of 150 attomoles. (C) cel miR 39 spike in level of 30 femtomoles.

2.5.2 Creatinine normalisation

To correct for diuretic effect, all urinary microRNAs were normalised to urinary creatinine. There was no difference in mean urinary creatinine levels across the 5 BMI groups (Figure 2.5A) and no correlation was observed between creatinine and BMI (Figure 2.5B, r=-0.14, p=0.35, Pearson correlation). These findings confirm the suitability of creatinine as an internal urinary standard and all urinary microRNA expression data in this report are shown relative to urinary creatinine concentration.

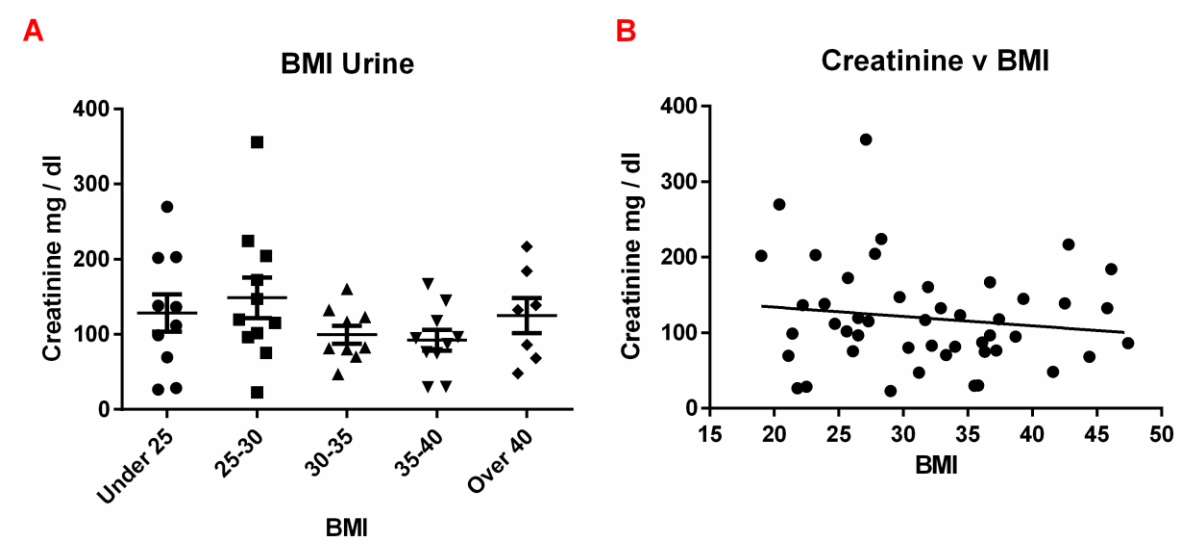

Figure 2.5: Urinary creatinine levels versus BMI.

(A) Urinary creatinine levels across 5 BMI groups. Data represents mean ± SEM. n=7-10 for BMI urine. (B) Pearson correlation between creatinine and BMI. n=47

2.5.3 Serum microRNA

The circulating levels of 8 microRNAs were measured in serum – miR 15a, miR 22-5p, miR 122, miR 125b, miR 142-3p, miR 145-5p, miR 192 and miR 221. These levels were correlated with BMI and clinical results from a standard blood biochemical profile.

2.5.3.1 miR 22-5p

A negative correlation was observed between miR 22-5p and BMI. Relative to levels in healthy individuals with a BMI under 25, levels of miR 22-5p remained virtually unchanged (0.99 fold) in individuals with a BMI between 25-30, but then miR 22-5p expression decreased with increasing BMI. Levels decreased 0.78 fold in individuals with a BMI between 30-35, decreased significantly 0.31 fold in individuals with a BMI between 35-40 and decreased 0.27 fold in morbidly obese individuals with a BMI over 40 (Figure 2.6A, p values 0.97, 0.58, 0.031 and 0.089 respectively, Student's t-test). The negative linear trend between miR 22-5p and increasing BMI was significant ($p=0.0107$, one-way ANOVA) and a statistically negative correlation was found between circulating levels of miR 22-5p and BMI (Figure 2.6B, $r=-0.41$, $p=0.0109$, Pearson correlation). Unsurprisingly, a similar correlation was found between miR 22-5p and weight (Figure 2.6C, $r=-0.46$, $p=0.0037$, Pearson).

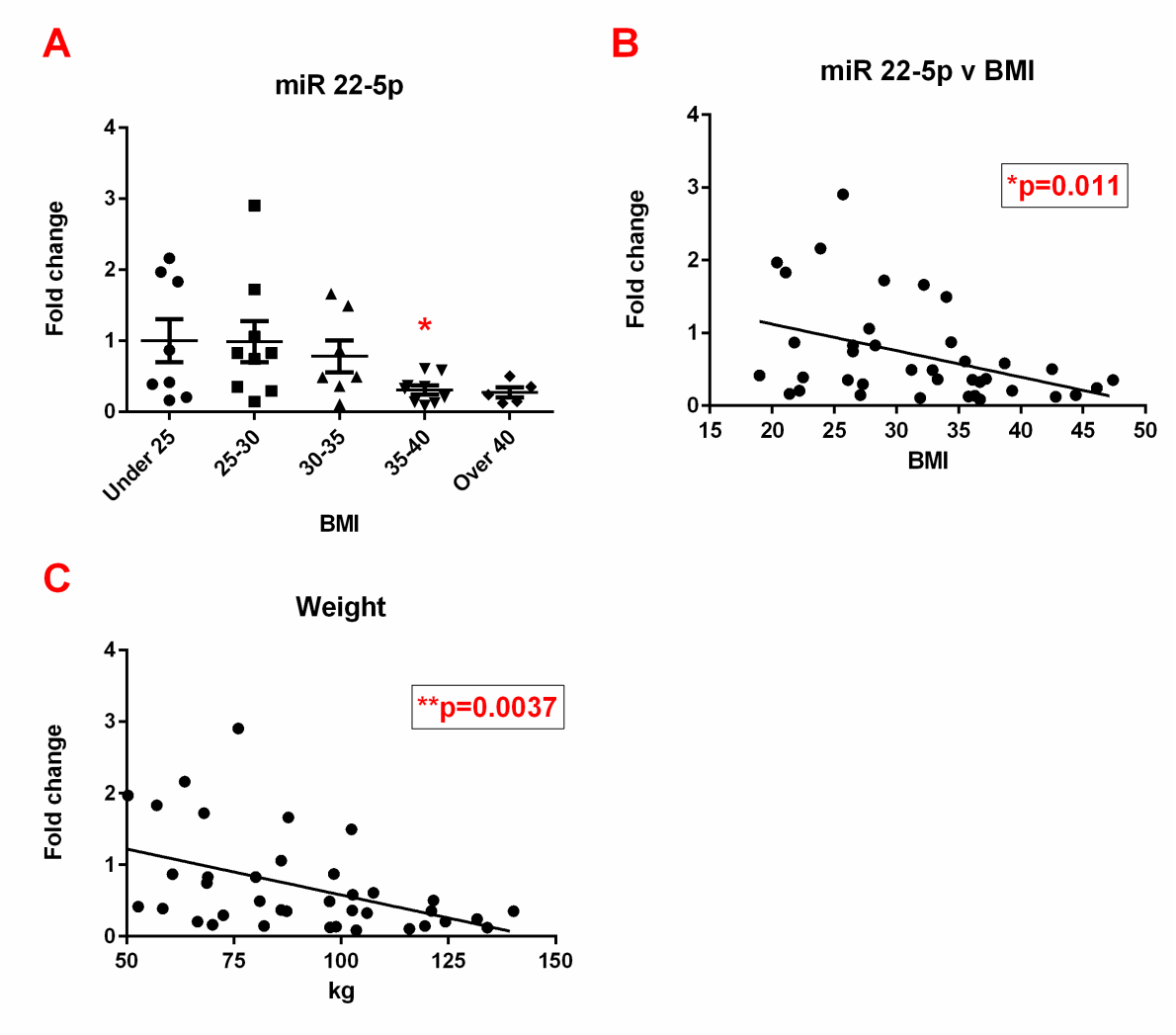

Figure 2.6: Serum miR 22-5p expression.

All microRNA data is represented as fold change relative to the under 25 BMI group. (A) miR 22-5p across 5 BMI groups. n=7-10 per group. Data represents mean ± SEM. *p<0.05 by Student's t-test. (B) Pearson correlation between miR 22-5p and BMI. (C) Pearson correlation between miR 22-5p and weight. n=30-47, *p<0.05, **p<0.01.

2.5.3.2 miR 145-5p

Similarly, a significant negative correlation was observed between circulating levels of miR 145-5p and BMI. Relative to levels in healthy individuals with a BMI under 25, levels of miR 145-5p decreased 0.55 fold in individuals with a BMI between 25-30, decreased 0.48 fold in individuals with a BMI between 30-35, decreased 0.28 fold in individuals with a BMI between 35-40 and decreased 0.27 fold in morbidly obese individuals with a BMI over 40 (Figure 2.7A). Although comparative two-way fold changes were not statistically significant (p values 0.34, 0.28, 0.13 and 0.18 respectively, Student's t-test), the linear trend with increasing BMI was statistically significant (p=0.031, one-way ANOVA). There was also a significant negative correlation between circulating levels of miR 145-5p and BMI (Figure 2.7B, r=-0.33, p=0.028, Pearson correlation) and weight (Figure 2.7C, r=-0.37, p=0.012, Pearson). Positive correlations were also observed between miR 145-5p serum levels and both baseline HDL (Figure 2.7D, r=0.42, p=0.019, Pearson) and baseline L-Phe:L-Tyr ratio (Figure 2.7E, r=0.37, p=0.039, Pearson).

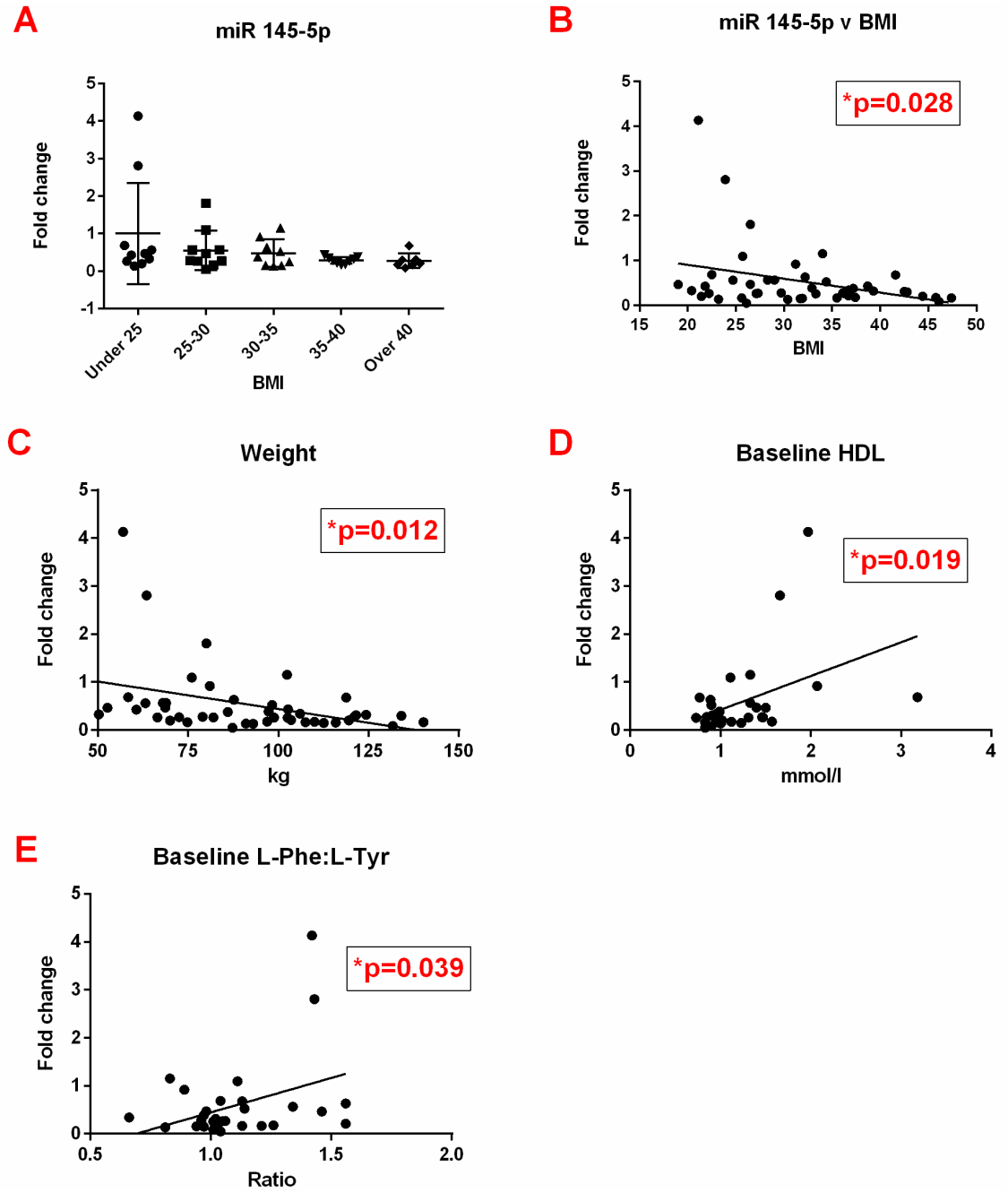

Figure 2.7: Serum miR 145-5p expression.

All microRNA data is represented as fold change relative to the under 25 BMI group. (A) miR 145-5p across 5 BMI groups. n=7-10 per group. Data represents mean ± SEM. (B) Pearson correlation between miR 145-5p and BMI. (C) Pearson correlation between miR 145-5p and weight. (D) Pearson correlation between miR 145-5p and baseline HDL. (E) Pearson correlation between miR 145-5p and baseline L-Phenylalanine:L-Tyrosine ratio. n=31-47, *p<0.05, **p<0.01.

2.5.3.3 miR 122

In contrast, no statistically significant relationship was also observed between circulating levels of miR 122 and BMI. Relative to levels in healthy individuals with a BMI under 25, levels of miR 122 decreased 0.89 fold in individuals with a BMI between 25-30, decreased 0.77 fold in individuals with a BMI between 30-35, decreased 0.53 fold in individuals with a BMI between 35-40 and decreased 0.41 fold in morbidly obese individuals with a BMI over 40 (Figure 2.8A). None of these fold changes were statistically significant (p values 0.88, 0.75, 0.46 and 0.45 respectively, Student's t-test). The linear trend was also not statistically significant (p=0.19, one-way ANOVA). Also, no significant correlation was found between circulating levels of miR 122 and BMI (Figure 2.8B, r=-0.19, p=0.2, Pearson correlation). However, miR 122 levels did correlate with fasting blood glucose (Figure 2.8C, r=0.38, p=0.032, Pearson) and baseline triglycerides (Figure 2.8E, r=0.42, p=0.018, Pearson) as well as bilirubin (Figure 2.8D, r=0.42, p=0.016, Pearson).

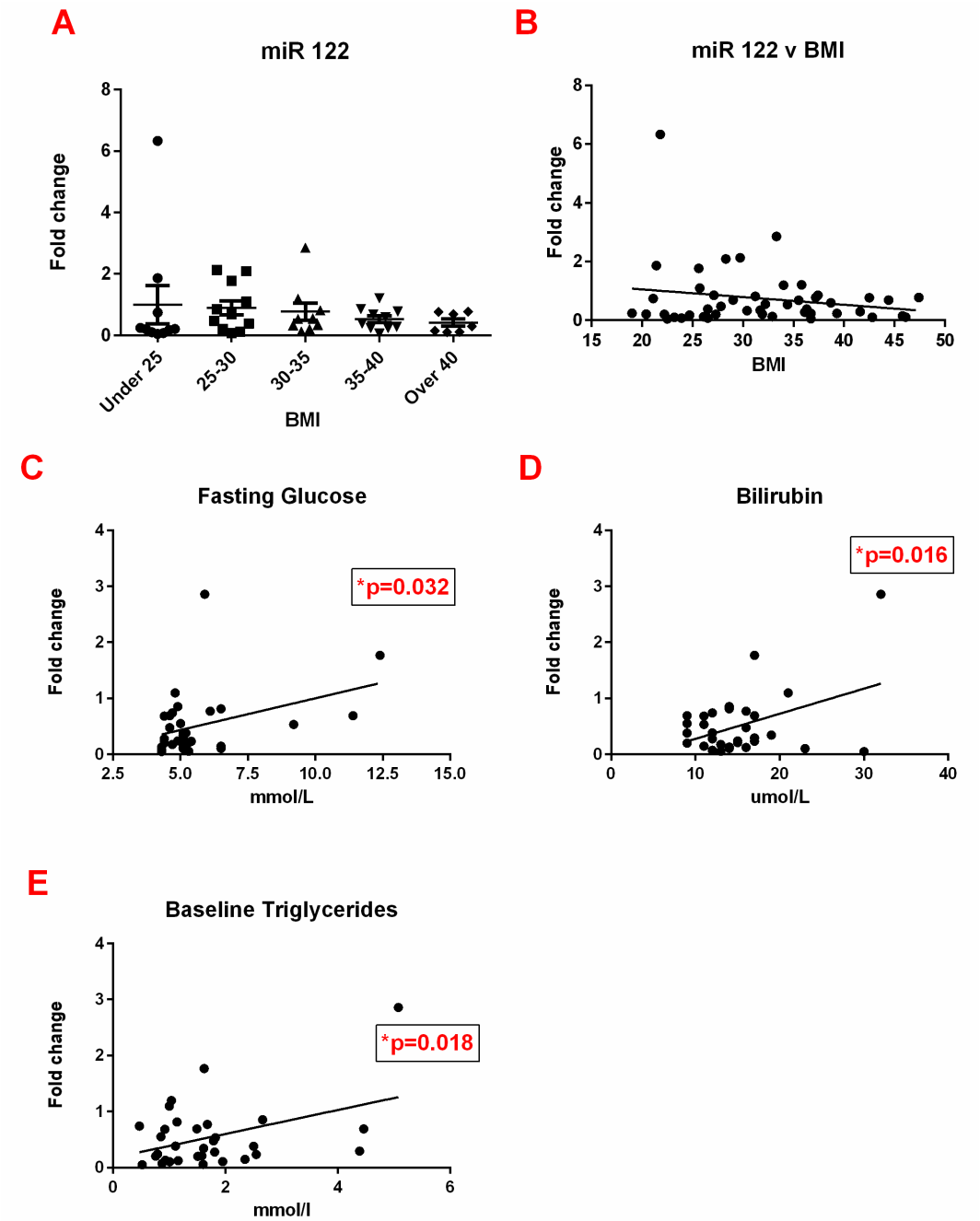

Figure 2.8: Serum miR 122 expression.

All microRNA data is represented as fold change relative to the under 25 BMI group. (A) miR 122 across 5 BMI groups. n=7-10 per group. Data represents mean ± SEM. (B) Pearson correlation between miR 122 and BMI. (C) Pearson correlation between miR 122 and fasting glucose. (D) Pearson correlation between miR 122 and bilirubin. (E) Pearson correlation between miR 122 and baseline triglycerides. n=30-47, *p<0.05.

2.5.3.4 miR 142-3p

No significant trend was observed between circulating levels of miR 142-3p and BMI. Relative to levels in healthy individuals with a BMI under 25, levels of miR 142-3p increased 1.58 fold in individuals with a BMI between 25-30, decreased 0.78 fold in individuals with a BMI between 30-35, decreased 0.45 fold in individuals with a BMI between 35-40 and decreased 0.84 fold in morbidly obese individuals with a BMI over 40 (Figure 2.9A). None of these fold changes were statistically significant (p values 0.31, 0.54, 0.097 and 0.72 respectively, Student's t-test). The linear trend was also not statistically significant (p=0.16, one-way ANOVA), and no statistically significant correlation was found between circulating levels of miR 142-3p and BMI (Figure 2.9B, r=-0.25, p=0.09, Pearson correlation). However, a significant negative correlation was found with weight (Figure 2.9C, r=-0.31, p=0.033, Pearson). Positive correlations were also found between serum levels of miR 142-3p and blood sodium (Figure 2.9D, r=0.37, p=0.036, Pearson).

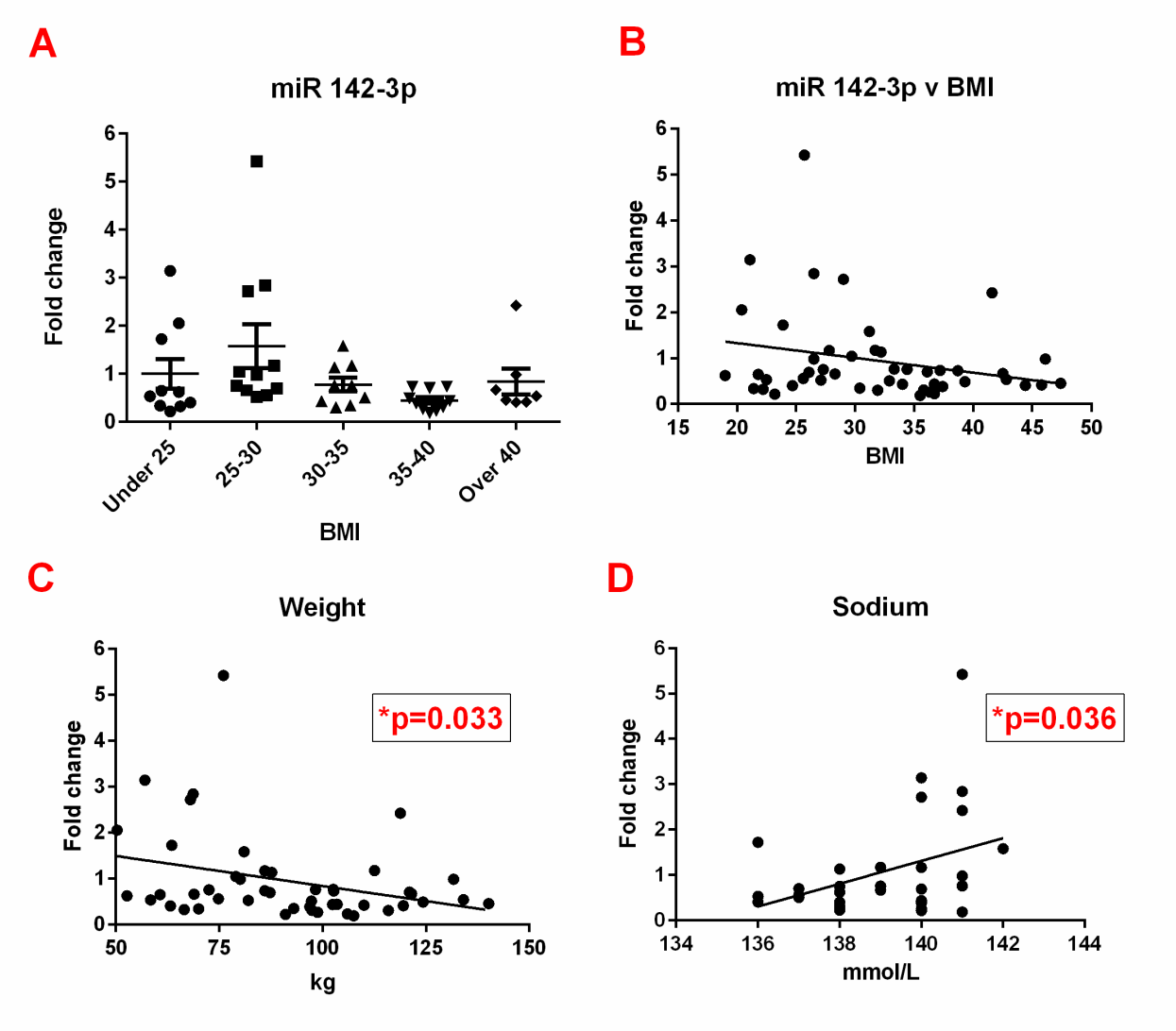

Figure 2.9: Serum miR 142-3p expression.

All microRNA data is represented as fold change relative to the under 25 BMI group. (A) miR 142-3p across 5 BMI groups. n=7-10 per group. Data represents mean ± SEM. (B) Pearson correlation between miR 142-3p and BMI. (C) Pearson correlation between miR 142-3p and weight. (B) Pearson correlation between miR 142-3p and sodium. n=30-47, *p<0.05.

2.5.3.5 miR 192

As with miR 142-3p, a significant negative correlation was found between circulating miR 192 levels and weight, but not BMI. Relative to levels in healthy individuals with a BMI under 25, levels of miR 192 increased 1.2 fold in individuals with a BMI between 25-30, decreased 0.73 fold in individuals with a BMI between 30-35, decreased 0.51 fold in individuals with a BMI between 35-40 and decreased 0.73 fold in morbidly obese individuals with a BMI over 40 (Figure 2.10A). None of these fold changes were statistically significant (p values 0.61, 0.58, 0.13 and 0.49 respectively, Student's t-test). The linear trend was also not statistically significant (p=0.15, one-way ANOVA). Also, no statistically significant correlation was found between circulating levels of miR 192 and BMI (Figure 2.10B, r=-0.26, p=0.17, Pearson correlation). In contrast, miR 192 levels significantly decreased with increasing weight (Figure 2.10C, r=-0.40, p=0.029, Pearson). A significant positive association was also found with blood bilirubin levels (Figure 2.10D, r=0.45, p=0.043, Pearson).

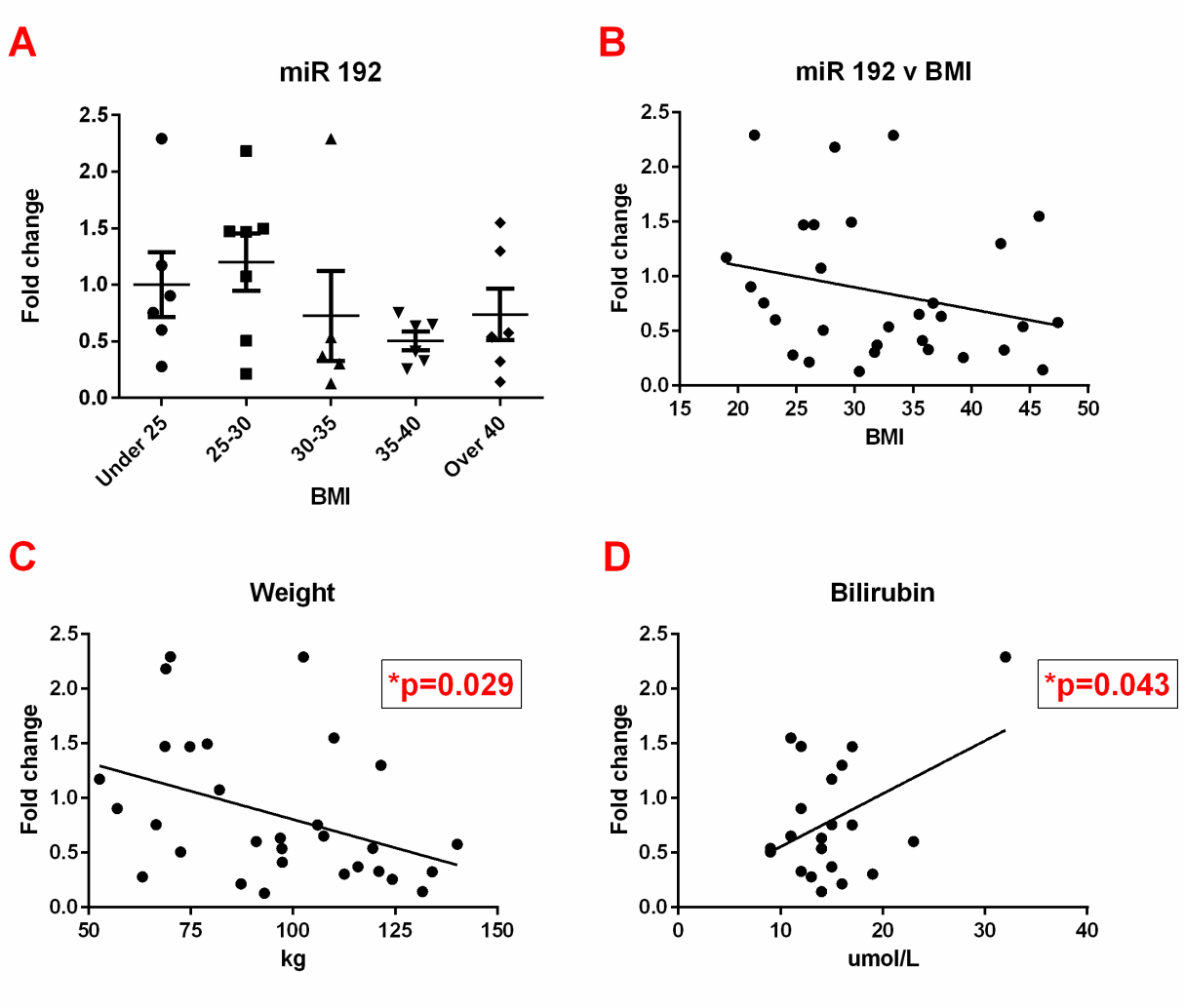

Figure 2.10: Serum miR 192 expression.

All microRNA data is represented as fold change relative to the under 25 BMI group. (A) miR 192 across 5 BMI groups. n=5-7 per group. Data represents mean ± SEM. (B) Pearson correlation between miR 192 and BMI. (C) Pearson correlation between miR 192 and weight. (D) Pearson correlation between miR 192 and bilirubin. n=30-47, *p<0.05.

2.5.3.6 miR 221

There was no significant relationship found between BMI and circulating miR 221. Relative to levels in healthy individuals with a BMI under 25, levels of miR 221 increased 2 fold in individuals with a BMI between 25-30, decreased 0.96 fold in individuals with a BMI between 30-35, increased 1.34 fold in individuals with a BMI between 35-40 and increased 4.94 fold in morbidly obese individuals with a BMI over 40 (Figure 2.11A). However, none of these fold changes were statistically significant (p values 0.27, 0.93, 0.68 and 0.25 respectively, Student's t-test). The linear trend was also not statistically significant (p=0.13, one-way ANOVA).

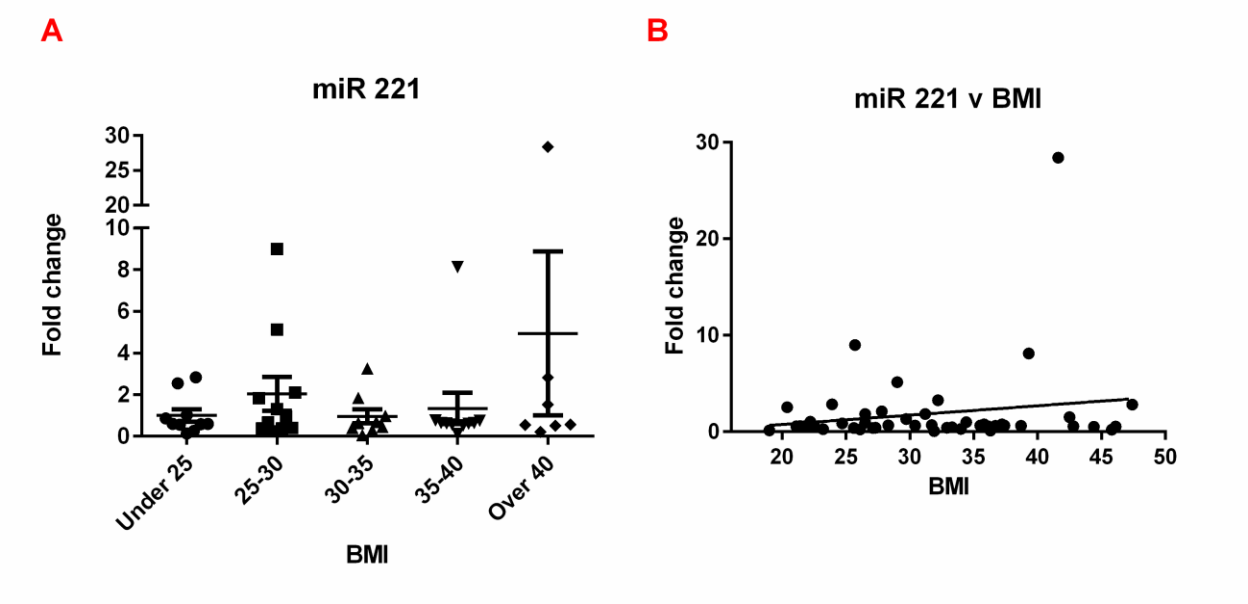

Figure 2.11: Serum miR 221 expression.

All microRNA data is represented as fold change relative to the under 25 BMI group. (A) miR 221 across 5 BMI groups. n=7-10 per group. Data represents mean ± SEM. (B) Pearson correlation between miR 221 and BMI. n=30-47.

2.5.3.7 miR 15a

Levels of miR 15a were not found to be differentially expressed with BMI. Relative to levels in healthy individuals with a BMI under 25, levels of miR 15a increased 1.26 fold in individuals with a BMI between 25-30, decreased 0.53 fold in individuals with a BMI between 30-35, decreased 0.31 fold in individuals with a BMI between 35-40 and increased 1.03 fold in morbidly obese individuals with a BMI over 40 (Figure 2.12A). None of these fold changes were statistically significant (p values 0.59, 0.25, 0.078 and 0.95 respectively, Student's t-test). The linear trend was also not statistically significant (p=0.3, one-way ANOVA). Also, no statistically significant correlation was found between circulating levels of miR 15a and BMI (Figure 2.12B, r=-0.2, p=0.17, Pearson correlation) or any blood biochemistry marker.

2.5.3.8 miR 125b

No relationship was found between BMI and circulating miR 125b. Relative to levels in healthy individuals with a BMI under 25, levels of miR 125b decreased 0.69 fold in individuals with a BMI between 25-30, decreased 0.95 fold in individuals with a BMI between 30-35, decreased 0.63 fold in individuals with a BMI between 35-40 and decreased 0.62 fold in morbidly obese individuals with a BMI over 40 (Figure 2.12C). None of these fold changes were statistically significant (p values 0.32, 0.9, 0.26 and 0.31 respectively, Student's t-test). The linear trend was also not statistically significant (p=0.24, one-way ANOVA), and no statistically significant correlation was found between circulating levels of miR 125b and BMI (Figure 2.12D, r=-0.17, p=0.27, Pearson correlation). No significant correlations were found with any blood biochemistry marker.

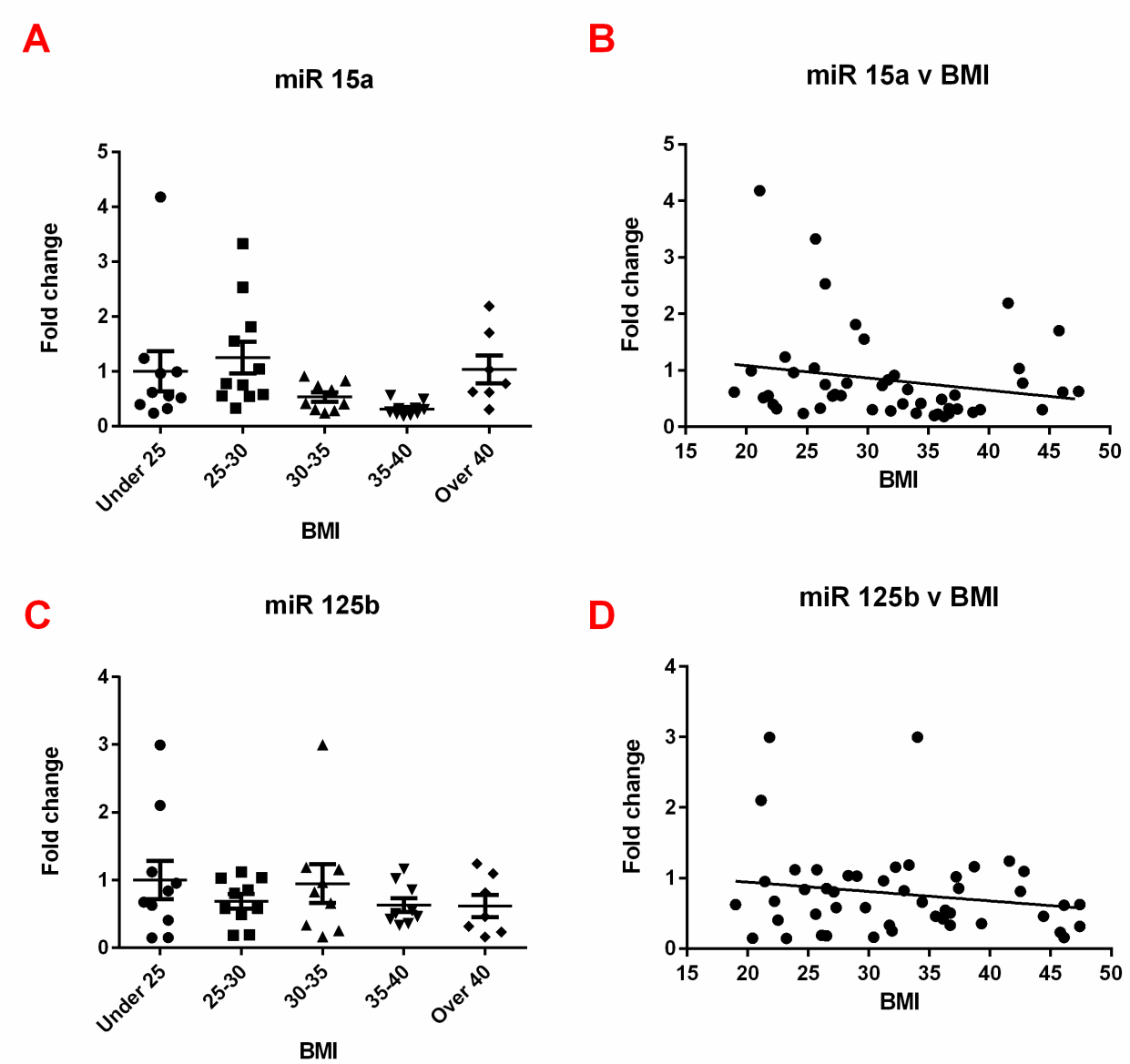

Figure 2.12: Serum microRNA expression of miR 15a and miR 125b.

(A-B) MiR 15a and (C-D) MiR 125b. Left panel illustrates microRNA fold change expression across 5 BMI groups. Fold change relative to under 25 BMI, n=7-10 per group. Data represents mean ± SEM. Right panel illustrates Pearson correlation between of BMI and fold change. n=30-47.

2.5.4 Urine

In the corresponding BMI urine samples expression of 3 miRNAs, miR 192, miR 200a and miR 200b, were measured. All three are kidney expressed miRNAs associated with the metabolic syndrome [178, 222].

2.5.4.1 miR 192

Urinary levels of miR 192 decreased with BMI but this was not statistically significant. Relative to levels in healthy individuals with a BMI under 25, urinary levels of miR 192 decreased 0.56 fold in individuals with a BMI between 25-30, decreased 0.39 fold in individuals with a BMI between 30-35, decreased 0.55 fold in individuals with a BMI between 35-40 and decreased 0.52 fold in morbidly obese individuals with a BMI over 40 (Figure 2.13A). None of these fold changes were statistically significant (p values 0.33, 0.17, 0.33 and 0.32 respectively, Student's t-test). There was also no linear trend (p=0.25, one-way ANOVA) and no correlation between urinary levels of miR 192 and BMI (Figure 2.13B, r=-0.23, p=0.13, Pearson correlation). However, a negative correlation was found with blood levels of urea (Figure 2.13C, r=-0.45, p=0.011, Pearson).

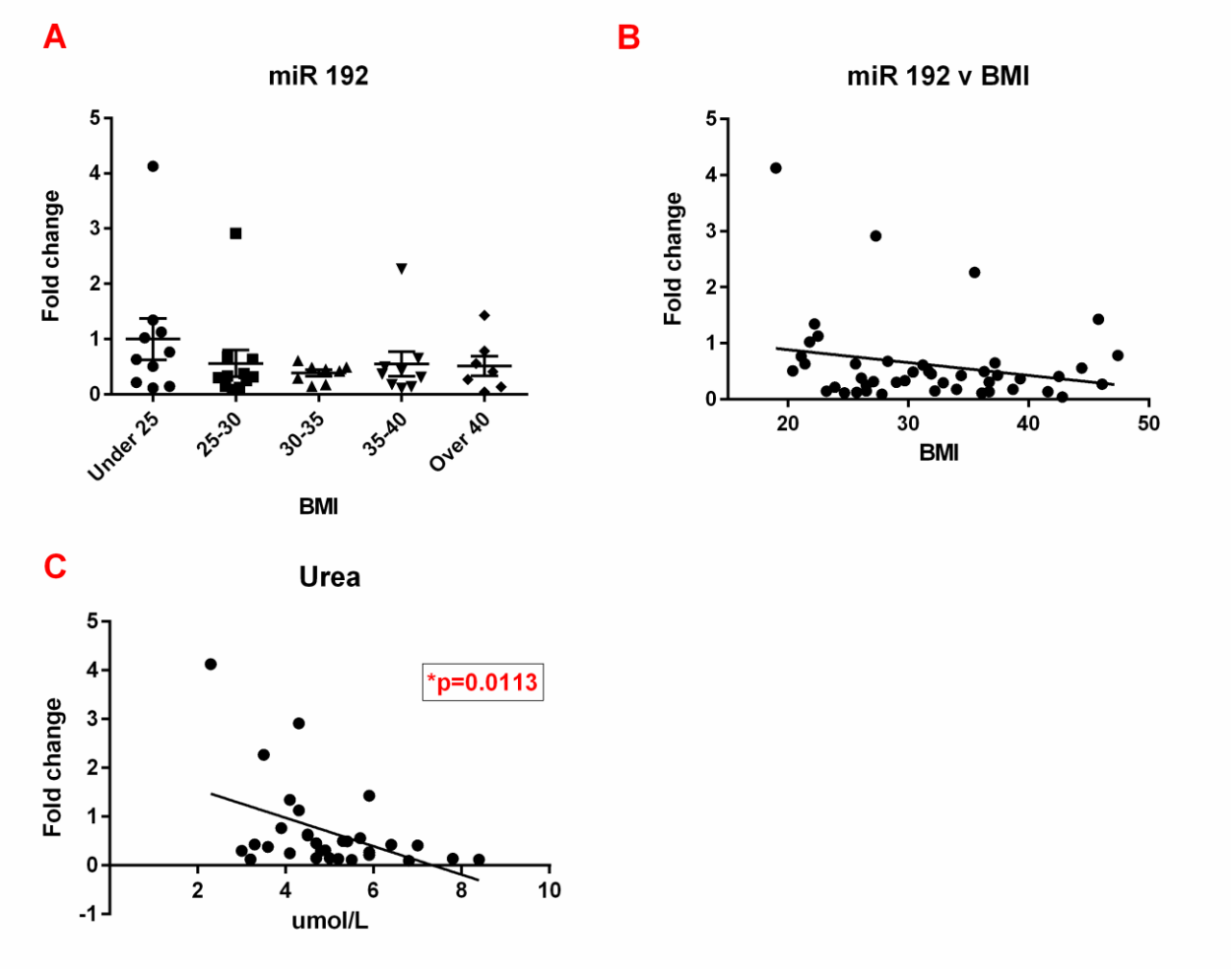

Figure 2.13: Urinary miR 192 expression.

All microRNA data is represented as fold change relative to the under 25 BMI group. (A) miR 192 across 5 BMI groups. n=7-10 per group. Data represents mean ± SEM. (B) Pearson correlation between miR 192 and BMI. (C) Pearson correlation between miR 192 and urea. n=30-47, *p<0.05.

2.5.4.2 miR 200a

There appeared to be a negative correlation between BMI and urinary levels of miR 200a, albeit this was not significant. Relative to levels in healthy individuals with a BMI under 25, urinary levels of miR 200a decreased 0.45 fold in individuals with a BMI between 25-30, decreased 0.16 fold in individuals with a BMI between 30-35, decreased 0.15 in individuals with a BMI between 35-40 and decreased 0.05 fold in morbidly obese individuals with a BMI over 40 (Figure 2.14A). However, none of these fold changes were statistically significant (p values 0.57, 0.44, 0.39 and 0.33 respectively, Student's t-test). There was also no significant linear trend (p=0.15, one-way ANOVA) and no correlation between urinary levels of miR 200a and BMI (Figure 2.14B, r=-0.33, p=0.07, Pearson). There was a significant negative correlation found with weight, however (Figure 2.14C, r=-0.37, p=0.041, Pearson correlation). A positive correlation was observed between urinary miR 200a and baseline L-Phe:L-Tyr levels (Figure 2.14D, r=0.5, p=0.026, Pearson).

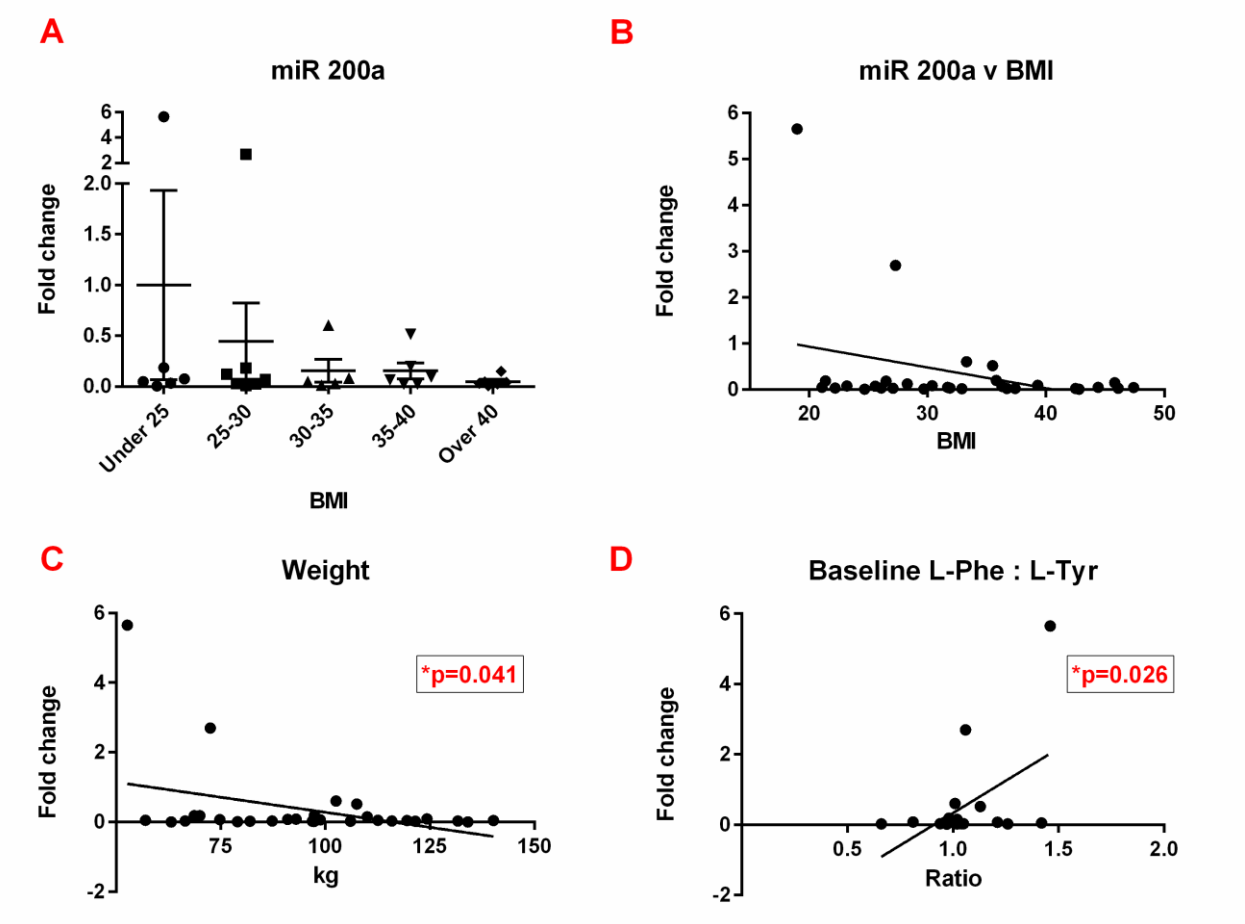

Figure 2.14: Urinary miR 200a expression.

All microRNA data is represented as fold change relative to the under 25 BMI group. (A) miR 200a across 5 BMI groups. n=7-10 per group. Data represents mean ± SEM. (B) Pearson correlation between miR 200a and BMI. (C) Pearson correlation between miR 200a and weight. (D) Pearson correlation between miR 200a and L-Phenylalanine:L-Tyrosine ratio. n=30-47, *p<0.05.

2.5.4.3 miR 200b

Similarly, there was a negative correlation between urinary levels miR 200b and BMI but this was not significant. Relative to levels in healthy individuals with a BMI under 25, urinary levels of miR 200b decreased 0.34 fold in individuals with a BMI between 25-30, decreased 0.21 fold in individuals with a BMI between 30-35, decreased 0.12 in individuals with a BMI between 35-40 and decreased 0.01 fold in morbidly obese individuals with a BMI over 40 (Figure 2.15A). However, none of these fold changes were statistically significant (p values 0.45, 0.38, 0.31 and 0.34 respectively, Student's t-test). There was also no significat linear trend (p=0.13, one-way ANOVA) and no correlation between urinary levels of miR 200b and BMI (Figure 2.15B, r=-0.29, p=0.0502, Pearson test). Urinary miR 200b did significantly correlate with weight, however (Figure 2.15C, r=-0.31, p=0.036, Pearson correlation). A correlation was also found with urea (Figure 2.15D, r=-0.35, p=0.049, Pearson correlation).

Complete tabulated Pearson correlations between all assessed circulating and urinary microRNAs and blood biochemistry markers can be found in the appendices (Tables 7.1-7.11).

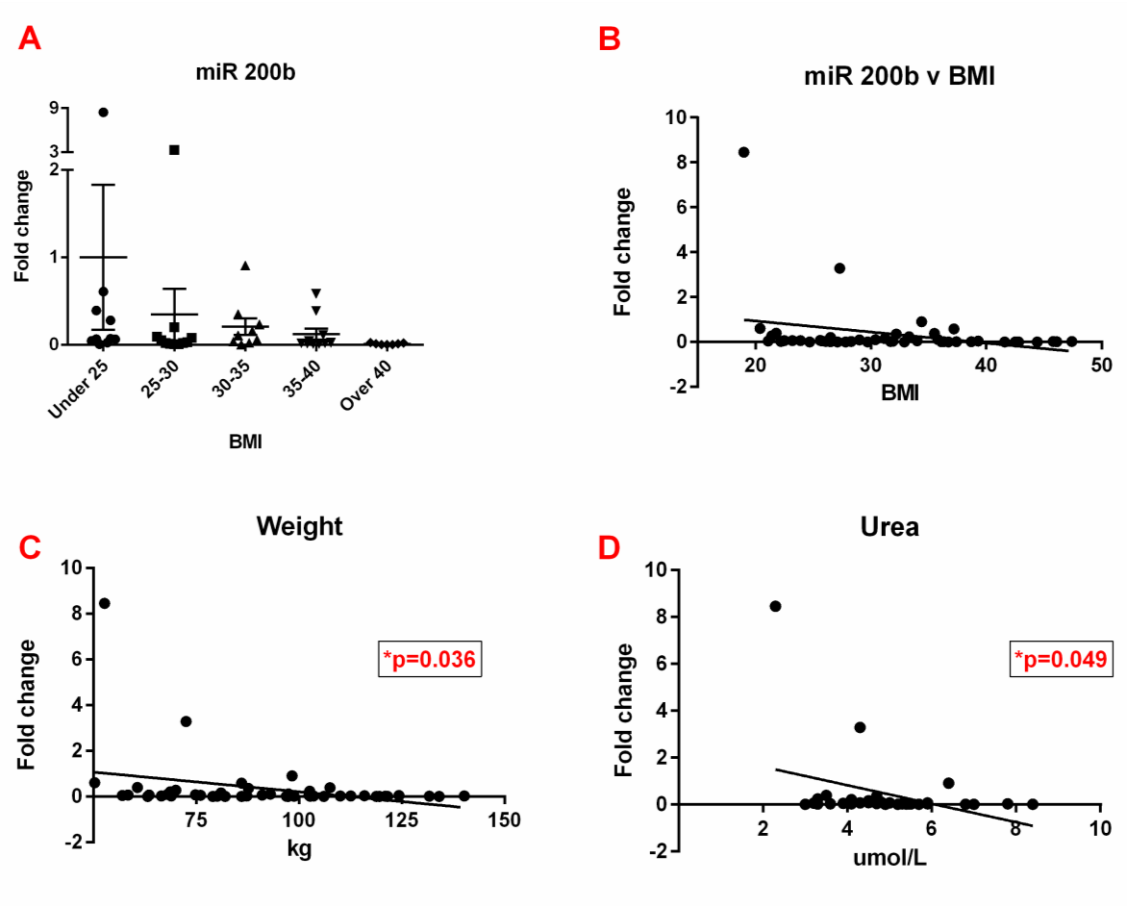

Figure 2.15: Urinary miR 200b expression.

All microRNA data is represented as fold change relative to the under 25 BMI group. (A) miR 200b across 5 BMI groups. n=7-10 per group. Data represents mean ± SEM. (B) Pearson correlation between miR 200b and BMI. (C) Pearson correlation between miR 200b and weight. (D) Pearson correlation between miR 200b and urea. n=30-47, *p<0.05.

2.6 Discussion

In this chapter a method to measure and normalise miRNA expression in serum and urine was developed and validated. Synthetic cel. miR-39 was used as an internal standard and urinary microRNA levels were normalised to creatinine concentrations to correct for diuretic effect. Baseline expression of select miRNAs associated with obesity and the metabolic syndrome was determined in both serum and urine. Circulating levels of miR 22-5p and miR 145-5p were found to be negatively correlated with BMI, suggesting they're biological effectors and may represent novel biomarkers for obesity. Serum miR 142-3p and miR 192 and urinary miR 200a and 200b were found to inversely correlate with weight.

Extensive published evidence has implicated miR 22 in cancer, both as an oncogene and a tumour suppressor. Cellular senescence, a state of permanent cell cycle arrest and a barrier to cancer progression, is induced by miR 22 in both human normal and cancer cells [223]. MiR 22 is also a reported tumour suppressor in colon cancer, inhibiting p21 and selectively determining p-53 induced apoptosis in response to cellular stress [224]. Additionally, miR 22 also inhibits the oncogene c-Myc by silencing c-Myc binding protein in a proliferation positive feedback loop [225]. However, miR 22 also reportedly inhibits the tumour suppressor PTEN [226] and displays oncogenic properties in haematological and breast cancers [227, 228]. MiR-22 is upregulated in myelodysplastic syndrome (MDS) and leukaemia and expression correlations with poor survival in both [227]. Transgenic mice conditionally expressing miR 22 in the haematopoietic compartment developed MDS and haematological malignancies [227]. In breast cancer miR 22 overexpression is associated with increased mammary hyperplasia, tumour development and poor survival [228]. The proto-oncogenic activity of miR 22 is exhibited through the direct targeting and inactivating TET2, which catalyses the conversion of 5-methylcytosine to 5-hydroxymethylcytosine. Mutations of TET2 are common in MDS and other malignancies and its overexpression has been found during haematopoietic differentiation [227, 229, 230].

The reported oncogenic and tumour suppressive functions of miR 22 underscores the multifaceted and complex nature of microRNA regulation, where each microRNA has multiple targets involved in a variety of pathways, and the biological function of microRNAs appears pleiotropic, specific to tissue and pathway. MiR 22 is reportedly upregulated in the gums of obese patients with periodontal disease [231]. This appears to be the only reported direct link between miR 22 and obesity as of yet. However, given that obesity is a well established risk factor to a number of different cancers [232], the inverse correlation found here between circulating expression of miR 22-5p and BMI supports the reported anti-cancer role of miR 22.

There is on the other hand evidence implicating miR 145 with obesity. Mir 145 is upregulated in the liver of genetic and dietary mouse models of obesity, and deficiency in miR 143-145 cluster leads to immunity from obesity-associated insulin resistance in mice [233]. MiR 145 has been found to be downregulated in isolated fat cells and intact subcutaneous white adipose tissue in obesity [165]. MicroRNA 145 expression is decreased in adipocyte cell differentiation and subcutaneous fat expression of miR 145 correlates with HDL-cholesterol and 2 hour oral glucose tolerance test levels [234]. MicroRNA 145 also reportedly promotes lipolysis by increasing the production and release of TNF-α (tumour necrosis factor α) and glycerol release through the activation of p65, a NF-κB (nuclear factor-κB) complex member. Lipolysis, the hydrolysis of triglycerides to into fatty acids and glycerol, is decreased in obesity resulting in the accumulation of fat mass [235]. MiR-145 also increases membrane bound TNF-α by targeting ADAM17, part of the metalloproteinase family [236]. There is also a reported negative correlation between miR 145 and leptin receptors in abdominal subcutaneous fat of morbidly obese individuals [237]. All this evidence is consistent with the inverse correlation between BMI and miR 145-5p found here. Interestingly, miR 145 has also been reported to be upregulated in the urinary exosomes of patients with microabluminuria and in the subcutaneous muscle cells of patients with type 2 diabetes when compared to non-diabetic patients [238, 239]. This is indicative of the proposed key regulatory role miR 145 has in lipid biology and obesity and the findings reported here support this assertion.

Circulating levels of miR 122 did not correlate with BMI here, inconsistent with Ortega *et al.* who reported a decrease in plasma miR 122 in patients with morbid obesity [208]. However, positive correlations between miR 122 and baseline triglycerides, fasting blood glucose and bilirubin were observed. The predominant microRNA in the liver, miR 122 is a key regulator of cholesterol and fatty acid metabolism [172]. Inhibition of miR 122 in mice on both normal and high-fat diets led to decreased fatty-acid and cholesterol synthesis in the liver, as well as a decrease in plasma triglycerides, but not plasma glucose [172]. Inhibition also triggered the activation of the central metabolic sensor AMPK, an important regulator in energy balance which is deregulated in the metabolic syndrome and a novel therapeutic target for type 2 diabetes [240]. Circulating levels of miR 122 and 192 are reported markers of liver damage [241], which may explain their correlation with bilirubin, a common marker for impaired liver function. Miravirsen, a miR 122 inhibitor, has been successful in a phase II clinical trial in treating Hepatitis C, an infection that primarily targets the liver. [242].

Inverse correlations with weight were also found with serum levels of microRNAs 142-3p and 192. This is in stark contrast to Ortega *et al.* who found circulatory miR 142-3p increases in cases of obesity and morbid obesity [208]. Mir 142-3p is reported to be upregulated in the adipose tissue of obese mice [243], but downregulated in diabetic cardiomyopathy [244]. MiR 192 is an anti-fibrotic microRNA typical of the kidney [178, 183] and its decrease in circulation has been reported in patients with type 2 diabetes [210], consistent with the decrease with weight found here. Urinary levels of miR 200a and miR 200b also decreased with weight. Both are kidney anti-fibrotic microRNAs and are decreased in diabetic nephropathy [222, 245]. Obesity did not influence serum levels of miR 15a, miR 125b or miR 221 here. All three were found to be decreased in obesity by Ortega *et al.* [208].

Due to financial and time restraints, the expression of only 8 microRNAs in circulation and 3 in urine were measured. Ideally, more microRNAs need to be assessed, either in a targeted PCR approach or

preferably through profiling, by next generation deep sequence, through microarrays or using predesigned microRNA PCR panels. This would provide a more complete picture of the obesity microRNA profile. However, employing a targeted manner this chapter has provided potential novel circulating biomarkers of obesity, in particular miR 145 and miR 22.

Determining a microRNA disease signature in biofluids is a field still in its infancy, as illustrated by the scant and differing findings. Validation of these findings is required in larger, more diverse, multicentre cohorts to with subgroups of the various obesity co-morbidities, including diabetes and cardiovascular disease. Temporal, prospective studies are required to assess the prognostic power of microRNAs in obesity. The role of microRNAs in biofluids is not fully understood and it is not known whether circulating microRNAs are functional factors in disease or simply biomarkers. Recently circulating microRNAs encompassed in exosomes and high- density lipoprotiens have been taken up in active form by recipient cells, suggesting a potential tissue-to-tissue communicative role for microRNAs [203, 204]. *In vitro* mechanistic studies are needed to decipher the precise function deregulated microRNAs have in obesity, to provide fresh mechanistic insights and to potentially uncover new avenues for obesity therapeutics.

To summarise, in this chapter a method of accurately measuring and normalising microRNA levels in circulation and urine was established. The expression levels of microRNAs associated with obesity was also determined, identifying potential novel circulating microRNA biomarkers for obesity and setting the phenotypic anchor for subsequent chapters assessing novel urinary and circulating microRNA biomarkers of the post-bariatric phenotype.

3 Urinary microRNA expression following bariatric surgery

3.1 Justification

Renal dysfunction is commonly associated with the metabolic syndrome [246]. Diabetes and obesity are independent risk factors of chronic kidney disease (CKD), characterised by decreased estimated glomerular filtration rate (eGFR) and increased urinary albumin. Obesity leads to a decline in renal function over time and increasing BMI leads to renal hyperfiltration and proteinuria which eventually culminates in hypofiltration and CKD. Diabetic nephropathy (DN) occurs in approximately one third of diabetics (both type 1 and type 2) and is the most common cause of CKD and end stage renal failure [247]. DN is characterised by microalbuminuria, thickening of the glomerular basement, mesangial expansion and tubulointerstitial fibrosis through accumulation of extracellular matrix proteins, namely collagen (encoded by Colα1) and fibronectin.

DN is mediated by transforming growth factor-β1 (TGF-β1) and TGF-β1 promoted fibrosis is mediated by an increasing number of fibroblasts, which are the effecter cells in the production and accumulation of the extracellular matrix. Epithelial-to-mesenchymal transition (EMT) is increasingly recognised as a key component in this process by promoting the transition of resident renal epithelial cells to a fibroblast phenotype [248]. MiR 192 and the miR 200 family suppress EMT by targeting zinc E-box binding homeobox 1 and 2 (ZEB1 and ZEB2), which encode transcriptional repressors for E-cadherin, essential for maintaining epithelial phenotype [178-180].

Weight loss, including that achieved surgically, leads to an improvement in renal function [249-251]. This chapter hypothesises that this is mediated by microRNAs, and their expression in urine are biomarkers for improvements in health induced by bariatric surgery.

3.2 Aims

1. To identify urinary microRNA biomarkers for clinical improvements following bariatric surgery

2. To determine the post-bariatric biological role of these microRNAs

3.3 Study design

Twenty seven morbidly obese individuals undergoing laparoscopic bariatric surgery provided urine samples under ethics approval 08/H0711/123. Urine samples were obtained preoperatively and at 2 periods postoperatively - between 2 and 6 months and between 1 and 2 years. Bariatric surgery was performed at Imperial College London. All patients fulfilled NICE qualifying criteria for bariatric surgery [49]. Twenty patients had a RYGB, 4 had a sleeve gastrectomy, 2 had a gastric band and 1 had a hybrid sleeve-bypass operation. Fifteen out of the 27 were diabetic or pre-diabetic preoperatively. Patients were stratified by surgical procedure and diabetes status. The average BMI was 51.6 kg/m^2. Females made up 70.4% of participants. A study summary table can be found in Table 3.1.

Table 3.1: Study Summary Table[ǂ]

All Patients	Total	T2DM/ Pre-T2DM	LRYGB	Sleeve	Gastric Band	Sleeve/Bypass
n	27	15	20	4	2	1
Age	47.2 (11.1)	51.9 (9.4)	45 (10.4)	49.1 (13.7)	62.3 (3.73)	52.1
Sex (Female)	19/27	10/27	14/27	2/4	2/2	1/1
BMI (kg/m^2)	50.9 (7.29)	47.5 (6.44)	50.3 (7.53)	55.7 (6.17)	43.4	53.5
Diabetes	9/27	9/15	8/20	1/4	0	0
Pre-diabetes	6/27	6/15	3/20	1/4	1/2	1/1

[ǂ]Values represent mean. Values in parenthesis represent standard deviation.

RNA was extracted from urine samples and the preoperative and postoperative expression of miR 192, 200a and 200b was measured by targeted qPCR. This was followed by *in vitro* functional studies manipulating expression of miR 192 in HK-2 cells, a human, non-cancerous cell line derived from the proximal tubule. Figure 3.1 is a flowchart outlining Chapter 3's study design.

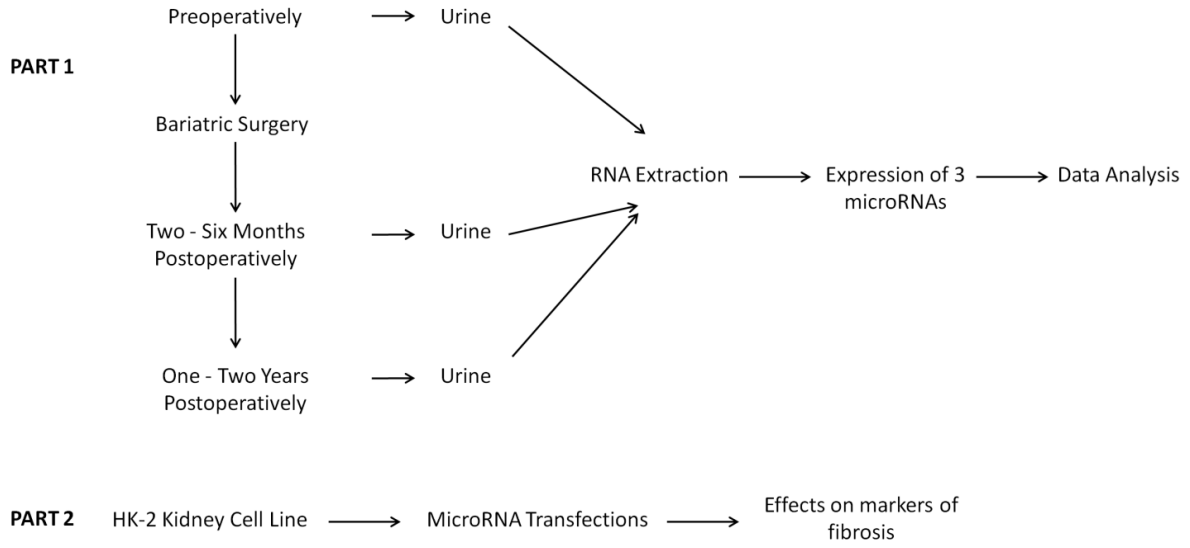

Figure 3.1: Flow chart illustrating the study design of chapter 3.

3.4 Materials and methods

3.4.1 Samples

All urine samples were collected in urine donation tubes. Samples were aliquoted into 0.2ml and 0.5ml aliquots. All samples were stored in -80^{o}C and filtered through a 0.2µm filter prior to analysis. Surgical clinical outcomes were obtained in collaboration with performing surgeons.

3.4.2 Urinary RNA extraction

RNA was extracted from urine samples using the *mir*Vana PARIS kit (Ambion). RNA was extracted from 250µl of urine. To normalise, 30 femtomoles of synthetic *C. elegans* miR-39 (Ambion) was spiked into the urine samples following denaturing. Cel. miR-39 was chosen as it lacks sequence homology with human miRNAs. RNA was eluted in 100µl nuclease free water. RNA extracts were stored at -20^{o}C until use. A detailed, step-wise protocol can be found in section 2.4.3 in the previous chapter.

3.4.3 Targeted quantitative PCR

RNA product was reverse transcribed using TaqMan MicroRNA Reverse Transcription kits (Applied Biosystems). Relative microRNAs levels were determined by real time, quantitative PCR using TaqMan Fast Universal Master Mix (Applied Biosystems). Quantitative PCR was performed in triplicate on the Applied Biosystems 7500 Fast System. All PCR and RT probes were obtained from Applied Biosystems. MicroRNA expression was normalised to cel. miR-39 levels and urinary microRNA expression was further normalised to creatinine. Relative expression was calculated using the $2^{-\Delta Ct}$ method [216]. A detailed, step-wise protocol can be found in section 2.4.4 in the previous chapter.

3.4.4 Creatinine assay

To correct for diuretic effect, urinary microRNA expression was normalised to urinary creatinine levels. Creatinine is a product of creatine metabolism in muscle and under normal conditions is excreted by the kidneys into urine at a relatively constant rate. Urinary levels were determined using a creatinine assay kit (R&D Systems). Briefly, urine samples were diluted 1 in 20 in distilled water and treated with an alkaline picrate to produce an orange-red complex. Following incubation at room temperature for 30 minutes, absorbance was measured at 490nm. Creatinine levels were determined using a standard curve. A detailed, step-wise protocol can be found in section 2.4.5 in the previous chapter.

3.4.5 Tissue culture

To determine the functional role of the urinary microRNAs found to be differentially expressed following bariatric surgery, microRNA expression was manipulated in an *in vitro* cell culture model.

3.4.5.1 Cell line

The human kidney-2 (HK-2) cell line was purchased from the American Type Culture Collection (ATCC) through LGC Standards (Teddington, UK). HK-2 cell line is a proximal tubular cell (PTC) line derived from a normal, adult, male, human renal cortex. The cell line was immortalised by transduction with human papilloma virus 16 E6/E7 genes and shares phenotypical and functional characteristics with well differentiated PTCs [252]. HK-2 cells are adherent, epithelial cells that double approximately every 48 hours (Figure 3.2). They have been used extensively as *in vitro* renal models to assess drug-induced nephrotoxicity and are capable of reproducing experimental results obtained from freshly isolated PTCs.

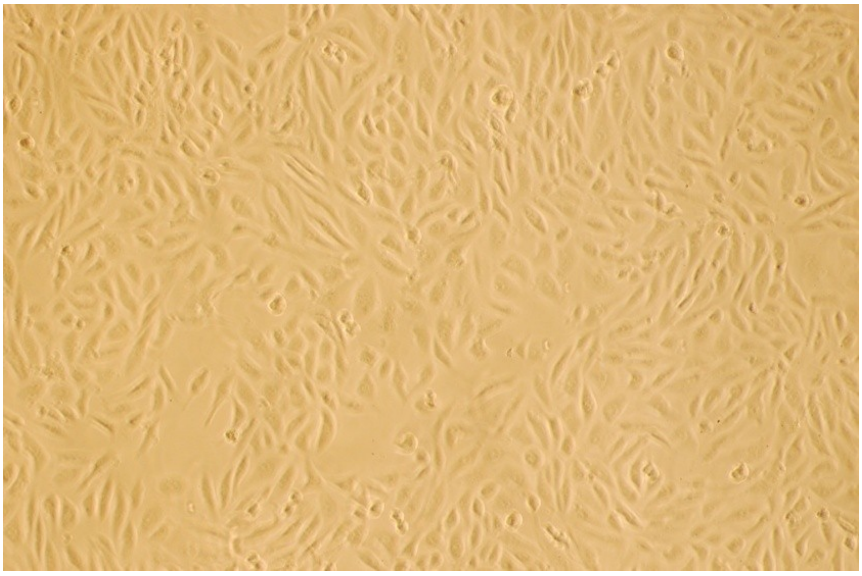

Figure 3.2: HK-2 cells in culture.

The image was taken under a light microscope.

3.4.5.2 Cell culture

For the successful growth and maintenance of cells *in vitro* appropriate culture conditions are required that resemble *in vivo* physiological conditions. Cell culture was carried out in Class II biological safety cabinets using reagents supplied by Life Technologies (Paisley, UK) and propagated in Corning (Loughborough, UK) standard tissue culture treated plasticware unless otherwise stated. Cells were cultured at 37^{o}C and 5% CO^{2} in a humidified incubator. HK-2 cells were maintained in DMEM/Ham's F12, supplemented with 10% v/v foetal bovine serum (FBS), 1% Penicillin/Streptomycin antibiotics (100U/ml, 100µg/ml respectively) and 1% Insulin-Transferrin-Sodium Selenite (Sigma-Aldrich, Gillingham, UK) to form complete media. Insulin-Transferrin-Sodium Selenite promotes glucose and amino acid uptake and reduces toxic oxidants and the need for FBS. FBS provides growth factors, hormones, essential fatty acids, binding and transport proteins and other supplements vital for cell growth, metabolism and proliferation [253].

3.4.5.3 Cell resuscitation

HK-2 cells were stored in the liquid phase of liquid nitrogen at 1-2x10^6 cells per vial. Cells were resuscitated from frozen by rapidly thawing a vial at 37^{o}C in a water bath. Cells were then transferred to a 15ml centrifuge tube. The vial was then washed with 1ml complete media, which was then added to the cells in the centrifuge tube, along with another 1ml of complete media. Cells were then centrifuged at 1,000g for 5 minutes. Storage media was aspirated and the cell pellet was suspended in 10ml complete media. Cells were transferred to a 25cm^3 culture flask and placed in an incubator until confluent, when they were transferred to a 75cm^3 culture flask. HK-2 cells typically double approximately every 48 hours. Media was refreshed every 2-3 days until confluence was reached.

Cells were maintained in culture until ~80% confluent. To passage cells, culture media was removed by suction and the cell adherent monolayer was washed in 1ml sterile phosphate-buffer saline (PBS) solution. To detach cells from the culture flask 5ml 0.05% trypsin-EDTA was added to the monolayer and the flask was incubated at 37^{o}C for 5 minutes. Trypsin was deactivated by the addition of equal volume complete media and the mixture was centrifuged at 1,000g for 5 minutes. The supernatant was removed by suction and the cell pellet was suspended in fresh complete media. Cells were then split into new culture flasks at a 1:3-1:4 ratio.

Cells were counted using a Neubauer haemocytometer and the trypan blue exclusion assay. Viable cells exclude trypan blue and thus can be differentiated. A 100µl aliquot of cell suspension was mixed with 20µl of trypan blue (0.4%), a dilution factor of 1.2. Then 10µl of the mixture was loaded into a haemocytometer and viable cells were scored in 4 squares under a microscope and averaged. Cell concentration was determined using the following equation:

$$Cells\ per\ ml = Number\ of\ viable\ cells\ x\ dilution\ factor\ x\ 10{,}000$$

3.4.5.4 Frozen cell stocks

Cells were harvested, scored and pelleted as described previously and suspended in 95% complete media plus 5% dimethylsulphoxide (DMSO), a cryoprotectant. Cells were aliquoted into cryovials at 1-2x10^6 cells/ml and frozen at -80^{o}C overnight before transfer to long-term storage in liquid nitrogen.

3.4.6 Transfections

Endogenous microRNA levels were manipulated in the HK-2 cells through the transfection of microRNA miR 192 mimic, a gain-of-function experiment designed to determine the biological function of miR 192. Two different transfection facilitators were used – Lipofectamine 2000 and siPORT NeoFX (both Life Technologies).

3.4.6.1 Mimics, inhibitors and mimic control

mIRIDIAN microRNA mimics, inhibitors and mimic controls were purchased from Dharmacon (Lafayette, CO, USA). RNA (5nmol) was diluted in 0.25ml siRNA dilution buffer to form a 20µM stock. Lipofectamine 2000 and siPORT NeoFX transfection reagents were used and transfection conditions were determined following protocol optimisation.

3.4.6.2 Transfection optimisation

Transfection conditions were optimised for volume of lipofectamine transfection reagent used. A fixed amount of a fluorescent FAM oligonucleotide (1µM) was incubated with 4 different volumes of lipofectamine reagent, forming transfection complexes of increasing strength. Transfection was performed over 24 hours as described in 3.4.6.3. Optimal transfection reagent volume was determined by balancing transfection efficiency, defined as the percentage of incubated oligonucleotide successfully transfected into cells, and cell viability, determined through the alamarBlue assay (Life Technologies). AlamarBlue is an indicator dye that can quantitatively assess proliferation of cells in culture and is used to determined cytotoxicity. The active compound in

alamarBlue is Resazurin, which is reduced to resorufin by viable cells, leading to a colour change from non-fluorescent blue to fluorescent red.

Following 24 hours of transfection with FAM oligonucleotides, transfection media was removed, cells were washed twice with PBS and 500µl of fresh antibiotic free media was added. Fluorescence was measured at 485nm excitation and 520nm emission. To measure viability another 500µl fresh antibiotic free media was added to cells (total volume 1ml) and incubated with 100µl of alamarBlue for 1 hour at 37^{o}C. Flourescence was read at 560nm excitation and 590nm emission. Viability was measured as a percentage of the viability of untreated cells.

3.4.6.3 Lipofectamine 2000

MicroRNA 192 mimic transfections were performed in a sterile 24 well cell culture plates following the manufacture's protocol. Cells (50,000) were seeded in growth media minus penicillin/streptomycin and incubated overnight. Cells were at approximately 70% confluence the following day, when media was removed by suction and replaced with 400µl Opti-MEM. Then, 2.5µl RNA was added to 100µl Opti-MEM and 8 µl lipofectamine was added to 50 µl Opti-MEM. Both mixtures were incubated at room temperature for 10 minutes. Then, diluted RNA and diluted lipofectamine were mixed 1:1 and incubated for 20 minutes at room temperature to allow transfection complexes to form. Transfection complexes (100µl) were then added to the seeded cells and incubated at 37^{o}C for 24 hours.

3.4.6.4 siPORT NeoFX

Transfections were performed in a sterile 24 well cell culture plates, with 50,000 cells seeded per well, following the manufacture's protocol. One hour prior to transfection HK-2 cells at approximately 80% confluence were trypsinised and suspended to 110,000 cells/ml in complete media. Three different mimic transfection concentrations were assessed – 10nM, 20nM and 50nM. The mimic:reagent ratio was kept constant across all 3 transfection concentrations. siPORT transfection reagent was diluted in Opti-MEM as described in Table 3.2.

Table 3.2: siPORT/Opti-MEM dilutions

Reagent	Transfection concentration		
	10nM	**20nM**	**50nM**
siPORT (µl)	0.2	0.4	1
Opti-MEM (µl)	25.8	25.6	25

Mixtures were incubated at room temperature for 10 minutes. Transfected RNA was diluted in Opti-MEM as described in Table 3.3.

Table 3.3: RNA/Opti-MEM dilutions

Reagent	Transfection concentration		
	10nM	**20nM**	**50nM**
RNA (µl)	0.25	0.5	1.25
Opti-MEM (µl)	29.75	29.5	28.75

Diluted RNA and diluted siPORT were then mixed 1:1 and incubated for 10 minutes at room temperature to allow transfection complexes to form. Then, 50µl was dispensed into assigned wells of a 24 well plate and 450µl of cell suspension was overlaid onto the transfection complexes. Cells were incubated at 37^{o}C for 48 hours.

3.4.7 Cell RNA extraction

Two different RNA extraction protocols were performed on *in vitro* cell samples. Trizol was used to extract RNA following lipofectamine transfections and *mir*VANA PARIS was used following SiPORT.

3.4.7.1 Trizol

Trizol is a solution containing guanidinium thiocyanate, sodium acetate, phenol and choloroform and is one of the most commonly used methods to separate RNA from DNA. When Trizol is mixed with biological samples and centrifuged, RNA remains in the upper aqueous phase and DNA and protein remain in the lower interphase and organic phase. RNA harvested in the upper aqueous is then recovered following precipitation with isopropanol [254].

Following transfection, transfection media was removed by aspiration and each transfection well was washed twice with PBS. To each well 0.5ml Trizol was added to disrupt and homogenise cells and lysates were collected and stored at -80^{o}C until extraction. To extract RNA samples were thawed and mixed with 100µl of chloroform and incubated at room temperature for 5 minutes before centrifugation at 12,000g for 15 minutes at 4^{o}C. The aqueous phase was then collected and precipitated in 250µl isopropanol and 1µl of glucagon. The mixture was incubated for 10 minutes at room temperature and centrifuged at 12,000g for 10 minutes at 4^{o}C. Following centrifugation the supernatant was discarded and the remnant RNA pellet was washed in 0.5ml 75% ethanol twice before being air dried under a sterile fume hood. Pellets were then dissolved in 50µl RNase free water and warmed at 55^{o}C for 10 minutes. RNA extracts were stored at -80^{o}C until use. RNA samples were quantified by nanadrop, micro-volume, ultraviolet visible spectrophotometry which measures absorbance between 220nm and 350nm to determine the concentration of nucleic acids and the presence of contaminates.

3.4.7.2 MirVANA PARIS

Following SiPORT transfection RNA was extracted from cells using the *mir*VANA PARIS kit (Ambion). Transfection media was aspirated and the attached cells were washed with 0.5ml ice-cold PBS twice. The cell culture plate was then placed on ice and 250µl of ice-cold cell disruption buffer was added to each well to lyse the cells. The plate was then left on ice for 5 minutes and the cell lysates were dispensed into sterile 2ml centrifuge tubes. Equal volume of denaturing buffer was then added to cell lysates and the RNA extraction was continued from this step as previously described in 2.4.2. RNA was eluted in 75µl nuclease free water.

3.4.7.3 RT-PCR

MicroRNA was reverse transcribed into cDNA using the TaqMan MicroRNA Reverse Transcription kit (Applied Biosystems) as previously described in 2.4.4.1. Messenger RNA (mRNA) was reverse transcribed using the High Capacity Reverse Transcription kit (Applied Biosystems), which differs from microRNA RT due to the use of random primers instead of specific primers. The manufacture's protocol was followed. Briefly, a master mix was made comprising of 2µl 10X RT buffer, 0.8µl 25x dNTP mix, 2µl 10x random primers, 1µl reverse transcriptase enzyme and 4.2µl RNase free water per sample (total volume 10µl). The master mix was then mixed manually and 10µl was dispensed into 0.2ml PCR polypropylene reaction tubes per reaction. To this 10µl RNA was added and mixed manually. Reaction tubes were loaded onto a MJ Research PTC-200 Thermo Cycler (GMI) and reactions were incubated at 25^{o}C for 10 minutes, 37^{o}C for 120 minutes, 85^{o}C for 5 minutes and finally 4^{o}C until the samples tubes were retrieved. cDNA products were stored at -20^{o}C until use. Real time, qPCR was performed in triplicate on the Applied Biosystems 7500 Fast System as outlined in 2.4.4.2. MicroRNA expression was normalised to U6 small nuclear RNA and mRNA expression was normalised to GAPDH, a frequently used housekeeping gene.

3.4.8 Statistical analysis

All PCR data is expressed as fold change relative to preoperative levels. Data is represented as mean ± standard error of mean (SEM). Statistical significance was determined using ANOVA (with a linear trend) and paired/unpaired Student's t-test where appropriate. Significance was considered as $p<0.05$. Statistical analysis was performed using GraphPad Prism.

3.5 Results

3.5.1 Clinical outcomes

Bariatric surgery induced substantial clinical improvements in all patients (Figure 3.3). Reduction in BMI was significant within 100 days of surgery and mean BMI decreased by almost 30% 100 days or more after surgery (Figure 3.3A, p=0.031 and 0.0001 respectively, Student's t-test). Mean levels of glycated haemoglobin (HbA1c) and fasting blood glucose, two established markers of diabetes, also decreased following bariatric surgery. HbA1c decreased from almost 7% preoperatively to 5.5% 100 days or more following surgery (Figure 3.3B, p=0.027, Student's t-test). Diabetes is defined as HbA1c equal to or greater than 6.5% [255]. Mean levels of fasting blood glucose decreased from 7.5mmol/L preoperatively to 5.6 mmol/L 100 days or more following surgery. Estimated glomerular filtration rate increased slightly from 73 ml/min/1.72msq preoperatively to 79.7ml/min/1.72msq at 100 days or more following surgery. Kidney function is often assessed by eGFR.

3.5.2 Creatinine normalisation

Urinary microRNA expression was corrected to urinary creatinine levels to account for diuretic effect. Mean creatinine levels were unchanged prior to and following bariatric surgery (Figure 3.4).

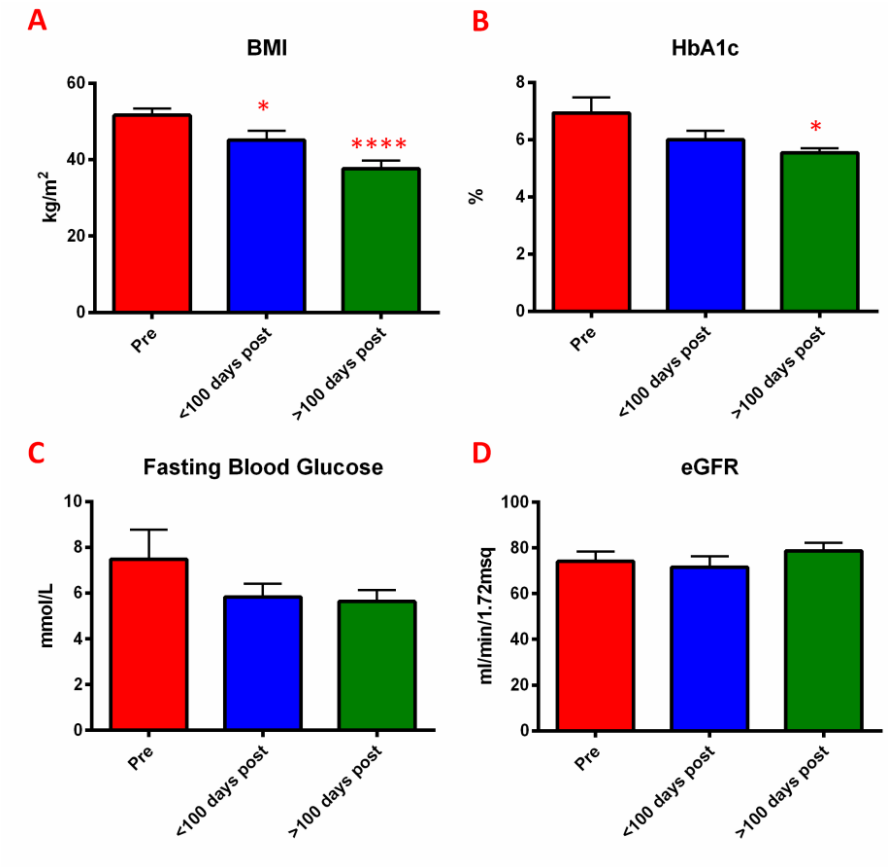

Figure 3.3: Clinical bariatric outcomes.

(A) BMI (B) HbA1c (C) fasting blood glucose and (D) eGFR levels preoperatively and at <100 days and >100 days following bariatric surgery. Data represent mean ± SEM. n=17-19. *p<0.05, ****p<0.0001 vs. preoperative level by Student's t-test.

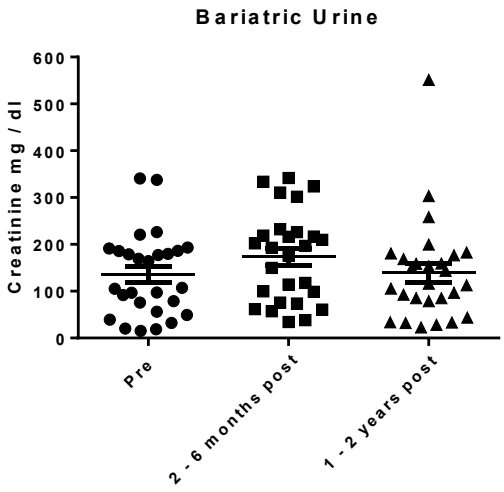

Figure 3.4: Urinary creatinine levels in bariatric urine.

Urinary creatinine levels preoperatively, 2-6 months and 1-2 years following bariatric surgery. Data represents mean ± SEM. n=27.

3.5.3 miR 192

Initially the urinary expression of miR 192, the preeminent microRNA in the kidney [256], was assessed. In patients who had laparoscopic RYGB, levels of miR 192 increased 1.28 and 2.8 fold respectively at 2-6 months and 1-2 years following surgery (Figure 3.5A, p=0.19 and 0.0012 respectively, paired t-test). A similar increase was observed in sleeve gastrectomy patients (Figure 3.5B). MiR 192 levels increased 1.27 fold at 2-6 months following sleeve procedures and 4.7 fold at 1-2 years postoperatively (p=0.68 and 0.013 respectively, paired t-test). Increase in urinary miR 192 levels was consistent when patients were stratified by preoperative diabetic status. In diabetic patients urinary levels of miR 192 increased 1.46 fold at 2-6 months and 3.6 fold at 1-2 years following bariatric surgery (Figure 3.6A, p=0.098 and 0.039 respectively, paired t-test). Pre-diabetic patients demonstrated a 1.54 fold increase at 1-2 years following surgery, although this was not statistically significant (Figure 3.6B). Non-diabetic patients demonstrated a significant 3 fold increase in miR 192 levels at 1-2 years following surgery (Figure 3.6C, p=0.031, paired t-test).

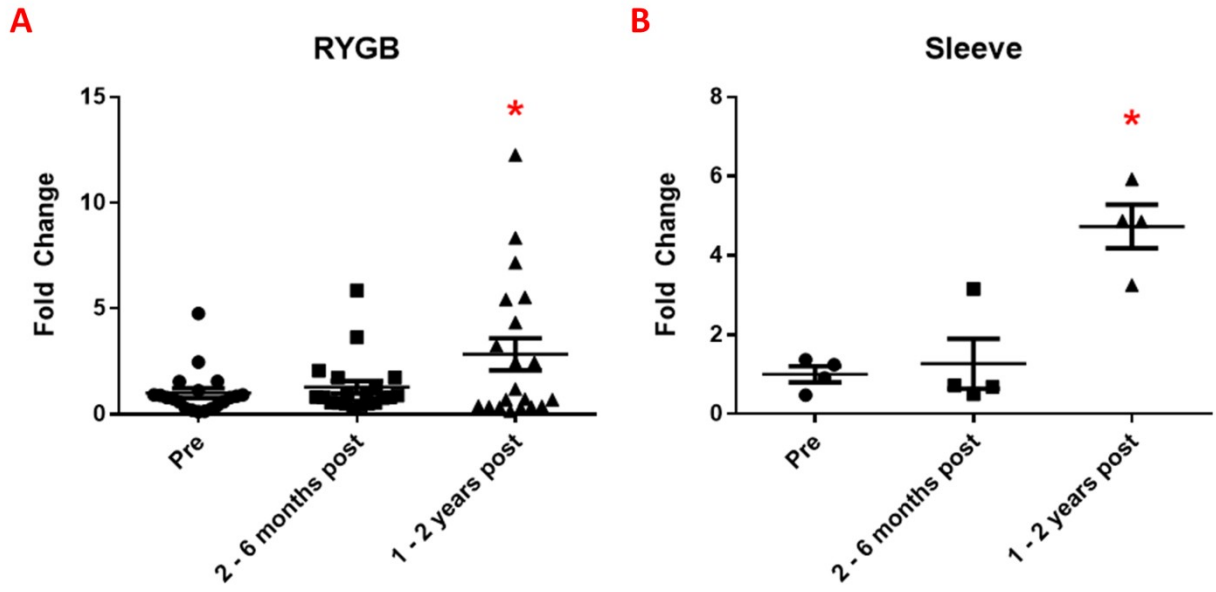

Figure 3.5: Urinary miR 192 expression following RYGB and Sleeve.

(A) RYGB patients. (B) Sleeve gastrectomy patients. Data represents mean fold change ± SEM relative to mean preoperative expression. n=20 for RYGB and n=4 for Sleeve. *p<0.05 vs. preoperative expression by paired t-test.

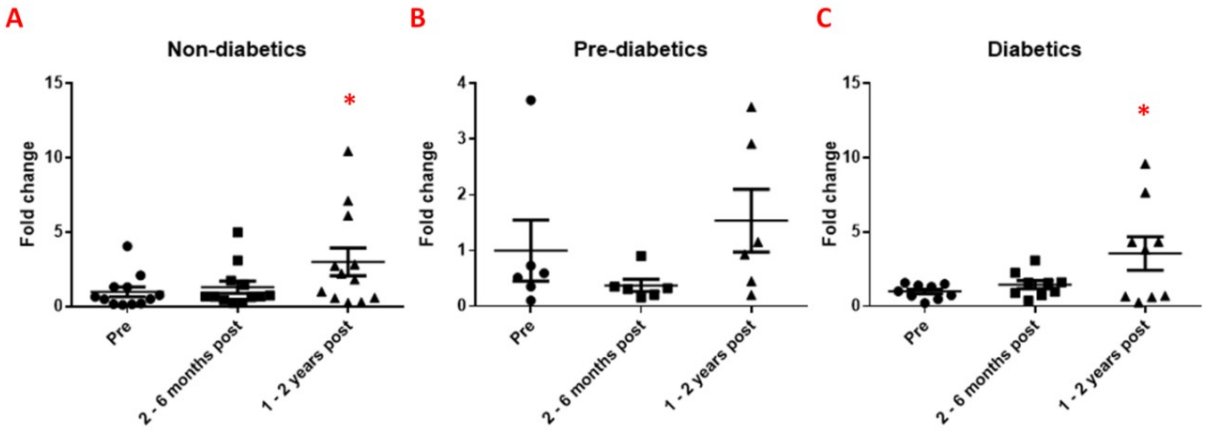

Figure 3.6: Urinary miR 192 expression following bariatric surgery across diabetic status.

(A) Non-diabetic, (B) pre-diabetic and (C) diabetic patients. Data represents mean ± SEM relative to mean preoperative expression. n=12 for non-diabetics, n=6 for pre-diabetics, n=9 for diabetics. *p<0.05 vs. preoperative expression by paired t-test.

Urinary miR 192 levels following bariatric surgery were compared to levels in a diverse BMI cohort described in the previous chapter. Relative to morbidly obese levels (BMI over 40), bariatric preoperative miR 192 levels were slightly lower (0.73 fold), likely reflecting the higher BMI in patients undergoing bariatric surgery (Figure 3.7A). MiR 192 expression was similar 2-6 months following surgery (0.76 fold). However, 1-2 years following bariatric surgery mean miR 192 level was nearly 2 fold higher relative to the morbidly obese cohort and was comparable to miR 192 levels in those with a healthy weight (BMI under 25). Although comparative two-way fold changes were not significant, the linear trend was (p=0.043, one-way ANOVA). An inverse correlation between fold change and BMI was also significant (p=0.0081, Pearson's correlation, Figure 3.7B). It appears bariatric surgery shifts urinary miR 192 expressions from levels observed in a morbidly obese population to levels observed in a healthy population.

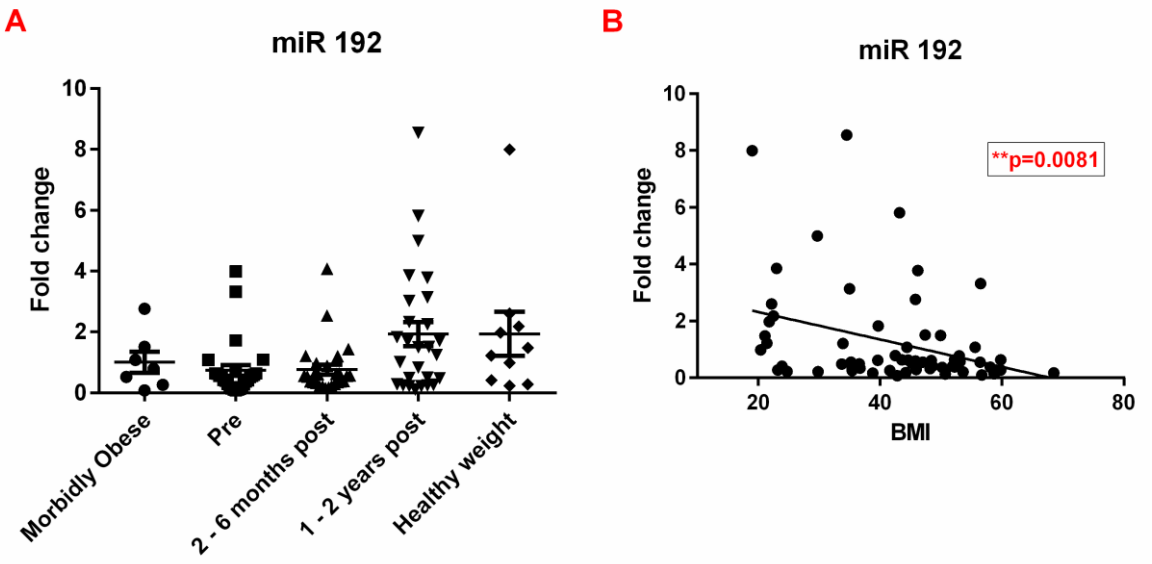

Figure 3.7: Bariatric urinary miR 192 expression relative to a morbidly obese cohort.

(A) Bariatric and healthy miR 192 expression relative to a morbidly obese population. Data represents mean ± SEM relative to mean preoperative expression. Morbidly obese is a BMI >40, healthy weight is a BMI <25. n=7 for morbidly obese, n=10 healthy weight, n=27 for preoperatively, 2 - 6 months and 1 - 2 years postoperatively. (B) Pearson correlation of miR 192 fold change against BMI. n=63, **p<0.01.

Of the 27 individuals who made up the bariatric cohort, 22 had increased urinary miR 192 expressions postoperatively relative to their preoperative levels, including 16 out of the 20 RYGB patients, 11 out of 15 diabetics and all 4 sleeve patients. A timecourse of postoperative miR 192 expressions in RYGB patients relative to their individual preoperative miR 192 levels can be found in Figure 3.8. A significant correlation was demonstrated between individual, personalised fold changed in miR 192 levels and days follow surgery (p=0.029, Pearson's correlation). This illustrates a trend of a gradual, general increase in miR 192 levels in urine which is enhanced and sustained with time.

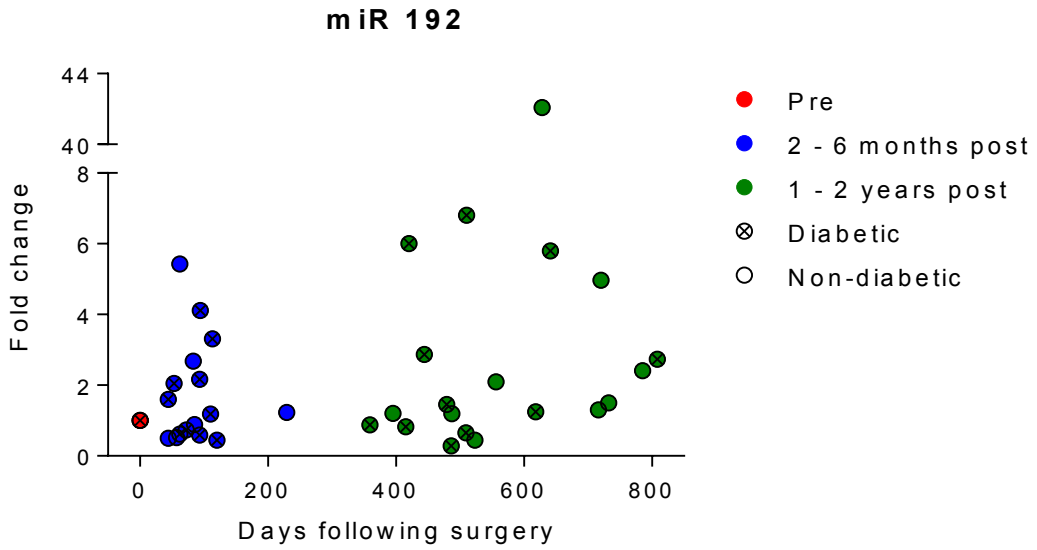

Figure 3.8: Timecourse of miR 192 expression following surgery.

Data represented as fold change relative to individual preoperative expression for 20 RYGB bariatric patients.

3.5.4 miR 200 family

Urinary levels of miR 200a and miR 200b were also measured. Both are expressed in the kidney and are involved in diabetic nephropathy. MiR 200a urine levels increased 2.5 fold at 2-6 months and 3.4 fold at 1-2 years following surgery (Figure 3.9A). Neither increase was statistically significant. MiR 200b levels increased 5.8 fold at 2-6 months and significantly 28.6 fold at 1-2 years postoperatively (p=0.003, Figure 3.9B, paired t-test). All but one patient demonstrated a postoperative increase of urinary miR 200a and miR 200b relative to their individual preoperative level. Significant correlations were observed between both miR 200a and miR 200b and days follow bariatric surgery (Figure 3.10, p=0.0071 and 0.044 respectively, Pearson's correlation).

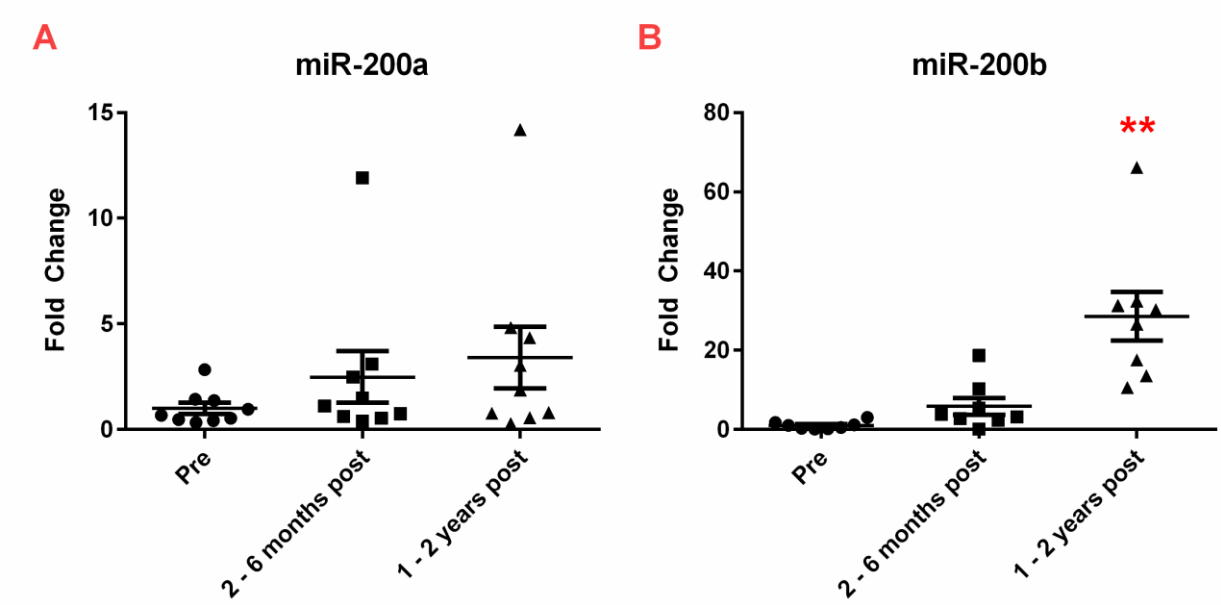

Figure 3.9: Urinary expression of miR 200 following bariatric surgery.

(A) miR-200a. n=9 (B) miR-200b. n=8. Data represents mean fold change ± SEM relative to mean preoperative expression. **p<0.01 vs. preoperative expression by paired t-test.

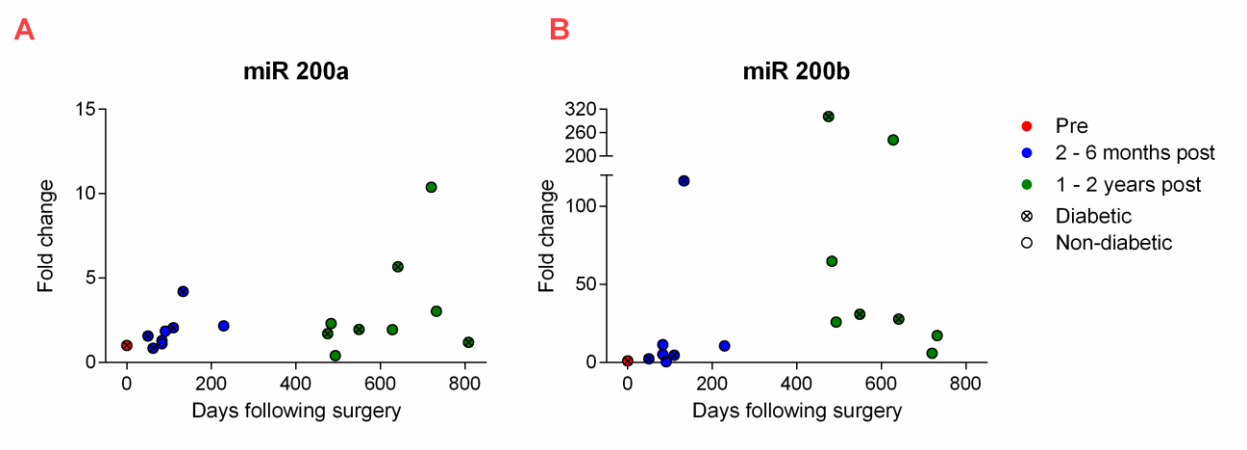

Figure 3.10: Timecourse of miR 200 expression following surgery.

(A) miR 200a. (b) miR 200b. Data represented as fold change relative to individual preoperative expression.

3.5.5 Transfections

3.5.5.1 Lipofectamine

Four different volumes of lipofectamine transfection reagents were assessed to determine the optimal delivery method for a set concentration of fluorescent oligonucleotide into HK-2 cells. Lipofectamine proved cytotoxic as only 53% of cells were viable after 24 hours with 2µl of Lipofectamine (Figure 3.11). However, increasing lipofectamine volume did not appear to decrease viability substantially, as quadrupling lipofectamine volume to 8µl only decreased viability a further 8% to 44%. However, transfection efficiency markedly increased with increasing lipofectamine. Transfection efficiency was 8% with 2µl of lipofectamine and that more than trebled to 26% with 8µl of lipofectamine. As a result 8µl of lipofectamine was used to transfect miR 192 mimic.

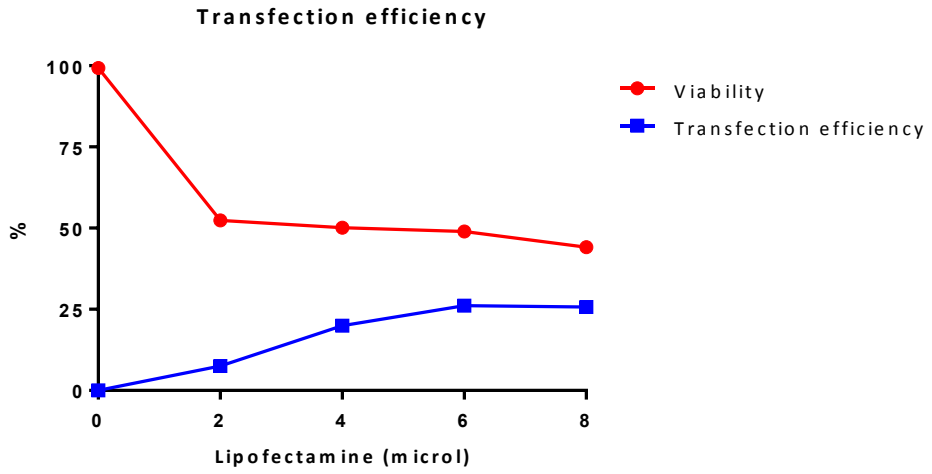

Figure 3.11: Transfection optimisation.

Transfection efficiency (blue) and viability (red) with increasing lipofectamine concentrations after 24 hours. Each point is a mean of two determinations.

HK-2 cells were transfected with miR 192 mimic (50nM final concentration) for 24 hours and RNA was extracted using Trizol. Transfection with miR 192 mimic resulted in an approximately 1,500 fold increase relative to cells transfected with a scrambled control (Figure 3.12, p=0.0012, Student's t-test). Incubation of the miR 192 alone without lipofectamine did not increase miR 192 levels relative to control cells, indicating the absence of any significant gymnotic transfection [257]. Levels of miR 192 were also unchanged in cells incubated with only lipofectamine and untreated cells.

Successful transfection of miR 192 however had no effect on miR 200a levels or the mRNA levels of ZEB1, ZEB2 or Colα1 relative to control-transfected cells (Figure 3.13).

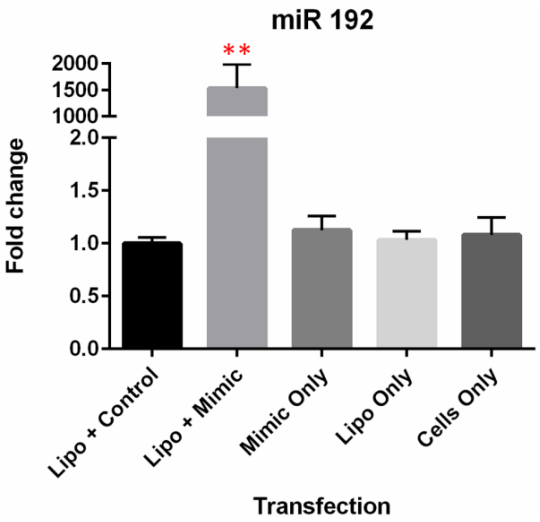

Figure 3.12: miR 192 expression following lipofectamine miR 192 mimic transfection.

Data represents mean ± SEM relative to transfection with a scrambled control. **<p=0.01, n=4.

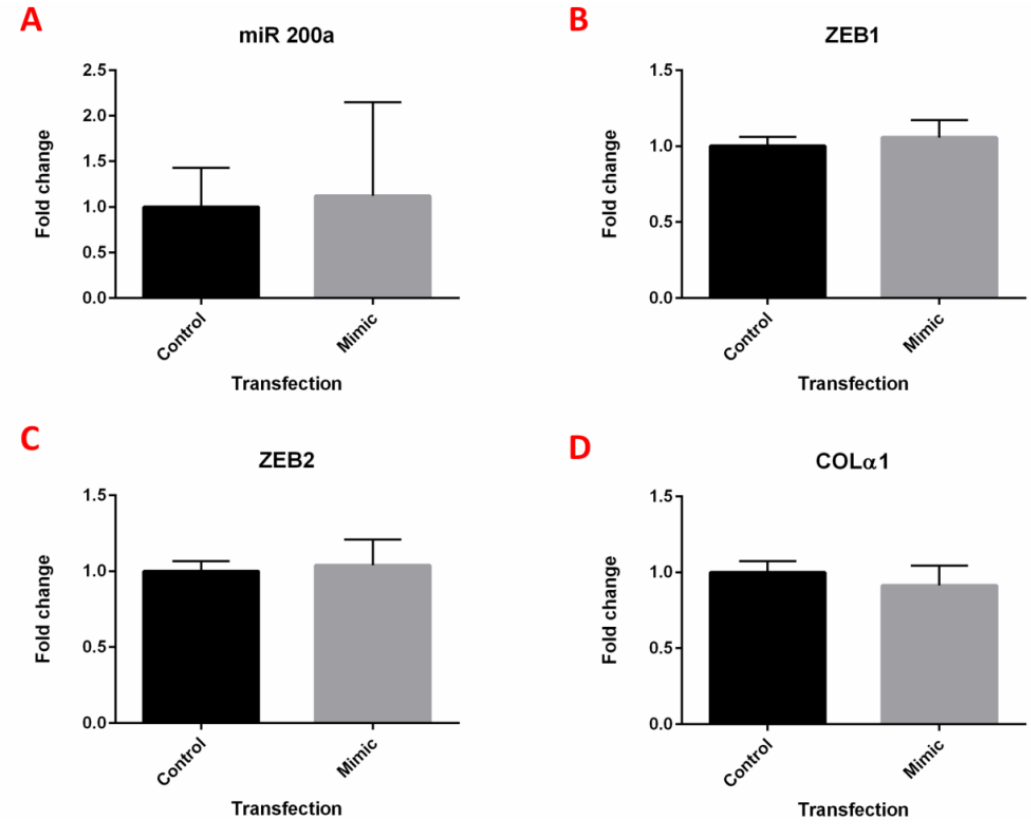

Figure 3.13: Effects of lipofectamine miR 192 mimic transfection.

Expression of (A) miR 200a (B) ZEB1 (C) ZEB2 and (D) Colα1 following after 24 hours of miR 192 mimic transfection. Data represents mean ± SEM relative to transfection with a scrambled control. n=4.

3.5.5.2 SiPORT

Due to the low transfection efficiency and considerable cytotoxicity observed with lipofectamine, HK-2 cells were also transfected with miR 192 mimic using siPORT NeoFX. Three transfection concentrations were assessed to determine the possibility of a dose response – 10nM, 20nM and 50nM. The mimic:reagent ratio was kept constant across all 3 transfection concentrations. The transfection time was also increased from 24 hours to 48 hours, doubling the time for miR 192 mimic to exert its activity. The mirVana PARIS kit was used to extract RNA instead of Trizol.

Transfection with all three concentrations of miR 192 mimic was successful and increased miR 192 expression 4,000 fold, 16,000 fold and 18,000 fold respectively relative to cells transfected with a scrambled control (Figure 3.14A, $p<0.001$ for all three, Student's t-test). However, only 10nM significantly increased miR 200a levels (Figure 3.14B, $p=0.015$, Student's t-test). Expression levels of ZEB1 and Colα1 were unaltered for all three miR 192 mimic concentrations (Figure 3.14C&E). However, transfection with 50nM miR 192 mimic concentration resulted in a significant 0.63 fold decrease in ZEB2 (Figure 3.14D, $p=0.04$, Student's t-test).

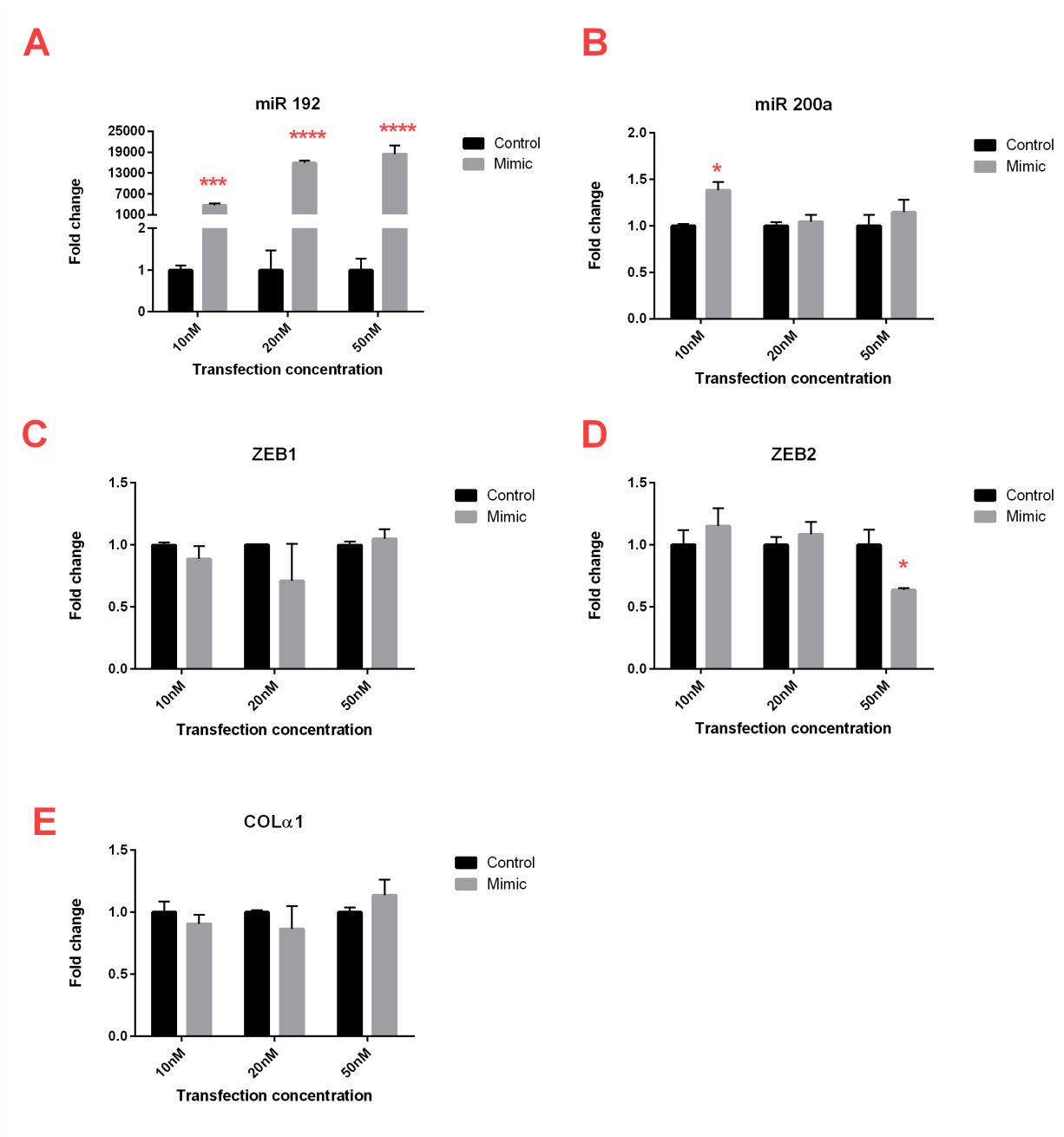

Figure 3.14: SiPORT miR 192 mimic transfection.

Expression of (A) miR 192 (B) miR 200a (C) ZEB1 (D) ZEB2 and (E) Colα1 following after 48 hours of 10nM, 20nM and 50nM miR 192 mimic transfection. Data represents mean ± SEM relative to transfection with a scrambled control. *p<0.05, **<p0.01, ***p<0.001, ****p<0.0001, n=3.

3.6 Discussion

Three kidney-expressed microRNAs, miR 192, miR 200a and miR 200b, were shown to be upregulated in urine following bariatric surgery, an increase that was consistent across surgical type and diabetic status and was sustained and enhanced with time. Upregulation of miR 192 and the miR 200 family was also accompanied by improvement in clinical parameters, including HbA1c. Bariatric surgery shifts urinary miR 192 expression from morbidly obese levels to levels seen in a healthy cohort, and the transfection of miR 192 in a kidney PTC cell line increased miR 200a and decreased ZEB2, a key transcriptional promoter of kidney fibrosis. These three microRNAs could potentially represent non-invasive, anti-fibrotic biomarkers for surgery-induced improvement in renal function.

The kidney-specific deletion of Dicer in mice leads to proteinuria, glomerular disease and tubular injury, illustrating the important functional roles of microRNAs in kidney pathophysiology [258-260]. MiR 192 is one of 5 microRNAs whose expression is higher in the kidney relative to other organs [256], and its levels are reduced in human renal biopsies from patients with advanced diabetic nephropathy, levels that correlate with tubulointerstitial fibrosis and decreased GFR, reflecting miR 192's key anti-fibrotic role [178]. *In vitro* incubation of PTCs with TGF-β1 decreases miR 192 expression and the overexpression of miR 192 suppresses ZEB1 and ZEB2, decreasing TGF-β1 mediated E-cadherin suppression [178]. In diabetic apoE mice, miR 192 expression was downregulated in the kidney and treatment of PTCs with TGF-β1 results in a reduction of miR 192 [183]. Renal levels of the miR 200 family are decreased in mouse models of renal scarring and by TGF-β1 in rat PTCs [222]. Injection of miR 200b precursor antagonises ZEB1/ZEB2 induction, decreases collagen synthesis and ameliorates fibrosis [245]. p53 tumor suppressor increases expression of miR 192 and miR 200, suppressing EMT [261]. MiR 200 expression is a strong biomarker for epithelial versus mesenchymal phenotype in cancer [262]. MiR 200 overexpression leads to mesenchymal to epithelial transition in mouse carcinomas and overexpressing miR 200 *in vitro* increases E-cadherin and represses EMT [179, 180]. Here, miR 192 transfection led to an

increase in miR 200a, indicating miR 192 acts upstream to miR 200 in a hierarchical regulation pathway, suggesting miR 192 is a master microRNA regulator in the kidney. Previously miR 192 has been shown to upregulate miR 200b/c expression in mesangial cells [263].

In contrast, miR 192 and miR 200 appear to have pro-fibrotic effect in mesangial cells. TGF-β1 increases miR 192 in mouse mesangial cells and repression of ZEB1/ZEB2 expression by miR 192 leads to collagen synthesis [181]. The inhibition of miR 192 in streptozotin-induced diabetic mice reduces proteinuria [182]. In mesangial cells, miR 200 family represses ZEB1/ZEB2, promoting fibrosis [263]. This likely reflects the complexity of the kidney and the pleiotropic roles miR 192 and miR 200 play in renal physiology appear to be cell specific. Indeed, the renal cortex and the medulla have different microRNA expression profiles [264]. It is worth noting that proximal tubular cells are further along the urinary tract than mesangial cells of the glomerulas and that urinary levels of miR 192 and miR 200 are decreased in patients with bladder cancer, correlating with increased EMT [265].

This study was only able to show a slight increase with eGFR following surgery, but other studies have found bariatric surgery significantly improves renal function. Weight loss is associated with a reduction in proteinuria, including weight loss achieved surgically [249-251]. Bariatric surgery improves renal function in patients with pre-existing glomerular hyperfiltration [250]. Surgery also leads to reduced levels of albuminuria one year postoperatively, and levels continue to decrease up to two years and were maintained up to 5 years post-surgery [79, 266]. Remission of microalbuminuria in diabetics can reach 60% 5 years following surgery. Surgery also has preventive effects, reducing the incidence of microalbuminuria by 80% and diabetic nephropathy by 60% compared to patients treated medically [79]. Bariatric surgery can also lead to improvement and remission in patients with established chronic kidney disease [267]. The results presented here suggest miR 192 may mediate these renal improvements following bariatric surgery.

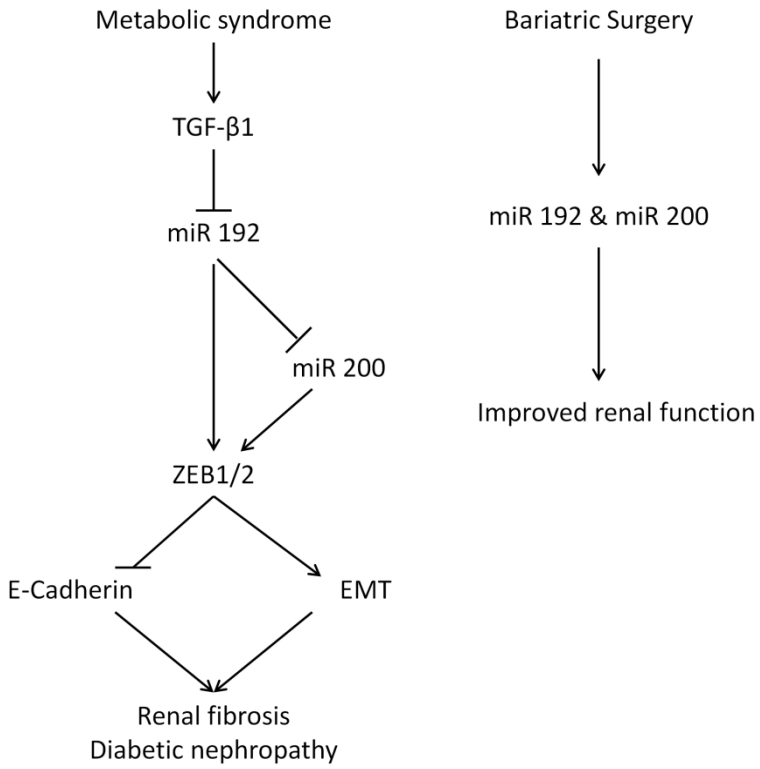

Figure 3.15: MiR 192 and 200 in renal function.

(Left) Mechanism for glucose-mediated renal fibrosis in the proximal tubular cells. Diabetes increases TGF-β which inhibits miR 192/200, lifting the suppression on ZEB and EMT. (Right) Mechanism following bariatric surgery.

The early detection of DN is important in preventing progression to renal failure. There are considerable limitations of conventional markers of kidney function. The sensitivity and specificity of proteinuria and eGFR is poor, particularly in obese patients, and only manifest late in the disease process. Novel markers of DN have been reported, including proteins, peptides and growth factors [268]. A number of studies have reported distinct microRNA profiles in urine, urinary sediments and circulation in cases of kidney diseases. MicroRNA 145 is upregulated in the urinary exosomes of type 1 diabetics with microalbuminuria [238] and urinary microRNA profiles can be used to differentiate various stages of diabetic nephropathy in individuals with type 1 diabetes [211]. In circulation, increased levels of miR 25, miR 27, miR 152 and miR 182 has been reported in patients with type 1 diabetes [269], and a recent report identified 10 elevated and 2 lowered microRNAs in diabetic

patients with DN relative to healthy controls [270]. Circulating microRNAs can select diabetic patients with DN from those with good renal function, suggesting prognostic potential [270]. This has led to interest in microRNAs as potential novel drug targets. The successful manipulation of miR 192 expression in the renal cortex of normal and diabetic mice suggests the same may be possible in humans [271].

Other microRNAs have been reported to be involved in DN, including miR 21, miR 25 and miR 29 [272-274]. The expression of more microRNAs need to be assessed in bariatric urine to get a more comprehensive representation of the post bariatric urinary microRNA profile. Over-expressing miR 192 decreased ZEB2 but the effects on fibronectin and collagen protein levels need to be assessed, as does the effects of glucose treatment of PTCs on microRNA. However, there are limitations to using *in vitro* models of renal function, as EMT is more commonly observed in immortalised cell lines than *in vivo* renal fibrosis [275]. The role of microRNAs in mediating the post-bariatric improvements in renal health needs to be confirmed in larger, prospective, multi-centre studies of bariatric patients including cohorts with varying degrees of kidney dysfunction.

To summarise, bariatric surgery increased the urinary expression of the anti-fibrotic microRNAs miR 192 and miR 200, providing fresh insights into the mechanisms behind improvements in renal function following bariatric surgery. MiR 192 and miR 200 represent potential novel, non-invasive biomarkers of obesity-associated renal function and could potentially be used to monitor operative outcomes and aid in patient selection.

4 Circulating microRNA profiling following bariatric surgery

4.1 Justification

Bariatric surgery is the most effective intervention strategy at achieving sustained weight loss. In addition, bariatric surgery leads to the remission of type 2 diabetes and a reduction in cancer risk [26, 116]. However, the precise mechanisms behind these beneficial effects are not completely understood. Recently, a microRNA study in a bariatric rat model found that surgery altered the expression of 14 circulating microRNAs and provided a mechanistic role for microRNAs in the altered postoperative metabolic changes and suggested an involvement in a gut-brain signalling axis [214]. Another study in humans reported that RYGB also modulates circulating microRNAs, but did not offer mechanistic insights [208].

The objective of this chapter was to assess the effect of RYGB on circulating microRNA expression profiles across a number of post-bariatric timepoints and to identify potential microRNA biomarkers associated with the health benefits of bariatric surgery. Consequently, a plasma sample was obtained preoperatively and at 1 month, 3 months, 6 months, 9 months and 12 months after RYGB (during standard postoperative check-up visits) and a circulatory microRNA profile was characterised.

4.2 Aim

To assess the effect of Roux-en-Y gastric bypass on circulating microRNA expression profiles.

4.3 Study design

Plasma samples were collected from 4 men and 5 women undergoing laparoscopic Roux-en-Y gastric bypass at Hull and East Yorkshire NHS Trust in the United Kingdom under ethics approval 10/H1304/13. All patients were morbidly obese prior to surgery and met qualifying criteria for bariatric surgery set out by NICE [49]. Plasma samples were collected and BMI and blood glucose were measured immediately preoperatively and at one month, three months, six months, nine months and one year postoperatively. All participants provided informed written consent prior to the study. A study summary table can be found in Table 4.1.

Table 4.1: Study Summary Table [ǂ]

Patients	Total
n	9
Age (years)	46.1 (9.8)
Sex (female)	5/9
Diabetics (T2DM)	2/9
BMI (kg/m^2)	49 (10)
Blood glucose (mmol/L)	7.5 (5.4)

[ǂ]Values represent mean unless otherwise stated. Values in parenthesis represent standard deviation.

RNA was extracted from plasma samples and circulating microRNA profiles were characterized at all time points using Exiqon's miRCURY LNA plasma/serum PCR panels, measuring expression of 179 microRNAs known to be expressed in circulation [276]. A study design flow chart can be found in Figure 4.1.

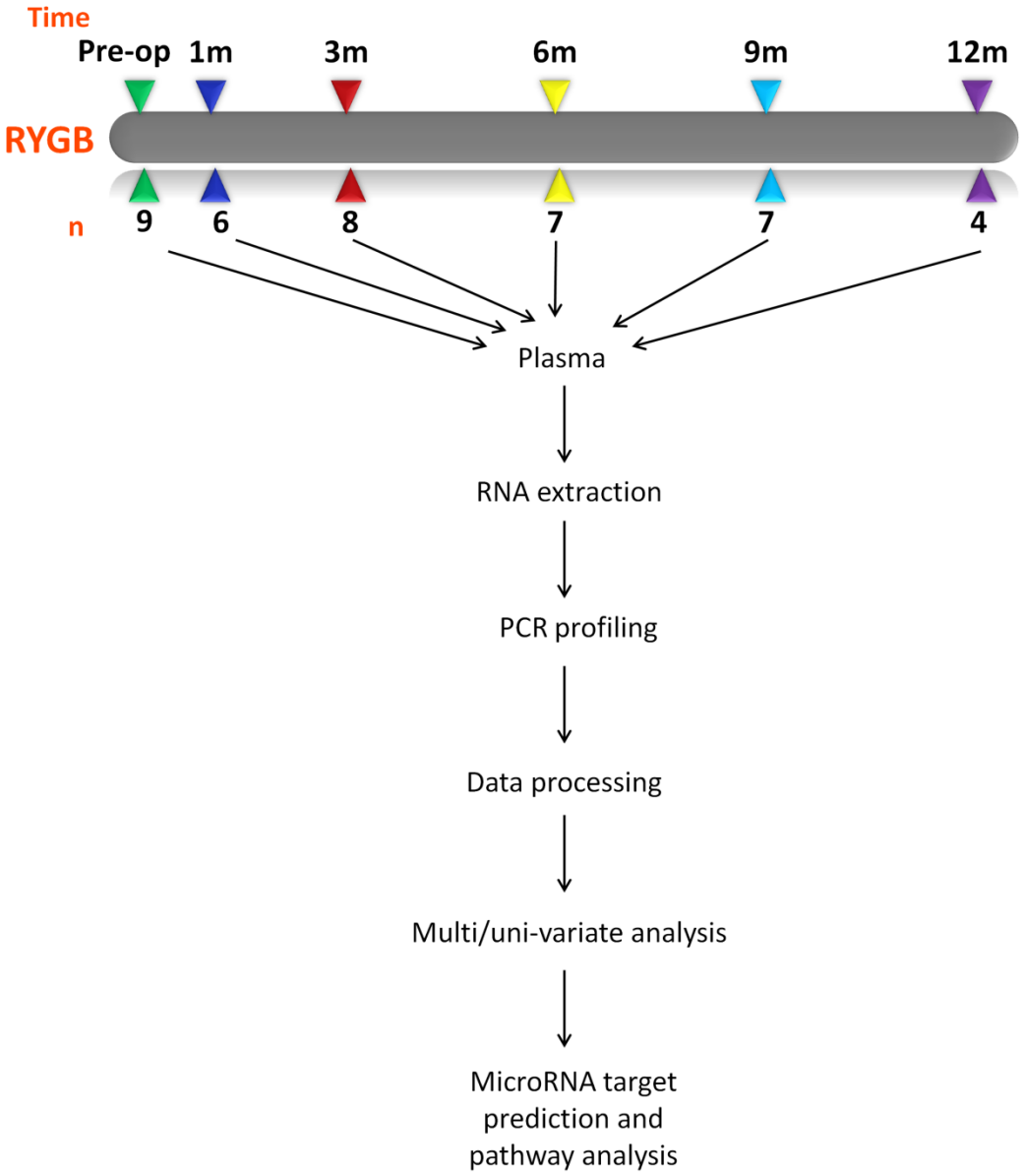

Figure 4.1: Flow chart illustrating the study design of chapter 4.

4.4 Materials and methods

4.4.1 Samples preparation and extraction

Plasma samples were acquired by standard venipuncture and centrifugation in EDTA-coated vacutainer tubes (Becton Dickinson) by collaborators at the University of Hull. Samples were stored in -80^{o}C until use. RNA was extracted from 100µl plasma using the *mir*Vana PARIS Isolation Kit (Life Technologies) and eluted in 100µl nuclease free water. A detailed, step-wise protocol can be found in section 2.4.2 in Chapter 2.

4.4.2 Profiling

Plasma samples were profiled using Exiqon's miRCURY locked nucleic acid (LNA) platform and Serum/Plasma Focus microRNA PCR panels. Panels consisted of two 96-well plates preloaded with LNA microRNA primers for 179 microRNAs, selected for their typical expression in circulation [276]. Panels also include primers for UniSp3 inter-plate calibrators and RNA spike-ins as well as blank wells as negative controls. This platform was selected for its high specificity, reproducibility and sensitivity in profiling circulating microRNAs [277].

Profiling was a two-step process:

1. Universal Reverse Transcription - a one first-strand cDNA synthesis that can be used as a template for multiple microRNA PCR reactions.
2. LNA PCR amplification with specific forward and reverse microRNA cDNA primers detected through the SYBR Green dye.

4.4.2.1 Universal reverse transcription

RNA was reverse transcribed into cDNA using the Universal cDNA Synthesis Kit (Exiqon). The manufacture's protocol was followed. A master mix was initially made consisting of 5X reaction buffer (which includes universal reverse transcription primer), enzyme mix, a synthetic UniSp6 RNA spike-in (10^8 copies/µl) and nuclease-free water as described in Table 4.2.

Table 4.2: RT Master Mix components

Component	Volume, per reaction (µl)
5X Reaction buffer (manufacturer's specification)	4
Enzyme mix	2
Synthetic UniSp6 RNA Spike in	1
Nuclease-free water	9
Total volume	16

Once created the master mix was manually mixed and 10µl was dispensed into a 0.2ml PCR polypropylene reaction tube per reaction. To this 4µl of RNA was added to produce a 20µl RT reaction. Reaction tubes were loaded onto an MJ Research PTC-200 Thermo Cycler (GMI) and reactions were incubated at 42°C for 60 minutes, then 95°C for another 5 minutes to heat-inactivate the reverse transcriptase, and finally 4°C until the samples tubes were retrieved. cDNA products were stored at -20°C until use.

4.4.2.2 Profiling of circulating microRNA

Before Serum/Plasma Focus microRNA PCR panels were used, the plates were centrifuged briefly. cDNA (20µl) was diluted 50X in 940µl nuclease-free water and 40µl ROX Dye, a passive reference dye whose fluorescence does not change during the reaction. Equal volume (1,000 µl) of SYBR Green PCR master mix was then added, which included DNA polymerase, dNTPs and the SYBR Green dye. This master mix was then manually mixed and 10µl was added to each well across the 2 plates that made up the panels. Once fully loaded, PCR plates were sealed with an optical film and centrifuged briefly. Quantitative PCR was carried out on the StepOnePlus 7500 PCR system (Life Technologies). Quantitative PCR reactions consisted of 95^{o}C for 10 minutes to allow for polymerase activation/denaturation, 45 amplification cycles of 95^{o}C for 10 seconds followed by 60^{o}C for 1 minute. Quantitative PCR reactions were concluded with a melting curve to disassociate the SYBR Green dye from amplification product, allowing the specificity of the amplification to be assessed.

4.4.2.3 Pre-processing

A threshold of 0.2 ΔRn was arbitrarily set and this remained consistent for every PCR reaction (explained in section 2.4.4.3). A C_t was obtained for every reaction, measured at the point the threshold is met by the amplification curve. Pre-processing and initial analysis of profiling data was performed with GenEx6 software (Exiqon) [278]. All data were subject to inter-plate calibration (through expression of UniSp3). Synthetic UniSp6 was added at the RT stage and this served as cDNA synthesis quality control. Threshold for expression was set as C_t <37, and microRNAs not expressed under this criteria in over 60% of samples were removed from consideration. All microRNA expression was normalised to four endogenous microRNAs, miR 223-3p, miR 26a, miR 101-3p and miR 19a, selected for their relative expression stability (see section 4.5.2) as determined by the geNorm [279] and Normfinder [280] algorithms. All microRNA expression levels were log transformed and expressed relative to preoperative mean.

4.4.3 Target prediction and pathway analysis

Each microRNA has hundreds of potential mRNA targets. Bioinformatic computational modelling was used to predict mRNA targets for each microRNA found to be differentially expressed following bariatric surgery. The miRWalk (v.2) database of predicted and validated microRNA targets [281] and the PANTHER (protein annotation through evolutionary relationship) classification system [282] was used to predict regulated pathways as previously described [214]. MiRWalk compiles putative mRNA targets from 10 target prediction algorithms – DIANA-mT, miRanda, miRDB, miRWalk, RNAhybrid, PICTAR4, PICTAR5, PITA, RNA22 and TargetScan. These algorithms predict mRNA targets by assessing 3'/5' UTR and coding sequence binding, sequence conservation, free energy stability and site accessibility and differ by their stringency criteria [283, 284]. To ensure confidence and accuracy in predicted targets only targets predicted by 2 or more algorithms were included in the analysis.

The PANTHER classification system is a comprehensive library of all protein coding genes from over 80 organisms (including humans) that have been annotated into 176 pathways [282]. Predicted targets obtained by miRWALK were uploaded into PANTHER's (v.10) gene list analysis tool and compared to PANTHER's datasets to determine which pathways were statistically overrepresented or underrepresented.

4.4.4 Data analysis

Principal component analysis (PCA) pattern recognition was applied to visualise differences in whole microRNA profiles prior to and following RYGB. PCA reduces multivariate data into components; the first component describes the greatest variation in the dataset, the second component describes the second greatest of variation and so on. MicroRNA profiles were converted into coordinates and plotted on a principal component space to allow clustering of similar profiles and separation of dissimilar profiles [285, 286].

Data is represented as mean ± SEM. Statistical significance was determined by Student's t-tests. The relationship between microRNA expression and clinical parameters was determined by Pearson's correlation. Significance was considered as $p<0.05$. All statistical analysis was performed on GraphPad Prism or R (www.r-project.org).

4.5 Results

4.5.1 Clinical outcomes

All patients demonstrated substantial time-dependent reduction in BMI following surgery (Figure 4.2A). Reduction in BMI was significant within 3 months following RYGB ($p=0.02$, Student's t-test) and continued to gradually decrease. Mean BMI at 12 months was 37% lower than mean preoperative BMI ($p=0.0056$, Student's t-test). Patients lost on average 15.7% of their preoperative BMI by 1 month postoperatively, 21.9% by 3 months postoperatively, 26.2% by 6 months postoperatively, 31.8% by 9 months postoperatively and 29.6% by 12 months postoperatively (Figure 4.2B). There were no significant changes in mean blood glucose following surgery (Figure 4.2C). Only 2 out of the 9 patients in this study were diabetic and both demonstrated decreases in postoperative blood glucose relative to their individual preoperative level (Figure 4.2D).

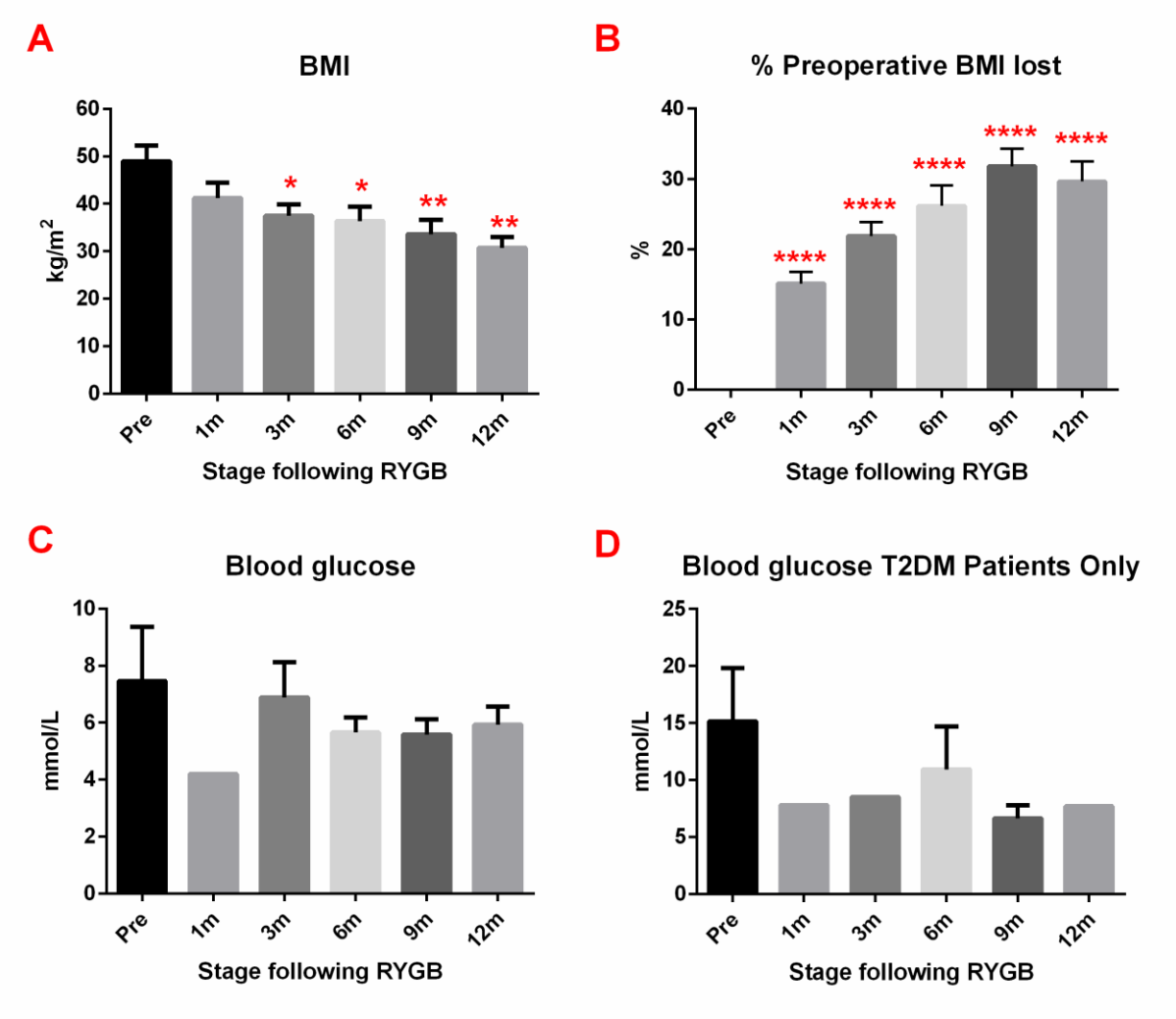

Figure 4.2: Clinical bariatric outcomes.

Changes in (A) BMI, (B) % preoperative BMI lost, (C) blood glucose following RYGB and (D) blood glucose following RYGB for patients that were diabetic preoperatively only. Data represent mean ± SEM. n=1-9. *p<0.05, **p<0.01, ****p<0.0001 vs. preoperative level by Student's t-test.

4.5.2 PCR validation

As the Exiqon plasma/serum microRNA panels are a quantitative PCR profiling platform, validation of profiling results with TaqMan PCR (section 2.4.4) was deemed unnecessary. The expression of only miR 122 was determined by both methods. Expression levels of miR 122 as measured by the two methods were comparable and correlated well (Figure 4.3, r=0.8252, p=0.0009, Pearson's correlation).

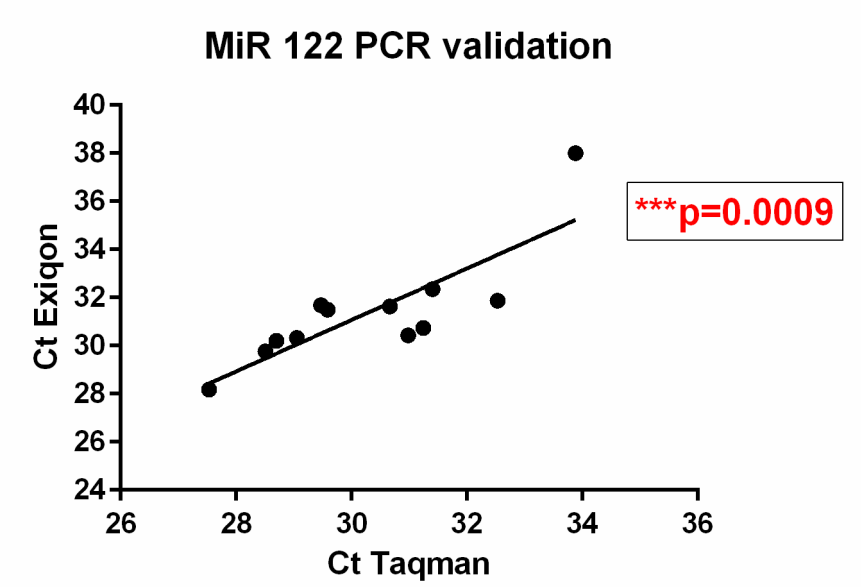

Figure 4.3: Raw Ct values of miR 122 expression as determined by Exiqon's PCR panel microRNA profiling and TaqMan quantitative PCR.

Pearson's correlation. ***p<0.001.

4.5.3 Normalisation

Profiling found 159 microRNAs that surpassed detection threshold. The large nature of profiling data leads to multiple normalising options to minimise technical variation. Four different normalising techniques were assessed. MicroRNA expressions were (1) not normalised, (2) normalised to the mean expression of all expressed microRNAs (global mean), (3) normalised to UniSp6, a synthetic RNA spiked in at the reverse transcription stage and (4) normalised to miR 223-3p, miR 26a, miR 101-3p and miR 19a, four endogenous microRNAs deduced and selected with the aid of GeNorm and Normfinder algorithms due to their relative stability in expression across all samples (Table 4.3). Overall variation was assessed through coefficient of variances (CV), calculated for each expressed microRNA for both the preoperative and postoperative groups. This was plotted against the cumulative distribution, as previously described [287] (Figure 4.4A).

Normalisation to global mean and UniSp6 significantly decreased mean CVs of the 50% least variable microRNAs compared to no normalisation ($p < 0.0001$ for both, unpaired t test; Figure 4.4B). However, the optimum method was normalisation to the four stable endogenous microRNAs, which displayed significantly lower mean CVs of the 50% least variable microRNAs compared to all other assessed methods (Figure 4.4B, $p < 0.0001$ v non normalised and global mean, $p = 0.0006$ v UniSp6, unpaired t test). As a result all profiling data was normalised to the miR 223-3p, miR 26a, miR 101-3p and miR 19a combination.

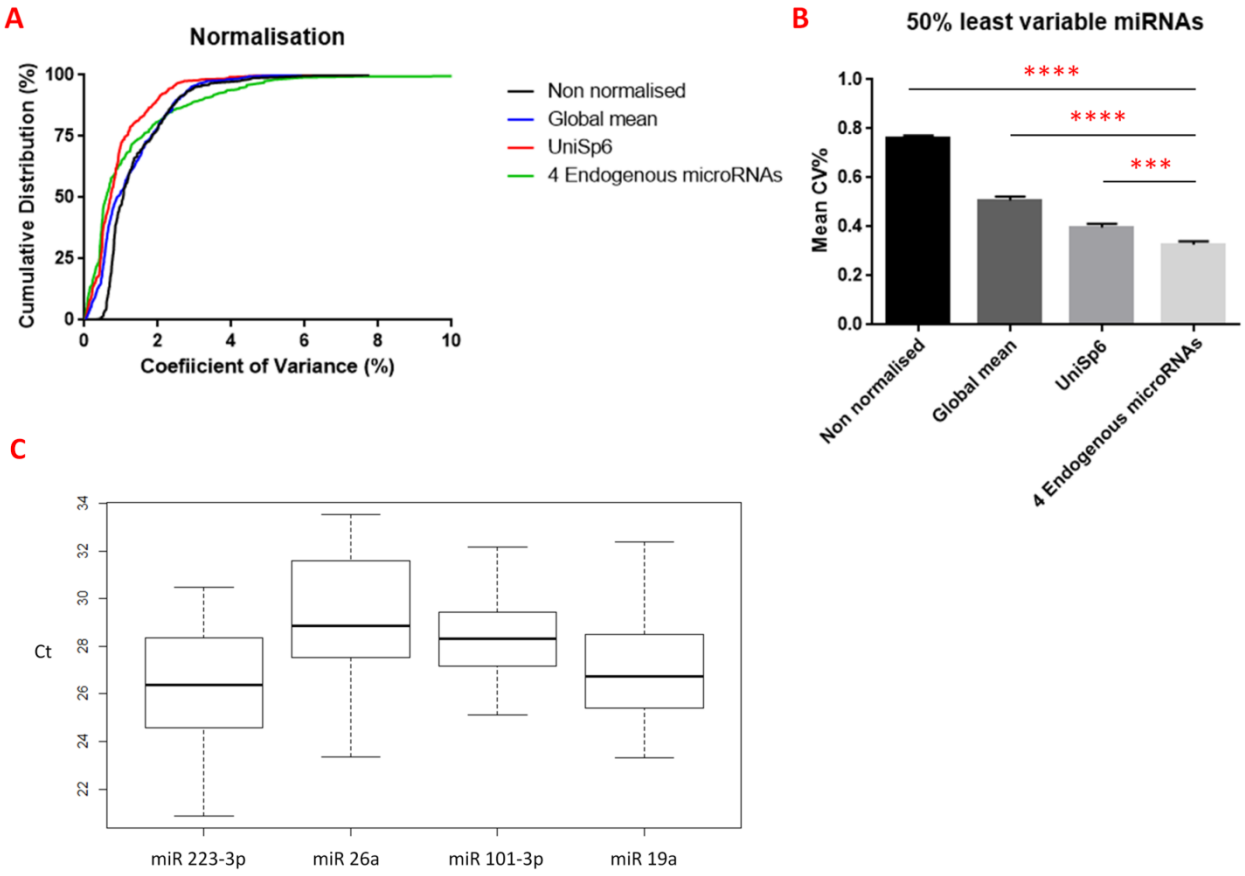

Figure 4.4: Normalisation of profiling data.

(A) Coefficient of variance against cumulative distribution for each expressed microRNA not normalised (black), normalised to global mean (blue), UniSp6 (red) and 4 endogenous microRNAs (green). (B) Mean coefficient of variance of the 50% least expressed microRNAs for the four different normalisation methods. Data represent mean ± SEM. ***p<0.001, ****p<0.0001 by Student's t-test. (C) Boxplots of raw Ct values of the 4 endogenous microRNAs used to normalise microRNA expression.

Table 4.3: Candidate normalising microRNAs ǂ.			
GeNorm		Normfinder	
MicroRNA	M-Value	MicroRNA	SD
miR-223-3p	0.532906148	**miR-101-3p**	0.4955
miR-26a-5p	0.532906148	**miR-19a-3p**	0.5597
miR-142-3p	0.69187472	**miR-19b-3p**	0.6936
miR-23a-3p	0.741792291	**miR-16-5p**	0.7727
miR-191-5p	0.895876676	**miR-191-5p**	1.0457
miR-19b-3p	1.006804913	**miR-142-3p**	1.1094
miR-19a-3p	1.051823548	**miR-23a-3p**	1.1125
miR-101-3p	1.110009752	**miR-106b-5p**	1.1482
miR-16-5p	1.135564234	**miR-21-5p**	1.2116
miR-451a	1.220766682	**miR-26a-5p**	1.2194
miR-144-3p	1.302659919	**miR-451a**	1.242
miR-106b-5p	1.365558024	**miR-144-3p**	1.2891
miR-21-5p	1.420741101	**miR-92a-3p**	1.357
miR-92a-3p	1.467133819	**miR-223-3p**	1.3766
miR-486-5p	1.51592891	**miR-486-5p**	1.5031
miR-320a	1.575285976	**miR-320a**	1.7919
miR-103a-3p	1.642058753	**miR-103a-3p**	1.8358
miR-425-5p	1.739905629	**miR-425-5p**	2.3032
miR-423-5p	1.855075269	**miR-423-5p**	2.7486
miR-93-5p	2.006345475	**miR-93-5p**	3.3277

ǂM-Value is the GeNorm stability value, defined as the variation of a microRNA compared to all other microRNAs [279]. SD is the Normfinder stability value, calculated as the sum of the estimated intragroup and intergroup variation [280].

4.5.4 Profiling

Multivariate pattern recognition algorithms are commonly used to visualise the similarities and differences in large datasets consisting of a large number of variables. PCA scores plot demonstrated separation between the preoperative and 5 postoperative groups (Figure 4.5A). There appeared to be discrete clustering of preoperative profiles (pink), 1 month postoperative profiles (red), 3 months postoperative profile (green), 6 month postoperative profiles (light blue), 9 month postoperative profiles (dark blue) and 12 month postoperative profiles (black). This is clearer in the trajectory PCA which plots the mean components of all 6 groups (Figure 4.5B). The preoperative and 1 month postoperative microRNA profiles are the most alike but there's a notable shift of increasing separation with each sequential postoperative timepoint.

A preoperative-postoperative comparative heatmap of relative expression of every expressed microRNA can be found in Figure 4.6A, presented with the clustering of microRNAs. The associated group cluster denodrogram (Figure 4.6B) illustrated distinct clustering of preoperative and 1m postoperative profiles and separate clustering of 3 months, 6 months, 9 months and 12 months postoperative profiles. Within the second cluster 3 month and 6 month profiles group together and 9 month and 12 month profiles group together. This, together with the PCA scores plots indicates bariatric circulating microRNA profiles display increasing variation from preoperative levels with each passing month.

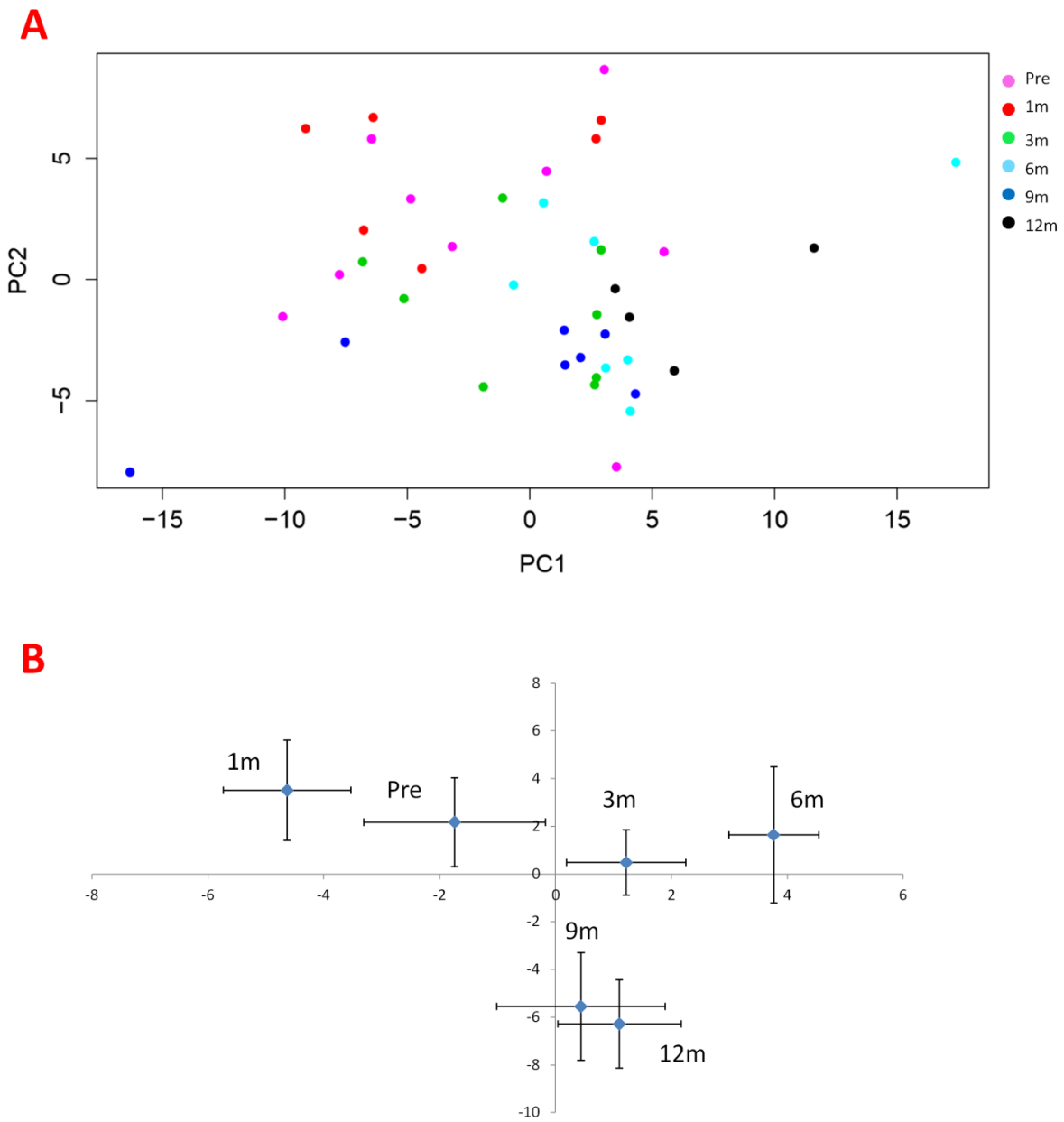

Figure 4.5: Principal Component Analysis of bariatric circulating microRNA profiles.

(A) PCA scores plot of preoperative (green), 1 month postoperative (blue), 3 month postoperative (red), 6 month postoperative (yellow), 9 month postoperative (light blue) and 12 month postoperative (purple). (B) Trajectory PCA scores plot of mean components ± standard deviation.

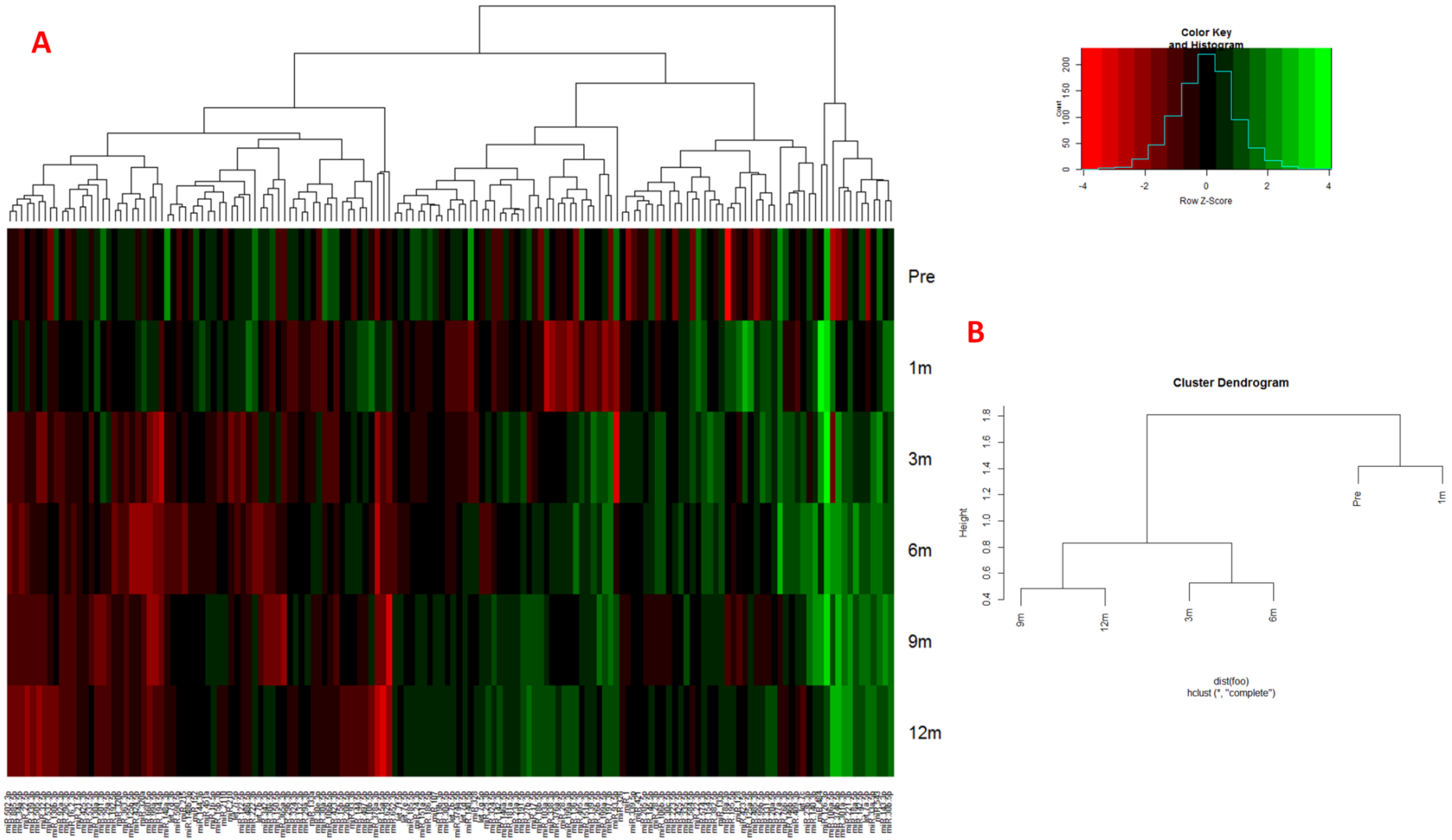

Figure 4.6: Comparative heat map of preoperative and postoperative mean relative microRNA expression and associated cluster dendrogram.

The majority of circulating microRNAs remained unaltered following RYGB. However, 49 out of the 159 detected microRNAs were differentially expressed in at least one post-bariatric timepoint compared to preoperative levels. A series of volcano plots of log microRNA fold change at each postoperative timepoint relative to preoperative levels can be found in Figure 4.7. At 1 month following surgery circulating microRNA levels were largely unchanged, with only one microRNA significantly upregulated and one microRNA significantly downregulated relative to preoperative levels. At 3 months only one microRNA was significantly increased and 4 microRNAs were significantly decreased relative to preoperative levels. The number of differentiated microRNAs continued to increase with each sequential timepoint following RYGB. The number of deregulated microRNAs at 6 months was 10 (4 increased, 6 decreased). At 9 months 28 microRNAs were significantly deregulated (1 increased, 27 decreased) and at 12 months 31 microRNAs were significantly deregulated (1 increased, 30 decreased).

All microRNAs significantly altered following RYGB are tabulated in Table 4.4 and all detected microRNA expression data is tabulated in Table 7.12 in the appendices.

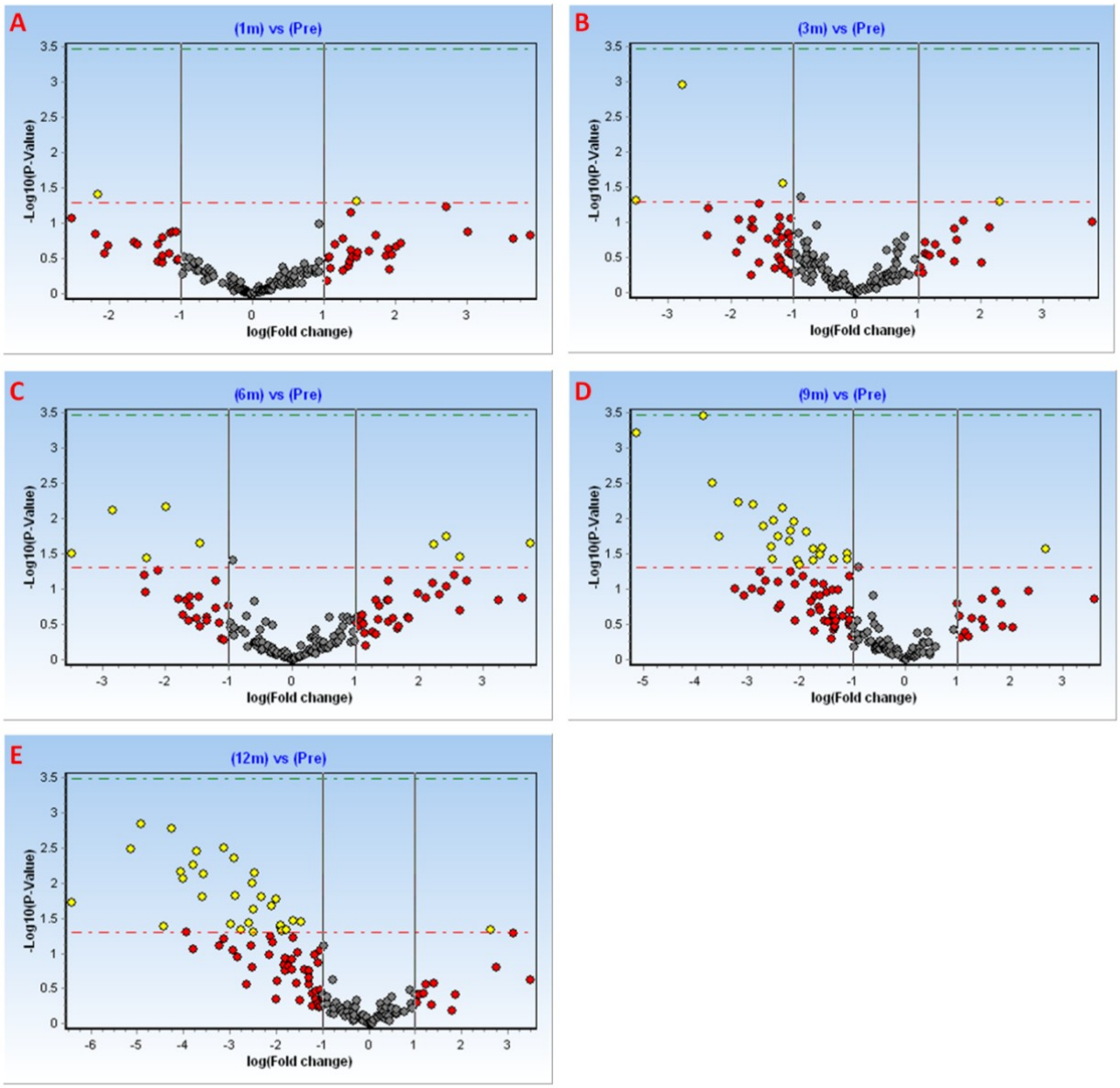

Figure 4.7: Volcano plots.

Log fold change against log p value by Student's t test of postoperative microRNA expression at (A) 1 month, (B) 3 months, (C) 6 months, (D) 9 months and (E) 12 month following RYGB relative to preoperative levels. Each data point represents an individual microRNA that has passed expression threshold. Data points in yellow are statistically significant.

Table 4.4: Circulating microRNAs significantly deregulated following RYGB.

(Pre) vs (1 Month)	Fold change	p
miR-338-3p	-4.48213	0.03853
miR-574-3p	2.74287	0.049

(Pre) vs (3 Month)	Fold change	p
let-7b-5p	-1.82723	0.04361
miR-106b-5p	-2.24716	0.02766
miR-194-5p	-6.79215	0.00111
miR-374b-5p	4.93347	0.05
miR-93-5p	-11.42136	0.04806

(Pre) vs (6 Month)	Fold change	p
let-7i-5p	-1.92065	0.03918
miR-125b-5p	-7.14436	0.00773
miR-192-5p	-3.9763	0.00694
miR-27a-3p	13.53321	0.02252
miR-301a-3p	5.37949	0.01795
miR-320a	-4.93124	0.03666
miR-33a-5p	4.73908	0.02358
miR-374b-5p	6.26218	0.03492
miR-378a-3p	-11.13685	0.03191
miR-590-5p	-2.72931	0.02227

(Pre) vs (9 Month)	Fold change	p
let-7d-3p	-2.147	0.03788
let-7i-5p	-2.15403	0.03174
miR-125b-5p	-3.06655	0.03318
miR-148a-3p	-2.57524	0.03815
miR-148b-3p	-1.86248	0.04963
miR-15a-5p	-6.5224	0.01269
miR-16-2-3p	-4.05593	0.04502
miR-192-5p	-3.68028	0.01581
miR-194-5p	-7.38657	0.00632
miR-21-5p	-2.99337	0.02618
miR-22-5p	-5.34766	0.01833
miR-28-3p	-3.38722	0.02715
miR-29c-3p	-4.36596	0.0111
miR-320a	-5.05808	0.00719
miR-320b	-3.36266	0.03971
miR-32-5p	-5.87211	0.02498
miR-363-3p	-4.16517	0.03886
miR-365a-3p	-14.39258	0.00036
miR-374b-5p	6.42042	0.0267
miR-378a-3p	-9.02419	0.00593
miR-423-3p	-4.64168	0.02109
miR-424-5p	-3.0694	0.02894
miR-502-3p	-5.75474	0.03794
miR-532-5p	-5.65122	0.01089
miR-629-5p	-34.77156	0.00061
miR-660-5p	-12.73778	0.00317
miR-92a-3p	-4.50946	0.015
miR-99a-5p	-11.74445	0.01831

(Pre) vs (12 Month)	Fold change	p
let-7d-3p	-2.76011	0.03541
miR-106b-5p	-3.74037	0.04017
miR-125b-5p	-3.70064	0.0481
miR-130b-3p	-13.8712	0.00552
miR-15a-5p	-84.90506	0.01922
miR-192-5p	-3.45762	0.04664
miR-194-5p	-8.75819	0.00318
miR-20b-5p	-5.5804	0.04966
miR-21-5p	-4.98989	0.01576
miR-22-5p	-19.12843	0.00171
miR-29a-5p	-5.74618	0.01011
miR-29b-3p	-3.09641	0.03521
miR-29c-3p	-7.43735	0.00451
miR-301a-3p	6.22679	0.04598
miR-30e-3p	-4.25004	0.02108
miR-320a	-5.63933	0.02424
miR-32-5p	-11.79701	0.00753
miR-339-3p	-11.9564	0.01566
miR-363-3p	-6.01488	0.03733
miR-378a-3p	-35.24316	0.00337
miR-423-3p	-4.01317	0.01692
miR-497-5p	-7.82366	0.03851
miR-502-3p	-13.22781	0.00365
miR-505-3p	-21.45293	0.04197
miR-532-3p	-16.70047	0.00699
miR-629-5p	-30.33645	0.00147
miR-660-5p	-16.14743	0.00885
miR-766-3p	-3.76456	0.04357
miR-92a-3p	-7.40402	0.01555
miR-93-3p	-5.51755	0.00722
miR-99a-5p	-6.78184	0.04712

4.5.5 Univariate analysis

The changes in circulating microRNA expression following RYGB can be categorised broadly into 5 types of response that are temporally dependent, referred to here as phases of response.

4.5.5.1 First phase

The first phase of the bariatric response with respect to circulating microRNAs occurred in the first few months following RYGB. The expression of the majority of circulating microRNAs were not significantly changed 1 month and 3 months following RYGB, and the circulating microRNA profiles at those two post-bariatric timepoints most resembled the preoperative stage. The few microRNAs that were differentially expressed during this phase were characterised by a significant change in expression at the early postoperative months before reverting back to preoperative expression levels at later postoperative months. This is best illustrated by miR 338, which relative to preoperative levels significantly decreased 4.48 fold at 1 month following RYGB relative to preoperative levels ($p=0.039$, Student's t test) but expression levels at subsequent timepoints following surgery were comparable to preoperative levels (Figure 4.8A). A similar pattern was observed with miR 93-5p, which relative to preoperative expression decreased 4.17 fold 1 month following RYGB and decreased significantly 11.4 fold at 3 months following RYGB ($p=0.27$ and 0.048 respectively, Student's t test) before reverting back to preoperative levels at 6 months, 9 months and 12 months following bariatric surgery (Figure 4.8B). Expression levels of neither miR 338 nor miR 93-5p correlated with BMI, % of preoperative BMI lost or blood glucose levels. As the expression of miR 338 and miR 93-5p was not transient following bariatric surgery this was expected.

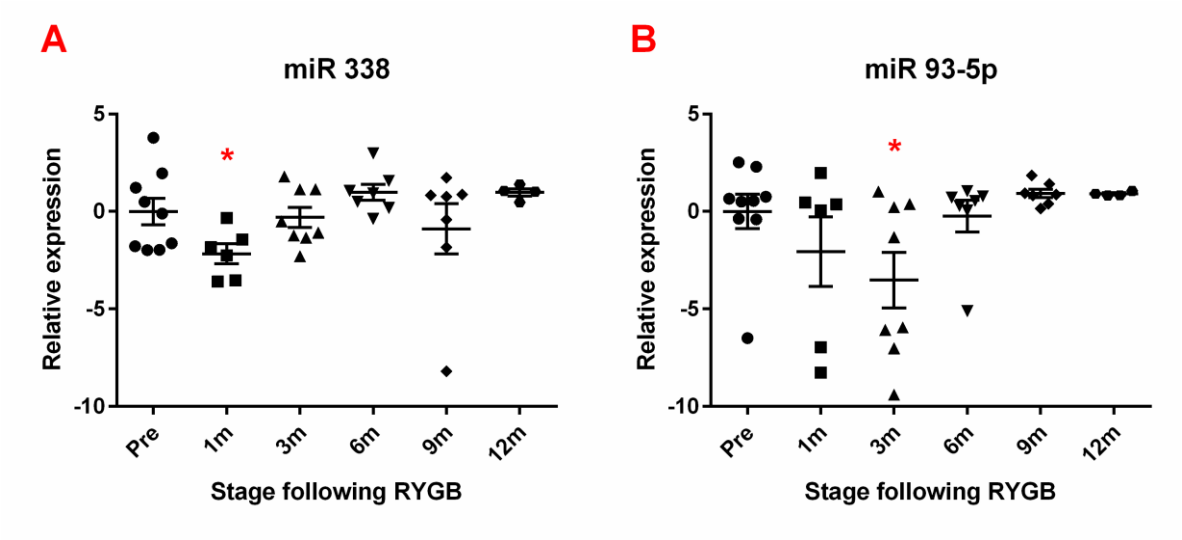

Figure 4.8: First phase of the bariatric circulating microRNA response.

Normalised logarithmic relative preoperative and postoperative expression of differentiated microRNAs. (A) miR 338 and (B) miR 93-5p. Data represents mean ± standard error of mean. *p<0.05 by Student's t test.

4.5.5.2 Second phase

The second phase of response followed a similar pattern to the first phase but with a later significant manifestation of the differentiated microRNA. Relative to preoperative expression circulating expression of miR 27a increases gradually 4 fold 1 month following RYGB, 3 fold 3 months following RYGB and significantly 13.5 fold 6 months following RYGB (p=0.21, 0.36 and 0.023 respectively, Student's t test) before returning to levels comparable to preoperative expression 9 months and 12 months following surgery (Figure 4.9A). Similarly circulating miR 33a expression increases 1.29 fold 1 month following surgery, 2.99 fold 3 months following surgery and significantly 4.74 fold 6 months following surgery (p=0.73, 0.12 and 0.024 respectively, Student's t test) before decreasing 9 months and 12 months following RYGB (Figure 4.9B). The inverse was observed for miR 590 which decreased gradually following RYGB to 1.2 fold 1 month following surgery, 1.19 fold 3 months following surgery and significantly 2.73 fold 6 months following surgery (p=0.82, 0.65 and 0.022 respectively, Student's t test) before gradually increasing back towards preoperative expression levels 9 months and 12 months following RYGB (Figure 4.9C). Circulating expression of miR 33a negatively correlated with BMI (r=-0.41, p=0.0085, Pearson's correlation) but not percentage of preoperative BMI lost nor blood glucose. Blood levels of miR 590 positively correlated with blood glucose (r=0.46, p=0.0054, Pearson's correlation). Expression of circulating miR 27a did not correlated with any of the measure clinical parameters.

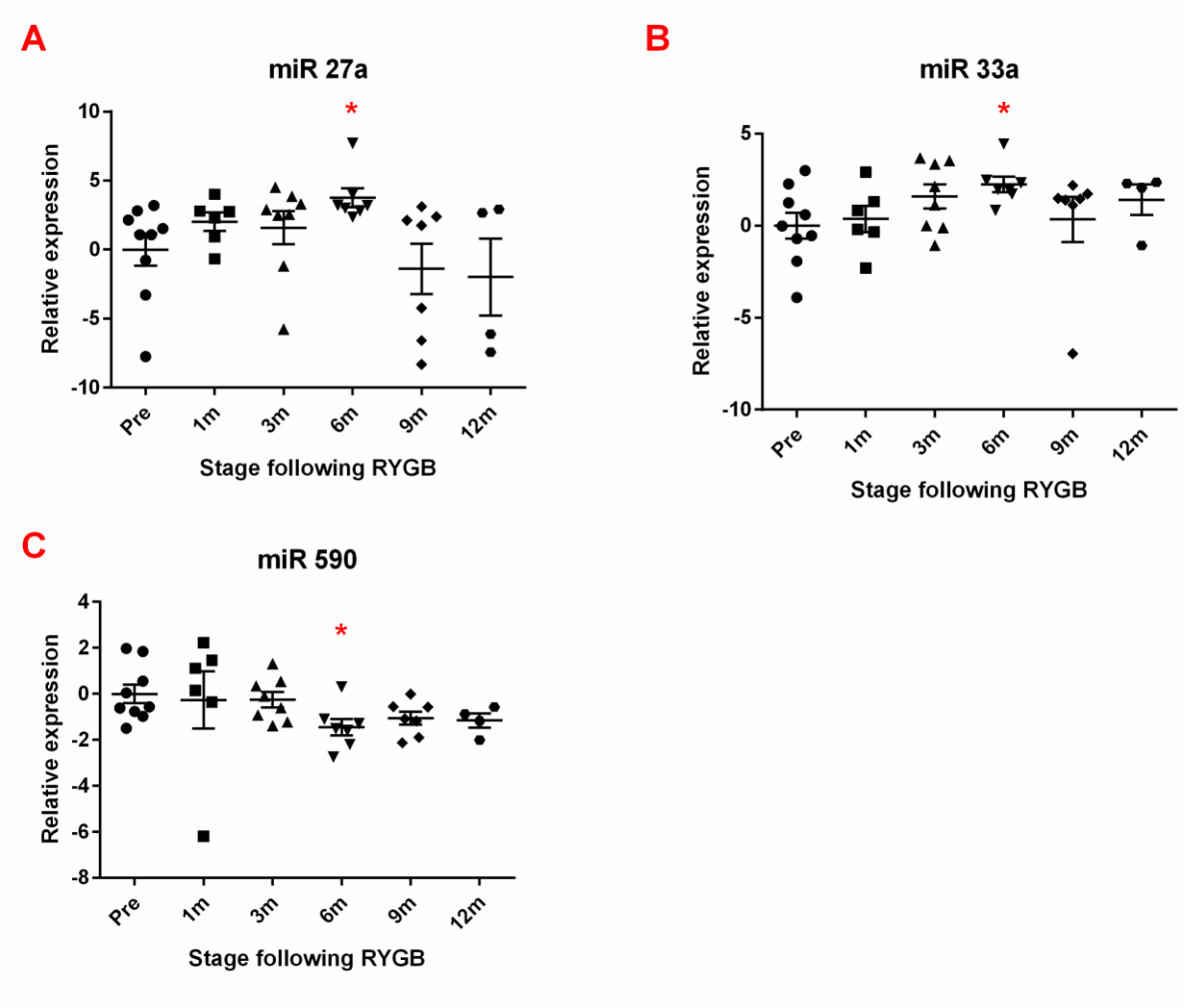

Figure 4.9: Second phase of the bariatric circulating microRNA response.

Normalised logarithmic relative preoperative and postoperative expression of differentiated microRNAs. (A) miR 27a, (B) miR 33a and (C) miR 590. Data represents mean ± standard error of mean. *$p<0.05$ by Student's t test.

4.5.5.3 Third phase

The third circulating microRNA bariatric phase consisted of microRNAs whose deregulation significantly manifested 6 months following surgery but unlike the microRNAs in the second response these changes in expression were maintained in subsequent post-bariatric timepoints. This includes miR 125b which relative to preoperative expression initially increased 1.22 fold 1 month after RYGB but then decreased 1.94 fold 3 months following RYGB, (neither significantly), decreased significantly 7.14 fold 6 months following RYGB, decreased significantly 3 fold 9 months following surgery and decreased significantly 3.7 fold 12 months following surgery (Figure 4.10A, p=0.75, 0.28, 0.0077, 0.033 and 0.048 respectively, Student's t test). MiR 192 followed a similar pattern, increasing initially 1.08 fold 1 month following surgery before decreasing 2.1 fold 3 months following surgery, significantly 3.98 fold 6 months following surgery, significantly 3.68 fold 9 months following surgery and significantly 3.46 fold 12 months following surgery (Figure 4.10B, p=0.87, 0.21, 0.0069, 0.015 and 0.047 respectively, Student's t test). Likewise miR 320a initially increased 2 fold following RYGB before decreasing 1.75 fold 3 months following surgery, significantly 4.93 fold 6 months following surgery, significantly 5.05 fold 9 months following surgery and significantly 5.64 fold 12 months following surgery (Figure 4.10D, p=0.31, 0.38, 0.037, 0.0072 and 0.024 respectively, Student's t test). MiR 378a circulating levels also decreased following RYGB, initially increasing 1.51 fold 1 month following surgery before decreasing 5.12 fold 3 months following surgery, significantly 11.1 fold 6 months following surgery, significantly 9.02 fold 9 months following surgery and significantly 35.2 fold 12 months following surgery (Figure 4.10, p=0.57, 0.16, 0.032, 0.0059 and 0.0033 respectively, Student's t test). Inversely, circulating miR 301a increased following RYGB. Relative to preoperative expression miR 301a initially decreased 1.05 fold 1 month following surgery before increasing 1.94 fold 3 months after surgery, increasing significantly 5.38 fold 6 months following surgery, increasing 2.77 fold 9 months following surgery and increasing significantly 6.23 following RYGB (Figure 4.10C, p=0.95, 0.34, 0.018, 0.14 and 0.046 respectively, Student's t test).

All 5 microRNAs demonstrated correlation with at least one assessed post-bariatric clinical parameter. Circulating miR 125b was found to positively correlate with BMI (r=035, p=0.29, Pearson's correlation) and to negatively correlate with percentage of preoperative BMI lost (r=-0.42, p=0.0065, Pearson's correlation). Negative correlations with percentage of preoperative BMI lost was also found with circulating miR 192 (r=-0.39, p=0.12, Pearson's correlation), miR 320a (r=-0.44, p=0.0041, Pearson's correlation) and miR 378a (r=-0.46, p=0.0031, Pearson's correlation). A positive correlation was also found between miR 320a and blood glucose (r=0.38, p=0.024). On the other hand, a negative correlation was demonstrated between circulating miR 301a and BMI (r=-0.59, p<0.0001, Pearson's correlation). A positive correlation was demonstrated between miR 301a and percentage of preoperative BMI lost (r=0.43, p=0.0057, Pearson correlation).

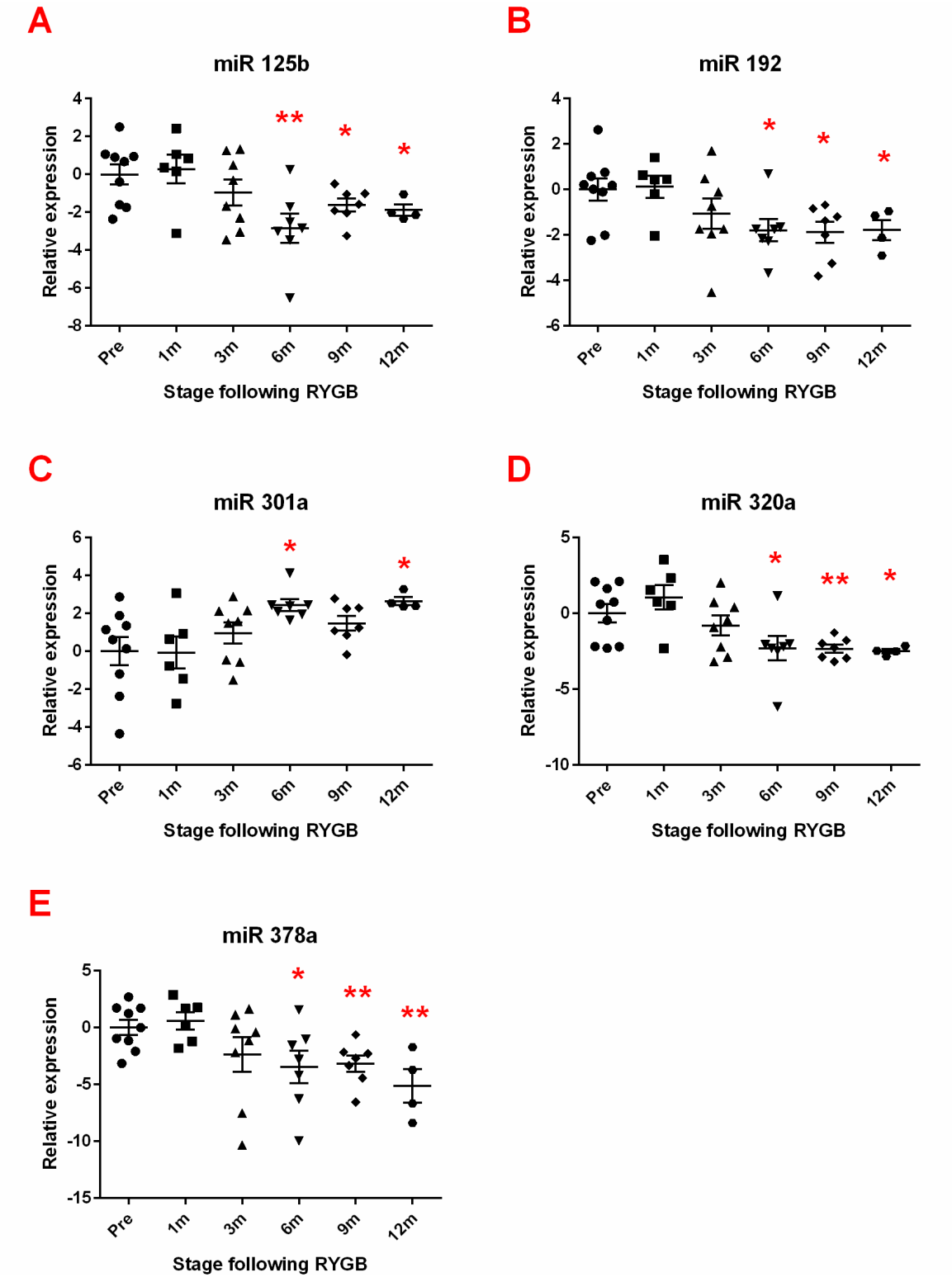

Figure 4.10: Third phase of the bariatric circulating microRNA response.

Normalised logarithmic relative preoperative and postoperative expression of differentiated microRNAs. (A) miR 125ba, (B) miR 192, (C) miR 301a, (D) miR 320a and (E) miR 378a. Data represents mean ± standard error of mean. *p<0.05, **p<0.01 by Student's t test.

4.5.5.4 Fourth phase

The fourth circulating microRNA bariatric phase consisted of microRNAs whose significant deregulation didn't manifest until 9 months following surgery but this deregulation not only persisted but was enhanced 12 month following surgery. Relative to preoperative levels circulating levels of miR 15a initially increased slightly 1.7 fold before gradually decreasing with each sequential post-bariatric timepoint. At 3 months following RYGB miR 15a decreased 2.4 fold and at 6 months following RYGB miR 15a decreased 2.22 fold. At 9 months following surgery miR 15a levels decreased significantly 6.52 fold and decreased further to 85 fold relative to preoperative levels 12 months following bariatric surgery (Figure 4.11A, p=0.53, 0.2, 0.3, 0.013 and 0.019 respectively, Student's t test). A similar trend was found with circulating levels if miR 22-5p, which increased 1.44 fold 1 month following surgery but then decreased 1.56 fold 3 months following surgery, decreased 1.96 fold 6 months following surgery, decreased significantly 5.35 fold and decreased significantly 19.1 fold 12 months following surgery (Figure 4.11B, p=0.61, 0.4, 0.31, 0.018 and 0.0017 respectively, Student's t test). Circulating miR 629 also initially increased following bariatric surgery before a gradual and eventually significant decrease. At 1 month following surgery miR 629 blood levels increased 2.13 fold but then decreased 3.54 fold 3 months following surgery, decreased 2.53 fold 6 months following surgery, decreased significantly 34.8 fold 9 months following surgery and decreased 30.3 fold 12 months following surgery (Figure 4.11C, p=0.44, 0.18, 0.29, 0.00061 and 0.0015, Student's t test). MiR 502 demonstrated a similar pattern. Circulating levels increased 1.33 fold 1 month following RYGB then decreased 2.39 fold 3 months postoperatively, 3 fold 6 months postoperatively, significantly 5.75 fold 9 months postoperatively and 13.2 fold 12 months following surgery (Figure 4.11D, p=0.68, 0.13, 0.13, 0.038 and 0.0036 Student's t test).

Although no correlations were found between circulating miR 15a and measured postoperative clinical outcomes, miR 22-5p circulating expression negatively correlated with percentage of preoperative BMI lost (r=-0.44, p=0.0042, Pearson's correlation). Similarly negative correlation were found between circulating levels of miR 629 (r=-0.4, p=0.0032) and miR 502 (r=-0.33, p=0.04) and percentage of preoperative BMI lost.

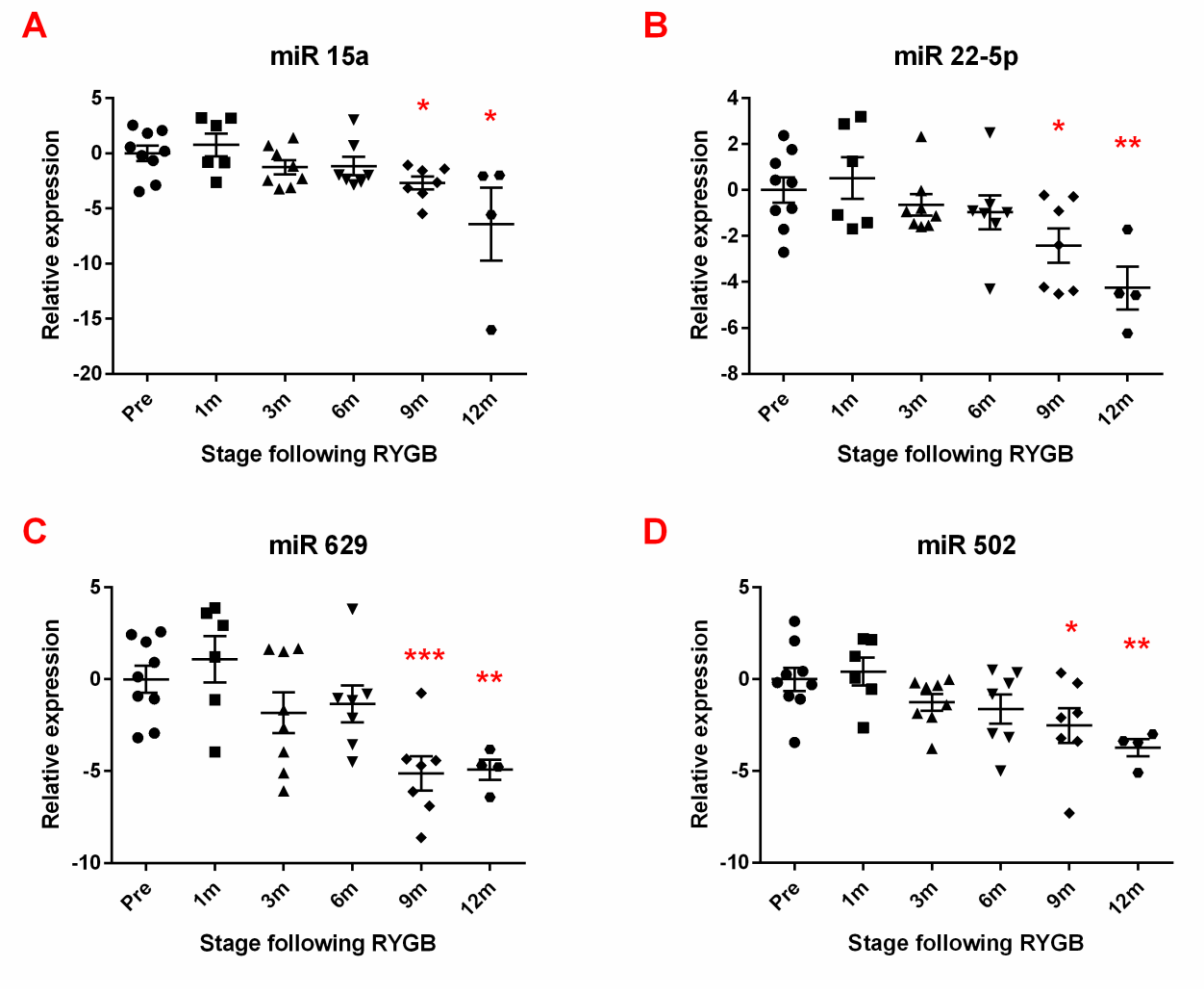

Figure 4.11: Fourth phase of the bariatric circulating microRNA response.

Normalised logarithmic relative preoperative and postoperative expression of differentiated microRNAs. (A) miR 15a, (B) miR 22-5p, (C) miR 629 and (D) miR 502. Data represents mean ± standard error of mean. *p<0.05, **p<0.01, ***p<0.001 by Student's t test.

4.5.5.5 Fifth phase

The fifth phase was characterised by microRNAs that remained unchanged relative to preoperative levels at the first few timepoints following bariatric surgery but demonstrated significant decreases at 12 months following surgery. These include miR 130b which relative to preoperative levels demonstrated comparable expression at 1 month, 3 months, 6 months and 9 months following RYGB. However, at 12 months following surgery miR 130b levels decreased significantly 13.9 fold (Figure 4.12A, p=0.0055 Student's t test). MiR 532-3p circulating levels remained stable at 1 month, 3 months and 6 months following surgery. An insignificant 3.32 fold decrease was followed by a significant 16.7 fold decrease 12 months after RYGB (Figure 4.12B, p=0.081 and 0.007 respectively, Student's t test). Similarly miR 339-6p levels were unchanged 1 month, 3 months and 6 months following surgery but decreased 4.3 fold 9 months postoperatively and significantly 12 fold 12 months postoperatively (Figure 4.12C, p=0.084 and 0.016 respectively, Student's t test). Circulating expression of miR 29a-5p also remained unchanged 1 month, 3 months and 6 months following RYGB. Levels decreased insignificantly 3.82 fold 9 months following surgery and decreased significantly 5.75 fold 12 months following RYGB (Figure 4.12D, p=0.066 and 0.01 respectively, Student's t test). No correlations were observed between these 4 microRNAs and any of the measured postoperative clinical outcomes.

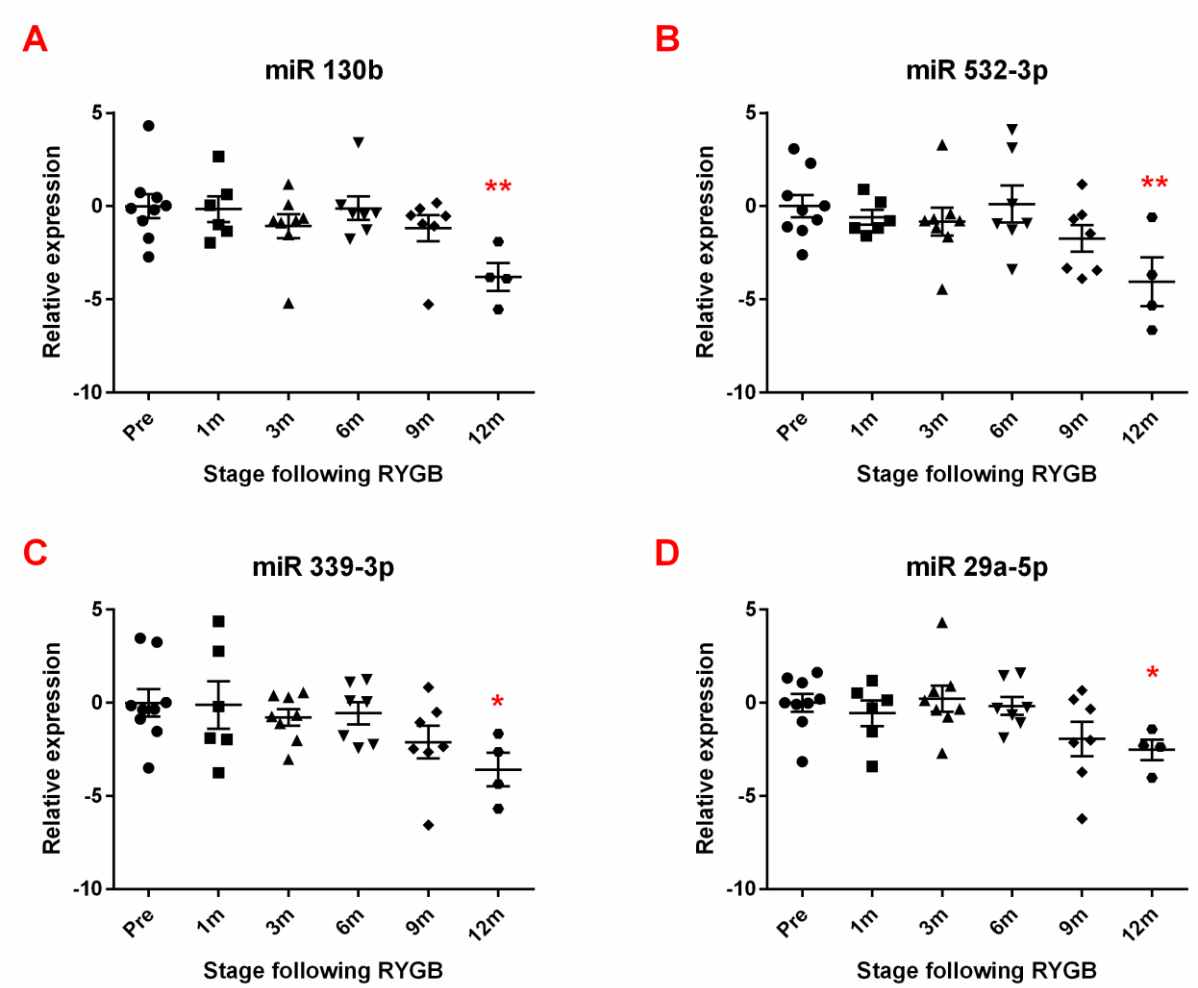

Figure 4.12: Fifth phase of the bariatric circulating microRNA response.

Normalised logarithmic relative preoperative and postoperative expression of differentiated microRNAs. (A) miR 130b, (B) miR 532-3p, (C) miR 339-3p and (D) miR 29a-5p. Data represents mean ± standard error of mean. *p<0.05, **p<0.01 by Student's t test.

Table 4.5: Circulating microRNA expression correlated with bariatric clinical outcomes[ǂ].							
Phase	**MicroRNA**	**BMI**		**% BMI lost**		**Blood glucose**	
		r	**p**	**r**	**p**	**r**	**p**
1	**miR-338-3p**	-0.2318	0.15	0.07554	0.6432	0.1006	0.5653
	miR-93-5p	0.02307	0.8876	0.1185	0.4665	0.02092	0.9051
2	**miR-33a-5p**	-0.4107	0.0085	0.228	0.1572	0.07564	0.6658
	miR-27a-3p	-0.0966	0.5533	0.07968	0.625	0.05217	0.766
	miR-590-5p	0.00154	0.9925	-0.2055	0.2033	0.4602	0.0054
3	**miR-301a-3p**	-0.5925	0.0001	0.4295	0.0057	0.1962	0.2587
	miR-125b-5p	0.3457	0.0289	-0.4235	0.0065	0.2246	0.1945
	miR-192-5p	0.2986	0.0613	-0.3929	0.0121	0.1238	0.4787
	miR-378a-3p	0.264	0.0997	-0.4564	0.0031	0.2314	0.1812
	miR-320a	0.2579	0.1081	-0.4439	0.0041	0.3817	0.0237
4	**miR-22-5p**	0.2064	0.2013	-0.4428	0.0042	0.2581	0.1344
	miR-15a-5p	0.1907	0.2384	-0.3005	0.0595	0.1948	0.262
	miR-629-5p	0.1834	0.2572	-0.4548	0.0032	0.321	0.0601
	miR-502-3p	0.1458	0.3692	-0.3263	0.0399	0.2487	0.1497
5	**miR-532-5p**	0.1111	0.4951	-0.1417	0.383	-0.1326	0.4476
	miR-29a-5p	0.0834	0.6089	-0.2452	0.1273	0.2563	0.1373
	miR-130b-3p	0.07258	0.6563	-0.2099	0.1937	-0.1307	0.4544
	miR-339-3p	-0.0037	0.9818	-0.2411	0.1339	0.09719	0.5786

[ǂ]Pearson correlations. Correlations in red are statistically significant.

4.5.6 Clinical correlations

Correlations of the expression of microRNAs involved in the 5 post-bariatric phases and clinical outcomes can be found in Table 4.5. However, significant correlations were found between clinical parameters and microRNAs that were not classified into the 5 post-bariatric phases. A total of 16 microRNAs significantly correlated with BMI, 23 significantly correlated with percentage preoperative BMI lost and 8 significantly correlated with blood glucose. All significant correlations are tabulated in Table 4.6 and all correlations are tabulated in Table 7.13 in the appendices.

Table 4.6: Significant Pearson correlation between circulating microRNA expression and measured clinical parameters.

BMI			
MicroRNA	**r**	**p**	**Significance**
miR-148a-3p	0.5195	0.0006	***
miR-33a-5p	-0.4107	0.0085	**
miR-148b-3p	0.4008	0.0104	*
miR-136-5p	-0.3881	0.0133	*
miR-191-5p	-0.3831	0.0147	*
miR-199a-5p	-0.3812	0.0152	*
let-7d-3p	0.3466	0.0285	*
miR-125b-5p	0.3457	0.0289	*
miR-107	-0.3347	0.0348	*
miR-424-5p	0.3329	0.0358	*
miR-20a-5p	-0.3319	0.0364	*
miR-103a-3p	-0.3231	0.042	*
miR-30d-5p	0.3203	0.0439	*
miR-142-5p	-0.32	0.0441	*
let-7i-5p	0.3165	0.0466	*
miR-23b-3p	-0.3159	0.0471	*

Blood glucose			
MicroRNA	**r**	**p**	**Significance**
let-7b-3p	0.4951	0.0025	**
miR-590-5p	0.4602	0.0054	**
miR-30a-5p	0.4038	0.0162	*
miR-346	-0.3917	0.02	*
miR-320a	0.3817	0.0237	*
miR-1	0.3594	0.034	*
miR-133a	0.356	0.0358	*
miR-30c-5p	0.3467	0.0413	*
miR-320b	0.3355	0.0488	*

% Preoperative BMI lost			
MicroRNA	**r**	**p**	**Significance**
miR-99a-5p	-0.4939	0.0012	**
miR-148a-3p	-0.4731	0.002	**
miR-378a-3p	-0.4564	0.0031	**
miR-629-5p	-0.4548	0.0032	**
miR-320a	-0.4439	0.0041	**
miR-22-5p	-0.4428	0.0042	**
miR-301a-3p	0.4295	0.0057	**
let-7d-3p	-0.4277	0.0059	**
miR-125b-5p	-0.4235	0.0065	**
miR-365a-3p	-0.4165	0.0075	**
let-7i-5p	-0.4127	0.0081	**
miR-374b-5p	0.4081	0.0089	**
miR-660-5p	-0.4026	0.01	*
miR-192-5p	-0.3929	0.0121	*
miR-194-5p	-0.369	0.0191	*
miR-423-3p	-0.3669	0.0199	*
miR-148b-3p	-0.3638	0.021	*
miR-92a-3p	-0.3394	0.0322	*
miR-32-5p	-0.3308	0.0371	*
miR-320b	-0.3264	0.0399	*
miR-502-3p	-0.3263	0.0399	*
miR-424-5p	-0.3216	0.043	*
miR-486-5p	-0.3174	0.0459	*

4.5.7 Pathway analysis

Pathways predicted to be regulated following bariatric surgery were determined for each of the five post-bariatric response phases described by a combination of miRWalk and PANTHER and are summarised in Tables 4.7-4.11. Affected pathways were ranked by number of microRNAs involved and by statistical significance. The top 6 predicted pathways regulated by both microRNAs involved in the first phase were angiogenesis, p53 pathway, PDGF (platelet derived growth factor) signalling pathway, Integrin signalling pathway and the apoptosis signalling pathway. All are pathways involved in cellular growth and proliferation. In fact, pathways involved in cell growth and proliferation form the majority of the top rank predicted affected pathways across all 5 response phases. Other regulated pathways include the TGF-β signalling pathway, Wnt signalling pathway, interleukin signalling pathway and chemokine/cytokine signalling pathways, all processes commonly associated with inflammation.

The top ranked pathway in the second phase was the gonadotropin releasing hormone receptor (GnRHR) pathway. In fact, the GnRHR pathway was found to be in the top 3 predicted affected pathways in the third, fourth and fifth phases, suggesting it has an important role in the post-bariatric phenotype. Despite not making the list of predicted pathways in the first, second or third phase, the Cholecystokinin receptor (CCKR) pathway was ranked 8th in the fourth phase and 7th in the fifth phase. The fourth and fifth phases were also predicted to activate β1 and β2 adrenergic receptor pathways. In addition, the later post-bariatric phases are predicted to regulate the cadherin signalling pathway.

Activation of pathways involved in the neurological process were predicted across all post-bariatric phases, including the metabotropic glutamate receptor group III pathway, Alzheimer disease-presenilin pathway, dopamine receptor mediated signalling pathway and the 5HT2 type receptor mediated signalling pathway.

Table 4.7: Regulated pathways in the first post-bariatric phase.

Rank	Pathway	93	338
1	Angiogenesis		
2	p53 pathway		
3	PDGF signaling pathway		
4	Integrin signalling pathway		
5	Apoptosis signaling pathway		
6	Gonadotropin releasing hormone receptor pathway		
7	TGF-beta signaling pathway		
8	Dopamine receptor mediated signaling pathway		
9	Endothelin signaling pathway		
10	EGF receptor signaling pathway		
11	Insulin/IGF pathway-mitogen activated protein kinase kinase/MAP kinase cascade		
12	Metabotropic glutamate receptor group III pathway		
13	Wnt signaling pathway		
14	FGF signaling pathway		
15	Alzheimer disease-presenilin pathway		
16	Interleukin signaling pathway		
17	Inflammation mediated by chemokine and cytokine signaling pathway		
18	Insulin/IGF pathway-protein kinase B signaling cascade		

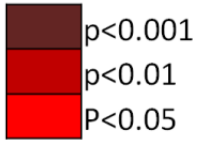

Table 4.8: Regulated pathways in the second post-bariatric phase.

Rank	Pathway	27a	33a	590
1	Gonadotropin releasing hormone receptor pathway			
2	PDGF signaling pathway			
3	Angiogenesis			
4	Integrin signalling pathway			
5	EGF receptor signaling pathway			
6	PI3 kinase pathway			
7	p53 pathway			
8	Wnt signaling pathway			
9	Apoptosis signaling pathway			
10	Metabotropic glutamate receptor group III pathway			
11	Dopamine receptor mediated signaling pathway			
12	Inflammation mediated by chemokine and cytokine signaling pathway			
13	Ras Pathway			
14	Endothelin signaling pathway			

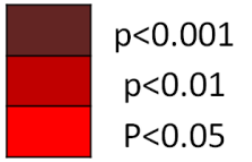

Table 4.9: Regulated pathways in the third post-bariatric phase.

Rank	Pathway	125b	192	301a	320a	378a
1	Angiogenesis					
2	Gonadotropin releasing hormone receptor pathway					
3	PDGF signaling pathway					
4	Integrin signalling pathway					
5	EGF receptor signaling pathway					
6	FGF signaling pathway					
7	Ras Pathway					
8	Cadherin signaling pathway					
9	Wnt signaling pathway					
10	Alzheimer disease-presenilin pathway					
11	TGF-beta signaling pathway					
12	Apoptosis signaling pathway					
13	Endothelin signaling pathway					
14	p53 pathway feedback loops 2					
15	Inflammation mediated by chemokine and cytokine signaling pathway					

p<0.001
p<0.01
P<0.05

Table 4.10: Regulated pathways in the fourth post-bariatric phase.

Rank	Pathway	15a	22	639	502
1	Angiogenesis				
2	Endothelin signaling pathway				
3	Gonadotropin releasing hormone receptor pathway				
4	PDGF signaling pathway				
5	EGF receptor signaling pathway				
6	Integrin signalling pathway				
7	Metabotropic glutamate receptor group III pathway				
8	CCKR signaling map				
9	p53 pathway				
10	FGF signaling pathway				
11	Apoptosis signaling pathway				
12	5HT2 type receptor mediated signaling pathway				
13	Ras Pathway				
14	VEGF signaling pathway				
15	Inflammation mediated by chemokine and cytokine signaling pathway				
16	Beta2 adrenergic receptor signaling pathway				
17	Dopamine receptor mediated signaling pathway				
18	Heterotrimeric G-protein signaling pathway-Gi alpha and Gs alpha mediated pathway				
19	Alpha adrenergic receptor signaling pathway				
20	TGF-beta signaling pathway				

p<0.001
p<0.01
P<0.05

Table 4.11: Regulated pathways in the fifth post-bariatric phase.

Rank	Pathway	130b	532	29a	339
1	p53 pathway				
2	Gonadotropin releasing hormone receptor pathway				
3	Integrin signalling pathway				
4	Angioenesis				
5	PDGF signaling pathway				
6	Wnt signaling pathway				
7	CCKR signaling map				
8	p53 pathway feedback loops 2				
9	Endothelin signaling pathway				
10	Alzheimer disease-presenilin pathway				
11	Beta1 adrenergic receptor signaling pathway				
12	Beta2 adrenergic receptor signaling pathway				
13	EGF receptor signaling pathway				
14	Inflammation mediated by chemokine and cytokine signaling pathway				
15	TGF-beta signaling pathway				
16	Cadherin signaling pathway				

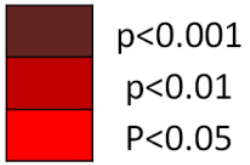

4.6 Discussion

The pathways predicted here to be regulated following RYGB include those involved in cell growth, inflammation and neurological processes, and at the later phases receptor pathways involved in gut hormone signalling, lipolysis and diabetic nephropathy. The link between inflammation and obesity is well established [288], and bariatric surgery alters transcription factors and microRNA profiles in adipose tissues [289, 290]. An obesity role in neurodegenerative disorders is also being increasingly recognised, as the metabolic syndrome contributes mechanistically to both Alzheimer's and Parkinson's diseases [291].

The GnRHR pathway was consistently one of the top predicted regulated pathways across the later bariatric microRNA phases. The GnRHR is a G-protein coupled receptor responsible for the release of gonadotropic luteinizing hormone (LH) and follicle stimulating hormone (FSH) and is therefore a key regulator of fertility [292]. Hyperinsulinemia resulting from obesity disrupts fertility through GnRH signalling [293]. Hypogonadism is common in morbidly obese males and this is reversed after bariatric surgery [294, 295], which may explain the activation of the GnRHR pathway and suggests the involvement of microRNAs in this process. MicroRNAs are essential for the proper gonadal function as the Gonadotrope-specific deletion of Dicer suppresses the release of gonadotropic hormones and impairs fertility [296].

The later bariatric phases were also predicted to regulate the β-adrenergic receptor pathways through miR 15a and miR 532. The β adrenergic receptors are a family of G protein coupled receptors that are key regulators of adipocyte lipid metabolism. Activation of the β2 adrenergic receptor stimulates lipolysis and the release of insulin [297]. Polymorphism in the β2 adrenergic receptor gene is common in obesity [298]. The β2 adrenergic receptor also modulates preprandial, postprandial and total energy expenditure [299]. MiR 532 is also predicted to regulate the β1 adrenergic receptor pathway, which promotes the secretion of ghrelin in the stomach when

activated [300]. The third bariatric phase is also predicted to regulate the cadherin signalling pathway through miR 192, which as described in the previous chapter has a central role in diabetic nephropathy [178].

Despite not making an appearance as the predicted affected pathways in the first three phases, the Cholecystokinin receptor pathway was ranked 8th in the fourth phase and 7th in the fifth phase. CCK is a gut hormone released after a meal in response to dietary fat and protein and acts on CCK receptors in the gastrointestinal tract and the central nervous system to inhibit gastric emptying and food intake and promote gallbladder contraction [301, 302]. CCK also regulates glucose homeostasis by promoting pancreatic glucagon release and pancreatic β cell differentiation [303]. In addition, CCK also stimulates the release of PYY [304] and suppresses the release of ghrelin [305]. The administration of exogenous CCK upregulates the Peptide YY type 2 receptor [306] and the appetite suppression neuropeptide transmitter cocaine and amphetamine regulated transcript (CART) [307] and inhibits synthesis of orexigenic neuropeptide transmitter melanin-concentrating hormone (MCH) and its receptor [307, 308]. CCK function is also modulated by leptin and insulin [309, 310]. Together this suggests CCK is a key master regulator of the vagal gut-brain satiety signalling axis.

Although high fat diets and obesity impairs CCK sensitivity and decreases its satiating effects [311-313], the bariatric role of CCK was initially largely dismissed [314, 315]. However, recently studies have demonstrated that RYGB increases the postprandial release of CCK within 2 weeks postoperatively [316] and this increase is maintained over 16 months following surgery [317]. Sleeve gastrectomy also increases postprandial CCK [318]. It has also been shown that RYGB passively increases the number of CCK releasing enteroendocrine cells in the Roux-limb but not the biliopancreatic limb [319]. This is consistent with the findings presented here that the CKK signalling pathway is regulated in the later bariatric phases by miR 22 and miR 130b, and suggests a microRNA role in the gut hormone modulated post-bariatric control of satiety and improved glucose homeostasis.

The benefits of bariatric surgery are plentiful and the mechanisms behind them are complex, multi-factorial, synergistic and enhanced with time. This is reflected in the bariatric microRNA profiles and the diverse array of pathways microRNAs are predicted to activate following RYGB. Here, it has been shown for the first time that bariatric surgery persistently and increasingly modulates circulating microRNAs with time so that there's an increasing departure in sequential postoperative profiles from the preoperative stage. In total, RYGB led to the differentiated expression of 49 circulating microRNAs across 5 post-bariatric phases characterised by the selective, time-dependent differentiation of specific circulating microRNAs and the predicted activation of pathways and physiological processes associated with obesity and T2DM. As such, circulating microRNAs are not only novel, minimally invasive biomarkers for bariatric surgery, they can also map the post-bariatric response and the development of the beneficial post-bariatric phenotype, activating specific pathways at different post-bariatric phases that may contribute to the establishment of the post-bariatric phenotype (Figure 4.13).

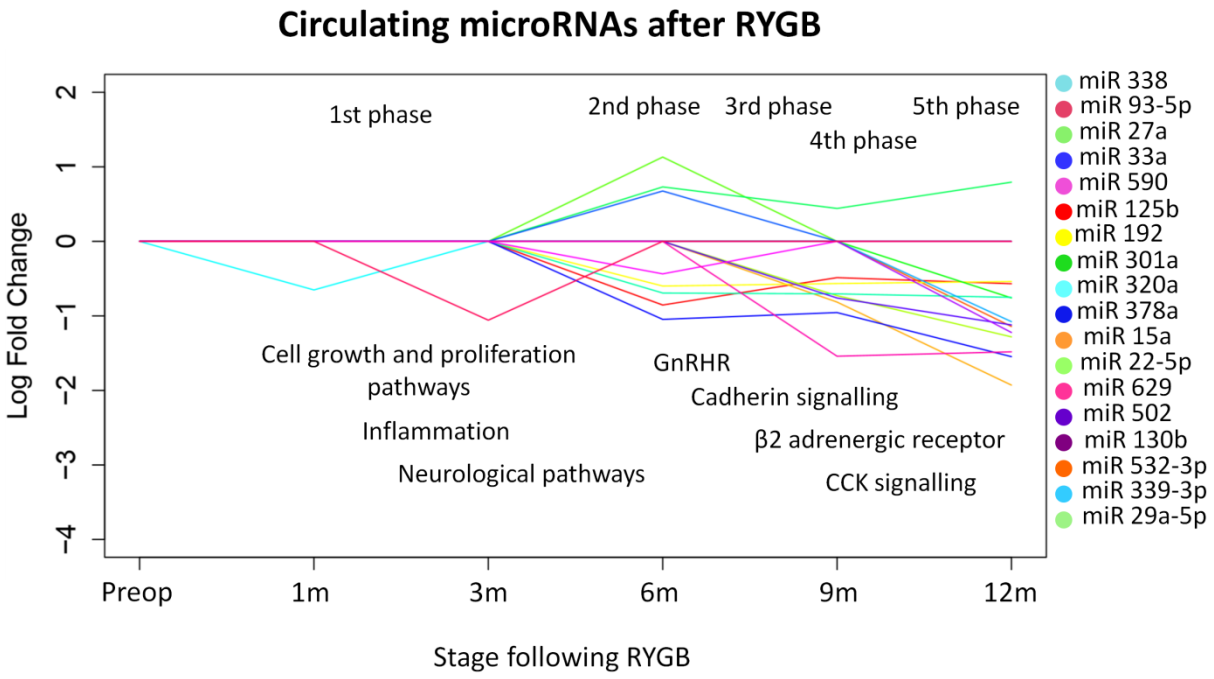

Figure 4.13: The post-bariatric circulating microRNA response in five phases.

Each line represents a microRNA.

A recently published study from our lab described circulating microRNA profiles in rat bariatric profiles and also concluded that altered gut-brain signalling established following bariatric surgery is mediated by microRNAs. Wu *et al.* found the differentiated expression of 14 circulating microRNAs in RYGB-operated Spreague Dawley rats compared to sham-operated rats, the predominant of which was miR 122 which decreased almost 60 fold [214]. MiR 122 is a liver microRNA responsible for regulating lipid metabolism [172]. Wu *et al.* demonstrated that diminished miR 122 was responsible for increase glucose transportation, accelerated glycolysis and the inhibition of gluconeogenesis following RYGB in rats [214]. This is supportive of the recent discovery that RYGB reprograms intestinal glucose metabolism by increasing glycolysis and glucose uptake [119], and suggests miR 122 could contribute to this effect. This study also found a consistent decrease in circulating miR 122 in humans following RYGB from 3 months onwards, although this was not statistically significant (Table 7.12, appendices). However, significant decreases in circulating levels of miR 93, miR 30e and miR 320 following RYGB were found both here and in Wu *et al*.

To our knowledge the only other study assessing post-bariatric circulating microRNAs was published in 2013 by Ortega and colleagues assessing 6 morbidly obese patients (3 men and 3 women) before and 12 months after RYGB [208]. They reported a significant modulation of 14 circulating microRNAs 12 months following RYGB, including a decrease in miR 122. Both Ortega *et al.* and this study found significant decreases in miR 125b and miR 16. Ortega *et al.* also reported increased circulating miR 221 expression, which in this study was consistently increased albeit not significantly across all post-operative timepoints (Table 7.12, appendices). However, Ortega *et al.* reported significant increases in the circulating levels of miR 130b and miR 21. Both microRNAs were significantly decreased in this study 12 months following RYGB. Ortega *et al.* were also unable to detect a change in miR 15a following surgery. In contrast, in this study miR 15a decreased almost 85 fold 12 months following RYGB, the most of any detected microRNA.

Many of the circulating microRNAs found here to be deregulated by RYGB have also been reported as circulating biomarkers of T2DM, including of miR 15a, miR 192, miR 130b and miR 125b [207, 210, 320]. The loss of circulating miR 126 in particular is reportedly a strong selector T2DM [320]. MiR 126 increased over 10 fold in each of the first 4 post-bariatric time points relative to preoperative levels, although none of the increases were statistically significant (Table 7.12, appendices). Blood glucose levels positivity correlated with circulating miR 320a, consistent with previous findings [207] and supporting its candidacy as a novel diabetic biomarker. In total, circulating levels of 9 microRNAs significantly correlated with blood glucose levels. It is important to note that of the 9 patients in this study only 2 were diabetic preoperatively. A larger, multi-centre, follow-up study with a bigger diabetic subset and more robust clinical endpoints are needed for the future development of this field.

MicroRNA profiles are rich in biological information as physiological responses and the mechanism behind them can be captured in the expression of the handful of microRNAs that regulate them. As such the deregulation of circulating microRNAs by bariatric surgery provides fresh mechanistic insights behind these procedures. MicroRNA can act as mediators or effectors in positive and negative feedback loops in wider regulation networks, but their precise function in circulation is still being debated. The presence of circulating microRNAs in exosomes and high-density lipoprotein complexes that can be taken up in the active form by recipient cells is suggestive of a potential tissue-to-tissue communicative role [203, 204] and that microRNAs have hormonal as well as biomarker potential [321]. Mechanistic *in vitro* studies and experimental validation of predicted microRNA targets are required to determine the exact role each differentiated microRNA plays following bariatric surgery. However, although the field is still in its infancy, bariatric surgery has been shown consistently to significantly alter circulating microRNA levels. Here, the deregulation of specific microRNAs at different post-bariatric phases leads to the time-dependent activation of obesity-associated pathways which may contribute to the beneficial effects of bariatric surgery.

5 Discussion

The underlying hypothesis of this thesis was that microRNAs are biomarkers of the beneficial effects of bariatric surgery. To this effect studies were designed and detailed in the preceding chapters that demonstrated the following:

1 After optimising a protocol to measure and normalise microRNA levels in urine and circulation, an obesity urinary and circulating microRNA baseline was established. Circulating levels of miR 22-5p and miR 145-5p, regulators of cancer and lipolysis respectively, both correlated with BMI were identified as potential biomarkers of obesity.

2 Bariatric surgery increased urinary levels of miR 192, miR 200a and miR 200b, regardless of operative procedure or diabetes status. All three microRNAs are expressed in the kidney and protect against fibrosis and diabetic nephropathy. Transfection of miR 192 into a kidney cell line inhibits ZEB2, a key transcriptional promoter of kidney fibrosis.

3 RYGB profoundly modulates circulating microRNA levels and produces distinct bariatric microRNA profiles that display increasing variation from the preoperative profile with time. Significant correlations were found between circulating microRNA expression and BMI, percentage of preoperative BMI lost and blood glucose. Post-bariatric phases are characterised by the selective differentiation of specific microRNAs and the accompanied activation of anti-obesity pathways including those that promote gut-hormone signalling and lipolysis.

MicroRNAs are a relatively new but an exceptionally exciting and fast moving area of gene regulation research. Over the past decade the role of microRNAs as important regulators of physiological processes in both health and disease has been increasingly recognised. Understanding changes in the expression patterns of this complex, wide-ranging network of post-transcriptional regulators is a key to understanding the processes behind physiological changes, such as those produced by bariatric surgery. Bariatric surgery has a number of beneficial effects on health beyond weight-loss, including the resolution of type 2 diabetes, improved cardiovascular health, improved kidney function and reduction in cancer risk. As outlined in the introduction the mechanisms by which these improvements of health are achieved are complex, multi-factorial and synchronistical. They include the suppression of appetite, modulation of gut hormone secretion, improved glucose management and increased energy expenditure.

The results outlined in this thesis demonstrate that both obesity and bariatric surgery deregulate microRNA expression in biofluids and that these microRNAs are involved in regulating pathways that are associated with obesity, the metabolic syndrome and the development of the beneficial post-bariatric phenotype. Bariatric surgery deregulates microRNAs that regulate pathways involved in kidney fibrosis, glucose homeostasis, gut hormone signalling and adipocyte lipolysis (Figure 5.1). This suggests that urinary and circulating microRNAs not only represent novel, minimally invasive biomarkers of health, they are potential post-bariatric biological effectors and can offer fresh mechanistic insights into the mechanisms behind bariatric surgery.

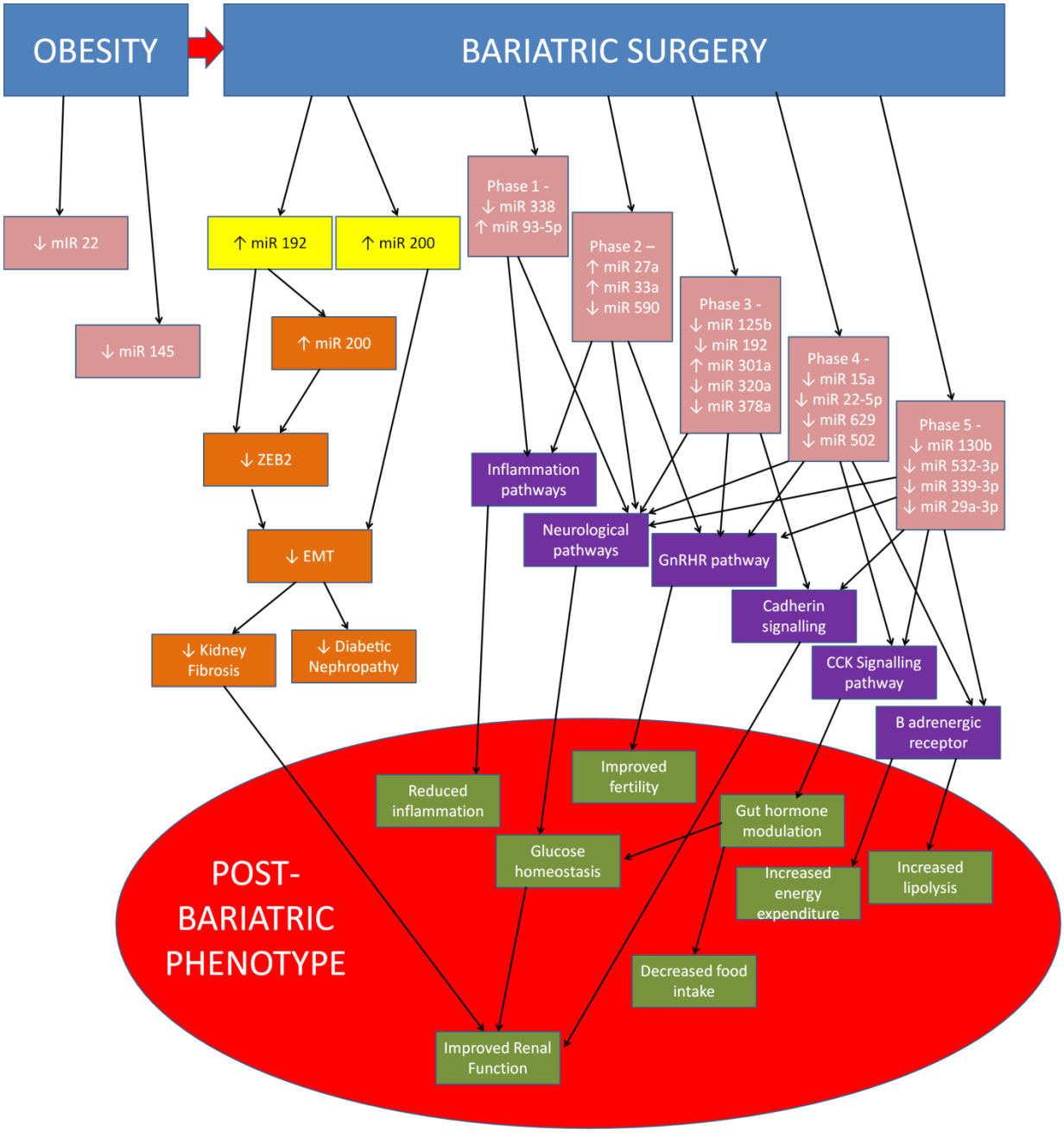

Figure 5.1: A summary of the main findings of this thesis.

Circulating microRNA changes are boxed in pink. Urinary microRNA changes are boxed in yellow.

One question that arises from this thesis is whether bariatric surgery shifts microRNA expression from an obesity state to levels similar to or approaching a healthy state, as the urinary miR 192 data suggests, or whether bariatric surgery produces microRNA expression profiles unique to bariatric patients. Bariatric surgery is often called metabolic surgery due to its profound health benefits beyond weight-loss and has also been suggested as a possible autobionic therapy, enhancing physiological function beyond normality [322]. Although the obesity microRNA baseline established in Chapter 2 demonstrated decreased levels of miR 22-5p and miR 145, miR 145 was unchanged following bariatric surgery and miR 22-5p decreased significantly at 9 months and 12 months following RYGB, forming part of the fourth post-bariatric phase. Similarly, Ortega *et al*. reported decreased miR 125b levels both in obesity and 12 months following RYGB [208] (here miR 125b remained unchanged with obesity but decreased at 6, 9 and 12 months following RYGB). As such subsequent profiling studies should include a healthy control group with a normal BMI.

There is increasing evidence to suggest microRNAs help to maintain system robustness, fine-tuning or 'buffering' gene expression in response to subtle internal or external stimuli [323]. Interestingly, as illustrated by the PCA scores plot of circulating microRNA profiles (Figure 3.7), at 1 month following RYGB the microRNA circulating profile shifts one way from the preoperative profile, before a pronounced and gradual shift in the opposite direction from 3 months onwards. A possible explanation is that the initial physiological response to bariatric surgery was to maintain the morbidly obese *status quo* which was reflected in the overall microRNA circulating profile. However, once a tipping point has been reached this homeostatic safety mechanism was overridden, placing the individual on the path to the post-bariatric phenotype. The early post-bariatric months demonstrated the fewest differentiated microRNAs, but the number of differentiated microRNAs increased with each passing month as the individual moved further physiologically and phenotypically from the morbidly obese state.

To date only one other study has attempted to assess the role of microRNAs in bariatric surgery [208]. Therefore, the findings presented here need to be confirmed in larger, prospective, randomised studies across international bariatric centres with a greater number of subgroups covering different bariatric procedures and obesity co-morbidities. Only a small number of patients in the studies outlined here were diabetic preoperatively and none presented with kidney dysfunction. Longer post-bariatric follow-ups and more robust clinical endpoints are required to affirm the bariatric biomarker and diagnostic potential of microRNAs.

MicroRNA targets and regulated pathways were largely predicted computationally through bioinformatics. Experimental mechanistic studies are required to validate these predictions, such as the gain or loss-of-function *in vitro* manipulation of microRNA used in Chapter 3. However, bariatric surgery altered the expression of a swathe of circulating microRNA, suggesting the post-bariatric microRNA response is holistic and not characterised by specific microRNAs. Of the 159 circulating microRNAs that passed the profiling detection threshold, 49 were differentially expressed in at least one timepoint following RYGB. That's over 30% of all assessed microRNAs, many of which shared not only regulatory pathways but specific mRNA targets, suggesting they function synergistically in a large, complex network. This concept is reflected in individual microRNA gene knockout studies that have show no significant changes in phenotype [324]. Focusing on individual or a few microRNAs may aid in the development of novel drug targets and diagnostic or prognostic biomarkers, however.

The question of whether urinary and circulating microRNAs are simply biomarkers of bariatric surgery or are causative players remains. As has been mentioned previously, there is evidence that extracellular microRNAs are packaged in membrane-covered exosomes or are present in complexes with high-density lipoproteins or argonaute protein, protecting them from ribonuclease degradation, and circulating miRNAs can be taken up in active form by recipient cells, suggesting a potential hormonal tissue-to-tissue communicative role [202-204]. One possible method to answer this question is to knock-out Dicer in rodent bariatric models, assessing whether this inhibits the

beneficial effects of bariatric surgery. Dicer-deficient mice have been used to demonstrate the essential roles of microRNA in angiogenesis, stem cell development and renal function. [140, 258-260, 325]. In humans, microRNA profiles could be determined in liver and adipose tissues obtained intraoperatively and through postoperative biopsies.

A PCR profiling platform that covered 179 microRNAs that are routinely found in circulation [276] was selected to profile circulating microRNAs. However, great strides have been made recently to improve the applicability and sensitivity of next generation profiling platforms and plasma/serum microRNA deep sequencing is now possible with as little as 500µl starting volume [326]. Urinary microRNA can also be deep sequenced but requires 20ml starting volume of urine [327]. Deep sequencing is high throughput and can detect novel microRNAs [193] and would provide a more comprehensive picture of the bariatric microRNA profile.

5.1 Conclusion

In conclusion, this thesis has demonstrated that microRNAs can act as biomarkers and are possible mediators of the beneficial bariatric effects, potentially contributing to the epigenetic development of the post-bariatric phenotype. Further development of this young field could eventually lead to the use of microRNAs as diagnostic tools, aiding in selecting patients for bariatric surgery and monitoring operative outcomes. Understanding the nature of their differential expression following bariatric surgery will help uncover the regulatory processes behind the mechanisms by which the beneficial effects of bariatric surgery are achieved, including potentially mechanisms previously unrecognised. Reverse engineering bariatric surgery will help improve bariatric procedures, accentuating and optimising their benefits and may lead to the development of a successful knifeless metabolic therapy for obesity and its many co-morbidites, encompassing all the benefits of bariatric surgery without the surgery itself. This possibility has been demonstrated recently by the transfer of gut microbiota from RYGB-treated mice to nonoperated, germ free mice, leading to weight loss and decreased fat mass [133].

6 References

1. WHO. *Obesity and overweight Fact Sheet N°311*. 2011; Available from: http://www.who.int/mediacentre/factsheets/fs311/en/index.html.
2. Ng, M., et al., *Global, regional, and national prevalence of overweight and obesity in children and adults during 1980-2013: a systematic analysis for the Global Burden of Disease Study 2013.* Lancet, 2014. **384**(9945): p. 766-81.
3. Health & Social Care Information Centre. *Statistics on Obesity, Physical Activity and Diet: England 2014*. 2014; Available from: http://www.hscic.gov.uk/catalogue/PUB13648/Obes-phys-acti-diet-eng-2014-rep.pdf.
4. McKinsey Global Institute. *Overcoming obesity: An initial economic analysis*. 2014; Available from: http://www.mckinsey.com/insights/economic_studies/how_the_world_could_better_fight_obesity.
5. Guh, D.P., et al., *The incidence of co-morbidities related to obesity and overweight: a systematic review and meta-analysis.* BMC Public Health, 2009. **9**: p. 88.
6. McGee, D.L. and C. Diverse Populations, *Body mass index and mortality: a meta-analysis based on person-level data from twenty-six observational studies.* Ann Epidemiol, 2005. **15**(2): p. 87-97.
7. Flegal, K.M., et al., *Association of all-cause mortality with overweight and obesity using standard body mass index categories: a systematic review and meta-analysis.* JAMA, 2013. **309**(1): p. 71-82.
8. House of Commons Health Committee. *Obesity*. 2004; Available from: http://www.publications.parliament.uk/pa/cm200304/cmselect/cmhealth/23/23.pdf.
9. Duncan, M., et al., *Certification of obesity as a cause of death in England 1979-2006.* Eur J Public Health, 2010. **20**(6): p. 671-5.
10. National Obesity Observatory. *The economic burden of obesity*. 2010; Available from: http://www.noo.org.uk/uploads/doc/vid_8575_Burdenofobesity151110MG.pdf.
11. WHO. *Metrics: Population Attributable Fraction (PAF)*. Available from: http://www.who.int/healthinfo/global_burden_disease/metrics_paf/en/.
12. Hammond, R.A. and R. Levine, *The economic impact of obesity in the United States.* Diabetes Metab Syndr Obes, 2010. **3**: p. 285-95.
13. Kahn, S.E., R.L. Hull, and K.M. Utzschneider, *Mechanisms linking obesity to insulin resistance and type 2 diabetes.* Nature, 2006. **444**(7121): p. 840-6.
14. Fox, C.S., et al., *Predictors of new-onset kidney disease in a community-based population.* JAMA, 2004. **291**(7): p. 844-50.
15. Fenske, W., et al., *Obesity-related cardiorenal disease: the benefits of bariatric surgery.* Nat Rev Nephrol, 2013. **9**(9): p. 539-51.
16. Colditz, G.A., et al., *Weight gain as a risk factor for clinical diabetes mellitus in women.* Ann Intern Med, 1995. **122**(7): p. 481-6.
17. Guariguata, L., et al., *Global estimates of diabetes prevalence for 2013 and projections for 2035.* Diabetes Res Clin Pract, 2014. **103**(2): p. 137-49.
18. Diabetes UK. *Diabetes: Facts and Stats*. 2014; Available from: https://www.diabetes.org.uk/Documents/About%20Us/Statistics/Diabetes-key-stats-guidelines-April2014.pdf.
19. Ferlay, J., et al., *Cancer incidence and mortality worldwide: sources, methods and major patterns in GLOBOCAN 2012.* Int J Cancer, 2015. **136**(5): p. E359-86.
20. Garfinkel, L. and S.D. Stellman, *Mortality by relative weight and exercise.* Cancer, 1988. **62**(8 Suppl): p. 1844-50.
21. Calle, E.E., et al., *Overweight, obesity, and mortality from cancer in a prospectively studied cohort of U.S. adults.* N Engl J Med, 2003. **348**(17): p. 1625-38.

22. Reeves, G.K., et al., *Cancer incidence and mortality in relation to body mass index in the Million Women Study: cohort study.* BMJ, 2007. **335**(7630): p. 1134.
23. Prospective Studies, C., et al., *Body-mass index and cause-specific mortality in 900 000 adults: collaborative analyses of 57 prospective studies.* Lancet, 2009. **373**(9669): p. 1083-96.
24. Renehan, A.G., et al., *Body-mass index and incidence of cancer: a systematic review and meta-analysis of prospective observational studies.* Lancet, 2008. **371**(9612): p. 569-78.
25. Lichtman, M.A., *Obesity and the risk for a hematological malignancy: leukemia, lymphoma, or myeloma.* Oncologist, 2010. **15**(10): p. 1083-101.
26. Ashrafian, H., et al., *Metabolic surgery and cancer: protective effects of bariatric procedures.* Cancer, 2010.
27. WHO. *Cardiovascular diseases (CVDs) Fact sheet N°317*. 2015; Available from: http://www.who.int/mediacentre/factsheets/fs317/en/.
28. Kenchaiah, S., et al., *Obesity and the risk of heart failure.* N Engl J Med, 2002. **347**(5): p. 305-13.
29. Rabkin, S.W., F.A. Mathewson, and P.H. Hsu, *Relation of body weight to development of ischemic heart disease in a cohort of young North American men after a 26 year observation period: the Manitoba Study.* Am J Cardiol, 1977. **39**(3): p. 452-8.
30. Hubert, H.B., et al., *Obesity as an independent risk factor for cardiovascular disease: a 26-year follow-up of participants in the Framingham Heart Study.* Circulation, 1983. **67**(5): p. 968-77.
31. Bastien, M., et al., *Overview of epidemiology and contribution of obesity to cardiovascular disease.* Prog Cardiovasc Dis, 2014. **56**(4): p. 369-81.
32. Roberto, C.A., et al., *Patchy progress on obesity prevention: emerging examples, entrenched barriers, and new thinking.* Lancet, 2015.
33. Sacks, F.M., et al., *Comparison of weight-loss diets with different compositions of fat, protein, and carbohydrates.* N Engl J Med, 2009. **360**(9): p. 859-73.
34. Dietz, W.H., et al., *Management of obesity: improvement of health-care training and systems for prevention and care.* Lancet, 2015.
35. Wadden, T.A., et al., *Lifestyle modification for obesity: new developments in diet, physical activity, and behavior therapy.* Circulation, 2012. **125**(9): p. 1157-70.
36. Diabetes Prevention Program Research, G., et al., *10-year follow-up of diabetes incidence and weight loss in the Diabetes Prevention Program Outcomes Study.* Lancet, 2009. **374**(9702): p. 1677-86.
37. Haskell, W.L., et al., *Physical activity and public health: updated recommendation for adults from the American College of Sports Medicine and the American Heart Association.* Med Sci Sports Exerc, 2007. **39**(8): p. 1423-34.
38. Mora, S., et al., *Physical activity and reduced risk of cardiovascular events: potential mediating mechanisms.* Circulation, 2007. **116**(19): p. 2110-8.
39. Jeffery, R.W., et al., *Physical activity and weight loss: does prescribing higher physical activity goals improve outcome?* Am J Clin Nutr, 2003. **78**(4): p. 684-9.
40. Yanovski, S.Z. and J.A. Yanovski, *Long-term drug treatment for obesity: a systematic and clinical review.* JAMA, 2014. **311**(1): p. 74-86.
41. Dietrich, M.O. and T.L. Horvath, *Limitations in anti-obesity drug development: the critical role of hunger-promoting neurons.* Nat Rev Drug Discov, 2012. **11**(9): p. 675-91.
42. Buchwald, H., et al., *Weight and type 2 diabetes after bariatric surgery: systematic review and meta-analysis.* Am J Med, 2009. **122**(3): p. 248-256 e5.
43. Buchwald, H., et al., *Bariatric surgery: a systematic review and meta-analysis.* JAMA, 2004. **292**(14): p. 1724-37.
44. Angrisani, L., et al., *Bariatric Surgery Worldwide 2013.* Obes Surg, 2015.
45. Buchwald, H. and S.E. Williams, *Bariatric surgery worldwide 2003.* Obes Surg, 2004. **14**(9): p. 1157-64.

46. Buchwald, H., et al., *Trends in mortality in bariatric surgery: a systematic review and meta-analysis.* Surgery, 2007. **142**(4): p. 621-32; discussion 632-5.
47. Chang, S.H., et al., *The effectiveness and risks of bariatric surgery: an updated systematic review and meta-analysis, 2003-2012.* JAMA Surg, 2014. **149**(3): p. 275-87.
48. The National Bariatric Surgery Registry. *The United Kingdom National Bariatric Surgery Registry - Second Registry Report*. 2014; Available from: http://www.bomss.org.uk/wp-content/uploads/2014/04/Extract_from_the_NBSR_2014_Report.pdf.
49. NICE. *Obesity: NICE Clinical Guideline 43.* 2006; Available from: http://www.nice.org.uk/CG43.
50. National Institute of Health. *Bariatric Surgery for Severe Obesity*. 2009; Available from: http://www.niddk.nih.gov/health-information/health-topics/weight-control/bariatric-surgery-severe-obesity/Documents/Bariatric_Surgery_508.pdf.
51. Cummings, D.E. and R.V. Cohen, *Beyond BMI: the need for new guidelines governing the use of bariatric and metabolic surgery.* Lancet Diabetes Endocrinol, 2014. **2**(2): p. 175-81.
52. NICE, *Obesity: identification, assessment and management of overweight and obesity in children, young people and adults*. 2014.
53. Alobaid H, A.A., Eltawil KM and Wells GA, *Bariatric Surgery for Obesity: A Systematic Review and Meta-Analysis.* Adv Obes Weight Manag Control, 2015. **2**(2).
54. Mason, E.E. and C. Ito, *Gastric bypass in obesity.* Surg Clin North Am, 1967. **47**(6): p. 1345-51.
55. Griffen, W.O., Jr., V.L. Young, and C.C. Stevenson, *A prospective comparison of gastric and jejunoileal bypass procedures for morbid obesity.* Ann Surg, 1977. **186**(4): p. 500-9.
56. Wittgrove, A.C., G.W. Clark, and L.J. Tremblay, *Laparoscopic Gastric Bypass, Roux-en-Y: Preliminary Report of Five Cases.* Obes Surg, 1994. **4**(4): p. 353-357.
57. Marceau, P., et al., *Biliopancreatic Diversion with a New Type of Gastrectomy.* Obes Surg, 1993. **3**(1): p. 29-35.
58. Buchwald, H. and D.M. Oien, *Metabolic/bariatric surgery Worldwide 2008.* Obes Surg, 2009. **19**(12): p. 1605-11.
59. Ashrafian, H., et al., *Metabolic surgery: an evolution through bariatric animal models.* Obes Rev, 2010. **11**(12): p. 907-20.
60. Sjostrom, L., et al., *Lifestyle, diabetes, and cardiovascular risk factors 10 years after bariatric surgery.* N Engl J Med, 2004. **351**(26): p. 2683-93.
61. Sjostrom, L., et al., *Effects of bariatric surgery on mortality in Swedish obese subjects.* N Engl J Med, 2007. **357**(8): p. 741-52.
62. Sjostrom, L., et al., *Bariatric surgery and long-term cardiovascular events.* JAMA, 2012. **307**(1): p. 56-65.
63. Dixon, J.B., et al., *Adjustable gastric banding and conventional therapy for type 2 diabetes: a randomized controlled trial.* JAMA, 2008. **299**(3): p. 316-23.
64. Mingrone, G., et al., *Bariatric surgery versus conventional medical therapy for type 2 diabetes.* N Engl J Med, 2012. **366**(17): p. 1577-85.
65. Schauer, P.R., et al., *Bariatric surgery versus intensive medical therapy in obese patients with diabetes.* N Engl J Med, 2012. **366**(17): p. 1567-76.
66. Schauer, P.R., et al., *Bariatric surgery versus intensive medical therapy for diabetes--3-year outcomes.* N Engl J Med, 2014. **370**(21): p. 2002-13.
67. Maggard, M.A., et al., *Meta-analysis: surgical treatment of obesity.* Ann Intern Med, 2005. **142**(7): p. 547-59.
68. Gloy, V.L., et al., *Bariatric surgery versus non-surgical treatment for obesity: a systematic review and meta-analysis of randomised controlled trials.* BMJ, 2013. **347**: p. f5934.
69. Pories, W.J., et al., *Who would have thought it? An operation proves to be the most effective therapy for adult-onset diabetes mellitus.* Ann Surg, 1995. **222**(3): p. 339-50; discussion 350-2.

70. Ikramuddin, S., et al., *Roux-en-Y gastric bypass vs intensive medical management for the control of type 2 diabetes, hypertension, and hyperlipidemia: the Diabetes Surgery Study randomized clinical trial.* JAMA, 2013. **309**(21): p. 2240-9.
71. Buse, J.B., et al., *How do we define cure of diabetes?* Diabetes Care, 2009. **32**(11): p. 2133-5.
72. American Diabetes, A., *Standards of medical care in diabetes--2012.* Diabetes Care, 2012. **35 Suppl 1**: p. S11-63.
73. Arterburn, D.E., et al., *A multisite study of long-term remission and relapse of type 2 diabetes mellitus following gastric bypass.* Obes Surg, 2013. **23**(1): p. 93-102.
74. Brethauer, S.A., et al., *Can diabetes be surgically cured? Long-term metabolic effects of bariatric surgery in obese patients with type 2 diabetes mellitus.* Ann Surg, 2013. **258**(4): p. 628-36; discussion 636-7.
75. Carlsson, L.M., et al., *Bariatric surgery and prevention of type 2 diabetes in Swedish obese subjects.* N Engl J Med, 2012. **367**(8): p. 695-704.
76. Cummings, D.E., *Endocrine mechanisms mediating remission of diabetes after gastric bypass surgery.* Int J Obes (Lond), 2009. **33 Suppl 1**: p. S33-40.
77. Cohen, R., et al., *Laparoscopic Roux-en-Y gastric bypass for BMI < 35 kg/m(2): a tailored approach.* Surg Obes Relat Dis, 2006. **2**(3): p. 401-4, discussion 404.
78. Lee, W.J., et al., *Gastrointestinal metabolic surgery for the treatment of diabetic patients: a multi-institutional international study.* J Gastrointest Surg, 2012. **16**(1): p. 45-51; discussion 51-2.
79. Heneghan, H.M., et al., *Effects of bariatric surgery on diabetic nephropathy after 5 years of follow-up.* Surg Obes Relat Dis, 2013. **9**(1): p. 7-14.
80. Hinojosa, M.W., et al., *Resolution of systemic hypertension after laparoscopic gastric bypass.* J Gastrointest Surg, 2009. **13**(4): p. 793-7.
81. Peterli, R., et al., *Early results of the Swiss Multicentre Bypass or Sleeve Study (SM-BOSS): a prospective randomized trial comparing laparoscopic sleeve gastrectomy and Roux-en-Y gastric bypass.* Ann Surg, 2013. **258**(5): p. 690-4; discussion 695.
82. Courcoulas, A.P., et al., *Weight change and health outcomes at 3 years after bariatric surgery among individuals with severe obesity.* JAMA, 2013. **310**(22): p. 2416-25.
83. Adams, T.D., et al., *Health benefits of gastric bypass surgery after 6 years.* JAMA, 2012. **308**(11): p. 1122-31.
84. Kashyap, S.R., et al., *Metabolic effects of bariatric surgery in patients with moderate obesity and type 2 diabetes: analysis of a randomized control trial comparing surgery with intensive medical treatment.* Diabetes Care, 2013. **36**(8): p. 2175-82.
85. Romeo, S., et al., *Cardiovascular events after bariatric surgery in obese subjects with type 2 diabetes.* Diabetes Care, 2012. **35**(12): p. 2613-7.
86. Christou, N.V., et al., *Surgery decreases long-term mortality, morbidity, and health care use in morbidly obese patients.* Ann Surg, 2004. **240**(3): p. 416-23; discussion 423-4.
87. Adams, T.D., et al., *Long-term mortality after gastric bypass surgery.* N Engl J Med, 2007. **357**(8): p. 753-61.
88. Batsis, J.A., et al., *Effect of bariatric surgery on the metabolic syndrome: a population-based, long-term controlled study.* Mayo Clin Proc, 2008. **83**(8): p. 897-907.
89. Ashrafian, H., et al., *Metabolic surgery and obstructive sleep apnoea: the protective effects of bariatric procedures.* Thorax, 2011.
90. Christou, N.V., et al., *Bariatric surgery reduces cancer risk in morbidly obese patients.* Surg Obes Relat Dis, 2008. **4**(6): p. 691-5.
91. Adams, T.D., et al., *Cancer incidence and mortality after gastric bypass surgery.* Obesity (Silver Spring), 2009. **17**(4): p. 796-802.
92. Kolotkin, R.L., et al., *Six-year changes in health-related quality of life in gastric bypass patients versus obese comparison groups.* Surg Obes Relat Dis, 2012. **8**(5): p. 625-33.

93. Ashrafian, H., A. Darzi, and T. Athanasiou, *Bariatric surgery - can we afford to do it or deny doing it?* Frontline Gastroenterol, 2011. **2**(2): p. 82-89.
94. Madsbad, S., C. Dirksen, and J.J. Holst, *Mechanisms of changes in glucose metabolism and bodyweight after bariatric surgery.* Lancet Diabetes Endocrinol, 2014. **2**(2): p. 152-64.
95. Miras, A.D. and C.W. le Roux, *Mechanisms underlying weight loss after bariatric surgery.* Nat Rev Gastroenterol Hepatol, 2013. **10**(10): p. 575-84.
96. Ashrafian, H., et al., *Metabolic surgery: an evolution through bariatric animal models.* Obesity Reviews, 2010. **11**(12): p. 907-920.
97. Shah, S., et al., *Prospective controlled study of effect of laparoscopic sleeve gastrectomy on small bowel transit time and gastric emptying half-time in morbidly obese patients with type 2 diabetes mellitus.* Surg Obes Relat Dis, 2010. **6**(2): p. 152-7.
98. Dixon, A.F., J.B. Dixon, and P.E. O'Brien, *Laparoscopic adjustable gastric banding induces prolonged satiety: a randomized blind crossover study.* J Clin Endocrinol Metab, 2005. **90**(2): p. 813-9.
99. Burton, P.R. and W.A. Brown, *The mechanism of weight loss with laparoscopic adjustable gastric banding: induction of satiety not restriction.* Int J Obes (Lond), 2011. **35 Suppl 3**: p. S26-30.
100. Maclean, P.S., et al., *Biology's response to dieting: the impetus for weight regain.* Am J Physiol Regul Integr Comp Physiol, 2011. **301**(3): p. R581-600.
101. Sumithran, P., et al., *Long-term persistence of hormonal adaptations to weight loss.* N Engl J Med, 2011. **365**(17): p. 1597-604.
102. le Roux, C.W., et al., *Gut hormone profiles following bariatric surgery favor an anorectic state, facilitate weight loss, and improve metabolic parameters.* Ann Surg, 2006. **243**(1): p. 108-14.
103. Kenler, H.A., R.E. Brolin, and R.P. Cody, *Changes in eating behavior after horizontal gastroplasty and Roux-en-Y gastric bypass.* Am J Clin Nutr, 1990. **52**(1): p. 87-92.
104. Olbers, T., et al., *Body composition, dietary intake, and energy expenditure after laparoscopic Roux-en-Y gastric bypass and laparoscopic vertical banded gastroplasty: a randomized clinical trial.* Ann Surg, 2006. **244**(5): p. 715-22.
105. Zheng, H., et al., *Meal patterns, satiety, and food choice in a rat model of Roux-en-Y gastric bypass surgery.* Am J Physiol Regul Integr Comp Physiol, 2009. **297**(5): p. R1273-82.
106. Wilson-Perez, H.E., et al., *The effect of vertical sleeve gastrectomy on food choice in rats.* Int J Obes (Lond), 2013. **37**(2): p. 288-95.
107. Tack, J., et al., *Pathophysiology, diagnosis and management of postoperative dumping syndrome.* Nat Rev Gastroenterol Hepatol, 2009. **6**(10): p. 583-90.
108. Ochner, C.N., et al., *Selective reduction in neural responses to high calorie foods following gastric bypass surgery.* Ann Surg, 2011. **253**(3): p. 502-7.
109. Scholtz, S., et al., *Obese patients after gastric bypass surgery have lower brain-hedonic responses to food than after gastric banding.* Gut, 2014. **63**(6): p. 891-902.
110. Seyfried, F., C.W. le Roux, and M. Bueter, *Lessons learned from gastric bypass operations in rats.* Obes Facts, 2011. **4 Suppl 1**: p. 3-12.
111. Kampe, J., et al., *Neural and humoral changes associated with the adjustable gastric band: insights from a rodent model.* Int J Obes (Lond), 2012. **36**(11): p. 1403-11.
112. Batterham, R.L., et al., *Gut hormone PYY(3-36) physiologically inhibits food intake.* Nature, 2002. **418**(6898): p. 650-4.
113. Dimitriadis, E., et al., *Alterations in gut hormones after laparoscopic sleeve gastrectomy: a prospective clinical and laboratory investigational study.* Ann Surg, 2013. **257**(4): p. 647-54.
114. Cummings, D.E., et al., *Plasma ghrelin levels after diet-induced weight loss or gastric bypass surgery.* N Engl J Med, 2002. **346**(21): p. 1623-30.

115. Barazzoni, R., et al., *Gastric bypass does not normalize obesity-related changes in ghrelin profile and leads to higher acylated ghrelin fraction.* Obesity (Silver Spring), 2013. **21**(4): p. 718-22.
116. Ashrafian, H., et al., *Diabetes resolution and hyperinsulinaemia after metabolic Roux-en-Y gastric bypass.* Obes Rev, 2011. **12**(5): p. e257-72.
117. Rubino, F. and J. Marescaux, *Effect of duodenal-jejunal exclusion in a non-obese animal model of type 2 diabetes: a new perspective for an old disease.* Ann Surg, 2004. **239**(1): p. 1-11.
118. Troy, S., et al., *Intestinal gluconeogenesis is a key factor for early metabolic changes after gastric bypass but not after gastric lap-band in mice.* Cell Metab, 2008. **8**(3): p. 201-11.
119. Saeidi, N., et al., *Reprogramming of intestinal glucose metabolism and glycemic control in rats after gastric bypass.* Science, 2013. **341**(6144): p. 406-10.
120. Ramos, A.C., et al., *Laparoscopic duodenal-jejunal exclusion in the treatment of type 2 diabetes mellitus in patients with BMI<30 kg/m2 (LBMI).* Obes Surg, 2009. **19**(3): p. 307-12.
121. Cohen, R., et al., *Role of proximal gut exclusion from food on glucose homeostasis in patients with Type 2 diabetes.* Diabet Med, 2013. **30**(12): p. 1482-6.
122. Thomas, C., et al., *TGR5-mediated bile acid sensing controls glucose homeostasis.* Cell Metab, 2009. **10**(3): p. 167-77.
123. Claudel, T., B. Staels, and F. Kuipers, *The Farnesoid X receptor: a molecular link between bile acid and lipid and glucose metabolism.* Arterioscler Thromb Vasc Biol, 2005. **25**(10): p. 2020-30.
124. Patti, M.E., et al., *Serum bile acids are higher in humans with prior gastric bypass: potential contribution to improved glucose and lipid metabolism.* Obesity (Silver Spring), 2009. **17**(9): p. 1671-7.
125. Kohli, R., et al., *Weight loss induced by Roux-en-Y gastric bypass but not laparoscopic adjustable gastric banding increases circulating bile acids.* J Clin Endocrinol Metab, 2013. **98**(4): p. E708-12.
126. Simonen, M., et al., *Conjugated bile acids associate with altered rates of glucose and lipid oxidation after Roux-en-Y gastric bypass.* Obes Surg, 2012. **22**(9): p. 1473-80.
127. Gerhard, G.S., et al., *A role for fibroblast growth factor 19 and bile acids in diabetes remission after Roux-en-Y gastric bypass.* Diabetes Care, 2013. **36**(7): p. 1859-64.
128. Ryan, K.K., et al., *FXR is a molecular target for the effects of vertical sleeve gastrectomy.* Nature, 2014. **509**(7499): p. 183-8.
129. Turnbaugh, P.J., et al., *An obesity-associated gut microbiome with increased capacity for energy harvest.* Nature, 2006. **444**(7122): p. 1027-31.
130. Zhang, H., et al., *Human gut microbiota in obesity and after gastric bypass.* Proc Natl Acad Sci U S A, 2009. **106**(7): p. 2365-70.
131. Li, J.V., et al., *Metabolic surgery profoundly influences gut microbial-host metabolic cross-talk.* Gut, 2011. **60**(9): p. 1214-23.
132. Furet, J.P., et al., *Differential adaptation of human gut microbiota to bariatric surgery-induced weight loss: links with metabolic and low-grade inflammation markers.* Diabetes, 2010. **59**(12): p. 3049-57.
133. Liou, A.P., et al., *Conserved shifts in the gut microbiota due to gastric bypass reduce host weight and adiposity.* Sci Transl Med, 2013. **5**(178): p. 178ra41.
134. Faria, S.L., et al., *Diet-induced thermogenesis and respiratory quotient after Roux-en-Y gastric bypass.* Surg Obes Relat Dis, 2012. **8**(6): p. 797-802.
135. Werling, M., et al., *Increased postprandial energy expenditure may explain superior long term weight loss after Roux-en-Y gastric bypass compared to vertical banded gastroplasty.* PLoS One, 2013. **8**(4): p. e60280.
136. Lee, R.C., R.L. Feinbaum, and V. Ambros, *The C. elegans heterochronic gene lin-4 encodes small RNAs with antisense complementarity to lin-14.* Cell, 1993. **75**(5): p. 843-54.

137. miRBase, H.s.m. 2012; Available from: http://www.mirbase.org/cgi-bin/mirna_summary.pl?org=hsa.
138. Lee, Y., et al., *MicroRNA genes are transcribed by RNA polymerase II.* EMBO J, 2004. **23**(20): p. 4051-60.
139. Bartel, D.P., *MicroRNAs: genomics, biogenesis, mechanism, and function.* Cell, 2004. **116**(2): p. 281-97.
140. Kanellopoulou, C., et al., *Dicer-deficient mouse embryonic stem cells are defective in differentiation and centromeric silencing.* Genes Dev, 2005. **19**(4): p. 489-501.
141. Wang, Y., et al., *DGCR8 is essential for microRNA biogenesis and silencing of embryonic stem cell self-renewal.* Nat Genet, 2007. **39**(3): p. 380-5.
142. Kim, V.N., J. Han, and M.C. Siomi, *Biogenesis of small RNAs in animals.* Nat Rev Mol Cell Biol, 2009. **10**(2): p. 126-39.
143. Krol, J., I. Loedige, and W. Filipowicz, *The widespread regulation of microRNA biogenesis, function and decay.* Nat Rev Genet, 2010. **11**(9): p. 597-610.
144. Bartel, D.P., *MicroRNAs: target recognition and regulatory functions.* Cell, 2009. **136**(2): p. 215-33.
145. Vasudevan, S., Y. Tong, and J.A. Steitz, *Switching from repression to activation: microRNAs can up-regulate translation.* Science, 2007. **318**(5858): p. 1931-4.
146. Orom, U.A., F.C. Nielsen, and A.H. Lund, *MicroRNA-10a binds the 5'UTR of ribosomal protein mRNAs and enhances their translation.* Mol Cell, 2008. **30**(4): p. 460-71.
147. Eiring, A.M., et al., *miR-328 functions as an RNA decoy to modulate hnRNP E2 regulation of mRNA translation in leukemic blasts.* Cell, 2010. **140**(5): p. 652-65.
148. Bueno, M.J. and M. Malumbres, *MicroRNAs and the cell cycle.* Biochim Biophys Acta, 2011. **1812**(5): p. 592-601.
149. Garzon, R., G.A. Calin, and C.M. Croce, *MicroRNAs in Cancer.* Annu Rev Med, 2009. **60**: p. 167-79.
150. Small, E.M., R.J. Frost, and E.N. Olson, *MicroRNAs add a new dimension to cardiovascular disease.* Circulation, 2010. **121**(8): p. 1022-32.
151. Tan, C.L., et al., *MicroRNA-128 governs neuronal excitability and motor behavior in mice.* Science, 2013. **342**(6163): p. 1254-8.
152. Jackson, A. and P.S. Linsley, *The therapeutic potential of microRNA modulation.* Discov Med, 2010. **9**(47): p. 311-8.
153. Abente, E.J., et al., *MicroRNAs in obesity-associated disorders.* Arch Biochem Biophys, 2015.
154. Arner, P. and A. Kulyte, *MicroRNA regulatory networks in human adipose tissue and obesity.* Nat Rev Endocrinol, 2015.
155. Ahn, J., et al., *MicroRNA-146b promotes adipogenesis by suppressing the SIRT1-FOXO1 cascade.* EMBO Mol Med, 2013. **5**(10): p. 1602-12.
156. Chen, L., et al., *MicroRNA-143 regulates adipogenesis by modulating the MAP2K5-ERK5 signaling.* Sci Rep, 2014. **4**: p. 3819.
157. Karbiener, M., et al., *MicroRNA-26 family is required for human adipogenesis and drives characteristics of brown adipocytes.* Stem Cells, 2014. **32**(6): p. 1578-90.
158. Mori, M., et al., *Essential role for miR-196a in brown adipogenesis of white fat progenitor cells.* PLoS Biol, 2012. **10**(4): p. e1001314.
159. Kim, Y.J., et al., *MicroRNA 21 regulates the proliferation of human adipose tissue-derived mesenchymal stem cells and high-fat diet-induced obesity alters microRNA 21 expression in white adipose tissues.* J Cell Physiol, 2012. **227**(1): p. 183-93.
160. Sun, L. and M. Trajkovski, *MiR-27 orchestrates the transcriptional regulation of brown adipogenesis.* Metabolism, 2014. **63**(2): p. 272-82.
161. Chen, Y., et al., *miR-155 regulates differentiation of brown and beige adipocytes via a bistable circuit.* Nat Commun, 2013. **4**: p. 1769.

162. Chen, L., et al., *MiR-540 as a novel adipogenic inhibitor impairs adipogenesis via suppression of PPARgamma.* J Cell Biochem, 2015. **116**(6): p. 969-76.
163. Poy, M.N., et al., *A pancreatic islet-specific microRNA regulates insulin secretion.* Nature, 2004. **432**(7014): p. 226-30.
164. Poy, M.N., et al., *miR-375 maintains normal pancreatic alpha- and beta-cell mass.* Proc Natl Acad Sci U S A, 2009. **106**(14): p. 5813-8.
165. Arner, E., et al., *Adipose tissue microRNAs as regulators of CCL2 production in human obesity.* Diabetes, 2012. **61**(8): p. 1986-93.
166. Yamauchi, T. and T. Kadowaki, *Adiponectin receptor as a key player in healthy longevity and obesity-related diseases.* Cell Metab, 2013. **17**(2): p. 185-96.
167. Xiao, F., et al., *A novel function of microRNA 130a-3p in hepatic insulin sensitivity and liver steatosis.* Diabetes, 2014. **63**(8): p. 2631-42.
168. Kornfeld, J.W., et al., *Obesity-induced overexpression of miR-802 impairs glucose metabolism through silencing of Hnf1b.* Nature, 2013. **494**(7435): p. 111-5.
169. Fu, X., et al., *MicroRNA-26a regulates insulin sensitivity and metabolism of glucose and lipids.* J Clin Invest, 2015. **125**(6): p. 2497-509.
170. Chen, Y.H., et al., *miRNA-93 inhibits GLUT4 and is overexpressed in adipose tissue of polycystic ovary syndrome patients and women with insulin resistance.* Diabetes, 2013. **62**(7): p. 2278-86.
171. McClelland, A.D. and P. Kantharidis, *microRNA in the development of diabetic complications.* Clin Sci (Lond), 2014. **126**(2): p. 95-110.
172. Esau, C., et al., *miR-122 regulation of lipid metabolism revealed by in vivo antisense targeting.* Cell Metab, 2006. **3**(2): p. 87-98.
173. Vickers, K.C., et al., *MicroRNA-27b is a regulatory hub in lipid metabolism and is altered in dyslipidemia.* Hepatology, 2013. **57**(2): p. 533-42.
174. Najafi-Shoushtari, S.H., et al., *MicroRNA-33 and the SREBP host genes cooperate to control cholesterol homeostasis.* Science, 2010. **328**(5985): p. 1566-9.
175. Rayner, K.J., et al., *MiR-33 contributes to the regulation of cholesterol homeostasis.* Science, 2010. **328**(5985): p. 1570-3.
176. Horie, T., et al., *MicroRNA-33 deficiency reduces the progression of atherosclerotic plaque in ApoE-/- mice.* J Am Heart Assoc, 2012. **1**(6): p. e003376.
177. Rayner, K.J., et al., *Inhibition of miR-33a/b in non-human primates raises plasma HDL and lowers VLDL triglycerides.* Nature, 2011. **478**(7369): p. 404-7.
178. Krupa, A., et al., *Loss of MicroRNA-192 promotes fibrogenesis in diabetic nephropathy.* J Am Soc Nephrol, 2010. **21**(3): p. 438-47.
179. Gregory, P.A., et al., *The miR-200 family and miR-205 regulate epithelial to mesenchymal transition by targeting ZEB1 and SIP1.* Nat Cell Biol, 2008. **10**(5): p. 593-601.
180. Korpal, M., et al., *The miR-200 family inhibits epithelial-mesenchymal transition and cancer cell migration by direct targeting of E-cadherin transcriptional repressors ZEB1 and ZEB2.* J Biol Chem, 2008. **283**(22): p. 14910-4.
181. Kato, M., et al., *MicroRNA-192 in diabetic kidney glomeruli and its function in TGF-beta-induced collagen expression via inhibition of E-box repressors.* Proc Natl Acad Sci U S A, 2007. **104**(9): p. 3432-7.
182. Putta, S., et al., *Inhibiting microRNA-192 ameliorates renal fibrosis in diabetic nephropathy.* J Am Soc Nephrol, 2012. **23**(3): p. 458-69.
183. Wang, B., et al., *E-cadherin expression is regulated by miR-192/215 by a mechanism that is independent of the profibrotic effects of transforming growth factor-beta.* Diabetes, 2010. **59**(7): p. 1794-802.
184. Zhang, Z., et al., *MicroRNA-21 protects from mesangial cell proliferation induced by diabetic nephropathy in db/db mice.* FEBS Lett, 2009. **583**(12): p. 2009-14.

185. Wang, Q., et al., *MicroRNA-377 is up-regulated and can lead to increased fibronectin production in diabetic nephropathy.* FASEB J, 2008. **22**(12): p. 4126-35.
186. Qin, W., et al., *TGF-beta/Smad3 signaling promotes renal fibrosis by inhibiting miR-29.* J Am Soc Nephrol, 2011. **22**(8): p. 1462-74.
187. Kato, M., et al., *TGF-beta activates Akt kinase through a microRNA-dependent amplifying circuit targeting PTEN.* Nat Cell Biol, 2009. **11**(7): p. 881-9.
188. van Rooij, E., et al., *Dysregulation of microRNAs after myocardial infarction reveals a role of miR-29 in cardiac fibrosis.* Proc Natl Acad Sci U S A, 2008. **105**(35): p. 13027-32.
189. Yang, B., et al., *The muscle-specific microRNA miR-1 regulates cardiac arrhythmogenic potential by targeting GJA1 and KCNJ2.* Nat Med, 2007. **13**(4): p. 486-91.
190. Shan, Z.X., et al., *Upregulated expression of miR-1/miR-206 in a rat model of myocardial infarction.* Biochem Biophys Res Commun, 2009. **381**(4): p. 597-601.
191. Duisters, R.F., et al., *miR-133 and miR-30 regulate connective tissue growth factor: implications for a role of microRNAs in myocardial matrix remodeling.* Circ Res, 2009. **104**(2): p. 170-8, 6p following 178.
192. Mitchell, P.S., et al., *Circulating microRNAs as stable blood-based markers for cancer detection.* Proc Natl Acad Sci U S A, 2008. **105**(30): p. 10513-8.
193. Pritchard, C.C., H.H. Cheng, and M. Tewari, *MicroRNA profiling: approaches and considerations.* Nat Rev Genet, 2012. **13**(5): p. 358-69.
194. Mestdagh, P., et al., *Evaluation of quantitative miRNA expression platforms in the microRNA quality control (miRQC) study.* Nat Methods, 2014. **11**(8): p. 809-15.
195. Wienholds, E., et al., *MicroRNA expression in zebrafish embryonic development.* Science, 2005. **309**(5732): p. 310-1.
196. Alvarez-Garcia, I. and E.A. Miska, *MicroRNA functions in animal development and human disease.* Development, 2005. **132**(21): p. 4653-62.
197. Lu, J., et al., *MicroRNA expression profiles classify human cancers.* Nature, 2005. **435**(7043): p. 834-8.
198. Rosenfeld, N., et al., *MicroRNAs accurately identify cancer tissue origin.* Nat Biotechnol, 2008. **26**(4): p. 462-9.
199. Boeri, M., et al., *MicroRNA signatures in tissues and plasma predict development and prognosis of computed tomography detected lung cancer.* Proc Natl Acad Sci U S A, 2011. **108**(9): p. 3713-8.
200. Frampton, A.E., et al., *microRNAs with prognostic significance in pancreatic ductal adenocarcinoma: A meta-analysis.* Eur J Cancer, 2015. **51**(11): p. 1389-1404.
201. Frampton, A.E., et al., *miR-15b and miR-17 Are Tumor-Derived Plasma MicroRNAs Dysregulated in Colorectal Neoplasia.* Ann Surg, 2014.
202. Arroyo, J.D., et al., *Argonaute2 complexes carry a population of circulating microRNAs independent of vesicles in human plasma.* Proc Natl Acad Sci U S A, 2011. **108**(12): p. 5003-8.
203. Valadi, H., et al., *Exosome-mediated transfer of mRNAs and microRNAs is a novel mechanism of genetic exchange between cells.* Nat Cell Biol, 2007. **9**(6): p. 654-9.
204. Vickers, K.C., et al., *MicroRNAs are transported in plasma and delivered to recipient cells by high-density lipoproteins.* Nat Cell Biol, 2011. **13**(4): p. 423-33.
205. Tijsen, A.J., et al., *MiR423-5p as a circulating biomarker for heart failure.* Circ Res, 2010. **106**(6): p. 1035-9.
206. Laterza, O.F., et al., *Plasma MicroRNAs as sensitive and specific biomarkers of tissue injury.* Clin Chem, 2009. **55**(11): p. 1977-83.
207. Karolina, D.S., et al., *Circulating miRNA profiles in patients with metabolic syndrome.* J Clin Endocrinol Metab, 2012. **97**(12): p. E2271-6.
208. Ortega, F.J., et al., *Targeting the circulating microRNA signature of obesity.* Clin Chem, 2013. **59**(5): p. 781-92.

209. Prats-Puig, A., et al., *Changes in circulating microRNAs are associated with childhood obesity.* J Clin Endocrinol Metab, 2013. **98**(10): p. E1655-60.
210. Ortega, F.J., et al., *Profiling of circulating microRNAs reveals common microRNAs linked to type 2 diabetes that change with insulin sensitization.* Diabetes Care, 2014. **37**(5): p. 1375-83.
211. Argyropoulos, C., et al., *Urinary microRNA profiling in the nephropathy of type 1 diabetes.* PLoS One, 2013. **8**(1): p. e54662.
212. Hanke, M., et al., *A robust methodology to study urine microRNA as tumor marker: microRNA-126 and microRNA-182 are related to urinary bladder cancer.* Urol Oncol, 2010. **28**(6): p. 655-61.
213. Yang, X., et al., *Identification of urinary microRNA profiles in rats that may diagnose hepatotoxicity.* Toxicol Sci, 2012. **125**(2): p. 335-44.
214. Wu, Q., et al., *Metabolic phenotype-microRNA data fusion analysis of the systemic consequences of Roux-en-Y gastric bypass surgery.* Int J Obes (Lond), 2015.
215. Chen, C., et al., *Real-time quantification of microRNAs by stem-loop RT-PCR.* Nucleic Acids Res, 2005. **33**(20): p. e179.
216. Livak, K.J. and T.D. Schmittgen, *Analysis of relative gene expression data using real-time quantitative PCR and the 2(-Delta Delta C(T)) Method.* Methods, 2001. **25**(4): p. 402-8.
217. Wyss, M. and R. Kaddurah-Daouk, *Creatine and creatinine metabolism.* Physiol Rev, 2000. **80**(3): p. 1107-213.
218. Wallimann, T., et al., *Intracellular compartmentation, structure and function of creatine kinase isoenzymes in tissues with high and fluctuating energy demands: the 'phosphocreatine circuit' for cellular energy homeostasis.* Biochem J, 1992. **281 (Pt 1)**: p. 21-40.
219. Gautier, J.C., et al., *Evaluation of novel biomarkers of nephrotoxicity in two strains of rat treated with Cisplatin.* Toxicol Pathol, 2010. **38**(6): p. 943-56.
220. Bonsnes, R.W. and H.H. Taussky, *On the colorimetric determination of creatinine by the Jaffe reaction.* Journal of Biological Chemistry, 1945. **158**(3): p. 581-591.
221. EXIQON. *Profiling of microRNA in serum/plasma and other biofluids*. 2012; Available from: http://www.exiqon.com/ls/Documents/Scientific/microRNA-serum-plasma-guidelines.pdf.
222. Wang, B., et al., *miR-200a Prevents renal fibrogenesis through repression of TGF-beta2 expression.* Diabetes, 2011. **60**(1): p. 280-7.
223. Xu, D., et al., *miR-22 represses cancer progression by inducing cellular senescence.* J Cell Biol, 2011. **193**(2): p. 409-24.
224. Tsuchiya, N., et al., *Tumor suppressor miR-22 determines p53-dependent cellular fate through post-transcriptional regulation of p21.* Cancer Res, 2011. **71**(13): p. 4628-39.
225. Xiong, J., Q. Du, and Z. Liang, *Tumor-suppressive microRNA-22 inhibits the transcription of E-box-containing c-Myc target genes by silencing c-Myc binding protein.* Oncogene, 2010. **29**(35): p. 4980-8.
226. Poliseno, L., et al., *Identification of the miR-106b~25 microRNA cluster as a proto-oncogenic PTEN-targeting intron that cooperates with its host gene MCM7 in transformation.* Sci Signal, 2010. **3**(117): p. ra29.
227. Song, S.J., et al., *The oncogenic microRNA miR-22 targets the TET2 tumor suppressor to promote hematopoietic stem cell self-renewal and transformation.* Cell Stem Cell, 2013. **13**(1): p. 87-101.
228. Song, S.J., et al., *MicroRNA-antagonism regulates breast cancer stemness and metastasis via TET-family-dependent chromatin remodeling.* Cell, 2013. **154**(2): p. 311-24.
229. Delhommeau, F., et al., *Mutation in TET2 in myeloid cancers.* N Engl J Med, 2009. **360**(22): p. 2289-301.
230. Jankowska, A.M., et al., *Loss of heterozygosity 4q24 and TET2 mutations associated with myelodysplastic/myeloproliferative neoplasms.* Blood, 2009. **113**(25): p. 6403-10.

231. Perri, R., et al., *MicroRNA modulation in obesity and periodontitis.* J Dent Res, 2012. **91**(1): p. 33-8.
232. Calle, E.E. and R. Kaaks, *Overweight, obesity and cancer: epidemiological evidence and proposed mechanisms.* Nat Rev Cancer, 2004. **4**(8): p. 579-91.
233. Jordan, S.D., et al., *Obesity-induced overexpression of miRNA-143 inhibits insulin-stimulated AKT activation and impairs glucose metabolism.* Nat Cell Biol, 2011. **13**(4): p. 434-46.
234. Kloting, N., et al., *MicroRNA expression in human omental and subcutaneous adipose tissue.* PLoS One, 2009. **4**(3): p. e4699.
235. Arner, P., et al., *Dynamics of human adipose lipid turnover in health and metabolic disease.* Nature, 2011. **478**(7367): p. 110-3.
236. Lorente-Cebrian, S., et al., *MicroRNAs regulate human adipocyte lipolysis: effects of miR-145 are linked to TNF-alpha.* PLoS One, 2014. **9**(1): p. e86800.
237. Viesti, A.C.R., et al., *The expression of LEP, LEPR, IGF1 and IL10 in obesity and the relationship with microRNAs.* PLoS One, 2014. **9**(4): p. e93512.
238. Barutta, F., et al., *Urinary exosomal microRNAs in incipient diabetic nephropathy.* PLoS One, 2013. **8**(11): p. e73798.
239. Riches, K., et al., *Elevated expression levels of miR-143/5 in saphenous vein smooth muscle cells from patients with Type 2 diabetes drive persistent changes in phenotype and function.* J Mol Cell Cardiol, 2014. **74**: p. 240-50.
240. Coughlan, K.A., et al., *AMPK activation: a therapeutic target for type 2 diabetes?* Diabetes Metab Syndr Obes, 2014. **7**: p. 241-53.
241. Starkey Lewis, P.J., et al., *Circulating microRNAs as potential markers of human drug-induced liver injury.* Hepatology, 2011. **54**(5): p. 1767-76.
242. Janssen, H.L., et al., *Treatment of HCV infection by targeting microRNA.* N Engl J Med, 2013. **368**(18): p. 1685-94.
243. Chartoumpekis, D.V., et al., *Differential expression of microRNAs in adipose tissue after long-term high-fat diet-induced obesity in mice.* PLoS One, 2012. **7**(4): p. e34872.
244. Chavali, V., S.C. Tyagi, and P.K. Mishra, *Differential Expression of Dicer, miRNAs, and Inflammatory Markers in Diabetic Ins2+/- Akita Hearts.* Cell Biochem Biophys, 2013.
245. Oba, S., et al., *miR-200b precursor can ameliorate renal tubulointerstitial fibrosis.* PLoS One, 2010. **5**(10): p. e13614.
246. Wang, Y., et al., *Association between obesity and kidney disease: a systematic review and meta-analysis.* Kidney Int, 2008. **73**(1): p. 19-33.
247. Molitch, M.E., et al., *Nephropathy in diabetes.* Diabetes Care, 2004. **27 Suppl 1**: p. S79-83.
248. Bowen, T., R.H. Jenkins, and D.J. Fraser, *MicroRNAs, transforming growth factor beta-1, and tissue fibrosis.* J Pathol, 2013. **229**(2): p. 274-85.
249. Chagnac, A., et al., *The effects of weight loss on renal function in patients with severe obesity.* J Am Soc Nephrol, 2003. **14**(6): p. 1480-6.
250. Agnani, S., et al., *Does treating obesity stabilize chronic kidney disease?* BMC Nephrol, 2005. **6**: p. 7.
251. Morales, E., et al., *Beneficial effects of weight loss in overweight patients with chronic proteinuric nephropathies.* Am J Kidney Dis, 2003. **41**(2): p. 319-27.
252. Ryan, M.J., et al., *HK-2: an immortalized proximal tubule epithelial cell line from normal adult human kidney.* Kidney Int, 1994. **45**(1): p. 48-57.
253. Brunner, D., et al., *Serum-free cell culture: the serum-free media interactive online database.* ALTEX, 2010. **27**(1): p. 53-62.
254. Chomczynski, P. and N. Sacchi, *The single-step method of RNA isolation by acid guanidinium thiocyanate-phenol-chloroform extraction: twenty-something years on.* Nat Protoc, 2006. **1**(2): p. 581-5.
255. WHO, *Use of Glycated Haemoglobin (HbA1c) in the Diagnosis of Diabetes Mellitus* 2011.

256. Sun, Y., et al., *Development of a micro-array to detect human and mouse microRNAs and characterization of expression in human organs.* Nucleic Acids Res, 2004. **32**(22): p. e188.
257. Soifer, H.S., et al., *Silencing of gene expression by gymnotic delivery of antisense oligonucleotides.* Methods Mol Biol, 2012. **815**: p. 333-46.
258. Ho, J., et al., *Podocyte-specific loss of functional microRNAs leads to rapid glomerular and tubular injury.* J Am Soc Nephrol, 2008. **19**(11): p. 2069-75.
259. Harvey, S.J., et al., *Podocyte-specific deletion of dicer alters cytoskeletal dynamics and causes glomerular disease.* J Am Soc Nephrol, 2008. **19**(11): p. 2150-8.
260. Shi, S., et al., *Podocyte-selective deletion of dicer induces proteinuria and glomerulosclerosis.* J Am Soc Nephrol, 2008. **19**(11): p. 2159-69.
261. Kim, T., et al., *p53 regulates epithelial-mesenchymal transition through microRNAs targeting ZEB1 and ZEB2.* J Exp Med, 2011. **208**(5): p. 875-83.
262. Park, S.M., et al., *The miR-200 family determines the epithelial phenotype of cancer cells by targeting the E-cadherin repressors ZEB1 and ZEB2.* Genes Dev, 2008. **22**(7): p. 894-907.
263. Kato, M., et al., *A microRNA circuit mediates transforming growth factor-beta1 autoregulation in renal glomerular mesangial cells.* Kidney Int, 2011. **80**(4): p. 358-68.
264. Tian, Z., et al., *MicroRNA-target pairs in the rat kidney identified by microRNA microarray, proteomic, and bioinformatic analysis.* Genome Res, 2008. **18**(3): p. 404-11.
265. Wang, G., et al., *Expression of microRNAs in the urine of patients with bladder cancer.* Clin Genitourin Cancer, 2012. **10**(2): p. 106-13.
266. Navarro-Diaz, M., et al., *Effect of drastic weight loss after bariatric surgery on renal parameters in extremely obese patients: long-term follow-up.* J Am Soc Nephrol, 2006. **17**(12 Suppl 3): p. S213-7.
267. Alexander, J.W., et al., *Improvement and stabilization of chronic kidney disease after gastric bypass.* Surg Obes Relat Dis, 2009. **5**(2): p. 237-41.
268. Fassett, R.G., et al., *Biomarkers in chronic kidney disease: a review.* Kidney Int, 2011. **80**(8): p. 806-21.
269. Nielsen, L.B., et al., *Circulating levels of microRNA from children with newly diagnosed type 1 diabetes and healthy controls: evidence that miR-25 associates to residual beta-cell function and glycaemic control during disease progression.* Exp Diabetes Res, 2012. **2012**: p. 896362.
270. Bijkerk, R., et al., *Circulating MicroRNAs Associate With Diabetic Nephropathy and Systemic Microvascular Damage and Normalize After Simultaneous Pancreas-Kidney Transplantation.* Am J Transplant, 2015.
271. Kato, M. and R. Natarajan, *Diabetic nephropathy--emerging epigenetic mechanisms.* Nat Rev Nephrol, 2014. **10**(9): p. 517-30.
272. Dey, N., et al., *MicroRNA-21 orchestrates high glucose-induced signals to TOR complex 1, resulting in renal cell pathology in diabetes.* J Biol Chem, 2011. **286**(29): p. 25586-603.
273. Fu, Y., et al., *Regulation of NADPH oxidase activity is associated with miRNA-25-mediated NOX4 expression in experimental diabetic nephropathy.* Am J Nephrol, 2010. **32**(6): p. 581-9.
274. Wang, B., et al., *Suppression of microRNA-29 expression by TGF-beta1 promotes collagen expression and renal fibrosis.* J Am Soc Nephrol, 2012. **23**(2): p. 252-65.
275. Kriz, W., B. Kaissling, and M. Le Hir, *Epithelial-mesenchymal transition (EMT) in kidney fibrosis: fact or fantasy?* J Clin Invest, 2011. **121**(2): p. 468-74.
276. Exiqon. *miRCURY LNA Universal RT microRNA PCR*. 2014; Available from: https://www.exiqon.com/ls/Documents/Scientific/Universal-RT-microRNA-PCR-manual-serum.pdf.
277. Jensen, S.G., et al., *Evaluation of two commercial global miRNA expression profiling platforms for detection of less abundant miRNAs.* BMC Genomics, 2011. **12**: p. 435.
278. Exiqon. *Exiqon GenEx qPCR Analysis Software*. Available from: http://www.exiqon.com/ls/documents/scientific/genex-product-flyer.pdf.

279. Vandesompele, J., et al., *Accurate normalization of real-time quantitative RT-PCR data by geometric averaging of multiple internal control genes.* Genome Biol, 2002. **3**(7): p. RESEARCH0034.
280. Andersen, C.L., J.L. Jensen, and T.F. Orntoft, *Normalization of real-time quantitative reverse transcription-PCR data: a model-based variance estimation approach to identify genes suited for normalization, applied to bladder and colon cancer data sets.* Cancer Res, 2004. **64**(15): p. 5245-50.
281. Dweep, H., et al., *miRWalk--database: prediction of possible miRNA binding sites by "walking" the genes of three genomes.* J Biomed Inform, 2011. **44**(5): p. 839-47.
282. Mi, H., et al., *Large-scale gene function analysis with the PANTHER classification system.* Nat Protoc, 2013. **8**(8): p. 1551-66.
283. Peterson, S.M., et al., *Common features of microRNA target prediction tools.* Front Genet, 2014. **5**: p. 23.
284. Witkos, T.M., E. Koscianska, and W.J. Krzyzosiak, *Practical Aspects of microRNA Target Prediction.* Curr Mol Med, 2011. **11**(2): p. 93-109.
285. Pearson, K., *LIII. On lines and planes of closest fit to systems of points in space.* Philosophical Magazine Series 6, 1901. **2**(11): p. 559-572.
286. Wold, S., K. Esbensen, and P. Geladi, *Principal component analysis.* Chemometrics and Intelligent Laboratory Systems, 1987. **2**(1–3): p. 37-52.
287. Mestdagh, P., et al., *A novel and universal method for microRNA RT-qPCR data normalization.* Genome Biol, 2009. **10**(6): p. R64.
288. Gregor, M.F. and G.S. Hotamisligil, *Inflammatory mechanisms in obesity.* Annu Rev Immunol, 2011. **29**: p. 415-45.
289. Dankel, S.N., et al., *Switch from stress response to homeobox transcription factors in adipose tissue after profound fat loss.* PLoS One, 2010. **5**(6): p. e11033.
290. Ortega, F.J., et al., *Inflammation triggers specific microRNA profiles in human adipocytes and macrophages and in their supernatants.* Clin Epigenetics, 2015. **7**(1): p. 49.
291. Ashrafian, H., et al., *Neurodegenerative disease and obesity: what is the role of weight loss and bariatric interventions?* Metab Brain Dis, 2013. **28**(3): p. 341-53.
292. Millar, R.P., et al., *Gonadotropin-releasing hormone receptors.* Endocr Rev, 2004. **25**(2): p. 235-75.
293. DiVall, S.A., et al., *Insulin receptor signaling in the GnRH neuron plays a role in the abnormal GnRH pulsatility of obese female mice.* PLoS One, 2015. **10**(3): p. e0119995.
294. Pellitero, S., et al., *Hypogonadotropic hypogonadism in morbidly obese males is reversed after bariatric surgery.* Obes Surg, 2012. **22**(12): p. 1835-42.
295. Samavat, J., et al., *Hypogonadism as an additional indication for bariatric surgery in male morbid obesity?* Eur J Endocrinol, 2014. **171**(5): p. 555-60.
296. Wang, H., et al., *Gonadotrope-specific deletion of Dicer results in severely suppressed gonadotropins and fertility defects.* J Biol Chem, 2015. **290**(5): p. 2699-714.
297. Porte, D., Jr., *Beta adrenergic stimulation of insulin release in man.* Diabetes, 1967. **16**(3): p. 150-5.
298. Large, V., et al., *Human beta-2 adrenoceptor gene polymorphisms are highly frequent in obesity and associate with altered adipocyte beta-2 adrenoceptor function.* J Clin Invest, 1997. **100**(12): p. 3005-13.
299. Masuo, K. and G.W. Lambert, *Relationships of adrenoceptor polymorphisms with obesity.* J Obes, 2011. **2011**: p. 609485.
300. Zhao, T.J., et al., *Ghrelin secretion stimulated by {beta}1-adrenergic receptors in cultured ghrelinoma cells and in fasted mice.* Proc Natl Acad Sci U S A, 2010. **107**(36): p. 15868-73.
301. Little, T.J., M. Horowitz, and C. Feinle-Bisset, *Role of cholecystokinin in appetite control and body weight regulation.* Obes Rev, 2005. **6**(4): p. 297-306.

302. Raybould, H.E., *Mechanisms of CCK signaling from gut to brain.* Curr Opin Pharmacol, 2007. **7**(6): p. 570-4.
303. Drucker, D.J., *The role of gut hormones in glucose homeostasis.* J Clin Invest, 2007. **117**(1): p. 24-32.
304. Lin, H.C., W.Y. Chey, and X. Zhao, *Release of distal gut peptide YY (PYY) by fat in proximal gut depends on CCK.* Peptides, 2000. **21**(10): p. 1561-3.
305. Brennan, I.M., et al., *Intravenous CCK-8, but not GLP-1, suppresses ghrelin and stimulates PYY release in healthy men.* Peptides, 2007. **28**(3): p. 607-11.
306. Burdyga, G., et al., *Cholecystokinin regulates expression of Y2 receptors in vagal afferent neurons serving the stomach.* J Neurosci, 2008. **28**(45): p. 11583-92.
307. de Lartigue, G., et al., *Cocaine- and amphetamine-regulated transcript: stimulation of expression in rat vagal afferent neurons by cholecystokinin and suppression by ghrelin.* J Neurosci, 2007. **27**(11): p. 2876-82.
308. Burdyga, G., et al., *Feeding-dependent depression of melanin-concentrating hormone and melanin-concentrating hormone receptor-1 expression in vagal afferent neurones.* Neuroscience, 2006. **137**(4): p. 1405-15.
309. Matson, C.A., et al., *Cholecystokinin and leptin act synergistically to reduce body weight.* Am J Physiol Regul Integr Comp Physiol, 2000. **278**(4): p. R882-90.
310. Riedy, C.A., et al., *Central insulin enhances sensitivity to cholecystokinin.* Physiol Behav, 1995. **58**(4): p. 755-60.
311. Covasa, M. and R.C. Ritter, *Rats maintained on high-fat diets exhibit reduced satiety in response to CCK and bombesin.* Peptides, 1998. **19**(8): p. 1407-15.
312. Torregrossa, A.M. and G.P. Smith, *Two effects of high-fat diets on the satiating potency of cholecystokinin-8.* Physiol Behav, 2003. **78**(1): p. 19-25.
313. Savastano, D.M. and M. Covasa, *Adaptation to a high-fat diet leads to hyperphagia and diminished sensitivity to cholecystokinin in rats.* J Nutr, 2005. **135**(8): p. 1953-9.
314. Rubino, F., et al., *The early effect of the Roux-en-Y gastric bypass on hormones involved in body weight regulation and glucose metabolism.* Ann Surg, 2004. **240**(2): p. 236-42.
315. Kellum, J.M., et al., *Gastrointestinal hormone responses to meals before and after gastric bypass and vertical banded gastroplasty.* Ann Surg, 1990. **211**(6): p. 763-70; discussion 770-1.
316. Jacobsen, S.H., et al., *Changes in gastrointestinal hormone responses, insulin sensitivity, and beta-cell function within 2 weeks after gastric bypass in non-diabetic subjects.* Obes Surg, 2012. **22**(7): p. 1084-96.
317. De Giorgi, S., et al., *Long-term effects of Roux-en-Y gastric bypass on postprandial plasma lipid and bile acids kinetics in female non diabetic subjects: A cross-sectional pilot study.* Clin Nutr, 2014.
318. Peterli, R., et al., *Metabolic and hormonal changes after laparoscopic Roux-en-Y gastric bypass and sleeve gastrectomy: a randomized, prospective trial.* Obes Surg, 2012. **22**(5): p. 740-8.
319. Mumphrey, M.B., et al., *Roux-en-Y gastric bypass surgery increases number but not density of CCK-, GLP-1-, 5-HT-, and neurotensin-expressing enteroendocrine cells in rats.* Neurogastroenterol Motil, 2013. **25**(1): p. e70-9.
320. Zampetaki, A., et al., *Plasma microRNA profiling reveals loss of endothelial miR-126 and other microRNAs in type 2 diabetes.* Circ Res, 2010. **107**(6): p. 810-7.
321. Cortez, M.A., et al., *MicroRNAs in body fluids--the mix of hormones and biomarkers.* Nat Rev Clin Oncol, 2011. **8**(8): p. 467-77.
322. Ashrafian, H., A. Darzi, and T. Athanasiou, *Autobionics: a new paradigm in regenerative medicine and surgery.* Regen Med, 2010. **5**(2): p. 279-88.
323. Ebert, M.S. and P.A. Sharp, *Roles for microRNAs in conferring robustness to biological processes.* Cell, 2012. **149**(3): p. 515-24.

324. Miska, E.A., et al., *Most Caenorhabditis elegans microRNAs are individually not essential for development or viability.* PLoS Genet, 2007. **3**(12): p. e215.
325. Yang, W.J., et al., *Dicer is required for embryonic angiogenesis during mouse development.* J Biol Chem, 2005. **280**(10): p. 9330-5.
326. Exiqon. *A guide to the microRNA and small RNA Sequencing Service* 2015; Available from: http://www.exiqon.com/ls/Documents/Scientific/Service-Customer-Information-NGS.pdf.
327. Cheng, L., et al., *Characterization and deep sequencing analysis of exosomal and non-exosomal miRNA in human urine.* Kidney Int, 2014. **86**(2): p. 433-44.

7 Appendices

Tables 7.1-7.11 are Pearson correlations between circulating and urinary microRNA expressions measured in an obese cohort described in Chapter 2 and blood biochemistry markers.

Table 7.12 tabulates mean fold changes in post-bariatric circulating microRNA expressions relative to mean preoperative levels. Table 7.13 tabulates Pearson correlations between circulating microRNA expressions in a bariatric cohort described in chapter 4 and measured clinical outcomes.

Red signifies statistical significance. Fold change statistical significance was determined by Student's t-tests.

Table 7.1: Serum miR 15a Pearson correlations with blood biochemistry markers.			
	miR 15a		
Clinical Parameter	**r**	**p**	**p significance**
BMI (kg/m^2)	-0.2024	0.1725	ns
Weight (kg)	-0.2386	0.1063	ns
Fasting Glucose (mmol/L)	-0.08298	0.6516	ns
Insulin (µIU/mL)	-0.2441	0.1711	ns
CRP (mg/L)	-0.2625	0.1611	ns
Hb (g/L)	0.09144	0.6187	ns
WCC (x10^9/L)	-0.1908	0.2955	ns
Platelet Count (x10^9/L)	-0.141	0.4415	ns
Sodium (mmol/L)	0.3114	0.0828	ns
Potassium (mmol/L)	-0.07898	0.6674	ns
Chloride (mmol/L)	0.06262	0.7335	ns
BiCarb (mmol/L)	0.03555	0.8468	ns
Urea (mmol/L)	-0.1723	0.3458	ns
Creatinine (umol/L)	0.01132	0.951	ns
eGFR (mL/min)	-0.1591	0.5283	ns
Calcium (mmol/L)	-0.0258	0.8885	ns
Phospate (mmol/L)	-0.1034	0.5735	ns
Bilirubin (umol/L)	0.09269	0.6139	ns
Alk Phos (iu/L)	-0.198	0.2774	ns
Albumin (g/L)	-0.011	0.9524	ns
Total protein (g/L)	-0.1936	0.2884	ns
Cholestrol (mmol/l)	0.02108	0.9088	ns
Triglycerides (mmol/l)	-0.0994	0.5883	ns
HDL (mmol/l)	0.09526	0.604	ns
LDL (mmol/L)	0.03185	0.8626	ns
L-Tyr (µM)	-0.261	0.1562	ns
L-Phe (µM)	-0.06536	0.7269	ns
L-Phe : L-Tyr Ratio	0.2925	0.1103	ns
GLP-1 (pM)	-0.2192	0.2445	ns
GIP (pg/mL)	-0.0783	0.6809	ns

Table 7.2: Serum miR 22-5p Pearson correlations with blood biochemistry markers.			
	miR 22-5p		
Clinical Parameter	r	p	p significance
BMI (kg/m^2)	-0.4085	0.0109	*
Weight (kg)	-0.4596	0.0037	**
Fasting Glucose (mmol/L)	-0.2417	0.2444	ns
Insulin (µIU/mL)	-0.2628	0.1945	ns
CRP (mg/L)	-0.3046	0.1478	ns
Hb (g/L)	0.08977	0.6696	ns
WCC (x10^9/L)	-0.06112	0.7717	ns
Platelet Count (x10^9/L)	0.0229	0.9135	ns
Sodium (mmol/L)	0.1137	0.5883	ns
Potassium (mmol/L)	-0.005556	0.979	ns
Chloride (mmol/L)	0.09567	0.6492	ns
BiCarb (mmol/L)	0.02642	0.9002	ns
Urea (mmol/L)	-0.124	0.5549	ns
Creatinine (umol/L)	-0.0445	0.8327	ns
eGFR (mL/min)	-0.08625	0.7794	ns
Calcium (mmol/L)	-0.11	0.6008	ns
Phospate (mmol/L)	0.1517	0.4691	ns
Bilirubin (umol/L)	0.02286	0.9136	ns
Alk Phos (iu/L)	-0.2131	0.3064	ns
Albumin (g/L)	-0.02086	0.9212	ns
Total protein (g/L)	0.0188	0.9289	ns
Cholestrol (mmol/l)	0.1268	0.537	ns
Triglycerides (mmol/l)	-0.361	0.07	ns
HDL (mmol/l)	0.1096	0.5939	ns
LDL (mmol/L)	0.3005	0.1359	ns
L-Tyr (µM)	-0.206	0.3232	ns
L-Phe (µM)	0.0681	0.7464	ns
L-Phe : L-Tyr Ratio	0.3882	0.0551	ns
GLP-1 (pM)	-0.2581	0.2234	ns
GIP (pg/mL)	-0.1686	0.431	ns

Table 7.3: Serum miR 122 Pearson correlations with blood biochemistry markers.			
	miR 122		
Clinical Parameter	r	p	p significance
BMI (kg/m^2)	-0.1912	0.1979	ns
Weight (kg)	-0.2195	0.1383	ns
Fasting Glucose (mmol/L)	0.3804	0.0317	*
Insulin (µIU/mL)	-0.03652	0.8401	ns
CRP (mg/L)	0.1043	0.5833	ns
Hb (g/L)	0.1209	0.5098	ns
WCC (x10^9/L)	0.02181	0.9057	ns
Platelet Count (x10^9/L)	0.1244	0.4975	ns
Sodium (mmol/L)	0.2456	0.1754	ns
Potassium (mmol/L)	-0.1116	0.5431	ns
Chloride (mmol/L)	-0.1163	0.526	ns
BiCarb (mmol/L)	0.1195	0.5148	ns
Urea (mmol/L)	-0.2858	0.1128	ns
Creatinine (umol/L)	-0.03351	0.8555	ns
eGFR (mL/min)	0.3849	0.1148	ns
Calcium (mmol/L)	0.1213	0.5085	ns
Phospate (mmol/L)	-0.03198	0.862	ns
Bilirubin (umol/L)	0.4235	0.0157	*
Alk Phos (iu/L)	0.1663	0.363	ns
Albumin (g/L)	0.2297	0.2061	ns
Total protein (g/L)	0.175	0.3381	ns
Cholestrol (mmol/l)	0.2357	0.1941	ns
Triglycerides (mmol/l)	0.4153	0.0181	*
HDL (mmol/l)	-0.1766	0.3337	ns
LDL (mmol/L)	0.1496	0.4138	ns
L-Tyr (µM)	0.01483	0.9369	ns
L-Phe (µM)	0.08123	0.664	ns
L-Phe : L-Tyr Ratio	-0.01044	0.9556	ns
GLP-1 (pM)	0.1879	0.3202	ns
GIP (pg/mL)	0.08403	0.6589	ns

Table 7.4: Serum miR 125b Pearson correlations with blood biochemistry markers.			
	miR 125b		
Clinical Parameter	**r**	**p**	**p significance**
BMI (kg/m^2)	-0.1692	0.2665	ns
Weight (kg)	-0.2252	0.1369	ns
Fasting Glucose (mmol/L)	-0.1745	0.3477	ns
Insulin (µIU/mL)	-0.1955	0.2835	ns
CRP (mg/L)	-0.1848	0.3372	ns
Hb (g/L)	0.06376	0.7333	ns
WCC (x10^9/L)	-0.167	0.3691	ns
Platelet Count (x10^9/L)	0.0001546	0.9993	ns
Sodium (mmol/L)	0.1044	0.5763	ns
Potassium (mmol/L)	-0.1026	0.5827	ns
Chloride (mmol/L)	0.05065	0.7867	ns
BiCarb (mmol/L)	-0.1523	0.4135	ns
Urea (mmol/L)	-0.1719	0.355	ns
Creatinine (umol/L)	-0.1591	0.3926	ns
eGFR (mL/min)	-0.1571	0.547	ns
Calcium (mmol/L)	0.05488	0.7694	ns
Phospate (mmol/L)	-0.06099	0.7445	ns
Bilirubin (umol/L)	0.0251	0.8934	ns
Alk Phos (iu/L)	-0.07366	0.6937	ns
Albumin (g/L)	0.1369	0.4627	ns
Total protein (g/L)	0.1404	0.4513	ns
Cholestrol (mmol/l)	0.2864	0.1183	ns
Triglycerides (mmol/l)	-0.05043	0.7876	ns
HDL (mmol/l)	0.1569	0.3992	ns
LDL (mmol/L)	0.3025	0.0981	ns
L-Tyr (µM)	-0.08076	0.6658	ns
L-Phe (µM)	-0.04568	0.8072	ns
L-Phe : L-Tyr Ratio	0.1539	0.4085	ns
GLP-1 (pM)	0.07855	0.6799	ns
GIP (pg/mL)	-0.05084	0.7896	ns

Table 7.5: Serum miR 142-3p Pearson correlations with blood biochemistry markers.			
	miR 142-3p		
Clinical Parameter	r	p	p significance
BMI (kg/m^2)	-0.2509	0.089	ns
Weight (kg)	-0.312	0.0328	*
Fasting Glucose (mmol/L)	-0.1752	0.3375	ns
Insulin (µIU/mL)	-0.2135	0.2328	ns
CRP (mg/L)	-0.2767	0.1388	ns
Hb (g/L)	0.01486	0.9357	ns
WCC (x10^9/L)	-0.167	0.3611	ns
Platelet Count (x10^9/L)	-0.007512	0.9675	ns
Sodium (mmol/L)	0.3729	0.0356	*
Potassium (mmol/L)	-0.04443	0.8092	ns
Chloride (mmol/L)	0.1775	0.3311	ns
BiCarb (mmol/L)	-0.001698	0.9926	ns
Urea (mmol/L)	-0.2127	0.2425	ns
Creatinine (umol/L)	-0.03333	0.8563	ns
eGFR (mL/min)	-0.1524	0.546	ns
Calcium (mmol/L)	-0.03377	0.8544	ns
Phospate (mmol/L)	0.1346	0.4626	ns
Bilirubin (umol/L)	0.09447	0.6071	ns
Alk Phos (iu/L)	-0.09721	0.5966	ns
Albumin (g/L)	-0.1377	0.4524	ns
Total protein (g/L)	-0.1974	0.2788	ns
Cholestrol (mmol/l)	0.1282	0.4845	ns
Triglycerides (mmol/l)	-0.1356	0.4592	ns
HDL (mmol/l)	0.1208	0.5101	ns
LDL (mmol/L)	0.1724	0.3454	ns
L-Tyr (µM)	-0.2206	0.233	ns
L-Phe (µM)	-0.034	0.8559	ns
L-Phe : L-Tyr Ratio	0.243	0.1878	ns
GLP-1 (pM)	-0.3332	0.072	ns
GIP (pg/mL)	-0.1256	0.5085	ns

Table 7.6: Serum miR 145-5p Pearson correlations with blood biochemistry markers.			
	miR 145-5p		
Clinical Parameter	r	p	p significance
BMI (kg/m^2)	-0.3277	0.028	*
Weight (kg)	-0.373	0.0116	*
Fasting Glucose (mmol/L)	-0.1974	0.2872	ns
Insulin (µIU/mL)	-0.2244	0.217	ns
CRP (mg/L)	-0.3087	0.1033	ns
Hb (g/L)	-0.1896	0.3069	ns
WCC (x10^9/L)	-0.1865	0.315	ns
Platelet Count (x10^9/L)	0.04471	0.8113	ns
Sodium (mmol/L)	-0.04803	0.7975	ns
Potassium (mmol/L)	-0.1516	0.4157	ns
Chloride (mmol/L)	-0.001392	0.9941	ns
BiCarb (mmol/L)	-0.05184	0.7818	ns
Urea (mmol/L)	-0.05991	0.7489	ns
Creatinine (umol/L)	-0.05129	0.7841	ns
eGFR (mL/min)	-0.3704	0.1433	ns
Calcium (mmol/L)	-0.1185	0.5256	ns
Phospate (mmol/L)	0.06655	0.7221	ns
Bilirubin (umol/L)	-0.09866	0.5975	ns
Alk Phos (iu/L)	-0.1672	0.3687	ns
Albumin (g/L)	0.04768	0.799	ns
Total protein (g/L)	-0.03342	0.8583	ns
Cholestrol (mmol/l)	0.1609	0.3871	ns
Triglycerides (mmol/l)	-0.3049	0.0954	ns
HDL (mmol/l)	0.4175	0.0194	*
LDL (mmol/L)	0.1453	0.4354	ns
L-Tyr (µM)	-0.3098	0.0898	ns
L-Phe (µM)	-0.1571	0.3987	ns
L-Phe : L-Tyr Ratio	0.3723	0.0392	*
GLP-1 (pM)	-0.1755	0.3535	ns
GIP (pg/mL)	-0.2536	0.1763	ns

Table 7.7: Serum miR 192 Pearson correlations with blood biochemistry markers.			
	miR 192		
Clinical Parameter	r	p	p significance
BMI (kg/m^2)	-0.2565	0.1712	ns
Weight (kg)	-0.3984	0.0292	*
Fasting Glucose (mmol/L)	0.2448	0.2849	ns
Insulin (µIU/mL)	-0.2271	0.3221	ns
CRP (mg/L)	-0.01676	0.9474	ns
Hb (g/L)	-0.07402	0.7498	ns
WCC (x10^9/L)	0.106	0.6474	ns
Platelet Count (x10^9/L)	0.274	0.2293	ns
Sodium (mmol/L)	0.263	0.2493	ns
Potassium (mmol/L)	0.003236	0.9889	ns
Chloride (mmol/L)	-0.316	0.1628	ns
BiCarb (mmol/L)	0.1636	0.4785	ns
Urea (mmol/L)	-0.2298	0.3163	ns
Creatinine (umol/L)	0.1293	0.5764	ns
eGFR (mL/min)	-0.0745	0.8277	ns
Calcium (mmol/L)	0.2929	0.1976	ns
Phospate (mmol/L)	0.1242	0.5917	ns
Bilirubin (umol/L)	0.4465	0.0425	*
Alk Phos (iu/L)	0.1619	0.4832	ns
Albumin (g/L)	0.2285	0.3191	ns
Total protein (g/L)	0.04143	0.8585	ns
Cholestrol (mmol/l)	0.2763	0.2383	ns
Triglycerides (mmol/l)	0.3526	0.1273	ns
HDL (mmol/l)	-0.003744	0.9875	ns
LDL (mmol/L)	0.1001	0.6747	ns
L-Tyr (µM)	-0.3321	0.1526	ns
L-Phe (µM)	-0.2452	0.2975	ns
L-Phe : L-Tyr Ratio	0.1857	0.4331	ns
GLP-1 (pM)	0.167	0.4944	ns
GIP (pg/mL)	0.0255	0.9175	ns

Table 7.8: Serum miR 221 Pearson correlations with blood biochemistry markers.			
		miR 221	
Clinical Parameter	r	p	p significance
BMI (kg/m^2)	0.169	0.256	ns
Weight (kg)	0.1496	0.3156	ns
Fasting Glucose (mmol/L)	-0.1075	0.5582	ns
Insulin (µIU/mL)	-0.1821	0.3105	ns
CRP (mg/L)	0.0436	0.819	ns
Hb (g/L)	0.2373	0.191	ns
WCC (x10^9/L)	-0.03578	0.8459	ns
Platelet Count (x10^9/L)	-0.1816	0.32	ns
Sodium (mmol/L)	0.2635	0.145	ns
Potassium (mmol/L)	0.1623	0.3749	ns
Chloride (mmol/L)	0.2807	0.1196	ns
BiCarb (mmol/L)	-0.5822	0.0005	***
Urea (mmol/L)	0.007609	0.967	ns
Creatinine (umol/L)	0.2576	0.1546	ns
eGFR (mL/min)	-0.3238	0.1899	ns
Calcium (mmol/L)	0.2665	0.1404	ns
Phospate (mmol/L)	-0.1071	0.5597	ns
Bilirubin (umol/L)	0.09852	0.5917	ns
Alk Phos (iu/L)	0.0023	0.99	ns
Albumin (g/L)	0.1049	0.5677	ns
Total protein (g/L)	0.05587	0.7614	ns
Cholestrol (mmol/l)	-0.006004	0.974	ns
Triglycerides (mmol/l)	0.3474	0.0514	ns
HDL (mmol/l)	-0.1577	0.3886	ns
LDL (mmol/L)	-0.1233	0.5015	ns
L-Tyr (µM)	-0.2097	0.2575	ns
L-Phe (µM)	-0.1684	0.3653	ns
L-Phe : L-Tyr Ratio	0.1183	0.5262	ns
GLP-1 (pM)	-0.121	0.524	ns
GIP (pg/mL)	-0.02148	0.9103	ns

Table 7.9: Urine miR 192 Pearson correlations with blood biochemistry markers.			
	miR 192		
Clinical Parameter	r	p	p significance
BMI (kg/m^2)	-0.2307	0.1274	ns
Weight (kg)	-0.285	0.0577	ns
Fasting Glucose (mmol/L)	-0.05647	0.7629	ns
Insulin (µIU/mL)	-0.222	0.2219	ns
CRP (mg/L)	0.2087	0.2772	ns
Hb (g/L)	-0.3424	0.0594	ns
WCC (x10^9/L)	0.1575	0.3974	ns
Platelet Count (x10^9/L)	0.1069	0.567	ns
Sodium (mmol/L)	-0.1126	0.5465	ns
Potassium (mmol/L)	-0.3078	0.0921	ns
Chloride (mmol/L)	-0.001099	0.9953	ns
BiCarb (mmol/L)	-0.01878	0.9201	ns
Urea (mmol/L)	-0.4491	0.0113	*
Creatinine (umol/L)	-0.2623	0.154	ns
eGFR (mL/min)	0.299	0.2436	ns
Calcium (mmol/L)	-0.1057	0.5714	ns
Phospate (mmol/L)	0.169	0.3634	ns
Bilirubin (umol/L)	-0.1206	0.5182	ns
Alk Phos (iu/L)	-0.117	0.5308	ns
Albumin (g/L)	-0.1624	0.3829	ns
Total protein (g/L)	-0.2245	0.2248	ns
Cholestrol (mmol/l)	-0.07378	0.6933	ns
Triglycerides (mmol/l)	-0.2108	0.2551	ns
HDL (mmol/l)	0.2303	0.2126	ns
LDL (mmol/L)	-0.1144	0.5401	ns
L-Tyr (µM)	-0.2018	0.2849	ns
L-Phe (µM)	-0.02369	0.9011	ns
L-Phe : L-Tyr Ratio	0.1914	0.3109	ns
GLP-1 (pM)	-0.2916	0.1248	ns
GIP (pg/mL)	-0.2458	0.1987	ns

Table 7.10: Urine miR 200a Pearson correlations with blood biochemistry markers.			
	miR 200a		
Clinical Parameter	r	p	p significance
BMI (kg/m^2)	-0.3326	0.0726	ns
Weight (kg)	-0.3747	0.0413	*
Fasting Glucose (mmol/L)	-0.132	0.5685	ns
Insulin (µIU/mL)	-0.3292	0.1451	ns
CRP (mg/L)	-0.02221	0.9303	ns
Hb (g/L)	-0.2015	0.3811	ns
WCC (x10^9/L)	0.3102	0.1711	ns
Platelet Count (x10^9/L)	0.2166	0.3456	ns
Sodium (mmol/L)	-0.1564	0.4985	ns
Potassium (mmol/L)	-0.263	0.2493	ns
Chloride (mmol/L)	0.003867	0.9867	ns
BiCarb (mmol/L)	-0.1804	0.4339	ns
Urea (mmol/L)	-0.4162	0.0606	ns
Creatinine (umol/L)	-0.1458	0.5283	ns
eGFR (mL/min)	0.3913	0.234	ns
Calcium (mmol/L)	0.1464	0.5265	ns
Phospate (mmol/L)	0.286	0.2088	ns
Bilirubin (umol/L)	-0.05784	0.8034	ns
Alk Phos (iu/L)	-0.1867	0.4177	ns
Albumin (g/L)	0.07435	0.7487	ns
Total protein (g/L)	-0.08569	0.7119	ns
Cholestrol (mmol/l)	-0.1115	0.6397	ns
Triglycerides (mmol/l)	-0.1759	0.4582	ns
HDL (mmol/l)	0.2895	0.2158	ns
LDL (mmol/L)	-0.1356	0.5688	ns
L-Tyr (µM)	-0.3979	0.0823	ns
L-Phe (µM)	-0.07222	0.7622	ns
L-Phe : L-Tyr Ratio	0.4972	0.0257	*
GLP-1 (pM)	-0.3684	0.1207	ns
GIP (pg/mL)	-0.4228	0.0713	ns

Table 7.11: Urine miR 200b Pearson correlations with blood biochemistry markers.			
		miR 200b	
Clinical Parameter	r	p	p significance
BMI (kg/m^2)	-0.2873	0.0502	ns
Weight (kg)	-0.3067	0.036	*
Fasting Glucose (mmol/L)	-0.05534	0.7636	ns
Insulin (µIU/mL)	-0.1258	0.4856	ns
CRP (mg/L)	-0.006918	0.9711	ns
Hb (g/L)	-0.1855	0.3095	ns
WCC (x10^9/L)	0.1815	0.3201	ns
Platelet Count (x10^9/L)	0.2185	0.2295	ns
Sodium (mmol/L)	-0.1354	0.46	ns
Potassium (mmol/L)	-0.1451	0.4281	ns
Chloride (mmol/L)	0.003286	0.9858	ns
BiCarb (mmol/L)	-0.06468	0.7251	ns
Urea (mmol/L)	-0.3515	0.0485	*
Creatinine (umol/L)	-0.1437	0.4328	ns
eGFR (mL/min)	-0.08875	0.7262	ns
Calcium (mmol/L)	0.08932	0.6269	ns
Phospate (mmol/L)	0.2353	0.1949	ns
Bilirubin (umol/L)	-0.09331	0.6115	ns
Alk Phos (iu/L)	-0.1474	0.4209	ns
Albumin (g/L)	0.06188	0.7365	ns
Total protein (g/L)	-0.1042	0.5703	ns
Cholestrol (mmol/l)	-0.1399	0.4451	ns
Triglycerides (mmol/l)	-0.1616	0.377	ns
HDL (mmol/l)	0.1113	0.5442	ns
LDL (mmol/L)	-0.1424	0.4368	ns
L-Tyr (µM)	-0.2368	0.1996	ns
L-Phe (µM)	-0.01756	0.9253	ns
L-Phe : L-Tyr Ratio	0.2986	0.1028	ns
GLP-1 (pM)	-0.2644	0.158	ns
GIP (pg/mL)	-0.3305	0.0744	ns

Table 7.12: Post-bariatric circulating microRNA fold changes relative to preoperative levels.										
	1 month		3 months		6 months		9 months		12 months	
MicroRNA	FC	p	FC	p	FC	p	FC	p	FC	p
let-7a-5p	-1.192	0.901	1.259	0.865	2.500	0.433	2.310	0.476	2.575	0.546
let-7b-3p	1.142	0.886	1.111	0.905	-3.172	0.145	-5.349	0.081	-1.505	0.629
let-7b-5p	-2.229	0.269	**-1.827**	**0.044**	-1.335	0.291	1.057	0.886	-1.213	0.585
let-7c	1.083	0.942	1.718	0.521	4.297	0.133	-1.002	0.990	-5.706	0.160
let-7d-3p	1.299	0.557	-1.729	0.286	-2.003	0.172	**-2.147**	**0.038**	**-2.760**	**0.035**
let-7d-5p	-2.045	0.328	-1.714	0.336	1.683	0.405	1.079	0.875	-1.240	0.750
let-7e-5p	-1.123	0.884	-1.169	0.774	-1.301	0.629	-1.983	0.341	1.039	0.959
let-7f-5p	-1.071	0.893	-1.303	0.664	-1.509	0.581	-1.214	0.760	-1.481	0.695
let-7g-5p	1.065	0.782	-1.138	0.551	-2.554	0.255	1.176	0.429	-1.081	0.745
let-7i-5p	1.903	0.102	-2.051	0.087	**-1.921**	**0.039**	**-2.154**	**0.032**	-2.054	0.091
miR-1	-1.225	0.663	1.354	0.594	1.369	0.648	-2.567	0.234	-2.600	0.170
miR-103a-3p	-5.757	0.085	-1.123	0.693	1.294	0.379	1.051	0.877	1.314	0.479
miR-106a-5p	3.763	0.459	-3.164	0.558	9.581	0.142	1.392	0.861	11.202	0.242
miR-106b-3p	1.137	0.890	2.289	0.301	2.411	0.415	-3.096	0.205	-1.533	0.661
miR-106b-5p	-1.031	0.956	**-2.247**	**0.028**	-1.002	0.990	-2.425	0.103	**-3.740**	**0.040**
miR-107	-1.031	0.951	-1.184	0.674	-1.082	0.863	-1.004	0.990	1.132	0.797
miR-10b-5p	4.244	0.193	-1.299	0.742	-1.376	0.708	-1.261	0.798	-9.328	0.078
miR-122-5p	1.911	0.343	-3.666	0.092	-1.382	0.572	-2.554	0.195	-4.186	0.070
miR-125a-5p	6.584	0.059	1.009	0.988	1.216	0.715	1.191	0.770	1.190	0.771
miR-125b-5p	1.221	0.755	-1.943	0.280	**-7.144**	**0.008**	**-3.067**	**0.033**	**-3.701**	**0.048**
miR-126-3p	12.599	0.167	13.881	0.099	12.412	0.136	12.175	0.139	1.355	0.907
miR-128	3.660	0.288	-1.741	0.642	1.092	0.938	-4.261	0.278	-1.767	0.695
miR-130a-3p	2.410	0.470	-1.297	0.850	1.300	0.819	-8.377	0.122	-6.195	0.280
miR-130b-3p	-1.115	0.875	-2.095	0.267	-1.082	0.904	-2.268	0.240	**-13.871**	**0.006**
miR-132-3p	-1.593	0.654	-1.247	0.834	-1.003	0.990	-1.468	0.698	-1.966	0.544
miR-133a	-1.762	0.362	-1.810	0.489	1.613	0.599	-3.487	0.148	-3.521	0.175
miR-133b	1.412	0.743	1.826	0.568	3.551	0.256	1.127	0.918	-1.429	0.789
miR-136-5p	-3.043	0.198	1.447	0.603	3.975	0.118	-1.483	0.702	1.305	0.771
miR-139-5p	-2.385	0.291	2.421	0.205	2.858	0.147	1.008	0.990	1.250	0.787
miR-140-3p	2.075	0.665	1.264	0.878	6.278	0.201	3.633	0.340	-1.263	0.903
miR-140-5p	-2.505	0.200	-2.639	0.171	1.580	0.468	-1.877	0.437	-1.852	0.415
miR-142-3p	-1.237	0.565	1.216	0.557	1.267	0.470	-1.102	0.781	1.419	0.412
miR-142-5p	1.113	0.926	1.241	0.824	3.164	0.363	2.086	0.500	1.345	0.828
miR-143-3p	3.094	0.252	1.422	0.699	2.561	0.271	3.574	0.159	1.913	0.602
miR-144-3p	2.228	0.200	-1.295	0.631	-1.232	0.678	-1.705	0.445	-2.002	0.413
miR-144-5p	2.636	0.306	-1.208	0.816	1.490	0.693	-2.913	0.287	-7.657	0.090
miR-145-5p	-1.047	0.957	1.262	0.653	1.751	0.339	-2.753	0.295	-1.319	0.786
miR-146a-5p	-1.208	0.725	1.660	0.227	1.302	0.546	-1.112	0.813	1.249	0.681
miR-146b-5p	-1.156	0.804	1.596	0.256	2.829	0.147	-2.082	0.273	-2.454	0.179
miR-148a-3p	1.278	0.648	-1.717	0.230	-2.309	0.076	**-2.575**	**0.038**	-3.092	0.061
miR-148b-3p	1.349	0.420	1.047	0.880	-1.501	0.151	**-1.862**	**0.050**	-1.967	0.077

MicroRNA	1 month		3 months		6 months		9 months		12 months	
	FC	p	FC	p	FC	p	FC	p	FC	p
miR-150-5p	1.129	0.871	1.506	0.576	-1.249	0.788	-9.519	0.099	-2.036	0.424
miR-151a-3p	-2.391	0.157	1.563	0.364	2.160	0.230	-1.100	0.859	-1.147	0.849
miR-151a-5p	-1.117	0.683	-1.630	0.496	1.099	0.642	1.109	0.681	1.191	0.523
miR-152	1.451	0.541	-1.061	0.908	-1.637	0.248	-1.410	0.372	-2.125	0.140
miR-154-5p	1.192	0.839	3.330	0.095	2.868	0.291	-1.031	0.969	-2.193	0.451
miR-15a-5p	1.710	0.528	-2.412	0.200	-2.226	0.301	**-6.522**	**0.013**	**-84.905**	**0.019**
miR-15b-3p	1.628	0.712	-2.457	0.448	-1.092	0.939	-1.183	0.876	-2.801	0.468
miR-15b-5p	1.220	0.766	-1.162	0.769	1.412	0.612	-2.087	0.309	-8.795	0.062
miR-16-2-3p	-1.074	0.939	-1.642	0.412	-1.897	0.465	**-4.056**	**0.045**	-5.841	0.078
miR-16-5p	1.370	0.493	-1.696	0.183	-1.415	0.380	-1.117	0.799	-1.375	0.542
miR-17-5p	-1.524	0.545	-1.437	0.480	1.881	0.279	1.297	0.594	1.411	0.600
miR-181a-5p	-1.039	0.954	1.249	0.700	1.034	0.950	1.213	0.680	1.147	0.825
miR-185-5p	-1.054	0.931	-1.528	0.112	-1.058	0.835	-1.507	0.314	-1.098	0.764
miR-186-5p	-1.156	0.830	-1.199	0.751	1.353	0.561	-1.428	0.654	1.203	0.779
miR-18a-3p	2.397	0.168	-1.104	0.810	1.179	0.834	-4.555	0.056	-1.253	0.670
miR-18a-5p	1.114	0.925	1.483	0.692	6.756	0.078	1.396	0.785	1.706	0.682
miR-18b-5p	-1.326	0.710	-1.237	0.737	1.743	0.255	2.002	0.160	1.868	0.333
miR-191-5p	-1.136	0.806	1.577	0.194	1.504	0.256	1.351	0.415	1.301	0.574
miR-192-5p	1.084	0.873	-2.103	0.206	**-3.976**	**0.007**	**-3.680**	**0.016**	**-3.458**	**0.047**
miR-194-5p	-1.935	0.297	**-6.792**	**0.001**	-3.465	0.141	**-7.387**	**0.006**	**-8.758**	**0.003**
miR-195-5p	2.764	0.255	-1.308	0.709	-1.176	0.787	-3.095	0.124	-1.107	0.883
miR-197-3p	-2.506	0.350	3.074	0.181	4.635	0.084	2.776	0.267	1.503	0.733
miR-199a-3p	-4.064	0.210	1.532	0.475	2.062	0.248	-1.469	0.673	1.511	0.619
miR-199a-5p	-4.574	0.144	1.717	0.511	5.884	0.065	1.493	0.653	1.348	0.782
miR-19b-3p	1.049	0.890	-1.061	0.821	-1.081	0.778	1.092	0.780	-1.015	0.967
miR-205-5p	1.458	0.689	1.011	0.990	1.981	0.558	-2.540	0.352	-2.127	0.526
miR-20a-5p	1.847	0.498	1.429	0.638	1.521	0.614	-1.958	0.666	2.068	0.509
miR-20b-5p	1.502	0.581	-1.009	0.989	1.626	0.565	-1.564	0.541	**-5.580**	**0.050**
miR-210	1.695	0.519	-3.081	0.123	-1.268	0.811	-2.526	0.343	-2.331	0.375
miR-2110	1.107	0.900	-1.383	0.607	1.151	0.858	-1.296	0.685	-3.563	0.146
miR-215	1.311	0.750	-1.591	0.570	-3.044	0.177	-1.961	0.436	-1.878	0.521
miR-21-5p	1.102	0.870	-1.507	0.371	-1.304	0.671	**-2.993**	**0.026**	**-4.990**	**0.016**
miR-221-3p	2.535	0.404	2.104	0.529	3.212	0.345	5.139	0.109	6.730	0.159
miR-222-3p	2.599	0.069	-2.909	0.377	-3.298	0.236	-1.213	0.648	1.015	0.978
miR-223-5p	1.365	0.635	-1.352	0.665	1.669	0.554	-1.397	0.702	-1.900	0.484
miR-22-3p	3.746	0.234	1.355	0.737	-1.040	0.967	-1.402	0.723	-2.079	0.571
miR-22-5p	1.437	0.609	-1.558	0.396	-1.958	0.305	**-5.348**	**0.018**	**-19.128**	**0.002**
miR-23a-3p	1.023	0.957	1.408	0.247	1.233	0.495	1.080	0.814	1.031	0.938
miR-23b-3p	1.449	0.721	-1.637	0.697	5.006	0.120	2.213	0.403	-2.331	0.568
miR-24-3p	-1.188	0.613	-1.952	0.505	1.022	0.936	-1.111	0.719	-1.099	0.791
miR-25-3p	1.022	0.986	1.193	0.838	-2.120	0.538	1.184	0.861	1.266	0.848
miR-26b-5p	-1.967	0.530	2.161	0.280	1.719	0.472	3.296	0.106	-2.085	0.585

MicroRNA	1 month		3 months		6 months		9 months		12 months	
	FC	p	FC	p	FC	p	FC	p	FC	p
miR-27a-3p	4.039	0.216	2.994	0.363	**13.533**	**0.023**	-2.634	0.513	-3.982	0.443
miR-27b-3p	-1.053	0.954	-2.062	0.545	-1.001	0.990	2.052	0.239	2.366	0.283
miR-28-3p	-1.583	0.480	1.736	0.163	2.881	0.078	**-3.387**	**0.027**	-1.631	0.507
miR-28-5p	-2.393	0.365	1.025	0.974	2.220	0.417	-2.022	0.476	1.507	0.708
miR-29a-3p	-1.231	0.792	-1.394	0.598	1.094	0.889	-1.351	0.615	-2.461	0.278
miR-29a-5p	-1.474	0.502	1.175	0.784	-1.119	0.818	-3.828	0.066	**-5.746**	**0.010**
miR-29b-3p	-1.836	0.317	-1.462	0.410	1.202	0.751	-1.866	0.279	**-3.096**	**0.035**
miR-29c-3p	-1.012	0.983	-1.888	0.142	-1.436	0.562	**-4.366**	**0.011**	**-7.437**	**0.005**
miR-301a-3p	-1.050	0.953	1.937	0.338	**5.379**	**0.018**	2.765	0.137	**6.227**	**0.046**
miR-30a-5p	-1.926	0.413	-2.347	0.318	-1.221	0.743	-1.963	0.439	-3.178	0.123
miR-30b-5p	3.854	0.275	2.006	0.536	3.569	0.263	2.830	0.359	3.660	0.395
miR-30c-5p	1.195	0.692	-1.211	0.695	1.290	0.502	-3.454	0.219	1.217	0.632
miR-30d-5p	-2.164	0.132	-1.767	0.196	-1.235	0.331	-1.516	0.124	-1.203	0.461
miR-30e-3p	-2.089	0.132	1.082	0.851	1.837	0.257	-2.612	0.103	**-4.250**	**0.021**
miR-30e-5p	-1.716	0.478	-1.605	0.300	-1.967	0.351	-7.573	0.100	-1.033	0.829
miR-320a	2.079	0.313	-1.752	0.383	**-4.931**	**0.037**	**-5.058**	**0.007**	**-5.639**	**0.024**
miR-320b	1.202	0.889	-2.035	0.291	-2.760	0.128	**-3.363**	**0.040**	-4.339	0.059
miR-324-3p	-1.861	0.425	-1.577	0.405	1.393	0.712	-1.303	0.703	-4.435	0.105
miR-324-5p	-1.686	0.354	-1.049	0.905	-1.445	0.504	1.272	0.564	1.082	0.888
miR-32-5p	1.634	0.523	-3.121	0.091	-1.499	0.569	**-5.872**	**0.025**	**-11.797**	**0.008**
miR-326	-1.449	0.564	1.195	0.715	1.250	0.782	-3.281	0.126	-3.131	0.172
miR-328	-1.210	0.800	-2.304	0.351	2.169	0.318	-1.635	0.406	-1.384	0.674
miR-331-3p	2.114	0.302	2.159	0.192	-1.009	0.990	-2.479	0.286	2.114	0.384
miR-335-5p	1.859	0.440	1.239	0.771	1.004	0.990	1.379	0.563	-1.983	0.382
miR-338-3p	**-4.482**	**0.039**	-1.230	0.737	1.967	0.274	-1.857	0.525	1.977	0.371
miR-339-3p	-1.080	0.936	-1.724	0.387	-1.476	0.576	-4.306	0.084	**-11.956**	**0.016**
miR-339-5p	1.020	0.979	1.420	0.550	1.249	0.743	-2.095	0.331	-2.041	0.422
miR-33a-5p	1.288	0.733	2.995	0.124	**4.739**	**0.024**	1.271	0.800	2.661	0.265
miR-342-3p	-1.139	0.848	1.494	0.502	-2.725	0.336	-6.749	0.107	-1.141	0.817
miR-34a-5p	-1.200	0.875	-2.275	0.426	-3.108	0.284	-5.222	0.167	-13.774	0.087
miR-363-3p	1.176	0.830	-2.919	0.055	-2.838	0.265	**-4.165**	**0.039**	**-6.015**	**0.037**
miR-365a-3p	-1.544	0.442	-2.269	0.164	-1.480	0.628	**-14.393**	**0.000**	-2.425	0.224
miR-374a-5p	-2.219	0.137	-1.404	0.308	1.292	0.653	-1.543	0.247	-1.703	0.244
miR-374b-5p	1.070	0.946	**4.933**	**0.050**	**6.262**	**0.035**	**6.420**	**0.027**	8.699	0.052
miR-376a-3p	-3.139	0.184	-1.012	0.987	1.954	0.412	-1.624	0.563	-1.247	0.821
miR-378a-3p	1.507	0.571	-5.183	0.156	**-11.137**	**0.032**	**-9.024**	**0.006**	**-35.243**	**0.003**
miR-382-5p	1.166	0.869	1.627	0.571	1.897	0.565	1.144	0.895	-1.696	0.675
miR-409-3p	-2.077	0.332	1.068	0.907	2.599	0.176	1.217	0.797	-2.966	0.270
miR-421	1.010	0.984	1.427	0.567	1.418	0.564	-1.401	0.543	-2.078	0.328
miR-423-3p	-1.671	0.465	-2.111	0.145	-1.660	0.418	**-4.642**	**0.021**	**-4.013**	**0.017**
miR-423-5p	8.054	0.132	1.595	0.674	1.029	0.981	-3.294	0.391	-1.689	0.732
miR-424-5p	1.516	0.473	-2.320	0.085	-5.042	0.063	**-3.069**	**0.029**	-2.873	0.099
miR-425-3p	1.609	0.472	-1.355	0.481	-1.085	0.901	-2.939	0.086	-3.326	0.155

MicroRNA	1 month		3 months		6 months		9 months		12 months	
	FC	p	FC	p	FC	p	FC	p	FC	p
miR-425-5p	1.547	0.718	1.154	0.886	2.494	0.436	-1.470	0.751	-1.240	0.878
miR-451a	1.716	0.448	-2.016	0.282	-1.727	0.374	-1.271	0.731	-1.558	0.592
miR-484	14.798	0.151	4.038	0.377	2.231	0.635	4.137	0.351	1.057	0.979
miR-485-3p	1.858	0.477	1.556	0.580	2.032	0.299	-3.134	0.180	-1.091	0.918
miR-486-5p	3.296	0.148	-1.854	0.343	-2.311	0.188	-2.796	0.111	-3.505	0.116
miR-495-3p	-1.512	0.609	2.221	0.287	2.078	0.338	-1.284	0.745	-1.486	0.637
miR-497-5p	2.616	0.244	1.405	0.641	1.244	0.806	-2.613	0.238	**-7.824**	**0.039**
miR-501-3p	1.183	0.877	1.693	0.569	-1.393	0.742	-6.811	0.057	-7.161	0.115
miR-502-3p	1.335	0.681	-2.393	0.135	-3.069	0.129	**-5.755**	**0.038**	**-13.228**	**0.004**
miR-505-3p	-1.029	0.981	-3.760	0.265	-1.625	0.660	-5.377	0.190	**-21.453**	**0.042**
miR-532-3p	-1.511	0.470	-1.769	0.397	1.078	0.923	-3.319	0.081	**-16.700**	**0.007**
miR-532-5p	1.171	0.828	-2.052	0.167	-1.199	0.848	**-5.651**	**0.011**	-2.192	0.347
miR-543	1.909	0.485	4.442	0.117	5.423	0.091	2.410	0.267	2.268	0.376
miR-574-3p	**2.743**	**0.049**	1.581	0.393	2.996	0.264	1.076	0.872	-1.267	0.740
miR-584-5p	2.759	0.303	2.068	0.443	1.450	0.687	-1.451	0.670	-3.960	0.244
miR-590-5p	-1.202	0.816	-1.190	0.648	**-2.729**	**0.022**	-2.087	0.065	-2.233	0.106
miR-629-5p	2.131	0.435	-3.544	0.180	-2.531	0.287	**-34.772**	**0.001**	**-30.336**	**0.001**
miR-652-3p	-1.090	0.888	-1.591	0.291	-1.903	0.376	-1.246	0.532	-1.270	0.579
miR-660-5p	1.478	0.642	-3.184	0.121	-4.952	0.110	**-12.738**	**0.003**	**-16.147**	**0.009**
miR-766-3p	-1.568	0.494	1.605	0.285	2.505	0.145	-1.327	0.622	**-3.765**	**0.044**
miR-885-5p	1.413	0.737	-2.183	0.474	-2.155	0.512	-6.271	0.076	-15.316	0.050
miR-92a-3p	1.236	0.747	-2.280	0.116	-1.882	0.350	**-4.509**	**0.015**	**-7.404**	**0.016**
miR-93-3p	1.655	0.371	1.283	0.430	2.139	0.282	-2.081	0.205	**-5.518**	**0.007**
miR-93-5p	-4.168	0.272	**-11.421**	**0.048**	-1.182	0.848	1.891	0.383	1.875	0.516
miR-99a-5p	1.772	0.461	-5.110	0.064	-4.344	0.055	**-11.744**	**0.018**	**-6.782**	**0.047**
miR-99b-5p	2.574	0.350	2.583	0.276	1.084	0.941	-2.574	0.385	1.026	0.982

Table 7.13: Pearson correlations between bariatric circulating microRNA expressions and clinical parameters.

MicroRNA	BMI		% Preop BMI lost		Blood glucose	
	r	p	r	p	r	p
let-7b-3p	0.02469	0.8798	-0.1838	0.2562	**0.4951**	**0.0025**
let-7b-5p	0.252	0.1168	-0.03617	0.8246	0.0275	0.8754
let-7c	0.074	0.65	0.009722	0.9525	-0.04249	0.8085
let-7d-3p	**0.3466**	**0.0285**	**-0.4277**	**0.0059**	0.09429	0.5901
let-7d-5p	-0.1591	0.3267	0.1148	0.4805	0.07089	0.6857
let-7e-5p	0.2546	0.1128	-0.2403	0.1353	0.08388	0.6319
let-7f-5p	-0.06739	0.6795	-0.1775	0.2731	0.2927	0.088
let-7g-5p	-0.1967	0.2237	-0.04721	0.7724	0.0679	0.6983
let-7i-5p	**0.3165**	**0.0466**	**-0.4127**	**0.0081**	0.1742	0.3168
miR-1	-0.2418	0.1328	0.01092	0.9467	**0.3594**	**0.034**
miR-103a-3p	**-0.3231**	**0.042**	0.1461	0.3685	0.1728	0.321
miR-106a-5p	-0.2061	0.202	0.1956	0.2265	-0.04955	0.7774
miR-106b-3p	-0.000729	0.9964	0.03009	0.8538	-0.009695	0.9559
miR-106b-5p	-0.09802	0.5474	-0.1599	0.3245	0.07866	0.6533
miR-107	**-0.3347**	**0.0348**	0.008081	0.9605	0.2033	0.2415
miR-10b-5p	0.1376	0.3972	-0.08126	0.6182	0.009655	0.9561
miR-122-5p	0.2242	0.1642	-0.2938	0.0658	0.2039	0.24
miR-125a-5p	0.08062	0.621	-0.147	0.3654	0.1924	0.2681
miR-125b-5p	**0.3457**	**0.0289**	**-0.4235**	**0.0065**	0.2246	0.1945
miR-126-3p	-0.247	0.1244	0.2654	0.098	0.1971	0.2565
miR-128	0.1282	0.4305	-0.173	0.2857	-0.05962	0.7337
miR-130a-3p	-0.0191	0.9069	-0.1837	0.2565	0.2375	0.1696
miR-130b-3p	0.07258	0.6563	-0.2099	0.1937	-0.1307	0.4544
miR-132-3p	-0.06356	0.6968	-0.05333	0.7438	0.3316	0.0516
miR-133a	-0.1824	0.26	-0.175	0.2802	**0.356**	**0.0358**
miR-133b	-0.08481	0.6029	0.05313	0.7447	0.005138	0.9766
miR-136-5p	**-0.3881**	**0.0133**	0.1255	0.4405	0.1953	0.2608
miR-139-5p	-0.1835	0.2571	0.1146	0.4815	0.161	0.3556
miR-140-3p	-0.2101	0.1932	0.1276	0.4327	0.1432	0.4119
miR-140-5p	0.00656	0.968	0.005003	0.9756	-0.2752	0.1097
miR-142-3p	-0.2293	0.1547	0.05257	0.7473	0.2257	0.1923
miR-142-5p	**-0.32**	**0.0441**	0.1897	0.241	0.06127	0.7266
miR-143-3p	-0.276	0.0848	0.2805	0.0795	0.009366	0.9574
miR-144-3p	-0.1361	0.4022	-0.07119	0.6625	0.106	0.5445
miR-144-5p	-0.1749	0.2805	-0.09053	0.5785	0.2958	0.0844
miR-145-5p	-0.06614	0.6851	-0.06063	0.7102	0.0672	0.7013
miR-146a-5p	0.05593	0.7318	-0.03155	0.8468	0.2216	0.2008
miR-146b-5p	-0.09773	0.5485	0.07658	0.6386	0.04566	0.7945
miR-148a-3p	**0.5195**	**0.0006**	**-0.4731**	**0.002**	0.04618	0.7922
miR-148b-3p	**0.4008**	**0.0104**	**-0.3638**	**0.021**	0.05604	0.7492

MicroRNA	BMI		% Preop BMI lost		Blood glucose	
	r	p	r	p	r	p
miR-150-5p	0.1481	0.3618	-0.1504	0.3542	0.04913	0.7793
miR-151a-3p	-0.1307	0.4214	0.07835	0.6308	-0.0878	0.616
miR-151a-5p	-0.01637	0.9201	0.06388	0.6954	0.06326	0.7181
miR-152	0.2464	0.1254	-0.2273	0.1584	0.08336	0.634
miR-154-5p	0.07499	0.6456	0.09192	0.5727	-0.02518	0.8858
miR-15a-5p	0.1907	0.2384	-0.3005	0.0595	0.1948	0.262
miR-15b-3p	-0.01747	0.9148	-0.04106	0.8014	0.05954	0.734
miR-15b-5p	0.09232	0.571	-0.1724	0.2873	0.08834	0.6138
miR-16-2-3p	0.001143	0.9944	-0.2115	0.1901	0.1952	0.2612
miR-16-5p	0.2089	0.1958	-0.099	0.5433	-0.2058	0.2356
miR-17-5p	-0.2066	0.201	0.2155	0.1818	0.07083	0.686
miR-181a-5p	-0.05945	0.7156	0.0407	0.8031	0.1863	0.2838
miR-185-5p	-0.1887	0.2435	-0.02768	0.8654	0.1432	0.4119
miR-186-5p	0.1052	0.5183	0.04153	0.7991	-0.05657	0.7469
miR-18a-3p	0.04131	0.8002	-0.1466	0.3668	0.02919	0.8678
miR-18a-5p	-0.1958	0.2259	0.2374	0.1402	-0.1344	0.4415
miR-18b-5p	-0.2205	0.1715	0.2619	0.1025	0.1803	0.2999
miR-191-5p	**-0.3831**	**0.0147**	0.2118	0.1895	0.1909	0.272
miR-192-5p	0.2986	0.0613	**-0.3929**	**0.0121**	0.1238	0.4787
miR-194-5p	0.193	0.2328	**-0.369**	**0.0191**	0.1291	0.4597
miR-195-5p	0.1886	0.2438	-0.2711	0.0906	0.1665	0.339
miR-197-3p	0.001588	0.9922	0.182	0.261	0.1624	0.3513
miR-199a-3p	0.04054	0.8038	1.128E-05	0.9999	0.1181	0.4991
miR-199a-5p	**-0.3812**	**0.0152**	0.2265	0.16	0.04164	0.8123
miR-19b-3p	-0.2402	0.1355	0.1324	0.4155	0.0065	0.9704
miR-205-5p	-0.08123	0.6183	0.02167	0.8944	-0.06271	0.7204
miR-20a-5p	**-0.3319**	**0.0364**	0.03544	0.8281	0.1167	0.5043
miR-20b-5p	0.06079	0.7094	-0.04246	0.7948	0.02331	0.8942
miR-210	-0.2856	0.074	-0.1064	0.5135	0.1622	0.3518
miR-2110	0.001971	0.9904	-0.04752	0.7709	0.1659	0.341
miR-215	0.03707	0.8204	-0.2454	0.1269	0.2024	0.2437
miR-21-5p	0.1557	0.3373	-0.2901	0.0694	0.2766	0.1078
miR-221-3p	-0.302	0.0582	0.1743	0.282	0.1311	0.4528
miR-222-3p	-0.06203	0.7038	-0.03221	0.8436	0.1832	0.2921
miR-223-5p	-0.06849	0.6745	-0.06866	0.6738	0.03172	0.8564
miR-22-3p	-0.1225	0.4513	-0.1116	0.4931	0.2023	0.2438
miR-22-5p	0.2064	0.2013	**-0.4428**	**0.0042**	0.2581	0.1344
miR-23a-3p	0.09437	0.5624	-0.005878	0.9713	0.08711	0.6188
miR-23b-3p	**-0.3159**	**0.0471**	0.1646	0.3102	0.155	0.3739
miR-24-3p	0.144	0.3753	-0.1043	0.5217	-0.04015	0.8189
miR-25-3p	-0.01727	0.9158	-0.003357	0.9836	0.03555	0.8393
miR-26b-5p	-0.1027	0.5281	0.09525	0.5588	0.09634	0.582

MicroRNA	BMI		% Preop BMI lost		Blood glucose	
	r	p	r	p	r	p
miR-27a-3p	-0.09657	0.5533	0.07968	0.625	0.05217	0.766
miR-27b-3p	-0.122	0.4531	-0.008877	0.9566	0.06936	0.6921
miR-28-3p	0.07332	0.653	-0.04745	0.7712	0.05087	0.7717
miR-28-5p	-0.1589	0.3275	0.001163	0.9943	0.226	0.1917
miR-29a-3p	0.2509	0.1184	-0.1014	0.5336	-0.06196	0.7237
miR-29a-5p	0.0834	0.6089	-0.2452	0.1273	0.2563	0.1373
miR-29b-3p	-0.1263	0.4373	-0.09505	0.5596	0.23	0.1838
miR-29c-3p	0.186	0.2504	-0.2977	0.0621	0.05115	0.7704
miR-301a-3p	**-0.5925**	**0.0001**	**0.4295**	**0.0057**	0.1962	0.2587
miR-30a-5p	-0.06924	0.6712	-0.1173	0.4709	**0.4038**	**0.0162**
miR-30b-5p	-0.1341	0.4094	0.2281	0.157	-0.07413	0.6722
miR-30c-5p	-0.1916	0.2364	-0.09934	0.5419	**0.3467**	**0.0413**
miR-30d-5p	**0.3203**	**0.0439**	-0.2471	0.1242	0.1678	0.3354
miR-30e-3p	-0.03267	0.8414	-0.1936	0.2314	0.2505	0.1467
miR-30e-5p	-0.2121	0.189	-0.09929	0.5422	0.1545	0.3754
miR-320a	0.2579	0.1081	**-0.4439**	**0.0041**	**0.3817**	**0.0237**
miR-320b	0.268	0.0945	**-0.3264**	**0.0399**	**0.3355**	**0.0488**
miR-324-3p	-0.02865	0.8607	-0.07504	0.6454	-0.1438	0.4098
miR-324-5p	-0.2259	0.1611	0.04119	0.8008	-0.06882	0.6945
miR-32-5p	0.09184	0.573	**-0.3308**	**0.0371**	0.2246	0.1945
miR-326	-0.06072	0.7097	-0.1227	0.4509	0.02954	0.8662
miR-328	-0.07584	0.6418	0.02052	0.9	-0.07006	0.6892
miR-331-3p	-0.1768	0.2752	0.01331	0.935	0.1524	0.3821
miR-335-5p	0.005219	0.9745	-0.05853	0.7198	0.1818	0.2959
miR-338-3p	-0.2318	0.15	0.07554	0.6432	0.1006	0.5653
miR-339-3p	-0.003726	0.9818	-0.2411	0.1339	0.09719	0.5786
miR-339-5p	-0.1663	0.305	-0.1278	0.4318	0.1669	0.3379
miR-33a-5p	**-0.4107**	**0.0085**	0.228	0.1572	0.07564	0.6658
miR-342-3p	-0.0822	0.6141	-0.0942	0.5632	0.1834	0.2915
miR-34a-5p	0.1511	0.352	-0.2672	0.0956	0.08434	0.63
miR-363-3p	0.02072	0.899	-0.2731	0.0882	0.2308	0.1823
miR-365a-3p	0.2311	0.1514	**-0.4165**	**0.0075**	0.07643	0.6626
miR-374a-5p	-0.1778	0.2724	-0.04062	0.8035	0.0529	0.7628
miR-374b-5p	-0.1509	0.3527	**0.4081**	**0.0089**	0.1614	0.3544
miR-376a-3p	-0.202	0.2112	0.03087	0.85	0.09109	0.6028
miR-378a-3p	0.264	0.0997	**-0.4564**	**0.0031**	0.2314	0.1812
miR-382-5p	-0.03511	0.8297	0.09181	0.5731	0.04492	0.7978
miR-409-3p	-0.2093	0.1949	0.04353	0.7897	-0.03217	0.8544
miR-421	-0.03206	0.8443	0.01591	0.9224	0.08119	0.6429
miR-423-3p	0.1308	0.4212	**-0.3669**	**0.0199**	0.07069	0.6866
miR-423-5p	-0.09214	0.5717	-0.1307	0.4215	0.3027	0.0772
miR-424-5p	**0.3329**	**0.0358**	**-0.3216**	**0.043**	0.1519	0.3838

MicroRNA	BMI		% Preop BMI lost		Blood glucose	
	r	p	r	p	r	p
miR-425-3p	-0.1108	0.4962	-0.2046	0.2053	0.2698	0.117
miR-425-5p	-0.04609	0.7776	0.007535	0.9632	0.1092	0.5323
miR-451a	0.2027	0.2098	-0.1116	0.4932	-0.1094	0.5315
miR-484	0.03356	0.8371	0.1021	0.5309	0.1048	0.5492
miR-485-3p	-0.01253	0.9388	-0.1151	0.4795	0.03507	0.8415
miR-486-5p	0.2955	0.0642	**-0.3174**	**0.0459**	0.266	0.1224
miR-495-3p	-0.06544	0.6883	0.08412	0.6058	-0.09751	0.5773
miR-497-5p	-0.1013	0.5339	-0.1019	0.5315	0.2197	0.2047
miR-501-3p	0.103	0.5269	-0.2985	0.0613	0.3104	0.0695
miR-502-3p	0.1458	0.3692	**-0.3263**	**0.0399**	0.2487	0.1497
miR-505-3p	0.1514	0.3511	-0.2921	0.0674	0.2263	0.1911
miR-532-3p	0.2847	0.0749	-0.2897	0.0698	0.1737	0.3182
miR-532-5p	0.1111	0.4951	-0.1417	0.383	-0.1326	0.4476
miR-543	-0.238	0.1391	0.184	0.2557	0.02228	0.8989
miR-574-3p	0.004511	0.978	0.04306	0.7919	-0.07358	0.6744
miR-584-5p	0.1216	0.4549	-0.1308	0.4212	0.001279	0.9942
miR-590-5p	0.001537	0.9925	-0.2055	0.2033	**0.4602**	**0.0054**
miR-629-5p	0.1834	0.2572	**-0.4548**	**0.0032**	0.321	0.0601
miR-652-3p	-0.1262	0.4377	-0.115	0.4799	0.1643	0.3458
miR-660-5p	0.1562	0.3358	**-0.4026**	**0.01**	0.2701	0.1166
miR-766-3p	-0.03222	0.8435	-0.08905	0.5848	0.212	0.2214
miR-885-5p	0.2426	0.1314	-0.2981	0.0617	0.06254	0.7212
miR-92a-3p	0.1935	0.2317	**-0.3394**	**0.0322**	0.08189	0.64
miR-93-3p	0.1319	0.4171	-0.1108	0.4962	-0.09724	0.5784
miR-93-5p	0.02307	0.8876	0.1185	0.4665	0.02092	0.9051
miR-99a-5p	0.3101	0.0515	**-0.4939**	**0.0012**	0.2539	0.1411
miR-99b-5p	0.01307	0.9362	-0.06759	0.6786	0.1593	0.3606